SECONDARY METABOLITES OF BACTERIA OBTAINED FROM THE NORTHEASTERN PACIFIC OCEAN: STRUCTURE ELUCIDATION AND BIOSYNTHETIC STUDIES

by

JUDY NEEDHAM

B.Sc., The University of Leeds, 1984

M.Sc., The University of British Columbia, 1988

A THESIS SUBMITTED IN PARTIAL FULFILLMENT OF

THE REQUIREMENTS FOR THE DEGREE OF

DOCTOR OF PHILOSOPHY

in

THE FACULTY OF GRADUATE STUDIES

(Department of Chemistry)

We accept this thesis as conforming

to the required standard

THE UNIVERSITY OF BRITISH COLUMBIA

December 1993

In presenting this thesis in partial fulfilment of the requirements for an advanced degree at the University of British Columbia, I agree that the Library shall make it freely available for reference and study. I further agree that permission for extensive copying of this thesis for scholarly purposes may be granted by the head of my department or by his or her representatives. It is understood that copying or publication of this thesis for financial gain shall not be allowed without my written permission.

(Signature)

Department of Chemistry

The University of British Columbia
Vancouver, Canada

Date 17th December 1993.

Abstract

Investigation of the organic extracts obtained from cultures of four species of bacteria isolated from the northeastern Pacific ocean led to the isolation of eight new and six previously known secondary metabolites. The structures of the new compounds were elucidated by extensive spectroscopic analysis. In addition, the biogenetic origins of the atoms in two of the bacterial metabolites were probed using stable isotope incorporation experiments.

A culture of the bacterium *Serratia odorifera*, isolated from a surface water sample taken near a Chinook salmon (*Oncorhyncus tshawytscha*) farm in Georgia Strait, British Columbia, produced the novel compound oncorhyncolide (**34**). Oncorhyncolide has a unique structure that is apparently not related to other known microbial metabolites isolated from terrestrial sources. Biosynthetic studies using stable isotopes have shown that all the carbons in oncorhyncolide are derived from acetate. The methyl branches in oncorhyncolide are derived from the C2 of acetate and are attached to carbon atoms derived from the carbonyl carbon, C1, of an acetate unit. This type of methyl branching is very rare in polyketide biosynthesis.

Examination of the ethyl acetate extracts of a solid agar culture of *Pseudomonas fluorescens* obtained from an unidentified tunicate in Moira Sound, Alaska, led to the isolation of moiramides A (**38**), B (**39**) and C (**40**) as well as the known compound andrimid (**41**). The crude extract had shown antibacterial activity against *Staphylococcus aureus* and methicillin-resistant *S. aureus*. Moiramide B and andrimid proved to be the compounds responsible for this activity. Biosynthetic studies on andrimid have shown that the acylsuccinimide ring is derived from valine, glycine and acetate. It has been proposed that the biosynthesis proceeds through a dipeptide-like intermediate formed from γ-amino-β-keto acids that are in turn formed from valine and glycine homologated with acetate, presumably via malonyl-CoA.

Liquid cultures of *Pseudomonas* sp. 91V47 obtained from an abalone collected off Cortez Island in Georgia Strait, British Columbia, gave an extract that exhibited potent in vitro cytotoxicity. Bioassay-guided fractionation of the crude extract led to the isolation of three new

δ-hydroxy acid rhizoxin analogs (**44** to **46**). The three new compounds showed significant in vitro activity against P388 murine leukemia.

A marine isolate of the bacterium *Bacillus pumilus*, obtained from a sediment sample collected in Georgia Strait, British Columbia, produced an extract that exhibited antimicrobial activity against *Staphylococcus aureus,* methicillin-resistant *S. aureus* and *S. saprophyticus*. The known compound AI-77-B (**54**), previously isolated from terrestrial and marine sources of *B. pumilus*, was found to be responsible for the antibacterial activity in the crude extract. A new AI-77-B analog, compound **57**, was also isolated. Compound **57** showed antibacterial activity only at high concentrations.

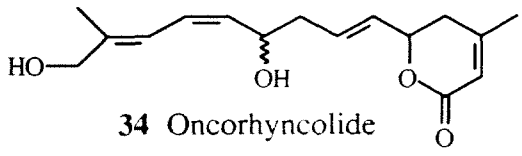

34 Oncorhyncolide

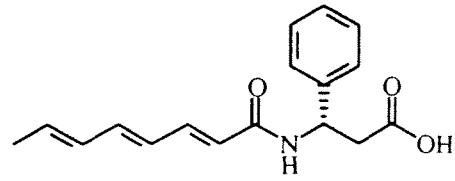

38 Moiramide A

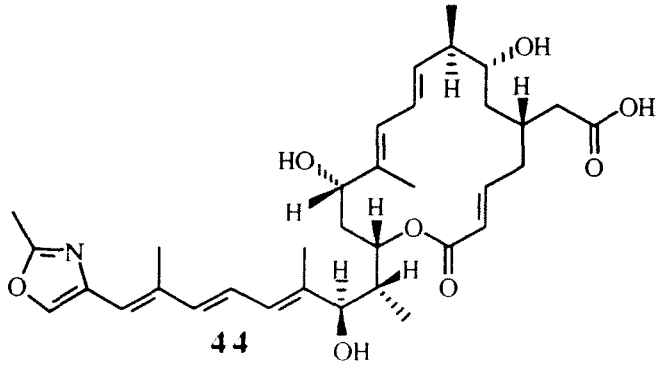

44

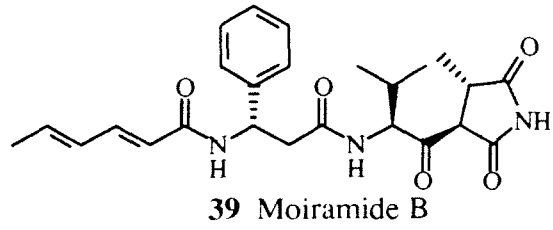

39 Moiramide B

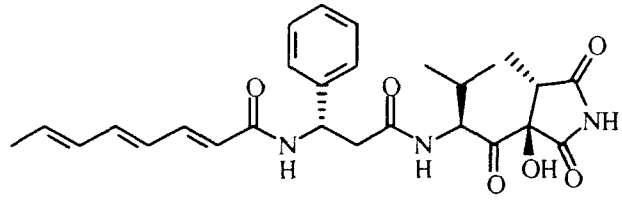

40 Moiramide C

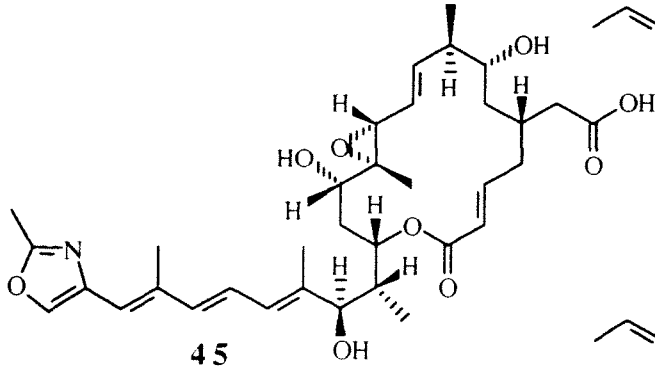

45

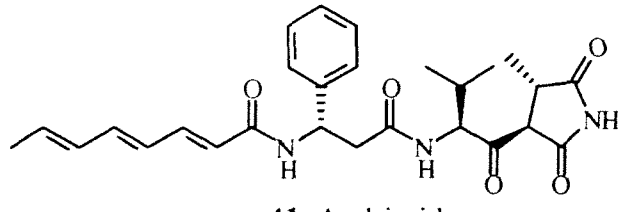

41 Andrimid

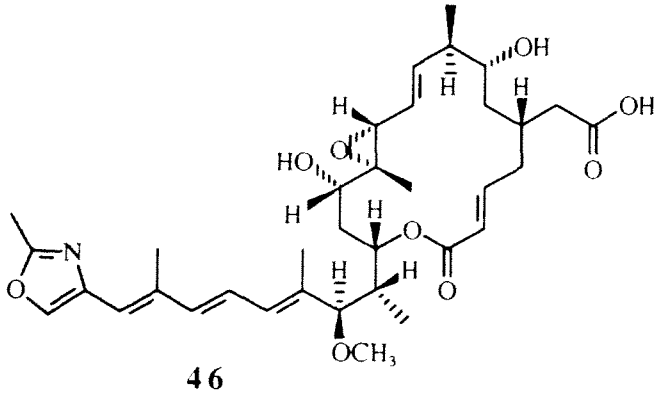

46

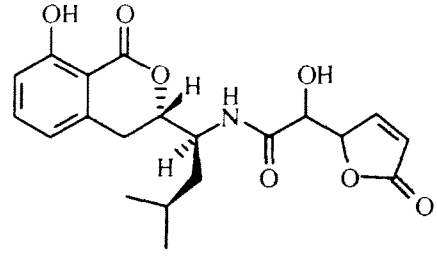

57

Table of Contents

Page

List of Figures

List of Tables

List of Abbreviations

Ac	acetyl
AcOH	acetic acid
APT	attached proton test
BIRD	bilinear rotation decoupling
br	broad
bs	broadened singlet
CD	circular dichroism
C_6D_6	benzene-d_6
$CDCl_3$	chloroform-d
CoA	coenzyme A
COLOC	correlation spectroscopy via long-range coupling
COSY	correlation spectroscopy
d	doublet
dd	doublet of doublets
ddd	doublet of doublets of doublets
1D	one-dimensional
2D	two-dimensional
DMSO-d_6	dimethyl sulfoxide-d_6
dt	doublet of triplets
ED_{50}	dose that is effective in 50 % of test subjects
EtOAc	ethyl acetate
FAS	fatty acid synthase
FID	free induction decay
FTIR	Fourier transform infrared spectroscopy
HETCOR	heteronuclear correlation
HIV	human immunodeficiency virus

HMBC	^{1}H-detected multiple-bond heteronuclear multiple-quantum coherence
HMQC	^{1}H-detected heteronuclear multiple-quantum coherence
HREIMS	high resolution electron impact mass spectrometry
HRLSIMS	high resolution liquid secondary ion mass spectrometry
HPLC	high-pressure liquid chromatography
i	signal due to an impurity
IC_{50}	inhibitory concentration resulting in 50 % response
IR	infrared spectroscopy
J	scalar coupling constant in Hertz
L1210	murine leukemia cell line L1210
LD_{50}	dose that is lethal to 50 % of test subjects
LH-20	Sephadex LH-20
LRDCIMS	low resolution desorption chemical ionization mass spectrometry
LREIMS	low resolution electron impact mass spectrometry
LRLSIMS	low resolution liquid secondary ion mass spectrometry
m	multiplet
M^+	molecular ion
m/z	mass-to-charge ratio
Me	methyl
MeOH	methanol
MIC	minimum inhibitory concentration
MIS	microbial identification system
mmu	millimass units
MS	mass spectrometry
NH_3	ammonia
NMR	nuclear magnetic resonance
NOE	nuclear Overhauser effect
P388	murine leukemia cell line P388

PKS	polyketide synthase
PPM, ppm	chemical shift in parts per million
q	quartet
R_f	ratio to front
s	signal due to solvent
s	singlet
SAM	S-adenosylmethionine
SCUBA	self-contained underwater breathing apparatus
sp.	species
t	triplet
TLC	thin layer chromatography
TMS	tetramethylsilane
UV	ultraviolet
w	signal due to water

$[\alpha]_D$	specific rotation at wavelength of sodium D line
δ	chemical shift in parts per million
ΔM	difference in mass
ϵ	extinction coefficient
λ_{max}	wavelength of absorbance maxima
$[\Theta]_\lambda$	molar ellipticity at wavelength λ

Acknowledgments

I would like to gratefully acknowledge the guidance, support and encouragement of my supervisor Dr. Raymond J. Andersen. His constant enthusiasm always provided an exciting environment for scientific research. It has been a great pleasure to be part of his research team.

I wish to thank members of Dr. Andersens research group, both past and present, for creating a pleasant and intellectually stimulating environment to work in.

Thanks are extended to Gary Hewitt of the Biological Services Laboratory in the Department of Chemistry for his help in culturing bacteria, and to Dr. M. Kelly for providing the microorganisms that made this work possible. I also wish to thank Lianne Darge for her assistance in running the 500 MHz NMR spectrometer. The staff of the Mass Spectrometry Laboratory in the Department of Chemistry are thankfully acknowledged.

I wish to express my heartfelt thanks to Mike Tyndall for his friendship, love, encouragement and unfailing support.

For Mike

"Of all the acts that confirm our unconscious need to reconsider Nature, few are as symbolic as descending into the ocean. As SCUBA divers or inside roving submersibles, we step off the land, leaving behind our urban alliance with concrete and asphalt. Underwater, our survival hinges on containers of portable air. Inside this strange inner space, we become weightless, drifting toward our aquatic origins."

"As trespassers in this other world, we are more susceptible to shifts in thinking and emotion. Our eyes are captured by unfamiliar colors and patterns of light and shadow. The pressurized air sliding in and out of our lungs remind us of our mortality. And from this, it is not a large intuitive leap to consider the mortality of the planet."

Joseph MacInnis; From *Saving the Oceans*,
Key Porter Books, Toronto, 1992, p12.

1. INTRODUCTION

1.1. General Introduction

Despite the availability of many clinically useful antibiotics for treating bacterial infections, there is still a need to search for new antimicrobial agents. The need for new antibiotics is driven by three main forces: i) more effective and less toxic antibiotics are needed to replace the older antimicrobial agents currently in use, ii) pathogenic bacteria have developed resistance to existing antibiotics, and iii) some human pathogens cannot be effectively treated with the currently available drugs.

The problem of antibiotic toxicity is illustrated by the aminoglycoside antibiotics gentamicin and streptomycin. Gentamicin, used for treating kidney infections, may cause kidney damage. Streptomycin, used to treat tuberculosis and infections of the intestines, kidneys and lungs, can cause hearing defects.

The growing problem in antibiotic resistance has been reviewed in a recent issue of Science.[1] Bacteria have responded to the widespread misuse and overuse of antibiotics by mutating and becoming immune to the killing effects of the antibiotics. Adding to the problem is that antibiotic resistance can be transferred from antibiotic-resistant bacteria to other bacteria. Antibiotic resistance is a problem in the community and hospitals. Multidrug-resistant strains of *Neisseria gonorrhoeae*, amphicillin-resistant *Haemophilus influenzae* and the multidrug-resistant enteric organisms *Shigella* and *Salmonella* are examples of community-acquired organisms. Hospital-acquired infections may be caused by multidrug-resistant *Enterobacteriaceae*, vancomycin-resistant enterococci and methicillin-resistant *Staphylococcus aureus*.

Human pathogens that cannot be treated effectively with currently available antibiotics include *Candida* sp. and *Enterococcus* sp. and no antibiotics are available to treat infections of *Mycobacterium avium-intracellulare* and *Pseudomonas cepacia*.

1.2. Microorganisms as a Source of Antibiotics

The discovery of the antibiotic penicillin by Alexander Fleming in 1929[2] revolutionized the treatment of infectious diseases. Fleming demonstrated the ability of penicillin, a secondary metabolite of the fungus *Penicillium notatum*, to kill the pathogenic bacterium *Staphylococcus aureus* in vitro. The use of penicillin as a therapeutic agent to treat infectious diseases in humans did not occur until the 1940's.[3]

Following the discovery of penicillin much attention was focused on soil microorganisms as sources of other antimicrobial chemotypes. In 1939 René J. Dubos isolated gramicidin from the soil microorganism *Bacillus brevis*.[4] Gramicidin was found to be toxic when given intravenously but it is used today as an external application for minor skin wounds. A major breakthrough came in 1943 when the soil microbiologist Selman Waksman and his group isolated streptomycin from the actinomycete *Streptomyces griseus*.[5] Streptomycin was found to be an excellent chemotherapeutic agent against *Mycobacterium tuberculosis*, the cause of tuberculosis. Waksman observed that many soil actinomycetes inhibited microbial growth.

Today it is accepted that a large proportion of microorganisms produce chemicals that inhibit the growth of other microorganisms and that these "antibiotics" help the organism compete for nutrients in their natural environment. The majority of antibiotics produced commercially and used to treat human infections are produced by the actinomycetes and endospore-forming bacteria. These include: bacitracin, chloramphenicol, erythromycin, kanamycin, lincomycin, neomycin, nystatin, polymyxin B, streptomycin and tetracycline. An exception are the β-lactam antibiotics which are produced by fungi.

1.3. Marine Bacteria as a Source of Antimicrobial Agents

Marine bacteria* are an under-explored source of bioactive natural products. Since many terrestrial microorganisms, especially actinomycetes, produce novel and biologically active secondary metabolites, it is not unreasonable to expect marine bacteria to be a rich source of structurally novel and clinically useful antibiotics and antitumour agents.

The marine environment offers a diverse range of habitats including high salinity, extreme pressure and temperatures and sediments rich in organics. Marine plants and animals provide a variety of host surfaces for bacteria. The microorganisms populating these habitats and hosts are expected to have developed unique biosynthetic and physiological capabilities leading to structurally unique compounds not observed from terrestrial microorganisms.

The presence of antagonistic bacteria in the marine environment was first demonstrated by the work of De Gaxia[6] in 1889. The first systematic study of antibiotic production by marine bacteria was carried out by Rosenfeld and Zobell[7] in 1947. A decade later, in 1958, Grein and Meyers[8] reported that approximately fifty percent of the actinomycetes recovered primarily from the Florida coast exhibited antibiotic activity against both Gram-positive and Gram-negative bacteria. Despite this early work, marine microorganisms as a source of biologically active secondary metabolites remain relatively unexplored.

1.4. Marine Bacteria

The classification of marine bacteria has been discussed in the literature.[9] A diverse range of microorganisms with different morphological, ecological and physiological characteristics exist in the marine environment. Gram-negative rods make up the majority of the microorganisms in the water column, while a higher proportion of Gram-positive bacteria are found in sediments.

---

* In this thesis, the term marine bacteria refers to bacteria isolated from the marine environment.

Many microorganisms isolated from the marine environment have features in common with terrestrial microorganisms and may not be indigenous to the marine environment. There is a large interest in the isolation of actinomycetes from the marine environment since it is well known that terrestrial actinomycetes produce many clinically useful antimicrobial and chemotherapeutic agents. It is questionable as to whether the actinomycetes, found in marine sediments, are part of the marine microflora since true marine bacteria may have a physiological requirement for salt. Actinomycetes are known to have a salt tolerance[10] and are able to produce resistant spores that may be washed into the ocean from terrestrial environments. A recent study by Jensen et al.[11] on the distribution of actinomycetes in near-shore tropical sediments suggests that different taxonomic groups vary in their adaptability to the marine environment. The 289 colonies of actinomycetes isolated were mainly assigned to the groups streptomycetes or actinoplanetes. The streptomycetes were found mainly along the shore in shallow mud. The fact that their numbers decreased with distance from the shore and their ability to grow without seawater, although growth was better in seawater, suggests that these streptomycetes were mainly of terrestrial origin but could grow in the marine environment. The highest number of actinoplanetes were isolated from the deepest sediments. It was found that actinoplanetes grew poorly or not at all in the absence of seawater and this could not be explained by the theory that they are dormant terrestrial bacteria. Therefore, it was suggested that the actinoplanetes had physiologically adapted to the marine environment.

Other Gram-positive bacteria such as *Bacillus* and *Clostridium* form stable endospores and may not be true marine bacteria, however, examples of these groups isolated from the marine environment require seawater for growth.

1.5. Secondary Metabolites from Marine Bacteria

Marine microorganisms live in very different environments than terrestrial organisms. These organisms may have developed novel biosynthetic capabilities leading to structurally novel secondary metabolites. A number of excellent reviews on metabolites produced by marine microorganisms have been published recently,[9b,12] therefore, a comprehensive review of the literature will not be presented in this thesis. However, a number of examples will be discussed to demonstrate the ability of marine bacteria to produce structurally novel and biologically active secondary metabolites.

Most of the attention has focused on marine actinomycetes. Novel metabolites produced by actinomycetes include altermicidin (**1**), the four new phenazine esters **2-5** and maduralide (**6**). The novel monoterpene alkaloid altermicidin (**1**) was obtained from cultures of the bacterium *Streptomyces sioyaensis* isolated from a sea-mud sample collected at Gamo, Miyagi Prefecture, Japan.[13] This altermicidin producing bacterium was identified during the screening of 200 actinomycete strains, isolated from the marine environment, with reference to brine shrimp toxicity. Altermicidin exhibited in vitro cytotoxicity against L1210 murine leukemia (IC_{50} = 0.84 μg/mL) and IMC carcinoma (IC_{50} = 0.82 μg/mL); potent in vivo toxicity in mice (LD_{50} = 0.3 mg/kg) would limit its use as a chemotherapeutic agent. Selective activity against the bacteria *Xanthomonas* sp. was also observed.

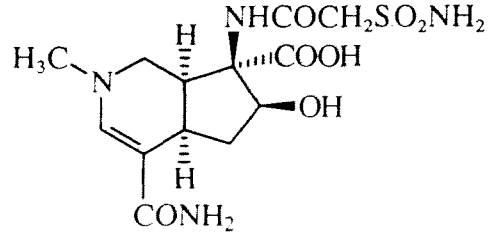

1 Altermicidin

A *Streptomyces* sp. isolated from a sediment sample collected in Bodega Bay, CA, produced four new alkaloid esters (**2**-**5**) of the rare phenazine class.[14] These compounds are phenazine esters of the rare sugar L-quinovose. Compounds **2** and **3** showed broad-spectrum activity against a number of Gram-positive and Gram-negative bacteria with MIC concentrations in the range 1-4 μg/mL.

Maduralide (**6**), a 24-membered ring macrolide isolated from a liquid culture of a marine actinomycete, obtained from a shallow mud sample collected at Bodega Bay, CA, exhibits weak activity against *Bacillus subtilus*.[15]

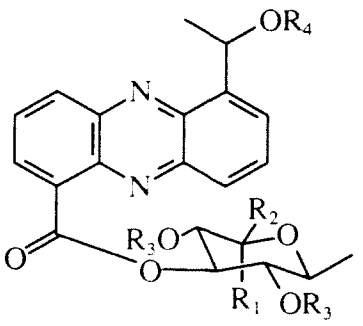

2 $R_1 = OH, R_2 = R_3 = R_4 = H$
4 $R_1 = R_3 = R_4 = H, R_2 = OH$

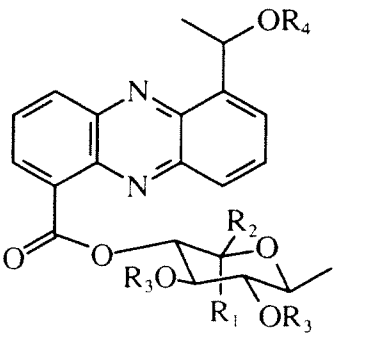

3 $R_1 = OH, R_2 = R_3 = R_4 = H$
5 $R_1 = R_3 = R_4 = H, R_2 = OH$

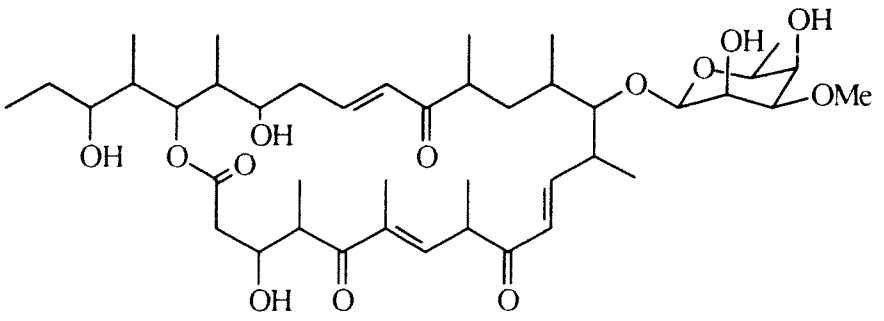

6 Maduralide

Bacteria inhabiting the dark deep sea may have unique biosynthetic capabilities since they must tolerate large in situ pressures. Novel metabolites produced by bacteria isolated from deep-

sea sediments include the macrolactins (for example **7**-**10**) and bisucaberin (**11**). An undefinable deep-sea bacterium #C-237 isolated from a sediment sample collected at a depth of 1000 meters along the California coast, produced the macrolactins (for example **7**-**10**) when cultured in a marine medium at atmospheric pressure.[16] The macrolactins are novel cytotoxic and antiviral macrolides. Macrolactin A accounted for the majority of the biological activity and was active in vitro against B16-F10 murine melanoma (IC_{50} = 3.5 μg/mL). This compound also inhibited a number of human viruses including *Herpes simplex* (IC_{50} = 10 μg/mL) and the human-immunodeficiency virus, HIV, (IC_{50} = 10 μg/mL).

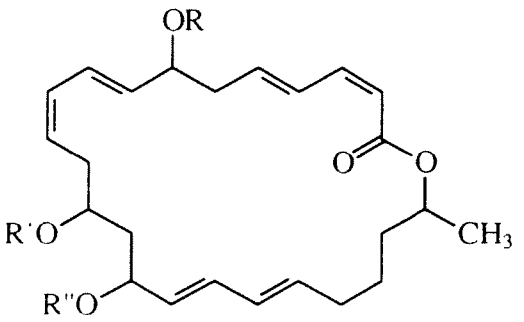

7 Macrolactin A R = R' = R" = H
8 Macrolactin B R = glucose R' = R" = H
9 Macrolactin C R = R' = H R" = glucose

10 Macrolactin D R =

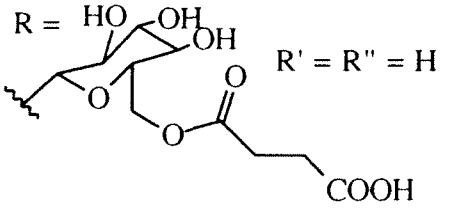

R' = R" = H

The bacterium *Alteromonas haloplanktis* isolated from a deep-sea mud off the coast of Aomari Prefecture, Japan, produced the new siderophore bisucaberin (**11**) only when grown in a marine medium supplemented with sardine and cuttlefish powders.[17] Bisucaberin sensitizes tumour cells to macrophage-mediated cytolysis making it a good candidate for use as an antitumour agent. Although the bacterium *Alteromonas haloplanktis* was isolated from a deep-

sea mud collected at about 3,300 meters in depth, this organism grew well at atmospheric pressure even though bacteria obtained from deep-sea sediments often require increased pressures for growth.

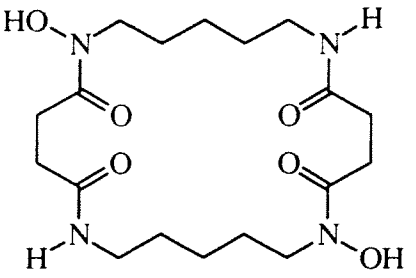

11 Bisucaberin

True marine bacteria might be expected to produce metabolites that are not observed from terrestrial microorganisms. It is interesting to note that some compounds isolated from near-shore actinomycetes have similar structures to metabolites produced by terrestrial actinomycetes. The first antibiotics to be isolated from a marine actinomycete were the aplasmomycins A (**12**), B (**13**) and C (**14**), produced by cultures of *Streptomyces griseus*, a common soil species, which had been isolated from shallow sea mud collected in Sagami Bay, Japan.[18] Antibiotic production was only observed in a medium that contained seawater salt concentrations suggesting that the bacterium had adapted to its marine environment. The aplasmomycins show in vitro antibacterial activity against the Gram-positive *Staphylococcus aureus, Bacillus subtilus, B. anthracis* and *Corynebacterium smegmatis*. The aplasmomycins are similar to the boron containing antibiotic, boromycin (**15**), first isolated from *Streptomyces antibioticus* obtained from an African soil sample.[19] A second bacterium, *Streptomyces tenjimariensis*, isolated from sea mud in Sagami Bay, Japan, produced the antibiotics istamycins A (**16**) and B (**17**) when grown in a marine medium.[20] The istamycins inhibit the growth of both Gram-positive and Gram-negative bacteria including many that are resistant to known aminoglycoside antibiotics. These two antibiotics are similar to fortimicin A (**18**),[21] isolated from a culture of *Micromonospora* species MK-70

obtained from a soil sample, and sporaricin A (**19**),[22] isolated from cultures of the soil organism *Saccharopolyspora hirsuta* subsp. *kobensis*.

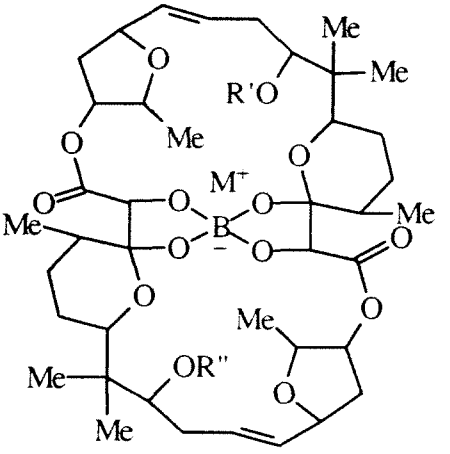

12 Aplasmomycin A R' = R'' = H
13 Aplasmomycin B R' = H R'' = Ac
14 Aplasmomycin C R' = Ac R'' = H

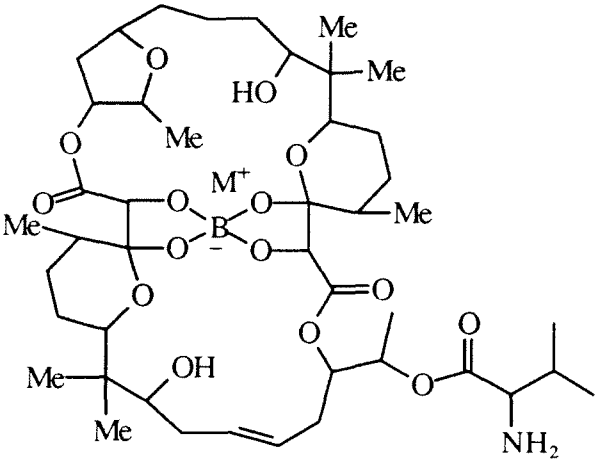

15 Boromycin

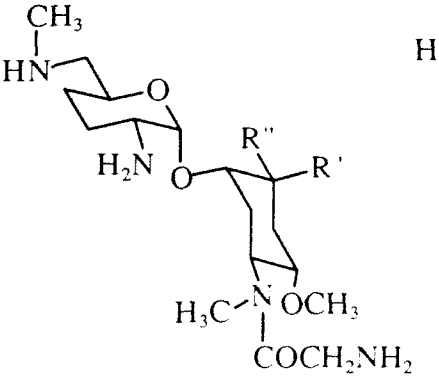

16 Istamycin A R' = NH_2 R'' = H
17 Istamycin B R' = H R'' = NH_2

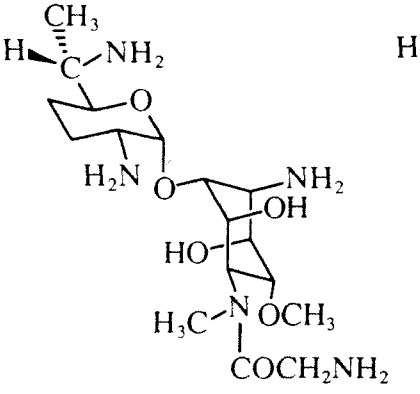

18 Fortimicin A

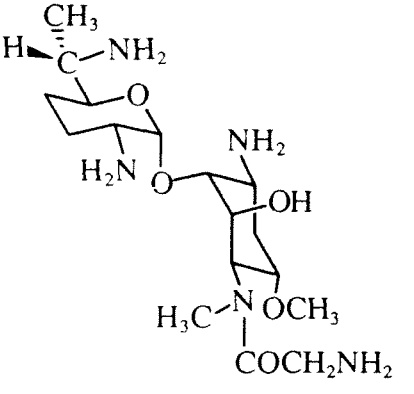

19 Sporaricin

An unidentified estuarine actinomycete isolated from a sediment sample produced two antibacterial metabolites, marinone (**20**) and debromomarinone (**21**), when cultured in a marine

medium.[23] Their structures are related to naphterpin (**22**)[24] and naphthgeranine A (**23**)[25] both isolated from cultures of terrestrial actinomycetes.

From the examples presented it is clear that marine bacteria have the biosynthetic capabilities to produce biologically active compounds with novel structures.

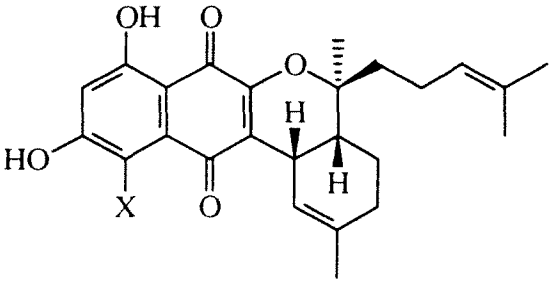

20 Marinone X = Br
21 Debromomarinone X = H

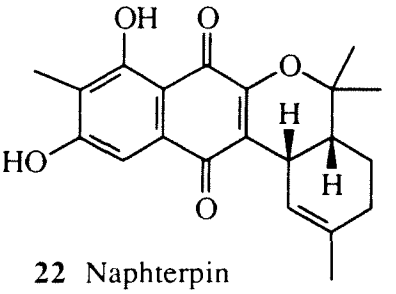

22 Naphterpin

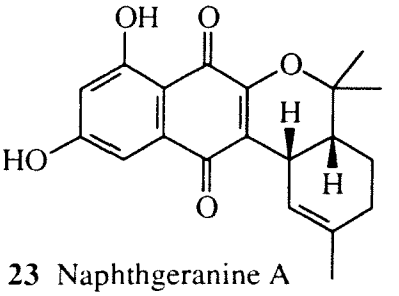

23 Naphthgeranine A

1.6. Symbiotic Marine Bacteria

Marine natural products chemists are also interested in marine bacteria from an ecological perspective. It has been postulated that many secondary metabolites isolated from marine invertebrates are actually being produced by symbiotic marine microorganisms since the metabolites produced are present in low concentrations and their occurrences violate taxonomic guidelines. Several recent examples have demonstrated the origin of some potent marine toxins. Neosurugatoxin (**24**), originally isolated from the digestive gland of the Japanese ivory shell, *Babylonia japonica*, the causative agent of food poisoning associated with the shellfish, has

been shown to be produced by a symbiotic coryneform bacterium isolated from the digestive gland of the organism.[26] Tetrodotoxin (**25**), the potent neurotoxin associated with pufferfish poisoning, is produced by cultures of a *Pseudomonas* sp. isolated from the skin of the pufferfish, *Fugu poecilonotus*.[27]

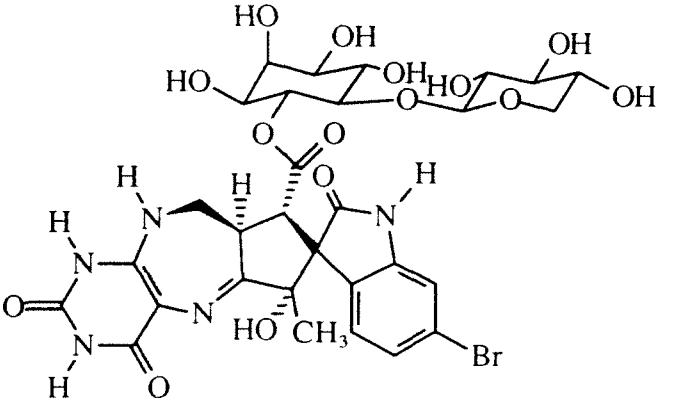

24 Neosurugatoxin

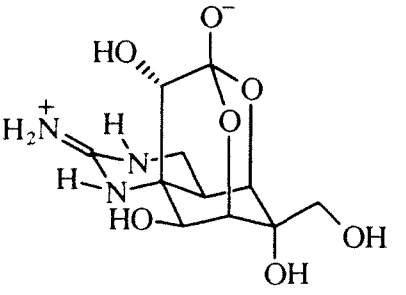

25 Tetrodotoxin

A study by Gil-Turnes et al. has demonstrated that marine bacteria may benefit their host. In this study the eggs of the estuarine shrimp, *Palaemon macrodactylus*, were found to be resistant to infection by the fungus *Lagenidium callinectes* when associated with the epibiotic bacterium *Alteromonas* sp.. When the bacteria were removed by antibiotic treatment the shrimp eggs were rapidly infested by pathogenic fungi, especially *Lagenidium callinectes*. Fermentation of an *Alteromonas* sp., obtained from the shrimp eggs, led to the isolation of the antifungal compound istatin (**26**).[28]

The first chemical evidence of a microbial symbiont associated with a sponge was provided when Stierle et al. isolated the diketopiperazines **27**-**29**, originally ascribed to the sponge *Tedania ignis*, from cultures of the symbiont marine *Micrococcus* sp..[29] Other chemical evidence for a symbiotic relationship was provided when cultures of the bacterium *Vibrio* sp.,

isolated from the sponge *Dysidea* sp., was found to produce the brominated phenyl ether **30**.[30] The tetrabrominated phenyl ether **30** was also isolated from the sponge *Dysidea* sp..

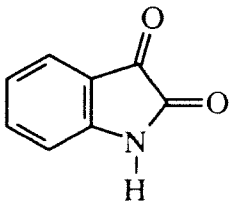

26 Istatin

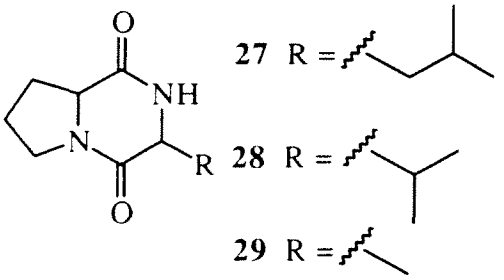

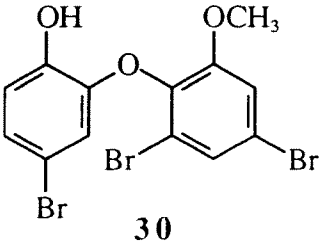

30

As part of a study to examine symbiotic bacteria associated with marine invertebrates a new tetracyclic alkaloid, alteramide (**31**), was isolated from cultures of the bacterium *Alteromonas* sp. obtained from the sponge *Halichondria okadai*.[31] Alteramide exhibited in vitro cytotoxicity against P388 murine leukemia (IC_{50} = 0.1 μg/mL), L1210 murine lymphoma (IC_{50} = 1.7 μg/mL) and the human epidermoid carcinoma KB cells (IC_{50} = 5.0 μg/mL). The authors did not provide any evidence for the symbiotic relationship between the *Alteromonas* sp. and the sponge *Halichondria okadai*.

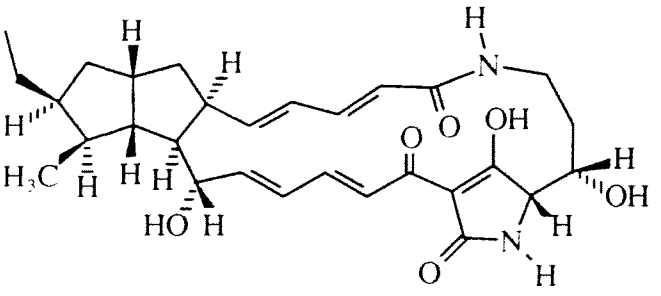

31 Alteramide

2. BACTERIA FROM THE NORTHEASTERN PACIFIC OCEAN

2.1. Research Objectives

The continuing need for new antibiotics and the fact that marine bacteria are capable of producing biologically active natural products, prompted us to investigate bacteria obtained from the northeastern Pacific ocean for the production of novel antibiotics. In collaboration with Dr. M. Kelly, bacteria were isolated from the marine environment and tested for antimicrobial activity. The promising antibiotic-producing organisms were grown in moderate scale culture. The objective of the research presented in this thesis was to isolate, elucidate the structures of, and study the biosynthesis of secondary metabolites produced by selected marine bacteria. Emphasis was placed on isolating compounds exhibiting antibacterial activity against clinically relevant human pathogens and to a lesser extent antitumour agents.

2.2. Isolation of Marine Bacteria[32]

Surface water, sediment, algal and invertebrate samples were collected from coastal marine environments ranging from southern British Columbia to Alaska. Surface water samples were collected in sterile Whirl-Pak bags. The water samples were passed through a 0.22 μm pore size membrane filter to collect any organisms present. The bacteria were cultured by placing the filter on the surface of an agar plate. Sediment samples, collected in sterile disposable plastic syringes by SCUBA or by a bottom-sampling device, were inoculated directly on the surface of the agar medium. Algal and invertebrate samples were collected using SCUBA in sterile Whirl-Pak bags and were inoculated directly to the agar plate. In some cases, the invertebrates were dissected and their intestinal contents were cultured directly on the agar medium.

The samples were inoculated to ten different media selected to represent the environmental conditions of the sample site and to provide a variety of conditions for the isolation of different microbial species. The culture media included: one half and full strength seawater agar, seawater agar plus 1 % peptone and 0.5 % glucose, seawater agar plus 1 % starch, 0.1 % yeast extract and 0.6 % glucose agar, Middlebrook 7H10 agar, Sabourad's agar, MacConkey agar, 5 % sheep blood agar and algal extract agar. Cultures were incubated at 18-22°C and examined for growth after one, two and seven days. Each unique morphological type was isolated by subculturing to a new plate of the same medium. The origins and the medium used for the isolation of antibiotic-producing marine bacteria are shown in Table 1.

Table 1. Origin and isolation media of antibiotic-producing marine bacteria.

Strain No.	Isolation Medium	Source	Location
91D13	algal extract agar	kelp	Georgia Strait
91D48	seawater agar (1/2 strength)	sponge	Georgia Strait
91K17	yeast extract agar	sediment	Georgia Strait
91Z50	yeast extract agar	sediment	Georgia Strait
91K3	blood agar	sediment	Georgia Strait
91BB19	seawater agar (full strength)	tunicate	Prince of Wales Is.
91W51	Middlebrook agar	algae	Georgia Strait
91QQ48	starch agar	tunicate	Prince of Wales Is.
91V47	blood agar	abalone	Georgia Strait
91-157	blood agar	water	Georgia Strait
91-162	blood agar	geoduck	Vancouver Is.

2.3. Screening Bacterial Isolates for Antibiotic Production[32]

Dr. Kelly has screened five hundred bacterial isolates for antibiotic production against ten test organisms chosen to provide a general assessment of activity and to indicate activity against organisms that are resistant to currently available antibiotics. *Candida albicans*, *Escherichia coli*, *Staphylococcus aureus* and *Staphylococcus saprophyticus* were chosen for the general assessment of activity. Organisms resistant to currently available antibiotics include: *Enterobacter cloacae*, *Enterococcus faecalis*, methicillin-resistant *Staphylococcus aureus*, *Pseudomonas aeruginosa*, *Pseudomonas cepacia* and *Xanthomonas maltophilia*. From the five hundred isolates screened eleven were found to produce antibiotics (Table 1, Table 2).

The spectrum of activity was quite different between the various marine bacteria. *Bacillus megaterium* 91K17 shows selective activity against the Gram-positive bacteria *Staphylococcus aureus* and *Enterococcus faecalis*. The isolate 91D13, identified as *Alcaligenes faecalis*, shows selective activity against the Gram-positive *S. aureus* and the Gram-negative *Pseudomonas aeruginosa* and *P. cepacia*. In addition, several bacterial isolates showed a broad spectrum of activity against several Gram-positive and Gram-negative bacteria, these include: *Serratia odorifera* 91-157, *S. odorifera* 91-162 and *P. chlororaphis* 91W51.

2.4. Identification of Antibiotic-Producing Strains[32]

The antibiotic-producing organisms were identified by traditional biochemical methods and by analysis of cellular fatty acid patterns. Traditional methods involve examining each isolate by the Gram-stain and by a series of growth dependent assays. The isolates were grown on a variety of media which include selective and differential media. A selective medium contains compounds that are added to selectively inhibit the growth of certain microorganisms. Differential media contain an indicator, usually a dye, to allow the identification of various reactions. These tests measure the presence or absence of enzymes involved in catabolism of the

substrate or substrates added to the differential medium. The MIDI automated Microbial Identification System (MIS) is a fully automated, commercially available (available from MIDI, Newark, Delaware), computerized, high-resolution gas chromatography system that analyzes the whole cell short-chain fatty acid methyl esters.

Table 2. Antibiotic activity of marine bacteria isolated form the northeastern Pacific ocean.

Bacterium (Strain No.) / Target Organism	*Staphylococcus aureus*	*Staphylococcus aureus* (MRSA)	*Staphylococcus saprophyticus*	*Enterococcus faecalis*	*Escherichia coli*	*Enterobacter cloacae*	*Pseudomonas aeruginosa*	*Pseudomonas cepacia*	*Xanthomonas maltophilia*	*Candida albicans*
Alcaligenes faecalis (91D13)	+	-	-	-	-	-	+	+	-	-
Alcaligenes faecalis (91D48)	+	+	+	+	-	-	+	-	-	-
Bacillus megaterium (91K17)	+	-	-	+	-	-	-	-	-	-
Bacillus pumilus (91Z50)	+	+	+	+	-	-	-	-	-	-
Bacillus pumilus (91K3)	+	+	+	+	-	-	-	-	-	-
Enterobacter intermedius (91BB19)	+	+	+	+	+	+	-	-	-	-
Pseudomonas chlororaphis (91W51)	+	+	+	+	+	+	+	+	-	+
Pseudomonas fluorescens (91QQ48)	+	+	+	+	+	+	-	-	-	-
Pseudomonas sp. (91V47)	+	+	+	+	-	-	-	+	-	-
Serratia odorifera (91-157)	+	+	+	+	+	+	+	-	-	-
Serratia odorifera (91-162)	+	+	+	+	+	+	+	-	-	-

2.5. Moderate Scale Culture of Antibiotic-Producing Bacterial Isolates

Antibiotic-producing organisms were grown in liquid culture or on solid agar. Bacterial isolates 91-157, 91Z50 and 91V47 were grown at room temperature in liquid shake cultures in one liter Erlenmeyer flasks containing 500 mL of tryptic soy broth supplemented with 1 % sodium chloride (except for 91-157 which was grown without a salt supplement). The cultures were harvested by centrifugation or filtration four of five days after inoculation. Isolate 91QQ48 was cultured as lawns on solid media containing tryptic soy broth, 1 % agar and 1 % sodium chloride at room temperature for three days after inoculation. The isolation of secondary metabolites from these organisms will be discussed elsewhere in this thesis.

3. SECONDARY METABOLITES FROM *SERRATIA ODORIFERA* (91-157)

3.1. Introduction

In January 1990 two bacterial isolates exhibiting broad-spectrum antibiotic activity, 91-157 and 91-162, were obtained from Dr. M. Kelly. Bacterial isolate 91-157, obtained from a surface water sample taken near a Chinook salmon (*Oncorhyncus tshawytscha*) farm in Georgia Strait, British Columbia, was identified as the Gram-negative *Serratia odorifera*. The marine isolate 91-162, obtained from the intestines of a geoduck collected off the coast of Vancouver Island, British Columbia, was also identified as the bacterium *Serratia odorifera*. Preliminary studies showed that liquid shake cultures of 91-157 gave an extract that exhibited antimicrobial activity against *Staphylococcus aureus*, *Bacillus subtilus*, the yeast *Candida albicans* and the fungus *Rhizoctonia solani*. Therefore, *Serratia odorifera* 91-157 was grown in moderate scale liquid culture in order to produce sufficient quantities of the antimicrobial metabolites for structure elucidation.

3.2. Results and Discussion

Serratia odorifera 91-157 was grown in liquid shake culture at room temperature in one liter Erlenmeyer flasks containing 500 mL of 1/2 strength tryptic soy broth medium. The cultures were harvested by centrifugation four days after inoculation and the supernatant was passed over a column of XAD-4 resin packed in water. Elution of the adsorbed organic material from the XAD-4 resin with methanol followed by evaporation of the methanol eluate in vacuo gave a crude residue which exhibited broad-spectrum antimicrobial activity. The crude residue was partitioned between water and ethyl acetate and the antimicrobial activity was found to reside in the organic extract. Fractionation of the ethyl acetate extract by Sephadex LH-20 chromatography

(eluent: 3:1 methanol/dichloromethane) yielded six fractions. The second fraction exhibited weak antibacterial activity and the sixth fraction showed activity against the fungus *Rhizoctonia solani*. Purification of the sixth fraction by reversed-phase HPLC (eluent: 4:6 water/methanol) led to the isolation of the known antimicrobial compound aminopyrrolonitrin (**32**) (1 mg).[33] The second fraction from the LH-20 column was applied to a reversed-phase Sep-Pak and eluted with a step gradient from 7:3 water/methanol to 100 % methanol. A late eluting fraction resulted in the isolation of the known antibacterial compound prodigiosin (**33**) (2 mg).[34] Prodigiosin was also isolated from the cell pellet after centrifugation. Purification of the first fraction from the Sep-Pak by reversed-phase HPLC (eluent: 4:6 water/methanol) gave pure oncorhyncolide (**34**) (16 mg).[35]

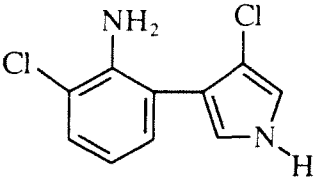

32 Aminopyrrolonitrin

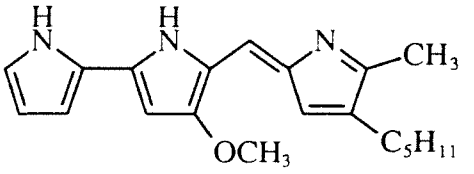

33 Prodigiosin

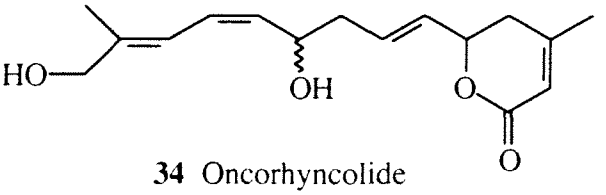

34 Oncorhyncolide

3.2.1. Oncorhyncolide

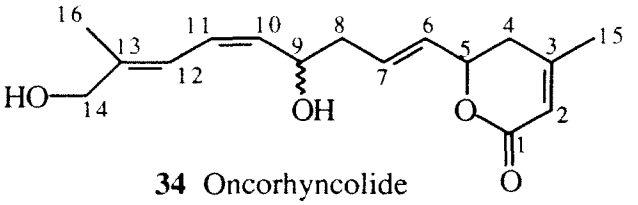

34 Oncorhyncolide

Oncorhyncolide (**34**) was isolated as an unstable, optically active ($[\alpha]_D$ -36°; c 3.1 (MeOH)), colourless oil. The HREIMS spectrum showed a molecular ion at m/z 278.1527 corresponding to a molecular formula of $C_{16}H_{22}O_4$ (ΔM +0.9 mmu). The molecular formula indicated that **34** had 6 sites of unsaturation. The IR spectrum contained a hydroxyl stretch at 3400 cm^{-1} and an adsorption band at 1690 cm^{-1} indicated the molecule contained an α,β-unsaturated carbonyl. Table 3 provides a summary of the NMR data acquired for compound **34**.*

The ^1H NMR spectrum (Figure 1) of oncorhyncolide (**34**) contains two allylic methyl singlets at δ 1.14 (H15) and δ 1.58 (H16) which integrated for three protons each. Analysis of the COSY spectrum (Figure 2) identified a twenty proton fragment, **A**. A methylene pair at δ 1.36 (H4) and δ1.54 (H4') was coupled to a multiplet, integrating for one proton, at δ 4.24 (H5). The chemical shift of the methine proton (H5) suggested that the proton was attached to a carbon atom bearing an oxygen atom. Long-range coupling was also observed between the H4/H4' methylene pair and the broad singlet at δ 1.14 (H15) which integrated for three protons. Allylic coupling was observed between the H15 methyl singlet and the proton at δ 5.56 (H2), a broad singlet which integrated for one proton. In addition, the signal at δ 4.24 (H5) showed a COSY correlation to an olefinic doublet of doublets at δ 5.33 (H6) which in turn was coupled to a multiplet integrating for one proton at δ 5.67 (H7). A methylene pair at δ 2.17 (H8) and δ 2.29 (H8') was coupled to the H7 multiplet (δ 5.67) and to a methine proton, a multiplet, at

* Appendix 1 provides a simple non-quantum mechanical description of the NOE difference, COSY, HMQC and HMBC experiments.

δ 4.53 (H9). Again the downfield chemical shift of this methine proton suggested that it was attached to a carbon atom bearing an oxygen atom.

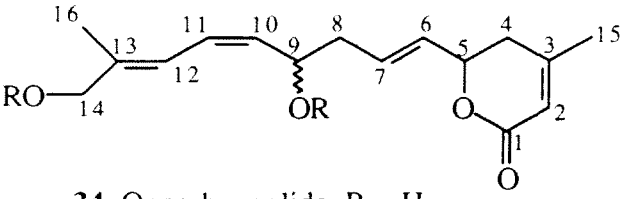

34 Oncorhyncolide R = H
35 Diacetate R = Ac

Table 3. ^{1}H and ^{13}C NMR data for oncorhyncolide (**34**) and oncorhyncolide diacetate **35**.

	Oncorhyncolide **34**		Diacetate **35**				
C#	^{1}H[a]	COSY	^{1}H[a]	COSY	NOEs[b]	^{13}C[c]	HMBC[d]
1	—	—	—			163.5	H2
2	5.56,bs	H4',H15	5.62,bs	H4',H15	H15	117.3	H15
3	—	—	—			154.9	H15
4	1.36,dd(17.7,4.4)	H4',H5',H15	1.41,dd(17.6,4.2,)	H4',H5		34.4	H2,H15
4'	1.54,ddm(17.7,10.3,≈1)	H4,H5,H15	1.63,m	H4,H5			
5	4.24m	H4,H4',H6	4.27,m	H4,H4',H6	H6,H7	76.3	
6	5.33,dd(15.5,5.9,)	H5,H7	5.39,dd(15.5,6.0)	H5,H7		131.5	H6,H7
7	5.67,m	H6,H8,H8'	5.52,m	H6,H8,H8'	H5	128.3	
8	2.17,m	H7,H8',H9	2.21,m	H7,H8',H9		37.9	H10
8'	2.29,m	H7,H8,H9	2.30,m	H7,H8,H9			
9	4.53,m	H8,H8',H10	5.93,m	H8,H8',H10	H12	69.0	H11
10	5.37,t(8.8)	H9,H11	5.37,t(10.0)	H9,H11		128.9	
11	6.23,dt(11.4,≈1)	H10,H12	6.21,dt(11.5,<1)	H10,H12	H10,H16	127.3	
12	6.41,dm(11.6,≈1)	H11,H14,H16	6.54,dm(11.5,≈1)	H11,H14,H14' H16	H9,H14 H14'	121.7	H10,H14 H16
13	—	—	—			136.0	H11,H14 H16
14	3.90,d(5.9)	H12,14-OH,H16	4.35,d(13.5)	H12,H14',H16		68.8	H12,H16
14'	—	—	4.44,d(13.5)	H12,H14,H16			
15	1.14,bs	H2,H4,H4'	1.19,bs	H2	H2	22.1	H2
16	1.58,bs	H12,H14	1.46,bs	H12,H14,H14'	H11	14.0	H12,H14
14-OH	1.87,t(6.0)	H14					
OAc	—	—	1.68,s; 1.75,s			20.4 20.7 169.5 169.8	

[a] Recorded in benzene-d_6 at 400 MHz. Chemical shifts in ppm relative to internal TMS.
[b] Proton in carbon # column irradiated.
[c] Recorded in benzene-d_6 at 125 MHz. Chemical shifts in ppm relative to solvent.
[d] Carbons in the carbon # column are correlated to the listed proton resonances.

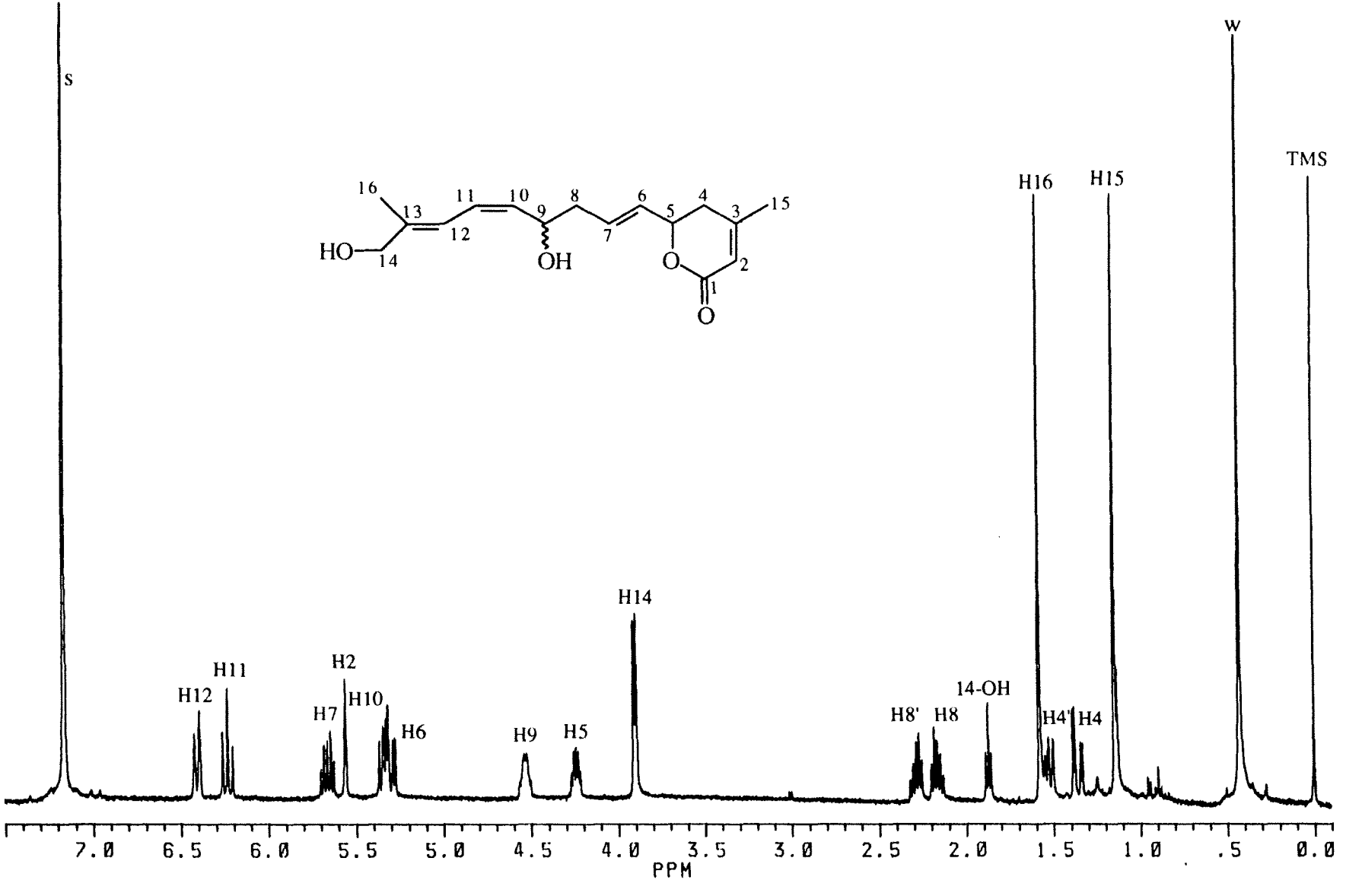

Figure 1. ^{1}H NMR spectrum of oncorhyncolide (**34**) (400 MHz, C_6D_6).

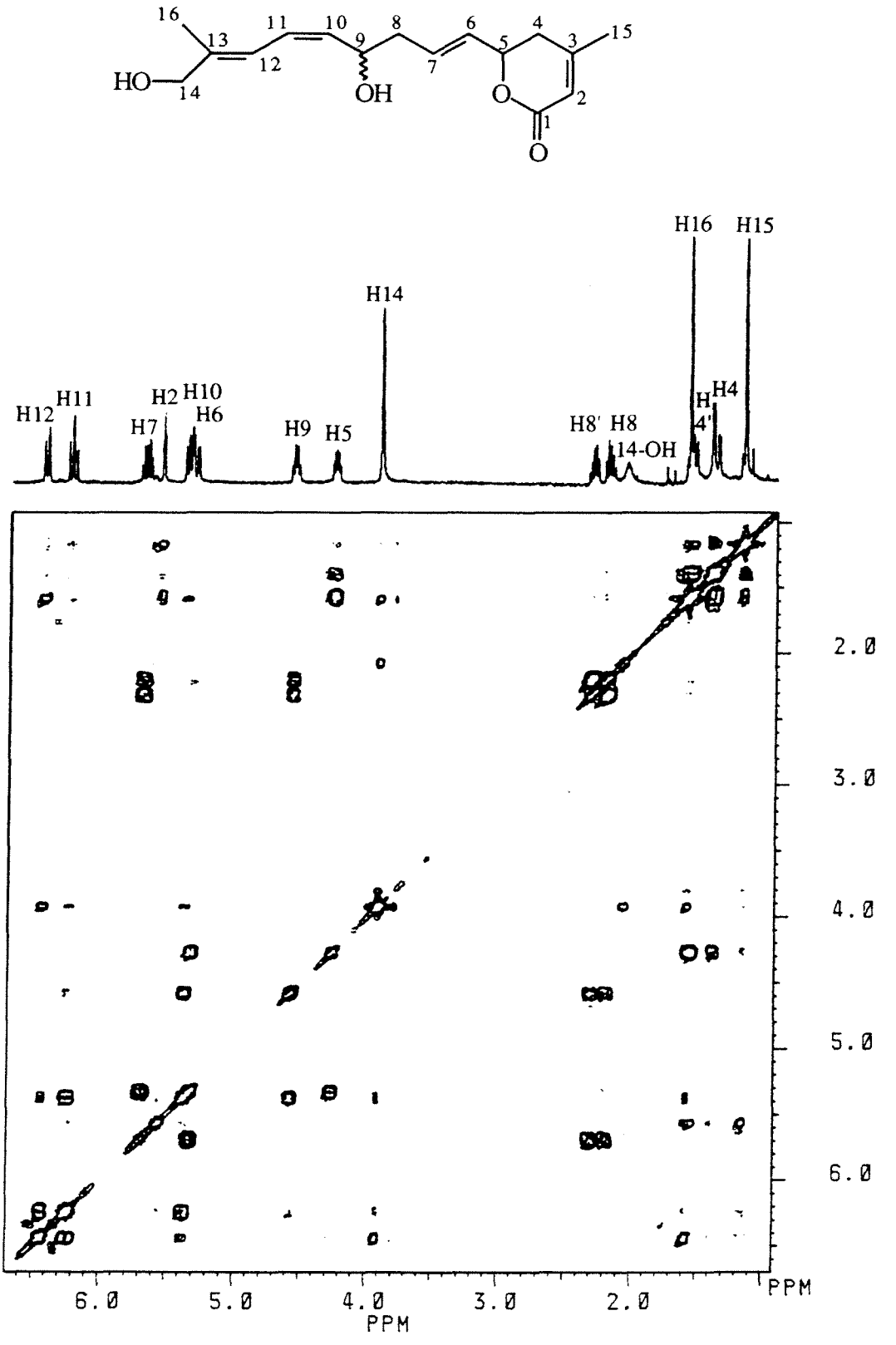

Figure 2. ^{1}H COSY spectrum of oncorhyncolide (**34**) (400 MHz, C_6D_6).

The methine proton at δ 4.53 (H9) showed a COSY correlation to an olefinic proton at δ 5.37 (H10) which in turn was coupled to another olefinic proton at δ 6.23 (H11). A COSY correlation was observed between the H11 olefinic proton and a doublet of multiplets at δ 6.41 (H12). Allylic coupling was also observed between the H12 proton and the methylene doublet at δ 3.90 (H14). The chemical shift of the methylene protons suggested that they were attached to a carbon atom bearing an oxygen atom. In addition, the H14 methylene protons showed a cross peak to the broad methyl singlet at δ 1.58 (H16).

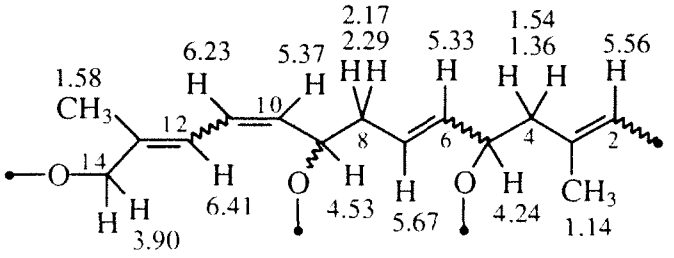

A

Oncorhyncolide was found to be quite unstable and readily decomposed. Acetylation of compound **34** resulted in the somewhat more stable oncorhyncolide diacetate **35**. The greater stability of **35** made it the compound of choice for structure determination by spectroscopic analysis.

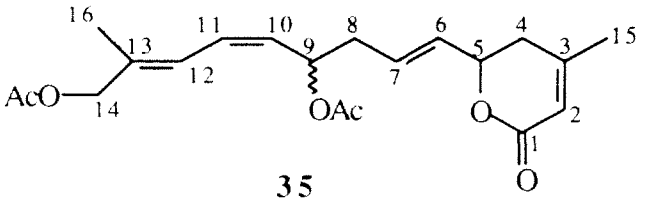

35

Oncorhyncolide diacetate **35** was isolated as a colourless oil. An intense molecular ion at m/z 380 ($C_{20}H_{26}O_6$ + NH_4) in the LRDCIMS was observed. The HREIMS did not show a

molecular ion but had a strong peak at m/z 302.1519 ($C_{18}H_{22}O_4$ ΔM +0.1 mmu) corresponding to the loss of AcOH from the molecular ion. The molecular formula indicated that **35** had eight sites of unsaturation. A summary of the NMR data for **35** is provided in Table 3.

The ^{13}C NMR spectrum of **35** (Figure 3) showed twenty well resolved carbon resonances, including three carbonyl and two quaternary carbons. An APT experiment (Figure 3) indicated four methyl, three methylene and eight methine groups accounting for the twenty-six protons in the molecule. The deshielded carbon at δ 163.5 in the ^{13}C NMR spectrum was assigned to an α,β-unsaturated ester carbonyl. A carbonyl stretching band at 1728 cm^{-1} in the IR spectrum of **35** was consistent with ester functionalities. The resonances at δ 20.4 (CH_3), δ 20.7 (CH_3), δ 169.5 (C) and δ 169.8 (C) in the ^{13}C spectrum and, δ 1.68 (s, 3H) and δ 1.75 (s, 3H) in the ^1H spectrum indicated two acetate groups. Resonances at δ 69.0 and δ 76.3 in the ^{13}C NMR spectrum suggested that the methine carbons were attached to oxygen and the resonance at δ 68.8 was indicative of a methylene carbon connected to an oxygen atom. ^{13}C NMR resonances at δ 117.3 (CH), 121.7 (CH), 127.3 (CH), 128.3 (CH), 128.9 (CH), 131.5 (CH), 136.0 (C) and 154.9 (C) were assigned to four olefinic functionalities. The four olefins and the three carbonyl functionalities accounted for seven of the eight sites of unsaturation in the molecule; the remaining site of unsaturation had to be a ring.

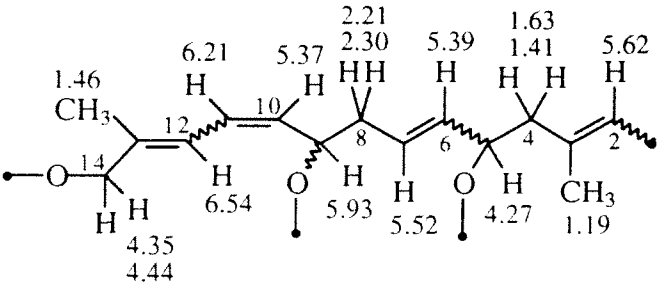

B

The ^1H NMR spectrum of the diacetate **35** (Figure 4) was well dispersed. Analysis of the COSY (Figure 5) and HMQC (Figure 6) data collected on the diacetate **35** identified the twenty proton fifteen carbon fragment **B** corresponding to fragment **A** identified in oncorhyncolide.

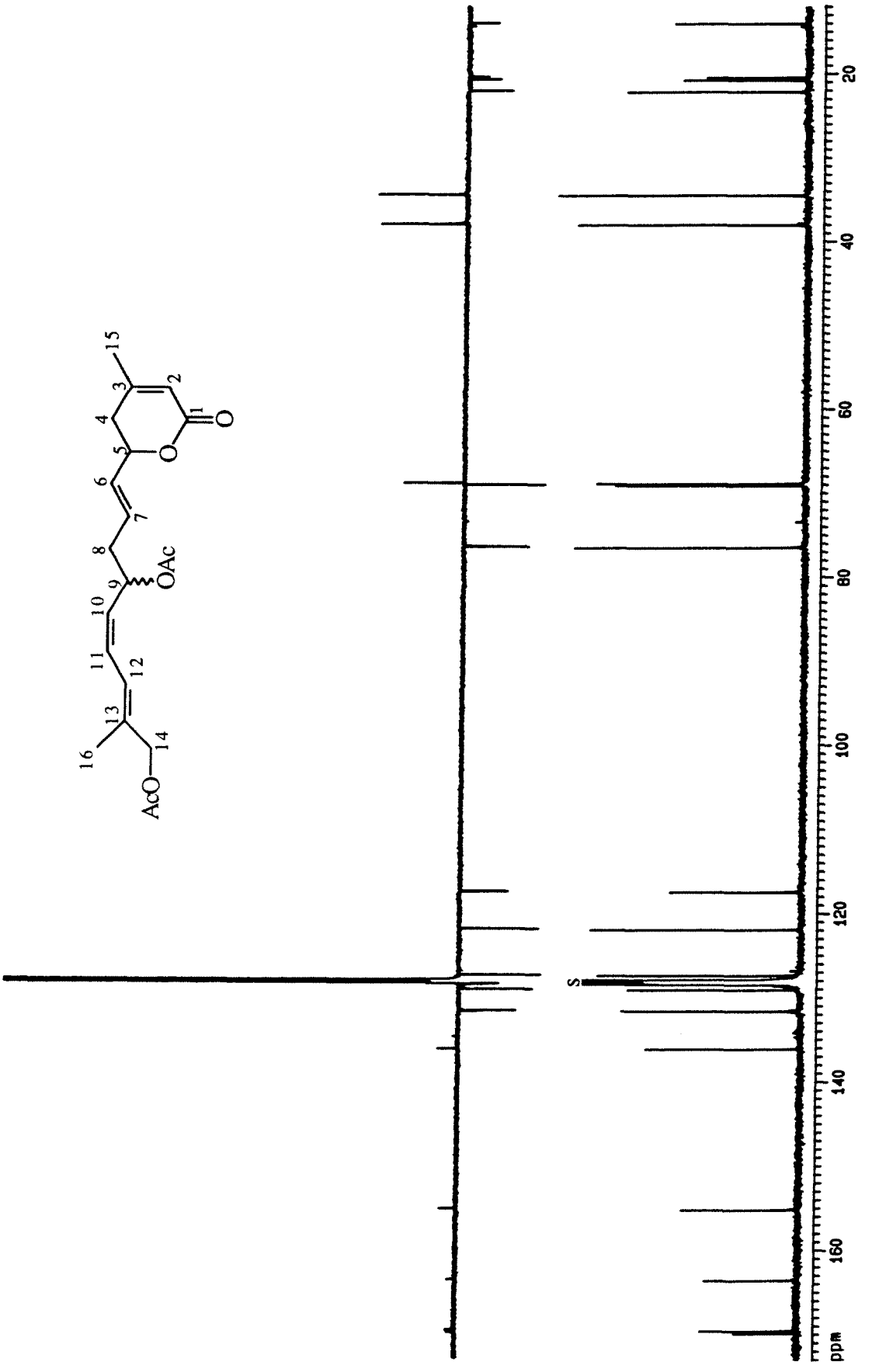

Figure 3. ^{13}C and APT NMR spectra of oncorhyncolide diacetate **35** (125 MHz, C_6D_6).

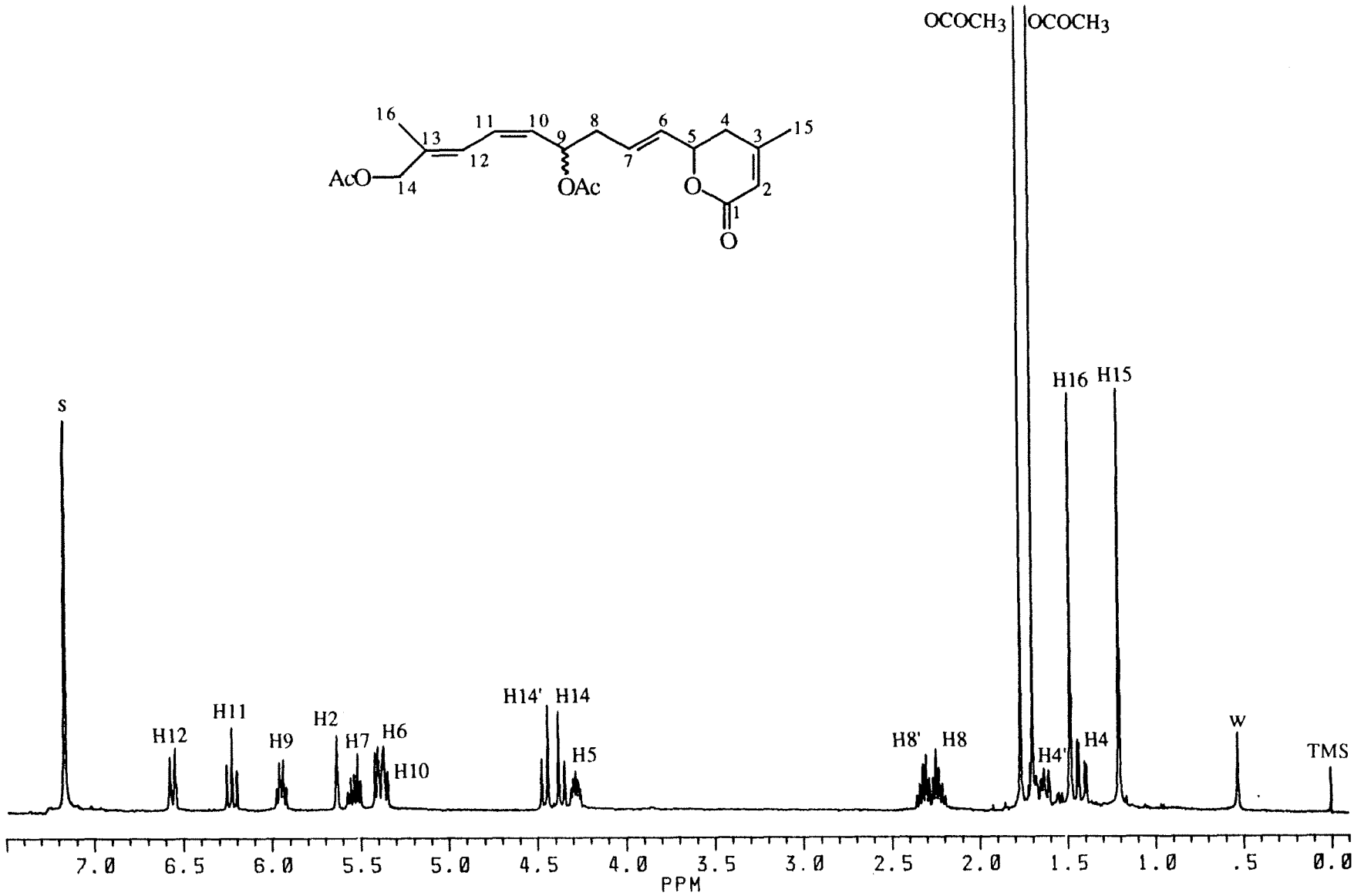

Figure 4. ^{1}H NMR spectrum of oncorhyncolide diacetate **35** (400 MHz, C_6D_6).

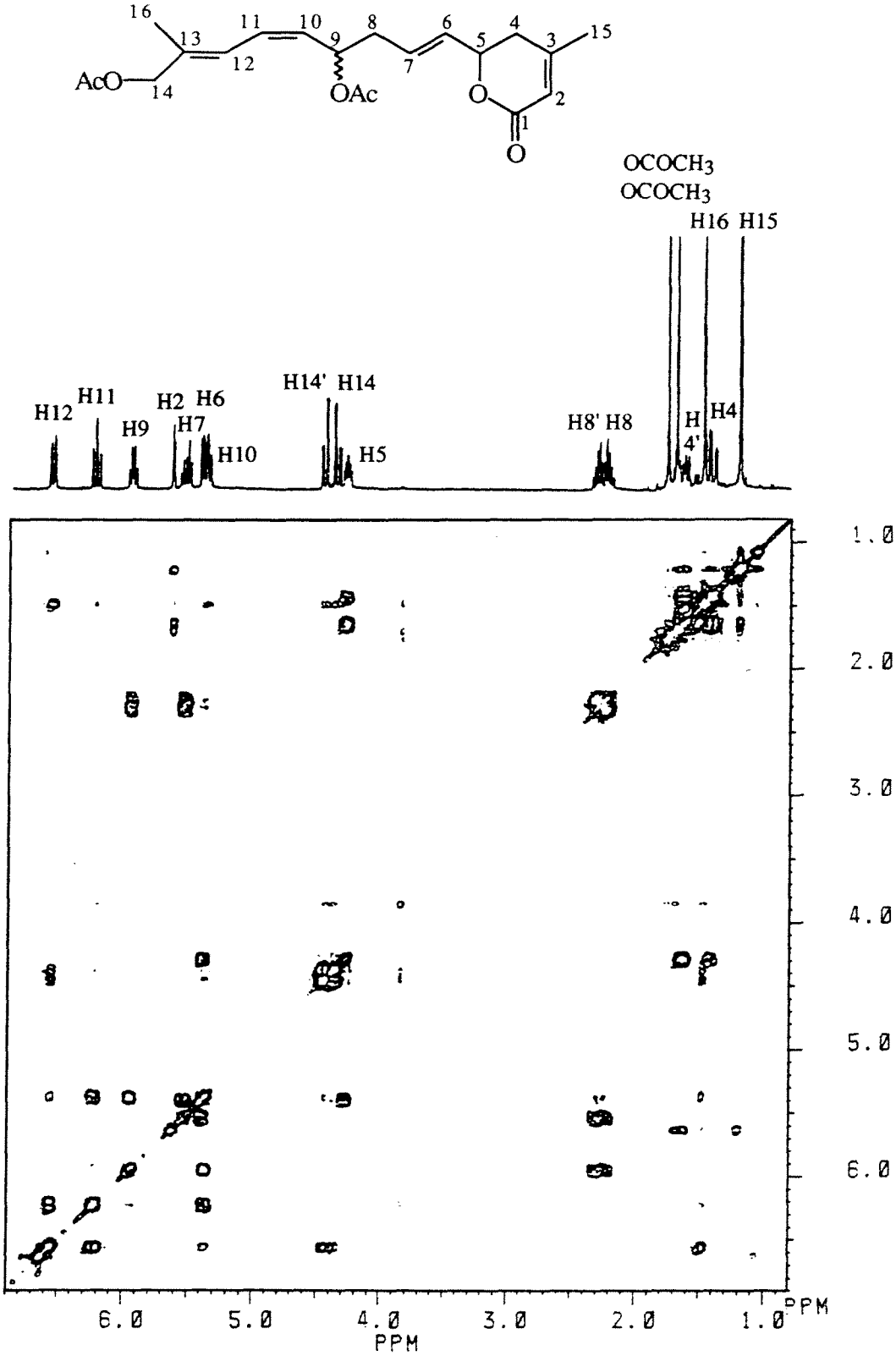

Figure 5. ^{1}H COSY spectrum of oncorhyncolide diacetate **35** (400 MHz, C_6D_6).

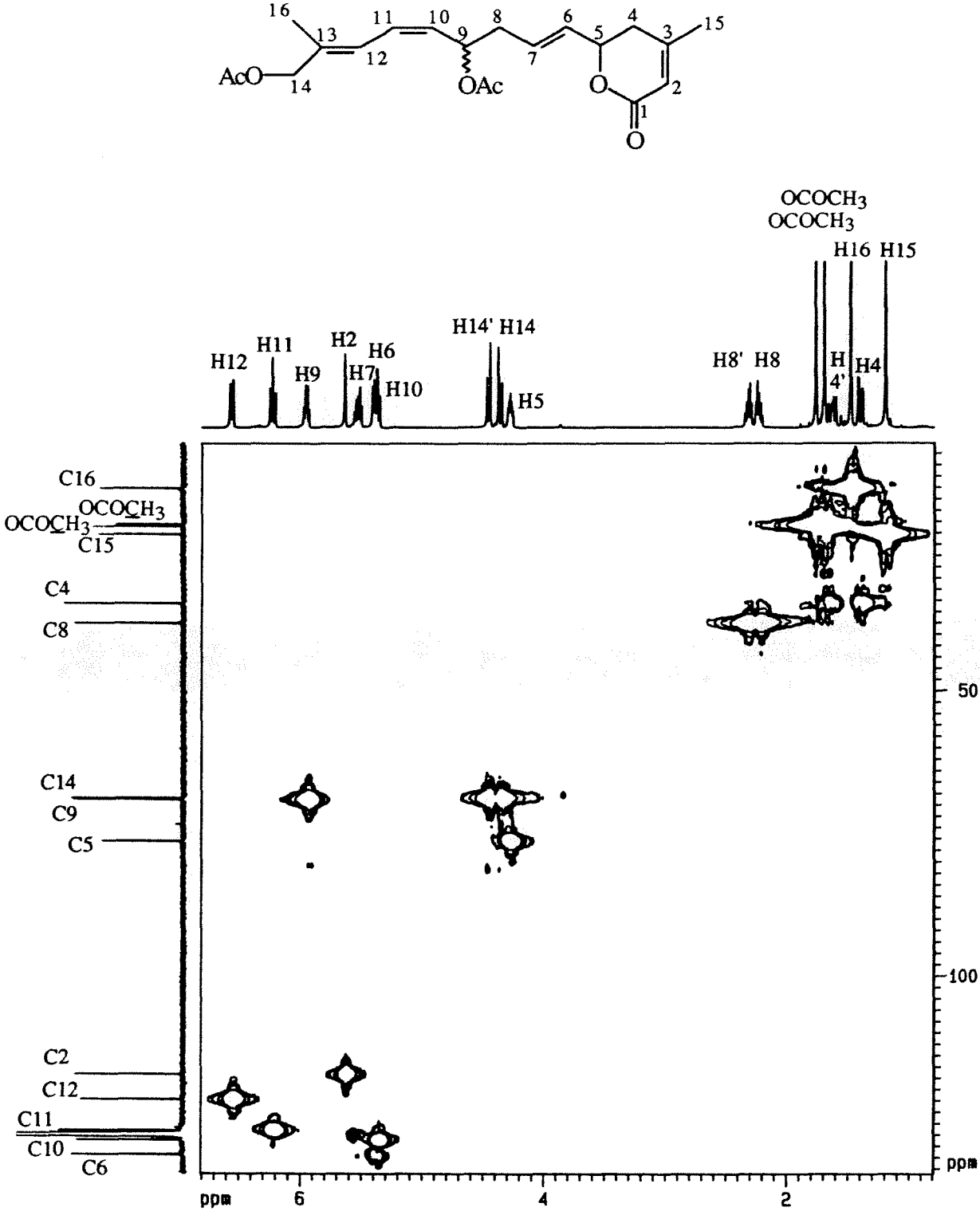

Figure 6. HMQC spectrum of oncorhyncolide diacetate **35** (500 MHz ^{1}H NMR, C_6D_6).

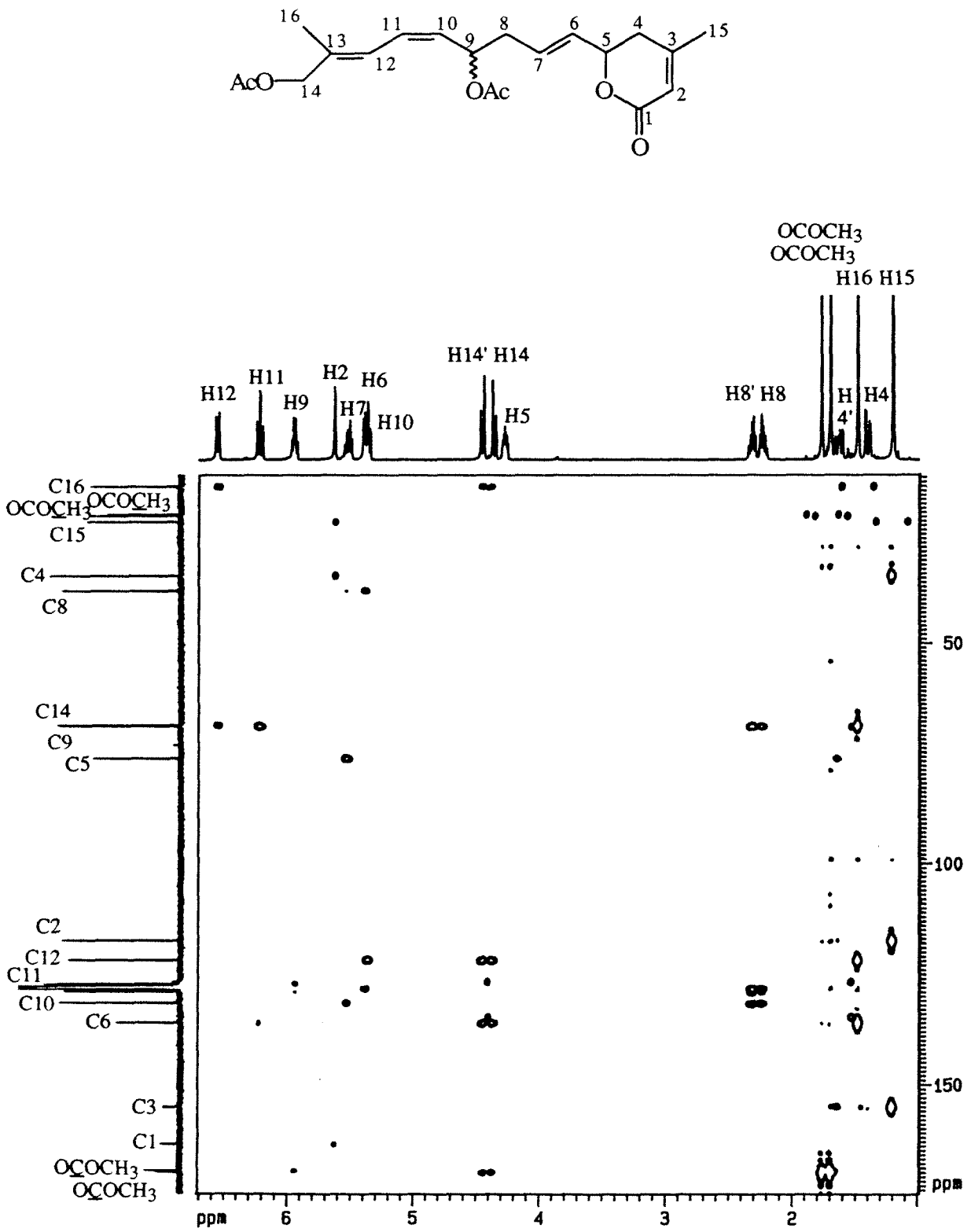

Figure 7. HMBC spectrum of oncorhyncolide diacetate **35** (500 MHz ^{1}H NMR, C_6D_6).

Double resonance experiments on H5, H7, H9 and H11 failed to provide chemical shifts and coupling constants of the two overlapping protons H6 and H10. These were assigned from NOE difference experiments by irradiating H5 and H11.

The ^{1}H NMR spectrum of **35** showed obvious acetylation shifts in the terminal H14/H14' methylene protons, (**34**: δ 3.90 (2H); **35**: δ 4.35 and δ 4.44), and in the H9 methine proton, (**34**: δ 4.53; **35**: δ5.93), resulting from the conversion of **34** to **35**. As mentioned earlier, the IR spectrum of oncorhyncolide contained an O-H stretch at 3400 cm^{-1}. This O-H stretch was not observed in the IR spectrum of the diacetate **35** indicating the loss of hydroxyl functionality in **35**. An HMBC correlation from the methine proton at δ 5.62 (H2) to the carbon at δ 163.5 placed the unsaturated ester carbon at C1 (Figure 8). Since C9 and C14 contained the acetate groups, the ester carbonyl (C1) had to be attached to the oxygen atom on C5 to generate the lactone and to account for the unassigned site of unsaturation. Additional correlations in the HMBC spectrum (Figure 7) were completely consistent with the proposed connectivity.

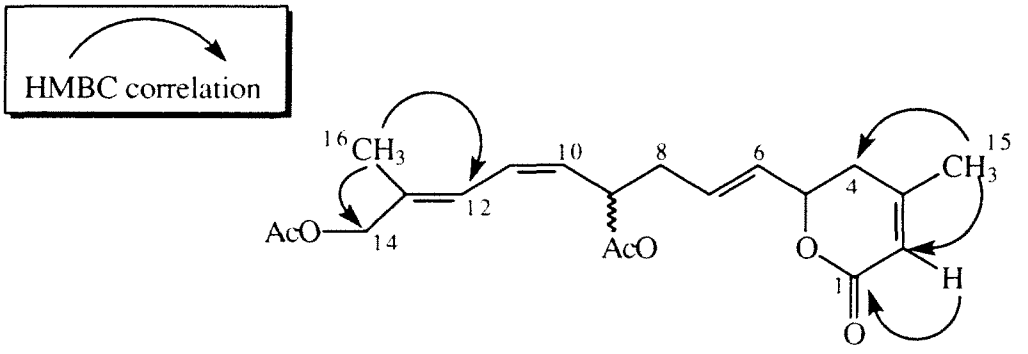

Figure 8. Selected HMBC correlations for oncorhyncolide diacetate **35**.

The configurations of the olefinic functionalities in **35** were determined by NOE experiments (Figure 9). Irradiation of the signal for H7 resulted in enhancement of the H5

methine signal suggesting an E configuration for the $\Delta^{6,7}$ double bond. The signals for H10 and H16 were enhanced by irradiation of the H11 resonance, demonstrating a Z configuration for the $\Delta^{10,11}$ olefin. The $\Delta^{12,13}$ double bond was assigned to an E configuration since irradiation of the H12 signal induced NOEs in the H14 and H14' resonances. The relative configurations at C5 and C9 were not determined.

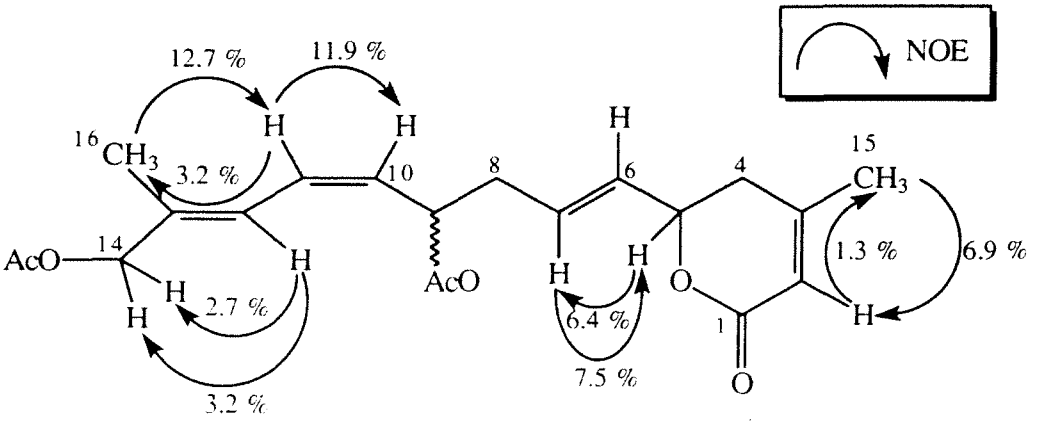

Figure 9. Results from selected NOE difference experiments on oncorhyncolide diacetate **35**.

3.2.2. Known Compounds from *Serratia odorifera*

Two known antimicrobial compounds, aminopyrrolonitrin (**32**) and prodigiosin (**33**) were also isolated from the ethyl acetate extract of a *Serratia odorifera* culture. Aminopyrrolonitrin was isolated as a yellow oil. Its structure was determined by comparison of its ^{1}H and ^{13}C NMR data (see experimental) with published results.[33] A molecular ion in the HREIMS at m/z 226.0067 confirmed the molecular formula $C_{10}H_8Cl_2N_2$ (ΔM +0.3 mmu).

The antibiotic aminopyrrolonitrin was first isolated from cultures of the soil bacterium *Pseudomonas aureofaciens*.[33a] It has also been isolated from cultures of *Pseudomonas cepacia* obtained from apple leaves.[33c] Biosynthetic studies[33b,36] have shown that pyrrolonitrin

(**36**), a compound related to aminopyrrolonitrin, is derived from tryptophan. It has been proposed that aminopyrrolonitrin is an intermediate in the biosynthesis of pyrrolonitrin.[33b,36]

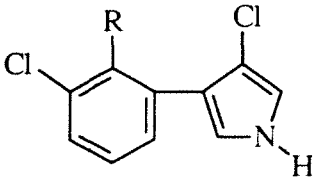

32 Aminopyrrolonitrin R = NH_2
36 Pyrrolonitrin R = NO_2

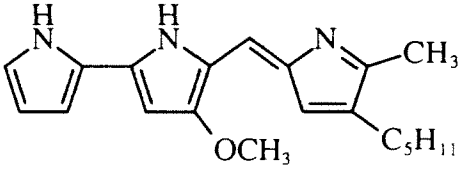

33 Prodigiosin

Prodigiosin, isolated as a red oil, was identified by comparing its MS and ^1H NMR data to literature values.[34p] A molecular ion in the HREIMS at m/z 323.1995 confirmed the molecular formula $C_{20}H_{25}N_3O$ (ΔM -0.2 mmu).

Prodigiosin (**33**) is the characteristic red pigment of the bacterium *Serratia marscens*.[34a] Its chemical structure was not deduced until 1960.[34k] The production of prodigiosin or of prodigiosin-like pigments is a common characteristic of bacteria in the genus *Serratia*. Bacteria belonging to other genera may also produce prodigiosin pigments.[37]

3.3. Conclusion

A culture of the bacterium *Serratia odorifera* (91-157) isolated from a surface water sample taken near a Chinook salmon (*Oncorhyncus tshawytscha*) farm in Georgia Strait, British Columbia, produced the new compound oncorhyncolide (**34**). Oncorhyncolide has a unique structure that is apparently not related to other known microbial metabolites isolated from terrestrial sources. It is interesting to note that the okadaic acid ester **37**, isolated from cultures of the dinoflagellate *Prorocentrum concavum*,[38] contains a seven-carbon ester fragment that

resembles the methyl branched diene system in oncorhyncolide (C1-C14, C16). The isolation of oncorhyncolide provides further evidence that bacteria isolated from the marine environment have the ability to produce unique metabolites.

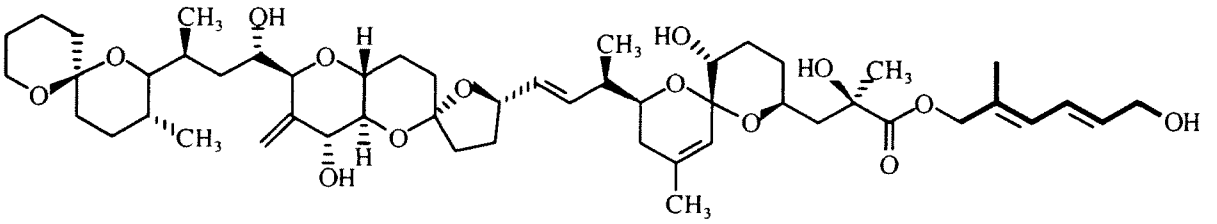

37

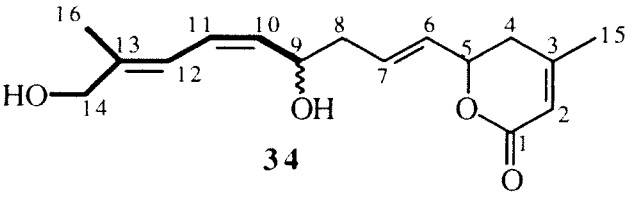

34

4. BIOSYNTHESIS OF ONCORHYNCOLIDE

4.1. Biogenesis

Although oncorhyncolide has a relatively simple structure its biogenetic origin is not immediately obvious. Several pathways may be proposed which include using exclusively acetate as the precursor, or a mixed biogenesis using acetate plus methionine or proprionate, or acetate and a five carbon unit derived from leucine, mevalonate, or valine. Three alternative biogenetic origins (**A**, **B**, **C**) that seemed reasonable possibilities at the outset of this study are given in Figure 10.*

The most straightforward possibility involves a linear heptaketide initiated with an acetate starter unit at C1/C2 as depicted in **A**. Two additional methyl groups are required at positions C3 and C13 to give the skeleton of oncorhyncolide (**34**). These methyl branches may be introduced from S-adenosylmethionine (SAM) or via propionate. Alternative **A** readily accounts for the formation of **34** but this pathway does not directly generate the correct oxidation patterns at C1, C5 and C9, since oxygen atoms are attached at these positions in oncorhyncolide. In addition, deoxygenation is required at C4 and C8 to form the natural product.

The pathway **B/B'** involves a linear heptaketide with an acetate starter unit at either C14/C13 or C16/C13. This is an attractive pathway since the oxygen atoms at C1, C5 and C9 exist in the precursor and only the carbon at C14 needs a change in oxidation state apart from the standard polyketide synthase (PKS) reduction-dehydration-reduction transformations. In **B** the formation of the C15 and C16 methyl groups may occur via an aldol-like condensation between an acetyl-SEnz group and the carbonyls at the C3 and C13 positions followed by subsequent

---

* Evidence is mounting for a so-called "processive" mode of polyketide biosynthesis in which the oxidation state at the keto group of the β-keto thioester is adjusted before the next carbon extension occurs.[39] Thus the "polyketides" in Figure 10 are formalisms used to illustrate the origin of the atoms in the natural product, and are not true proposed intermediates.

decarboxylation. This is similar to the reactions leading to the formation of an isoprene unit. A similar mechanism for the formation of methyl branches from the C2 of acetate has been previously reported in the biosynthesis of the virginiamycins.[40]

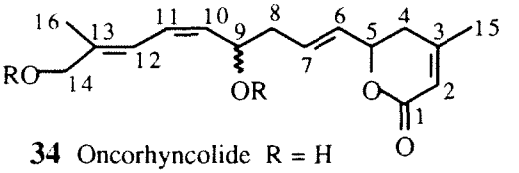

34 Oncorhyncolide R = H
35 Diacetate R = Ac

Polyketide C1/C2 starter unit

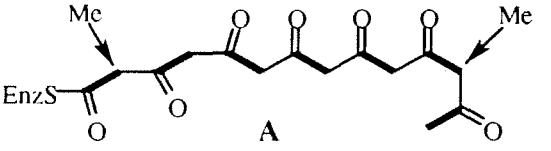

Polyketide C14/C13 or C16/C13 starter unit

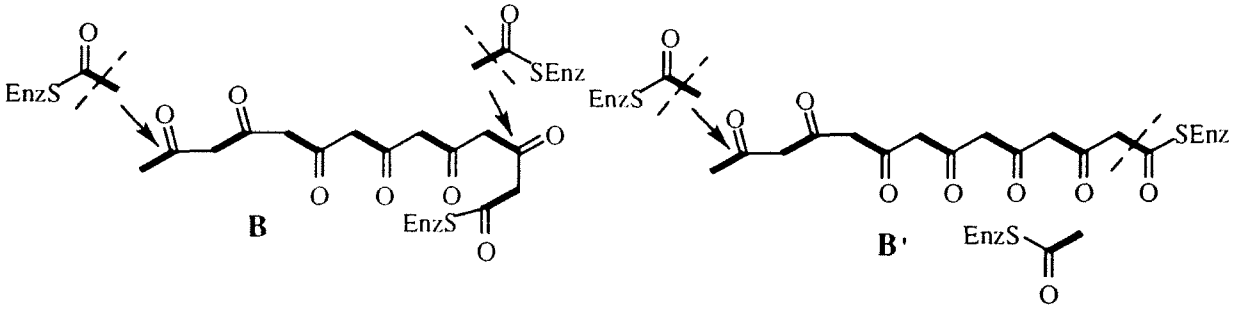

Five carbon starter unit

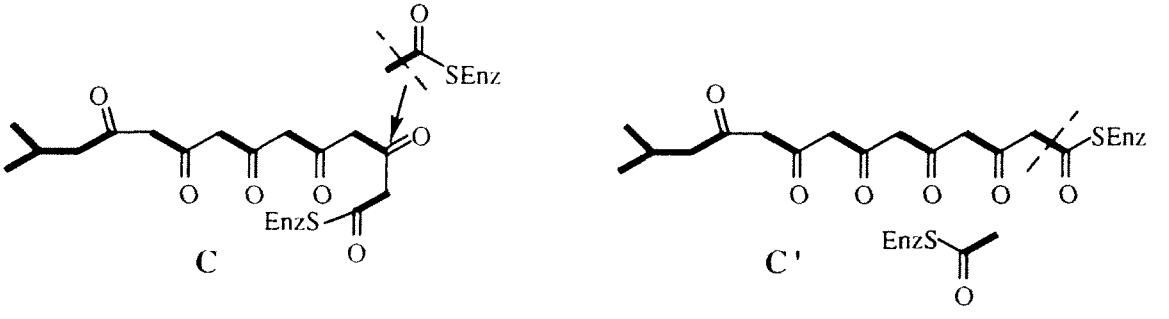

Figure 10. Alternative biogenetic origins for oncorhyncolide (**34**).

Pathway **B'** involves a linear heptaketide with C15 being formed by decarboxylation of the linear chain and C1/C2 is introduced as a separate intact acetate unit. Methylation at C13 is again from the C2 of acetate.

The pathway **C/C'** involves a five carbon starter unit, possibly derived from leucine, mevalonate or valine. The correct pattern of oxygen atoms at C1, C5 and C9 exists and only one methylation is required.

In an attempt to distinguish between the various possible biogenetic origins of oncorhyncolide depicted in Figure 10 a number of stable isotope feeding experiments were proposed. A feeding experiment using [1-^{13}C]sodium acetate would distinguish between the polyketide pathway **A** and pathways **B/B'** or **C/C'**. Incorporation of [2-^{13}C]sodium acetate into oncorhyncolide should provide complementary results to the [1-^{13}C]acetate experiment. If the biogenetic origin of oncorhyncolide is from either pathway **B/B'** or **C/C'** this experiment may determine the origin of the C15 and C16 methyl branches. The origin of these methyl branches may also be probed by feeding ^{13}C labelled sodium propionate or methionine. The use of [1,2-$^{13}C_2$]sodium acetate will show intact acetate units. In addition, separate labelling experiments using ^{13}C labelled leucine, mevalonate or valine may provide insight into the five carbon starter unit of pathways **C/C'**.

4.2. Results and Discussion

Liquid shake cultures of *Serratia odorifera* 91-157 (12 x 1 L flasks each containing 500 mL of 1/2 strength tryptic soy broth) were fed [1-^{13}C: 1 g], [2-^{13}C: 0.5 g], [1,2-$^{13}C_2$: 0.25 g] and [2-^{13}C,$^{2}H_3$: 0.5 g] labelled sodium acetate in separate experiments. The labelled precursors were added in two pulses 30 and 50 hours after inoculation and the cultures were harvested by centrifugation after four days. The supernatant was passed over a column of XAD-4 resin and the adsorbed organic material was eluted with methanol. Evaporation of the methanol eluate in vacuo gave a crude residue which was partitioned between water and ethyl acetate. The ethyl

acetate extract was fractionated by Sephadex LH-20. The fraction containing oncorhyncolide was acetylated and purified by radial thin layer chromatography (silica gel) which yielded the pure oncorhyncolide diacetate **35**.

The incorporation of the labelled precursors into oncorhyncolide diacetate **35** was determined by the comparison of the ^{13}C NMR spectrum of the diacetate with that of a natural abundance spectrum run under identical conditions. The specific incorporation, that is the percent enhancement above natural abundance, for a particular carbon equals 1.1 % x ([integrated peak area of the enriched signal - integrated peak area of the natural abundance signal] / integrated peak area of the natural abundance signal).[41] The specific incorporations were normalized to an unenriched carbon and the results are summarized in Table 4.[42]

Table 4. Stable isotope incorporation data for oncorhyncolide diacetate **35**.

C #	δ ^{13}C[a]	Specific Incorporation[b] [1-^{13}C]	[2-^{13}C]	$^{1}J_{C,C}$ Hz	# of ^{2}Hs incorporated [2-$^{13}C/^{2}H_3$]
1	163.5	7.8	0.2	68.3	—
2	117.3	0.6	2.9	68.3	1
3	154.9	9.9	0.1	37.7	—
4	34.4	0.0	3.5	36.9	2
5	76.3	7.9	0.0	49.8	—
6	131.5	0.4	4.0	50.6	1
7	128.3	9.6[c]	0.4[c]	43.1[c]	—
8	37.9	0.0	4.6	43.1[c]	2
9	69.0	11.4	0.3	50.2	—
10	128.9	0.4	4.5	49.8	1
11	127.3	10.0	0.3	56.2	—
12	121.7	0.0	3.6	56.2	1
13	136.0	10.3	0.3	47.4	—
14	68.8	0.6	4.5	47.4	2
15	22.1	0.3	2.6	s	2
16	14.0	0.4	4.1	s	2
Ac	20.4	0.4	0.2		
Ac	20.7	0.3	0.0		
Ac	169.5	-0.3	0.1		
Ac	169.8	0.7	0.0		

[a] Recorded in C_6D_6 at 125 MHz.
[b] Specific Incorporation = 1.1 % x ([integrated peak area of the enriched signal - integrated peak area of the natural abundance signal] / integrated peak area of the natural abundance signal).[41]
[c] Recorded in acetone-d_6 at 125 MHz.

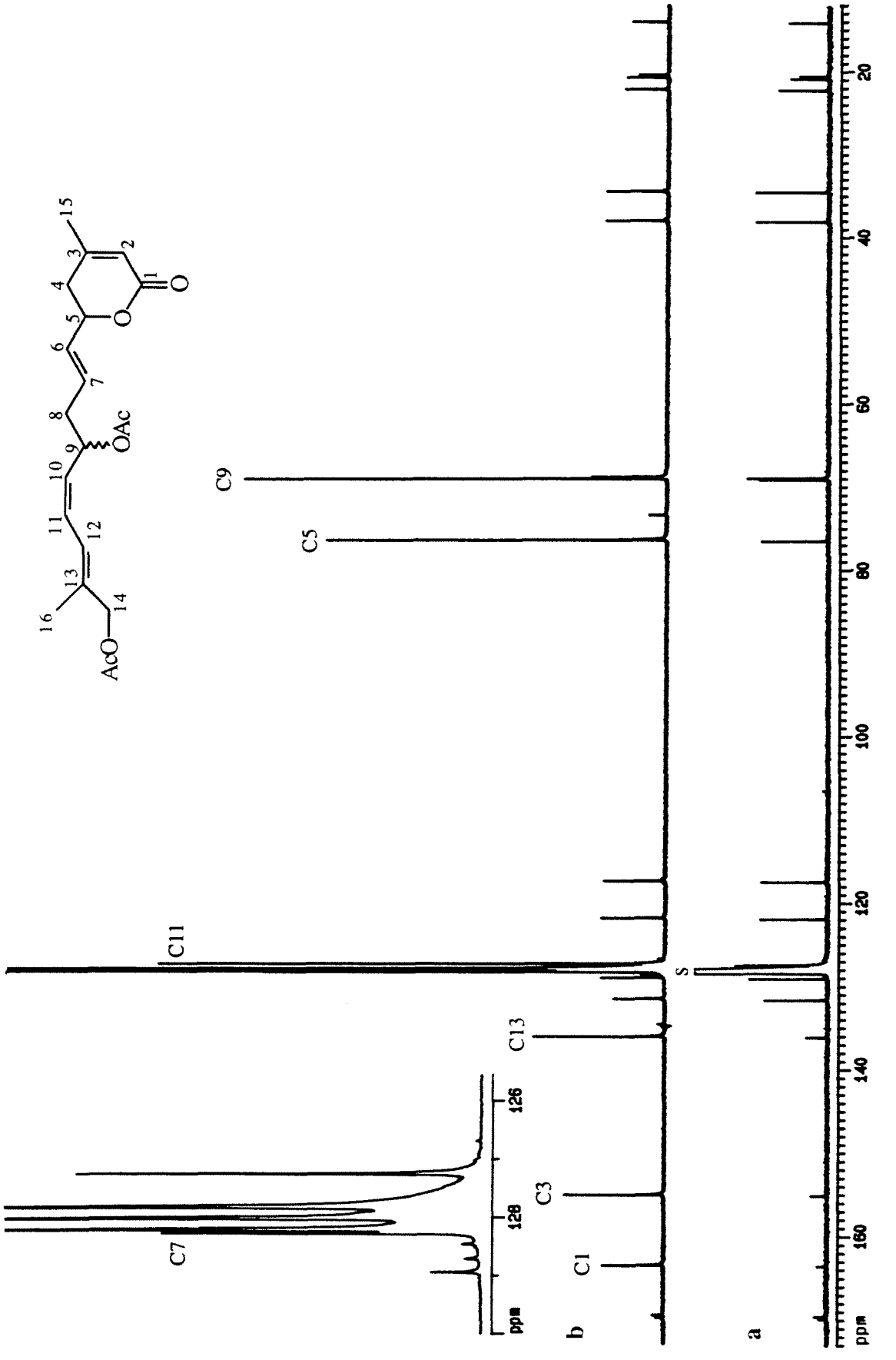

Figure 11. ^{13}C NMR spectra of a) oncorhyncolide diacetate **35** and b) **35** labelled by [1-^{13}C]sodium acetate (125 MHz, C_6D_6).

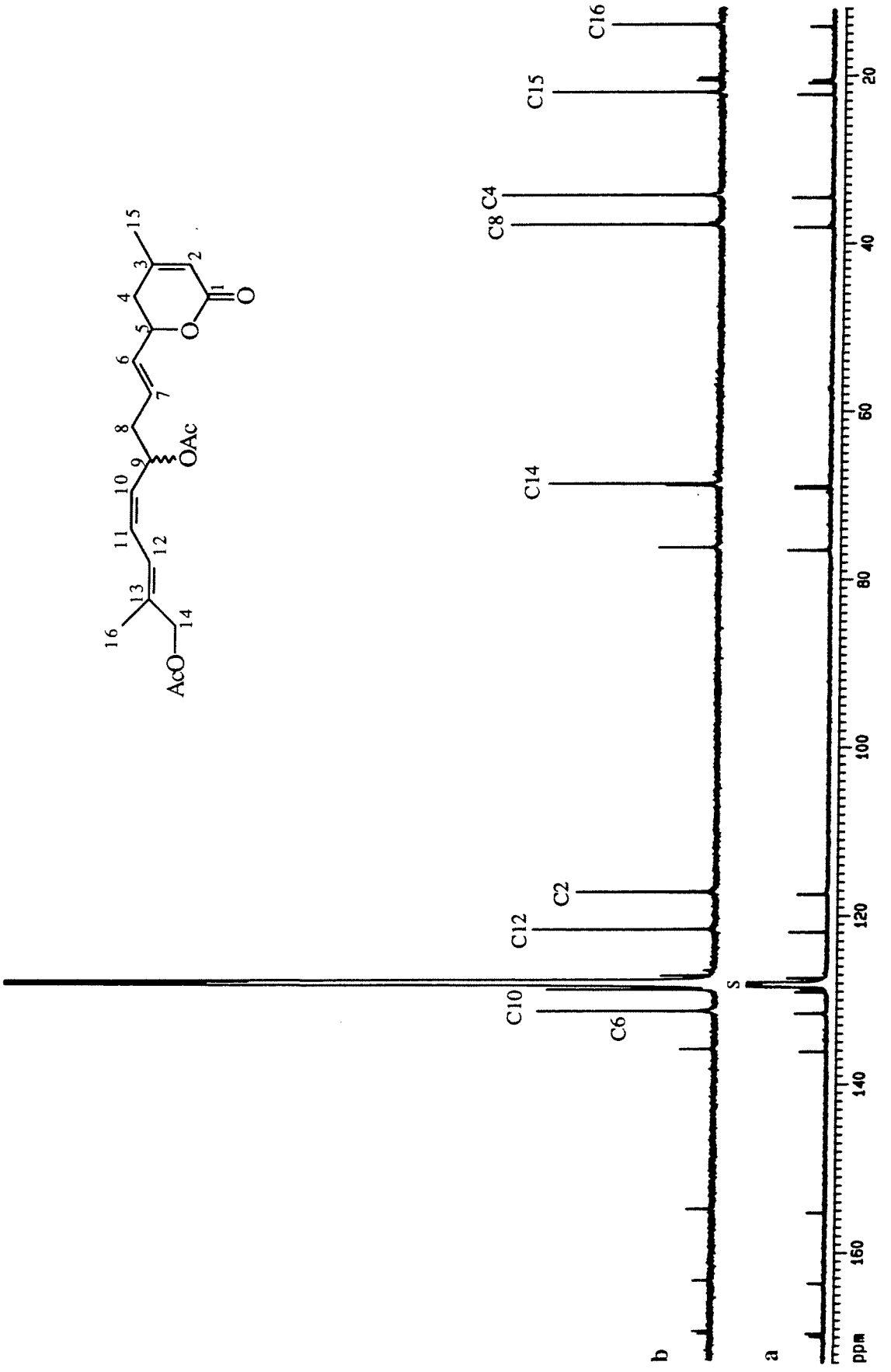

Figure 12. ^{13}C NMR spectra of a) oncorhyncolide diacetate **35** and b) **35** labelled by [2-^{13}C]sodium acetate (125 MHz, C_6D_6).

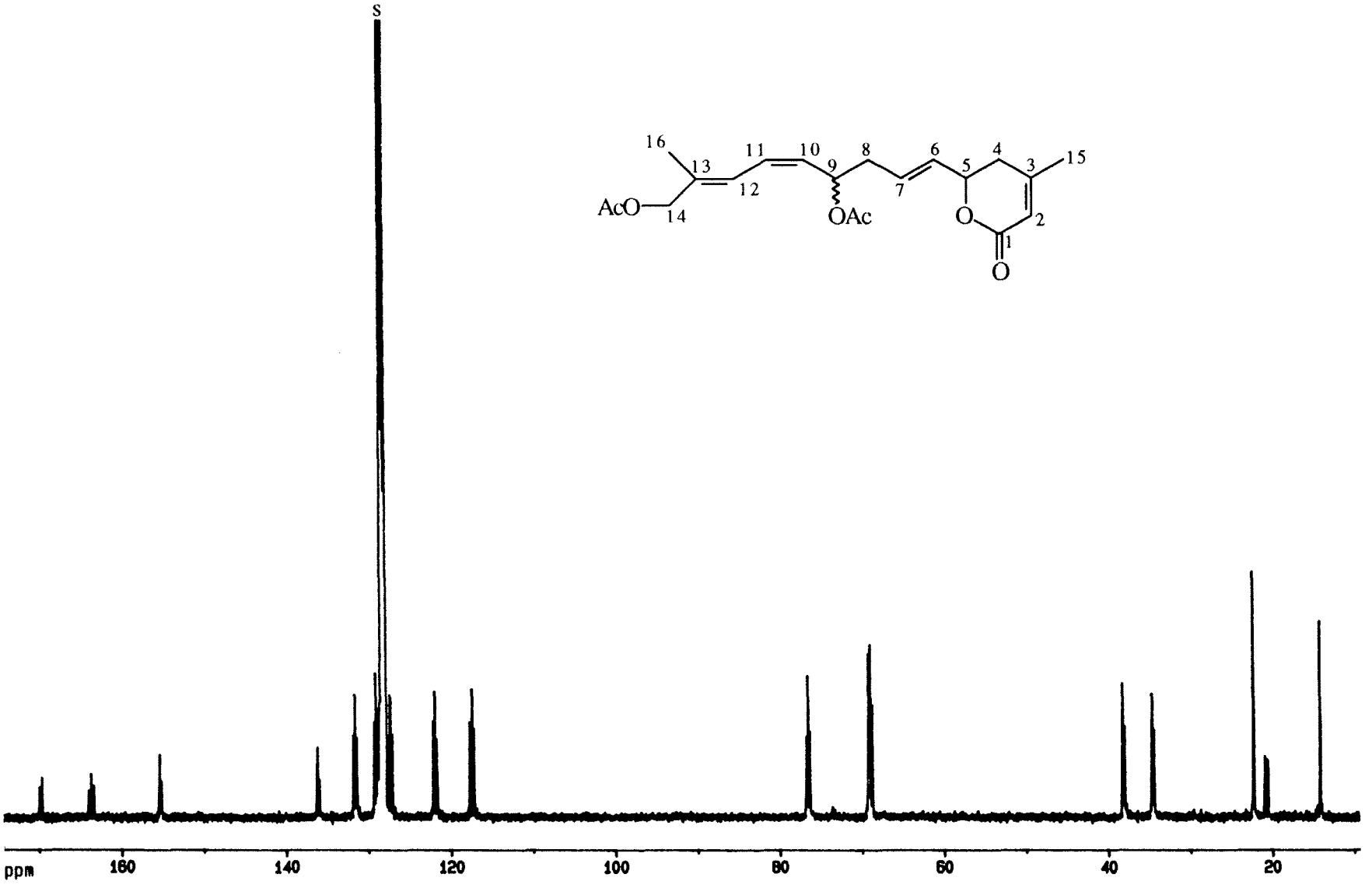

Figure 13. ^{13}C NMR spectrum of oncorhyncolide diacetate **35** labelled by [1,2-$^{13}C_2$]sodium acetate (125 MHz, C_6D_6).

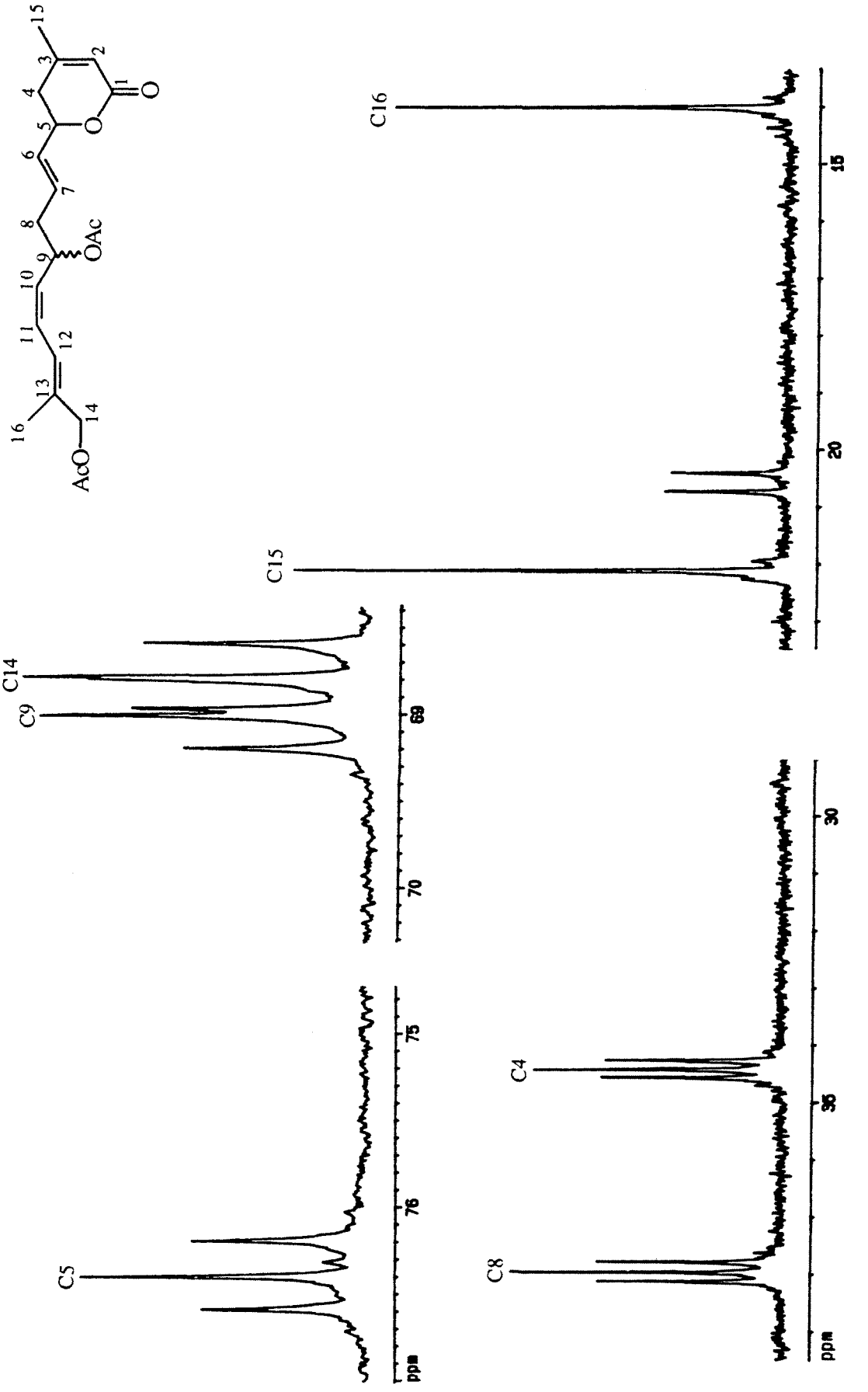

Figure 14. ^{13}C NMR spectrum of oncorhyncolide diacetate **35** labelled by [1,2-$^{13}C_2$]sodium acetate (125 MHz, C_6D_6).

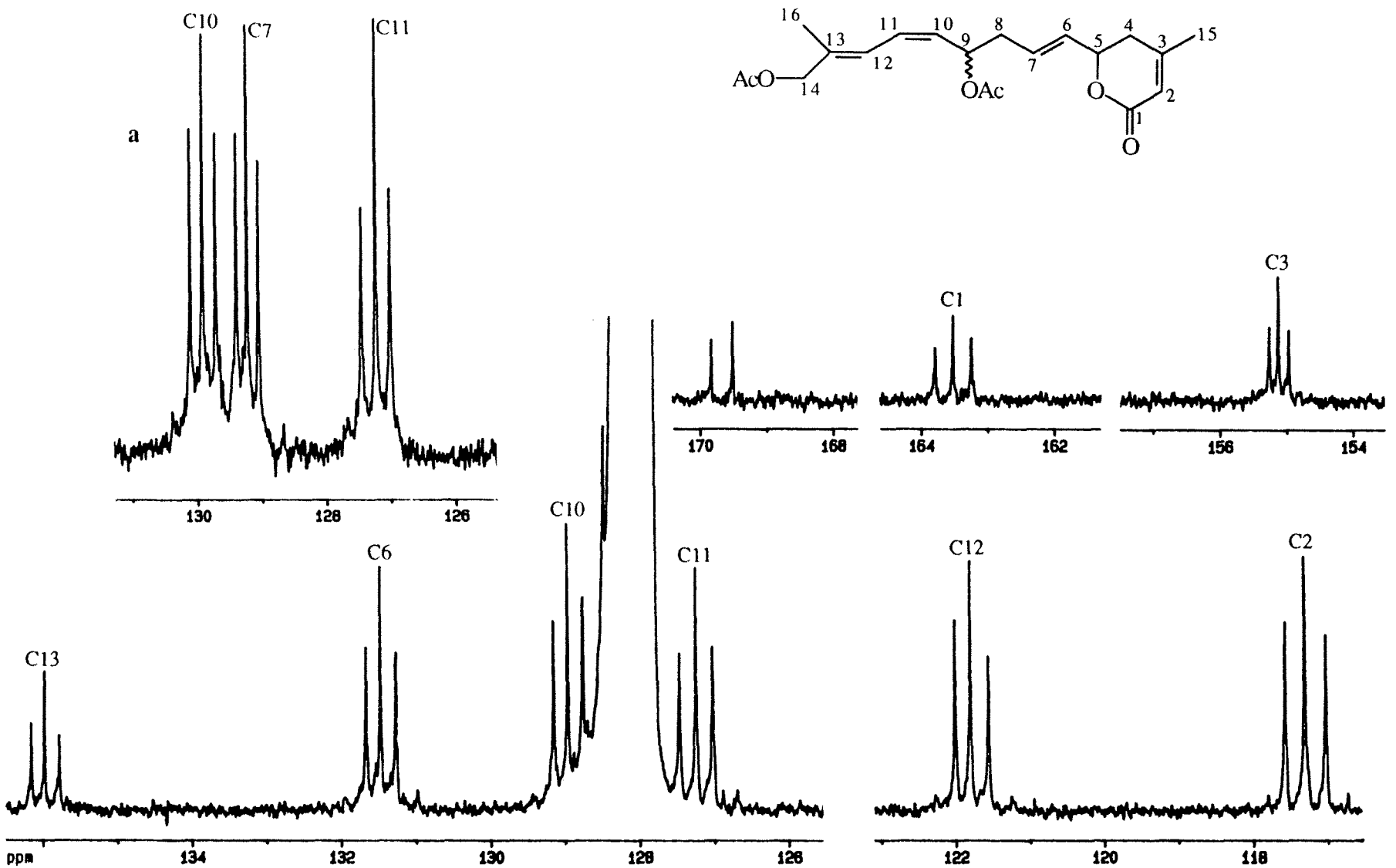

Figure 15. ^{13}C NMR spectrum of oncorhyncolide diacetate **35** labelled by [1,2-$^{13}C_2$]sodium acetate (125 MHz, C_6D_6), a) (125 MHz, acetone-d_6).

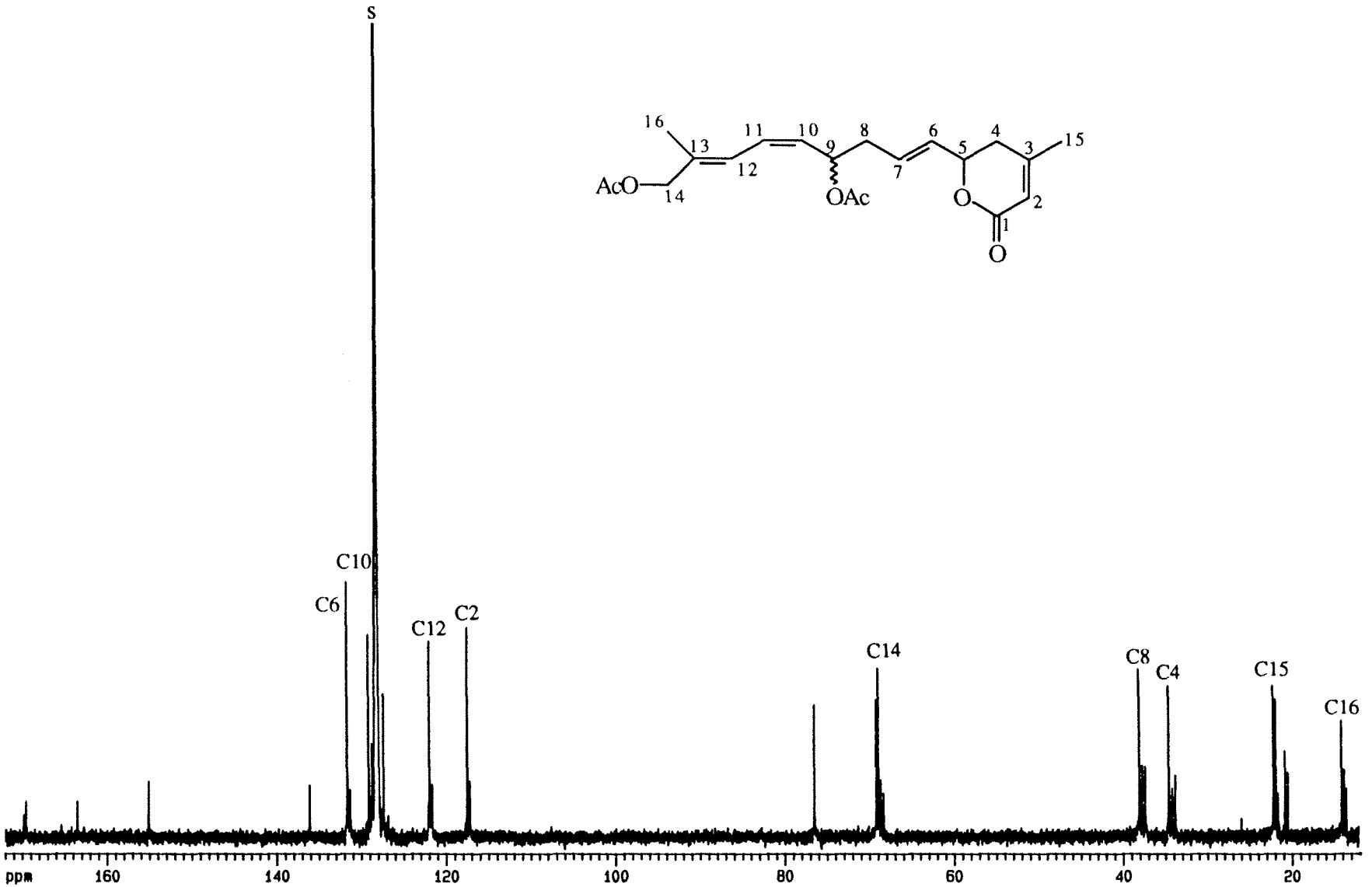

Figure 16. ^{13}C NMR spectrum of oncorhyncolide diacetate **35** labelled by [2-^{13}C,$^{2}H_3$]sodium acetate (125 MHz, C_6D_6).

The diacetate **35**, obtained from the feeding experiment with [1-^{13}C]sodium acetate, displayed seven enhanced signals in the ^{13}C NMR spectrum (Figure 11, Table 4) with enrichment at C1, C3, C5, C7, C9, C11 and C13. This suggests that seven molecules of acetate were used in the biosynthesis of the carbons C1 to C14 in oncorhyncolide. The observed labelling patterns from this sodium acetate feeding experiments ruled out the biogenetic pathway **A**. Pathway **A**, with a C1/C2 acetate starter unit, would have shown enhancement at the C2, C4, C6, C8, C10 and C12 resonances on feeding [1-^{13}C]sodium acetate.

An incorporation study with [2-^{13}C]sodium acetate provided complementary results to the [1-^{13}C] experiment. Nine non-acetate carbons were enhanced, C2, C4, C6, C8, C10, C12, C15 and C16 (Figure 12, Table 4) suggesting that these carbons were derived from the methyl carbon of acetate. From these two experiments an all acetate biosynthesis was established since all the carbons in oncorhyncolide were enhanced on feeding [1-^{13}C] and [2-^{13}C] labelled sodium acetate. These experiments eliminated pathways **C/C'** with a leucine or valine derived starter unit. The acetate pathways **B/B'** and the mixed acetate and mevalonate pathways **C/C'** would result in the observed labelling pattern.

The use of uniformly labelled [1,2-$^{13}C_2$]sodium acetate identified the intact acetate units. The proton decoupled ^{13}C NMR spectrum (Figure 13, Figure 14, Figure 15) of the diacetate **35** exhibited doublets flanking a central singlet for the carbons C1 to C14 representing seven intact acetate units. The doublets are due to ^{13}C/^{13}C coupling in doubly labelled molecules and the central singlet represents the natural abundance ^{13}C in unlabelled molecules. The ^{13}C/^{13}C coupling constants are given in Table 4. The carbon resonances for C15 and C16 appeared as singlets.

The [2-^{13}C,$^{2}H_3$]sodium acetate feeding experiment identified the location of ^{13}C-^{2}H bonds and the number at each site. A ^{1}H and ^{2}H broadband decoupled ^{13}C NMR spectrum (Figure 16) showed the presence of the ^{13}C-^{1}H resonance and one or two isotopically shifted resonances indicating the presence of one or two ^{2}H atoms. The results (Table 4) showed that the maximum number of ^{2}H atoms, derived from the C2 of acetate, were incorporated at each site in

the heptaketide chain. Two ^{2}H atoms were also incorporated at both the C15 and C16 methyls. This provided further evidence that these methyl groups were derived from the C2 of acetate.

In an attempt to distinguish between the acetate derived pathways **B/B'** and the acetate and mevalonate derived pathways **C/C'**, a feeding study was conducted with [2-^{13}C: 100 mg] mevalonolactone following the same protocol used for the acetate studies. The ^{13}C NMR spectrum of the isolated oncorhyncolide diacetate **35** showed no evidence for the incorporation of mevalonolactone. This negative evidence does not prove that mevalonic acid is not on the biosynthetic pathway to oncorhyncolide. However, if the biosynthesis of oncorhyncolide proceeded from acetate, via mevalonate, then it would not be unreasonable to expect carbons C11, C12, C13, C14 and C16 to show lower incorporation levels. These carbons have virtually the same incorporation levels as the other carbons in the molecule. Considered together, the uniform labelling and the negative incorporation of mevalonolactone suggests that mevalonate is probably not an intermediate in oncorhyncolide biosynthesis.

The biosynthesis of polyketides is thought to proceed via a mechanism similar to that of fatty acid biosynthesis which is carried out by an enzyme system known as the fatty acid synthase (FAS) system. Fatty acid biosynthesis involves the successive extension of an acyl chain by two methylene groups obtained, via malonate, from acetate.[43] Polyketide biosynthesis is thought to be carried out by a set of enzymes known as the polyketide synthase (PKS) system (Figure 17).[44] A more complex molecule can be biosynthesized from this system by omitting some of the reduction-dehydration-reduction steps normally used to convert the acetate keto group to a methylene group or olefin.

Evidence is mounting for a so-called "processive" polyketide biosynthesis in which the oxidation state at the keto group of the β-keto thioester is adjusted before the next carbon extension occurs.[39] In addition, it has been suggested that the intermediates in polyketide biosynthesis remain enzyme-bound and are released only for final modifications such as cyclization and oxidation.[44]

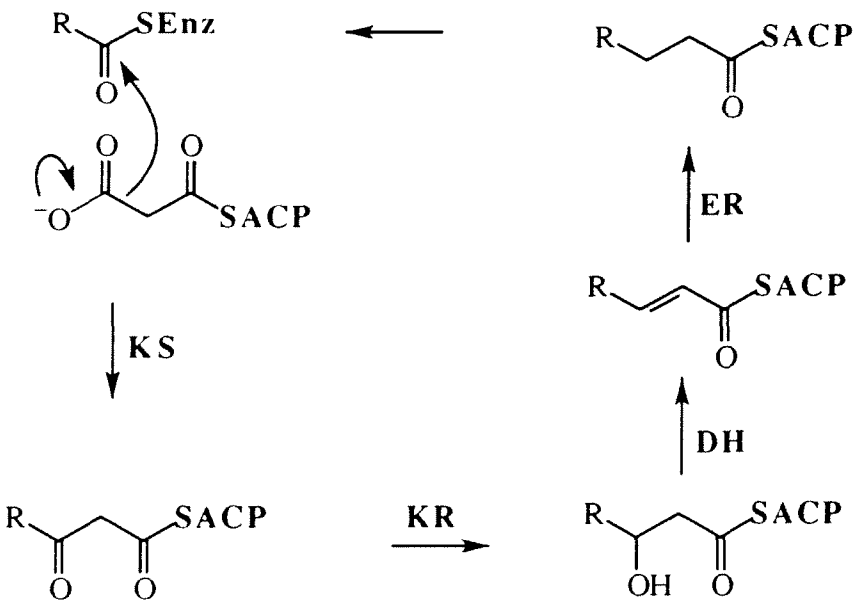

Figure 17. Proposed polyketide synthase system.[44]

ACP acyl carrier protein
KS ketone synthase
KR ketone reductase
DH dehydratase
ER enoyl reductase

The biosynthesis of oncorhyncolide is unusual because of the methyl branches at chain carbons derived from the carbonyl carbons of acetate units. The feeding studies indicated that oncorhyncolide biosynthesis is initiated by an acetate starter unit at C14/C13. This is followed by addition of a second acetate unit, via malonate, to form acetoacetyl-SEnz. Malonate is derived from acetate and is activated by coenzyme A (CoA). If oncorhyncolide is biosynthesized by a "processive" mechanism then one would expect the introduction of the methyl branch at this stage and a proposed mechanism is given in Figure 18. A third acetate unit, presumably from malonate, is added via an aldol-like condensation and subsequent decarboxylation results in a five carbon enzyme-bound unit.

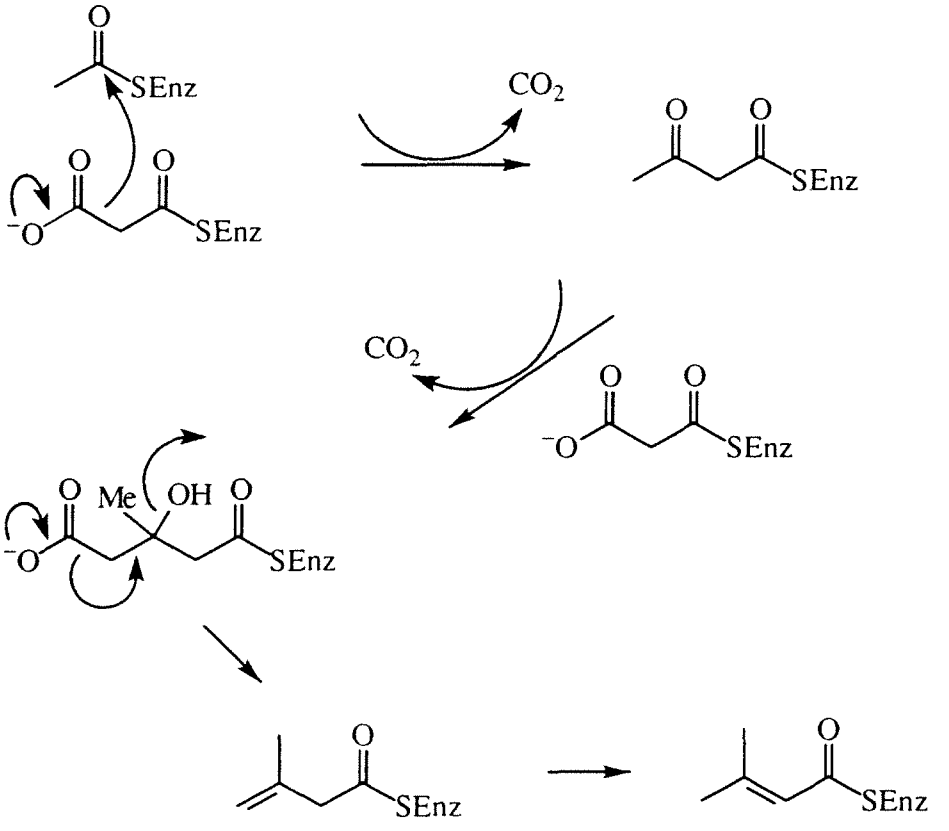

Figure 18. Proposed mechanism for methyl branching at C16 in oncorhyncolide.

The enzyme-bound five carbon unit undergoes an addition of five acetate units in the PKS system and after each addition the oxidation state at the β-keto group is adjusted (Figure 19 **A-G**). The introduction of the methyl branch at C3 may arise by the addition of an acetate group at C3 (**F**) and subsequent decarboxylation, or by the addition of an intact acetate unit at C1/C2 (**G**) and decarboxylation of the straight chain. It is not possible to distinguish between these two possibilities and both lead to intermediate **H** and finally to oncorhyncolide (**34**).

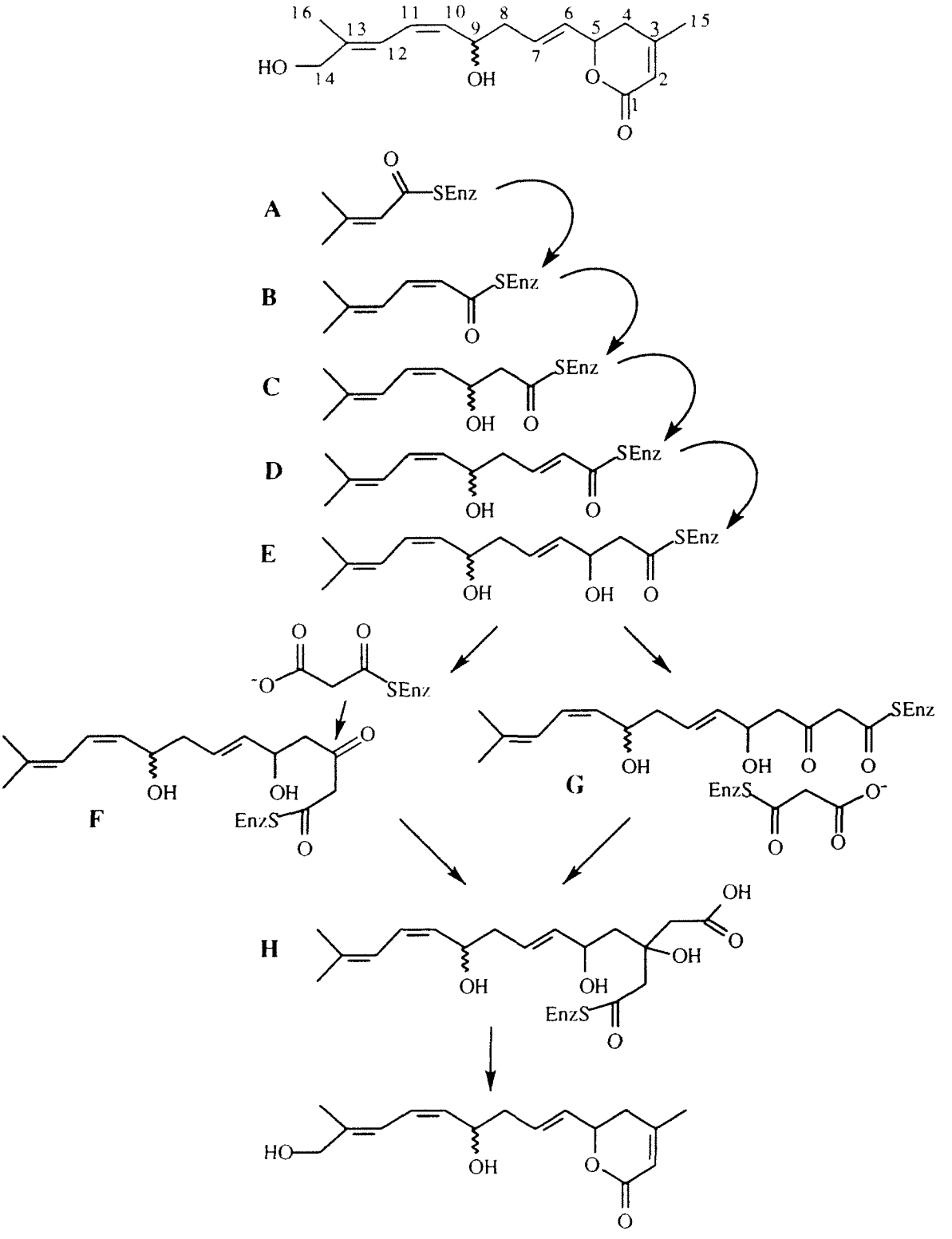

Figure 19. Proposed enzyme-bound thioester intermediates in the "processive" mechanism of oncorhyncolide biosynthesis.

4.3. Conclusion

Stable isotope studies on oncorhyncolide have shown that all the carbons are derived from acetate. Analysis of the labelling patterns revealed the incorporation of seven intact acetate units in the linear carbon chain extending from C1 to C14. These results are consistent with the biogenetic pathway **B/B'** shown in Figure 10. The methyl branches at C15 and C16 are derived from the C2 of acetate and are attached to carbon atoms derived from the carbonyl carbon, C1, of an acetate unit. This type of methyl branching, formed by the decarboxylation of an acetate unit, is quite rare in polyketide biosynthesis and has only been reported from bacterial metabolites including the aurantinins,[45] myxopyronin,[46] myxovirescin A[47] and the virginiamycins.[40] An exception is cylindrocyclophane D which is produced by a cyanobacteria.[48] The results presented in this thesis do not provide any insight into the mechanism of this unusual methyl branching and further studies involving the incorporation of more advanced precursors are required.

Oncorhyncolide (**34**) has a unique structure that is apparently not related to other known microbial metabolites isolated from terrestrial sources. As mentioned earlier, the okadaic ester **37**, isolated from cultures of the dinoflagellate *Prorocentrum concavum*, contains a seven-carbon ester fragment that resembles the methyl branched diene system in oncorhyncolide. This seven-carbon ester fragment in **37** is also derived completely from acetate.[49]

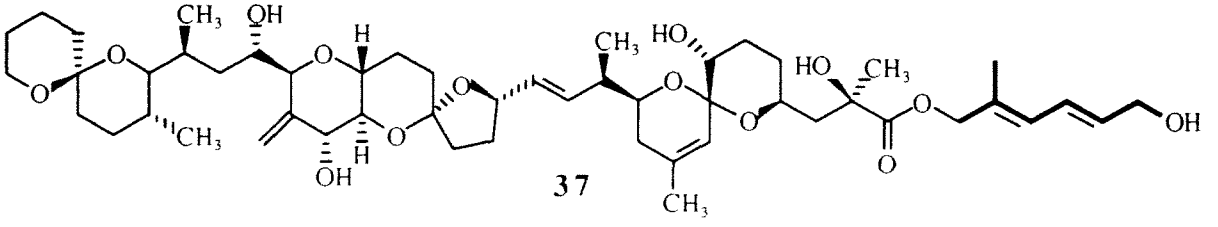

37

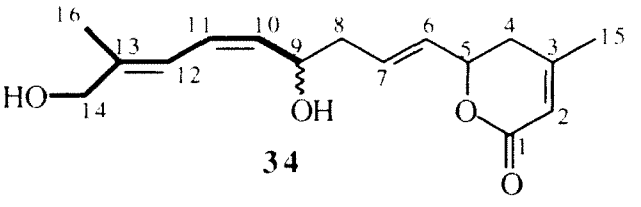

34

5. SECONDARY METABOLITES FROM *PSEUDOMONAS FLUORESCENS* (91QQ48)

5.1. Introduction

The marine isolate 91QQ48 was obtained from tissues of an unidentified tunicate collected from rock ledges off Prince of Wales Island in Moira Sound, Alaska. The tunicate was sectioned and inoculated directly to the surface of a variety of media. Isolate 91QQ48 was recovered from starch agar. Initial screening by Dr. M. Kelly showed that the marine isolate 91QQ48 exhibited antibacterial activity against Gram-positive bacteria including several organisms that are resistant to currently available antibiotics (see Table 2, page 16). The organism was identified as the Gram-positive bacterium *Pseudomonas fluorescens* by using classical biochemical methods and cellular fatty acid analysis (MIDI system, Newark, Delaware).

Preliminary studies showed that extracts of liquid shake cultures of *P. fluorescens* had no antibacterial activity. However, cultures grown on solid media resulted in extracts which, at low concentrations, inhibited methicillin-resistant *Staphylococcus aureus*. Therefore, *P. fluorescens* was grown in moderate scale culture on solid media.

5.2. Isolation of secondary metabolites from *Pseudomonas fluorescens*[50]

Forty-six aluminium trays (23 x 33 x 5 cm) each containing 500 mL of tryptic soy broth medium, 1 % agar and 1 % sodium chloride were each inoculated with 2 mL of an actively growing liquid culture of *P. fluorescens*. The cultures were incubated for 3 days at room temperature at which time the cells were gently scraped off the solid media. The scraped media was sectioned into 3 x 3 cm cubes and immersed in ethyl acetate. After 24 hours the ethyl acetate was decanted, dried over sodium sulfate, and concentrated in vacuo to give a pungent dark red

oil. The ethyl acetate extraction of the agar cubes was repeated three times to yield 12.4 g of the crude oil.

The crude extract was processed in a batchwise manner beginning with reversed-phase silica column chromatography (eluent: 65:35 methanol/0.025 M phosphate buffer, pH 6.86). The chromatographic fractions were pooled into four fractions on the basis of their TLC behaviour and antimicrobial activity. Each of the four pooled fractions was concentrated in vacuo to remove the methanol and the aqueous residue was exhaustively extracted with ethyl acetate. The fastest eluting fraction (6.4 g) was chromatographed on Sephadex LH-20 (eluent: ethyl acetate/ methanol/water 8:2:1) and again the chromatographic fractions were pooled into fractions on the basis of their TLC behaviour and antimicrobial activity. Further purification of the pooled antimicrobial fractions from the Sephadex LH-20 column by reversed-phase HPLC (eluent: methanol/0.025 M phosphate buffer, pH 6.86) yielded pure samples of moiramide A (**38**) (25 mg), moiramide B (**39**) (27 mg) and andrimid[51] (**41**) (1 g) as well as a partially pure sample of moiramide C (**40**).[52] Final purification of the impure moiramide C via normal phase silica gel HPLC (eluent: ethyl acetate/hexane 7:3) yielded 1.5 mg of pure compound. The slowest eluting fraction from the reversed-phase silica column contained a red pigment that was identified as prodigiosin (**33**).[34]

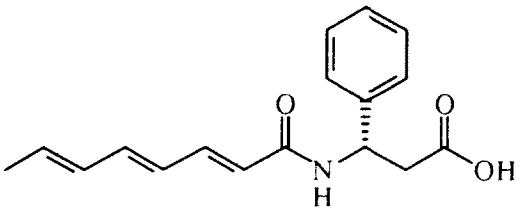

38 Moiramide A

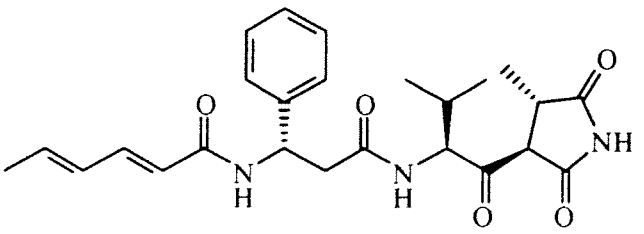

39 Moiramide B

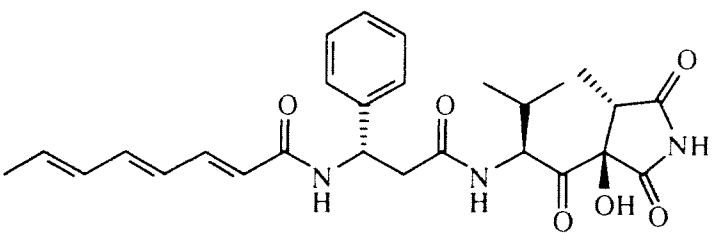

40 Moiramide C

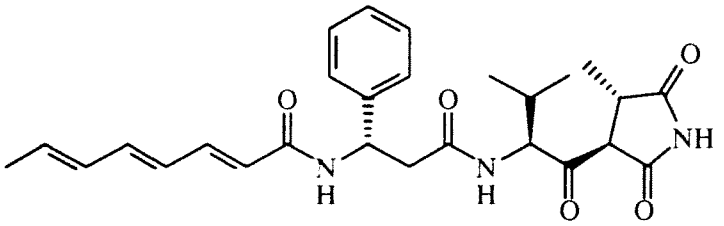

41 Andrimid

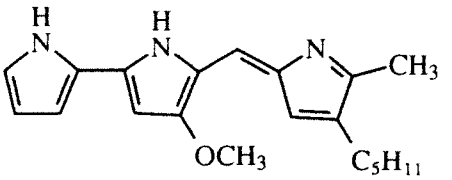

33 Prodigiosin

5.3. Results and Discussion

5.3.1. Moiramide A (38)

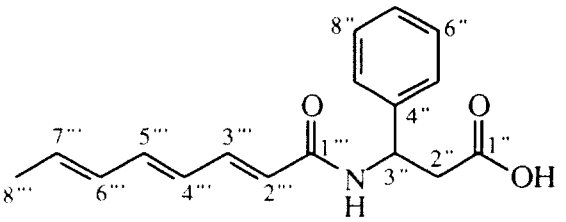

38

Moiramide A (**38**) was isolated as an amorphous white solid. The HREIMS spectrum showed a molecular ion at m/z 285.1366 corresponding to a molecular formula of $C_{17}H_{19}NO_3$ (ΔM +0.1 mmu). The molecular formula indicated that **38** had 9 sites of unsaturation. Table 5 provides a summary of the NMR data acquired for compound **38**. The ^{1}H NMR spectrum (Figure 20) of moiramide A contained a methyl doublet at δ 1.76, a methylene resonance at δ 2.68 and a downfield methine resonance at δ 5.25. Six olefinic protons were observed from δ 5.89 to 7.00 ppm, and five aromatic protons from δ 7.2 to δ 7.3 indicated the presence of a phenyl ring. A doublet at δ 8.48 in the ^{1}H NMR spectrum showed no HMQC correlation to a

carbon resonance and was assigned to an amide proton. The broad singlet at δ 12.25 had no attached carbon and was assigned to a carboxylic acid proton.

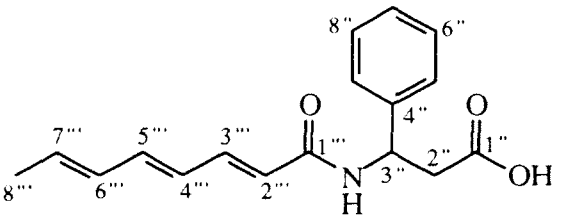

38

Table 5. ^{1}H and ^{13}C NMR data for moiramide A (**38**).

C#	^{13}C[a]	^{1}H[b]	COSY	HMBC[c]
1"	171.6	—	—	H2",H3"
2"	40.9	2.68,m	H3"	H3"
3"	49.5	5.25,dd(15.3,8.3)	H2",NH	H2"
4"	142.6	—	—	H2",H3"
5"	126.4	7.30,d(4.1)	—	—
6"	128.2	7.30,d(4.1)	—	—
7"	126.9	7.22,m	—	—
8"	128.2	7.30,d(4.1)	—	—
9"	126.4	7.30,d(4.1)	—	—
NH	—	8.48,d(8.3)	H3"	—
1'''	164.2	—	—	H3",NH,H2''',H3'''
2'''	124.1	6.00,d(15.0)	H3'''	—
3'''	139.4	7.00,dd(15.0,11.3)	H2''', H4'''	H5'''
4'''	128.0	6.25,dd(14.8,11.3)	H3''',H5'''	H2''',H5''',H6'''
5'''	138.9	6.53,dd(14.8,10.7)	H4''',H6'''	H3''',H4''',H7'''
6'''	131.4	6.18,ddd(15.0,10.7,1.5)	H5''',H7'''	H4''',H8'''
7'''	133.3	5.89,m	H6''',H8'''	H5''',H8'''
8'''	18.2	1.76,d(6.6)	H7'''	H6''',H7'''
1-OH	—	12.25,bs	—	—

[a] Recorded in DMSO-d_6 at 125 MHz. Chemical shifts in ppm relative to solvent.
[b] Recorded in DMSO-d_6 at 400 MHz. Chemical shifts in ppm relative to solvent.
[c] Carbons in the carbon # column are correlated to the listed proton resonances.

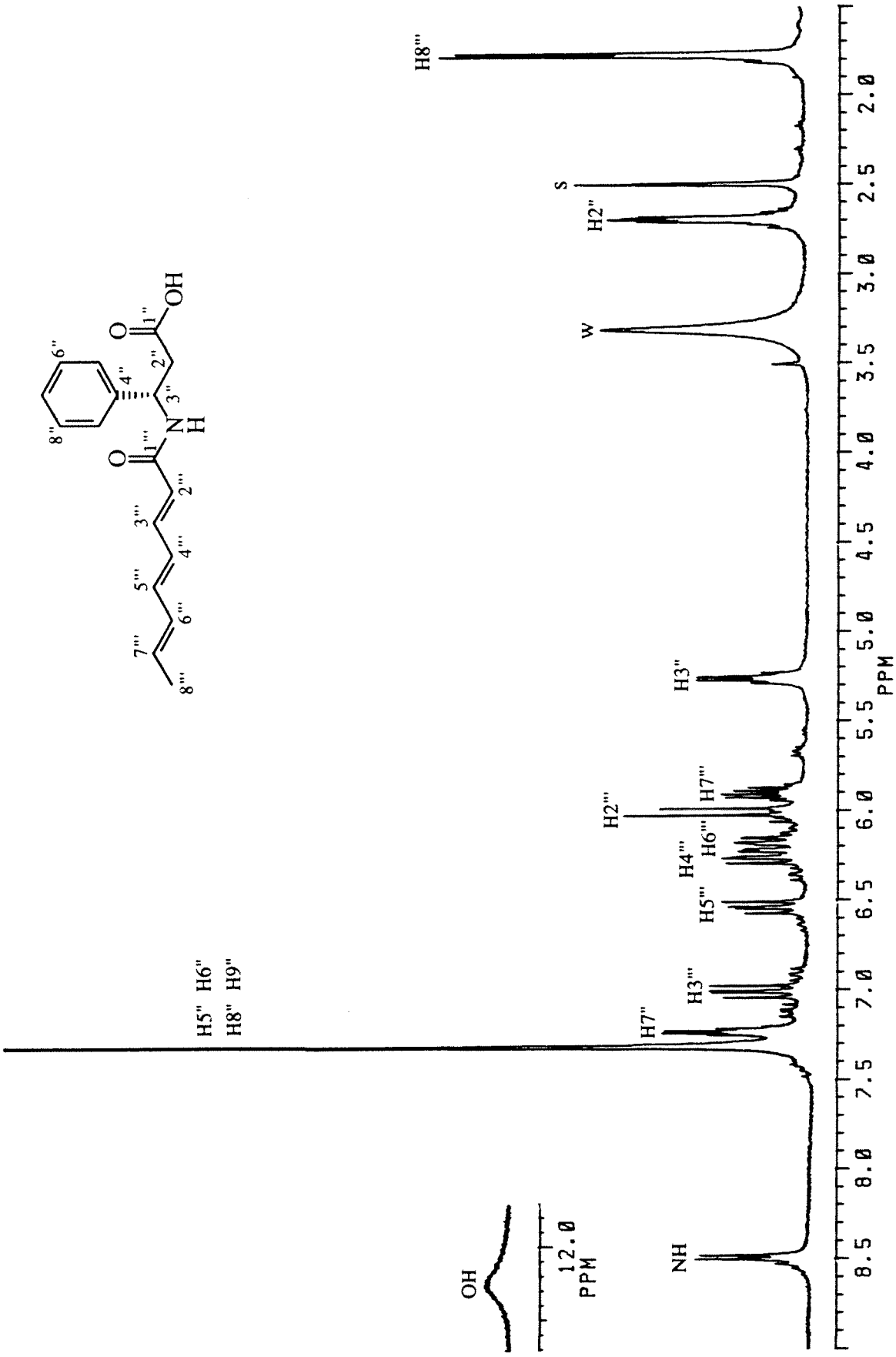

Figure 20. ^{1}H NMR spectrum of moiramide A (400 MHz, DMSO-d_6).

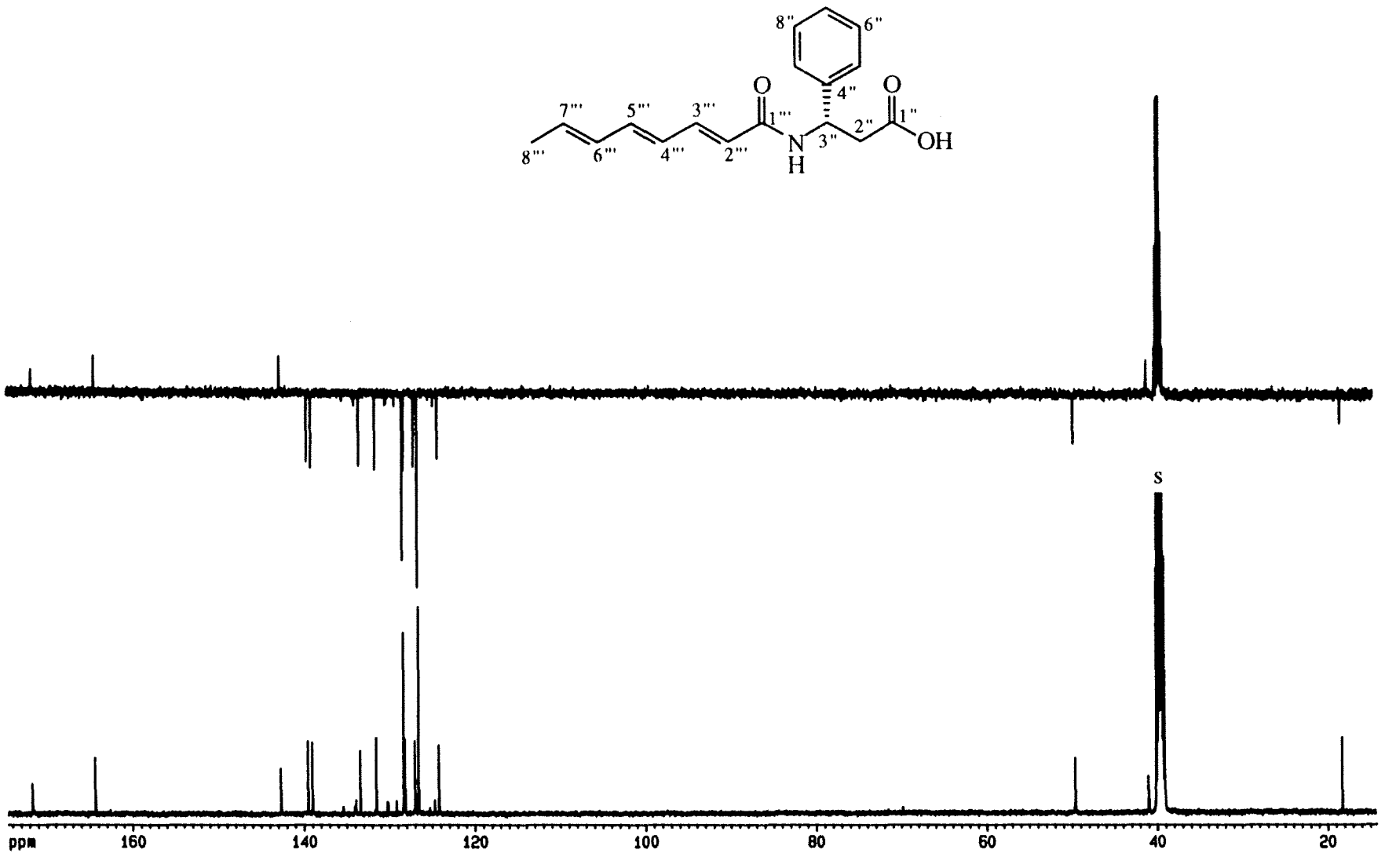

Figure 21. ^{13}C and APT NMR spectra of moiramide A (**38**) (125 MHz, DMSO-d_6).

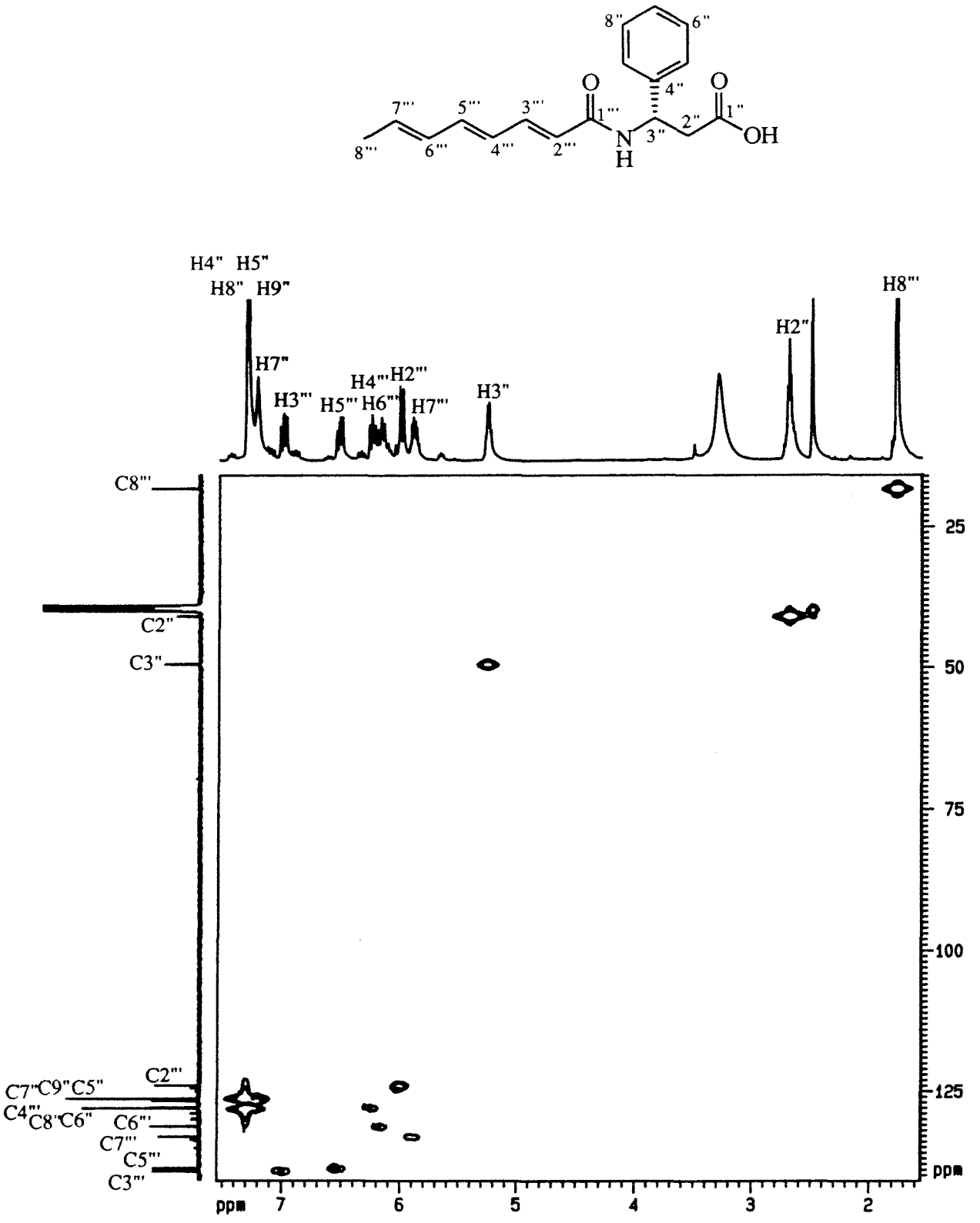

Figure 22. HMQC NMR spectrum of moiramide A (**38**) (500 MHz ^{1}H NMR, DMSO-d_6).

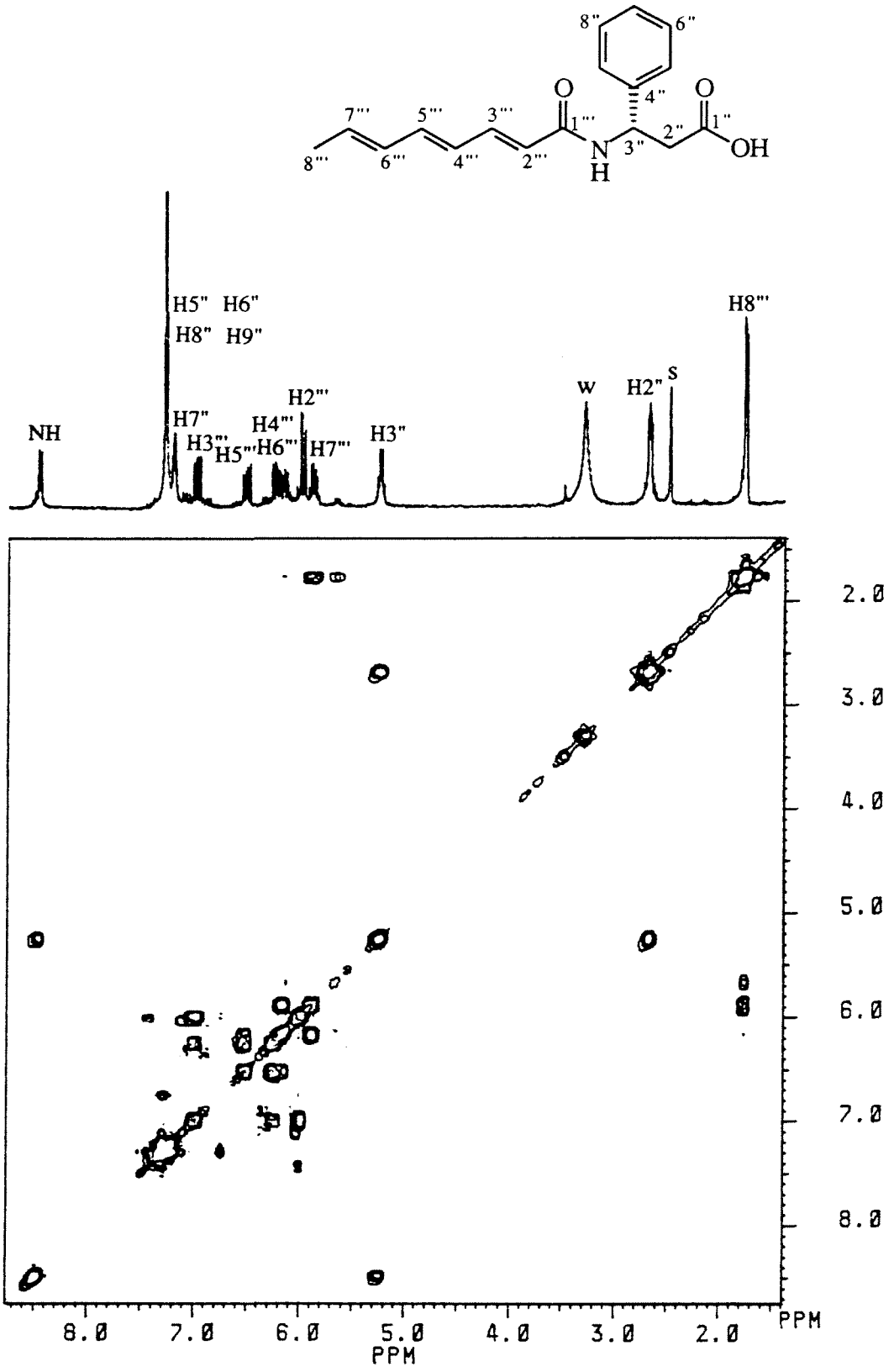

Figure 23. ^{1}H COSY NMR spectrum of moiramide A (**38**) (400 MHz, DMSO-d_6).

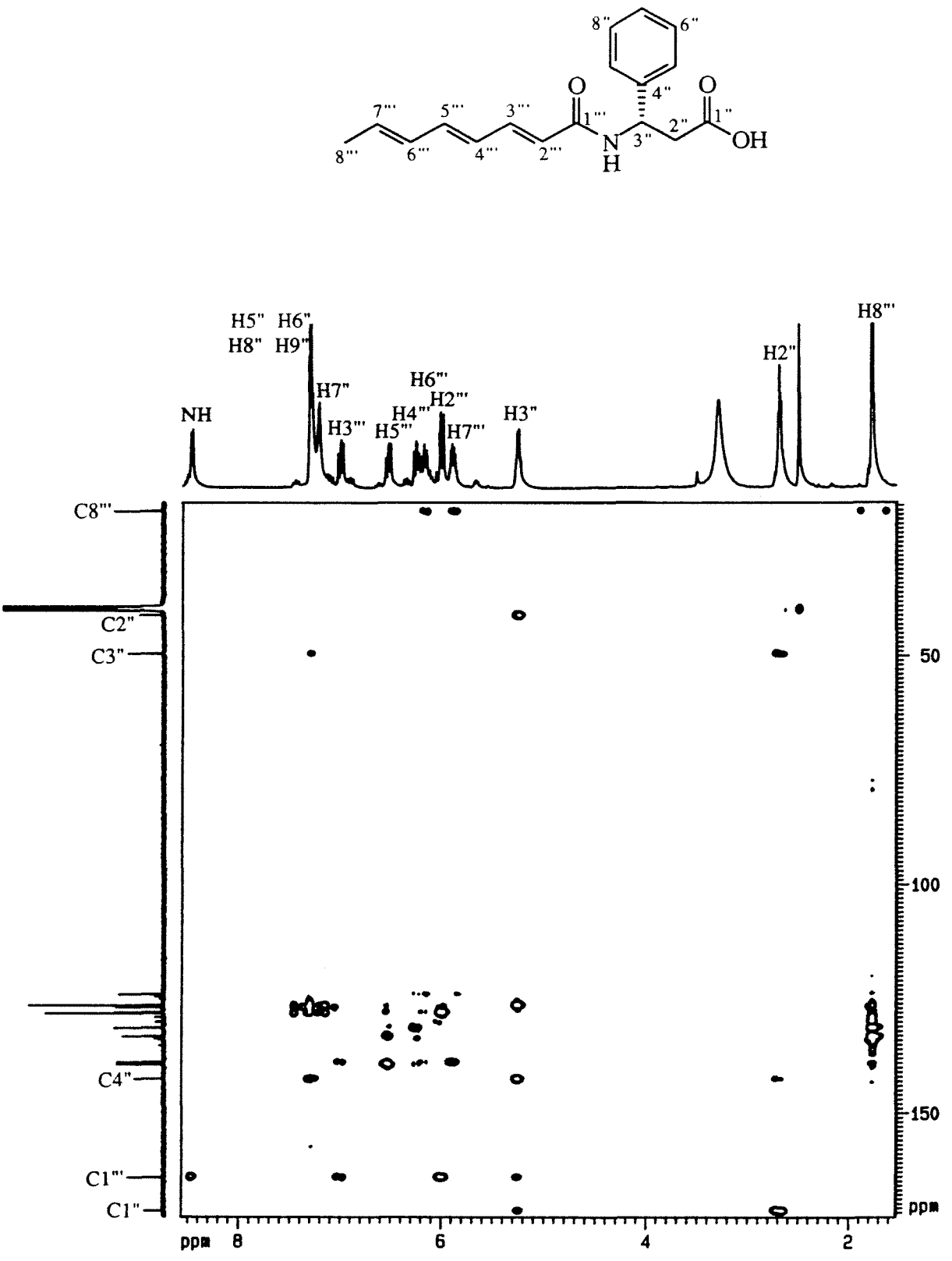

Figure 24. HMBC NMR spectrum of moiramide A (**38**) (500 MHz ^{1}H NMR, DMSO-d_6).

The ^{13}C NMR spectrum of **38** (Figure 21) showed fifteen resolved carbon resonances. Analysis of the APT (Figure 21) and HMQC (Figure 22) NMR data demonstrated the presence of a mono-substituted aromatic ring. The five aromatic proton resonances from δ 7.2 to δ 7.3 were attached to three ^{13}C resonances at δ 126.4, δ 126.9 and δ 128.2. This data was consistent with a symmetrically substituted benzene ring where C5" and C9" as well as C6" and C8" are chemically equivalent. Since the ^{13}C resonances at δ 126.4 and δ 128.2 accounted for two carbons each, the ^{13}C NMR spectrum confirmed the presence of seventeen carbon atoms. An APT experiment (Figure 21) indicated one methyl, one methylene and twelve methine groups accounting for seventeen of the nineteen protons in the molecule. The deshielded resonances at δ 171.6 and δ 164.2 in the ^{13}C NMR spectrum were assigned to the carbonyl carbons of a carboxylic acid and an amide group, respectively. Six olefinic carbons were identified, corresponding to the ^{13}C NMR resonances at δ 124.1 (CH), 128.0 (CH), 131.4 (CH), 133.3 (CH), 138.9 (CH) and 139.4 (CH). ^{13}C NMR resonances at δ 126.4 (2 x CH), 126.9 (CH), 128.2 (2 x CH) and 142.6 were assigned to aromatic carbons. The six olefinic carbon resonances and the two carbonyl functionalities account for five of the nine sites of unsaturation in the molecule and the remaining four sites of unsaturation were assigned to a phenyl ring.

Analysis of the ^{1}H, COSY (Figure 23) and HMQC (Figure 22) NMR data of moiramide A identified three fragments, **A**, **B** and a phenyl ring. Together these fragments accounted for eighteen of the nineteen protons in the molecule. The remaining proton was assigned to that of a carboxylic acid. A methyl doublet at δ 1.76 (H8"'), integrating for three protons, was coupled to an olefinic proton, a multiplet at δ 5.89 (H7"'), which in turn showed a correlation to the olefinic proton at δ 6.18 (H6"'). The H6"' proton was also coupled to an olefinic proton at δ 6.53 (H5"'). The H5"' doublet of doublets was coupled to the H4"' olefinic proton at δ 6.25 which in turn showed a correlation to the doublet of doublets at δ 7.00 (H3"'). A correlation from the H3"' proton to the doublet at δ 6.00 (H2"') completed fragment **A**.

In fragment **B** a multiplet at δ 2.68 (H2"), integrating for two protons, was coupled to a methine proton at δ 5.25 (H3"). The downfield chemical shift of this proton together with a ^{13}C chemical shift of 49.5 ppm for its attached carbon suggested that the methine carbon was attached

to a nitrogen atom. A COSY correlation was observed between the H3" methine proton and a doublet at δ 8.48 (NH). The proton at δ 8.48 was not attached to a carbon and was therefore assigned to an amide proton due to its downfield chemical shift.

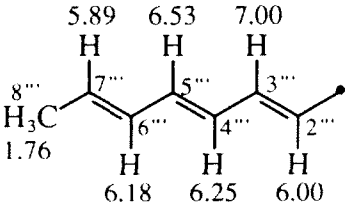

A

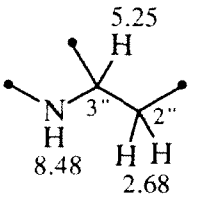

B

Examination of the HMBC spectrum (Figure 24) of moiramide A connected the three fragments and assigned the two carbonyl groups. HMBC correlations between the carbonyl carbon at δ 164.2 (C1''') and the protons at δ 5.25 (H3"), δ 8.48 (NH), δ 6.00 (H2''') and δ 7.00 (H3''') positioned the carbonyl carbon C1''' between the olefinic carbon C2''' of fragment **A** and the nitrogen of fragment **B**. HMBC correlations from the methylene protons at δ 2.68 (H2") and the methine proton at δ 5.25 (H3") to the quaternary carbon at δ 142.6 on the phenyl ring and HMBC correlations from the protons at δ 2.68 (H2") and δ 5.25 (H3") to the carbonyl carbon at δ 171.6 give rise to two possible structures depicted in Figure 25. The HMBC data is consistent with the attachment of either the phenyl ring or the carboxylic acid to C3" or C2". Structure **38a** gives rise to the normal amino acid phenylalanine, whereas **38** gives rise to a β-phenylalanine moiety.

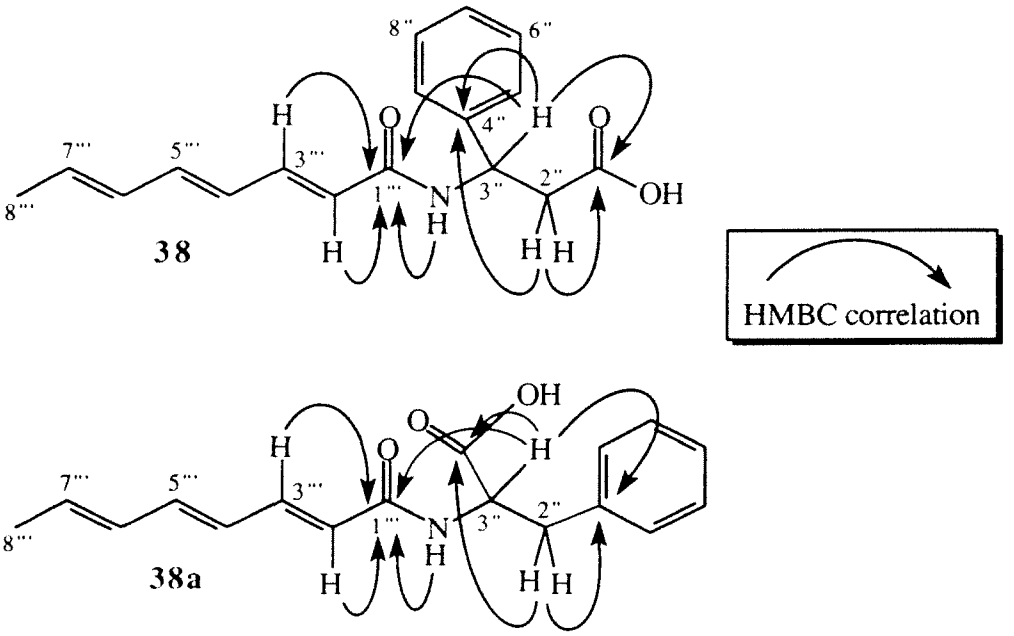

Figure 25. HMBC correlations for moiramide A.

The observed HMBC correlation from a proton at δ 7.30 on the phenyl ring to C3" (δ 49.5) (Figure 24) would be a three bond correlation in **38** but a four bond correlation in **38a** (Figure 26). Since the HMBC experiment is optimized for two and three bond correlations, this correlation unambiguously attaches the phenyl ring to C3" and supports the proposed constitution for **38**.

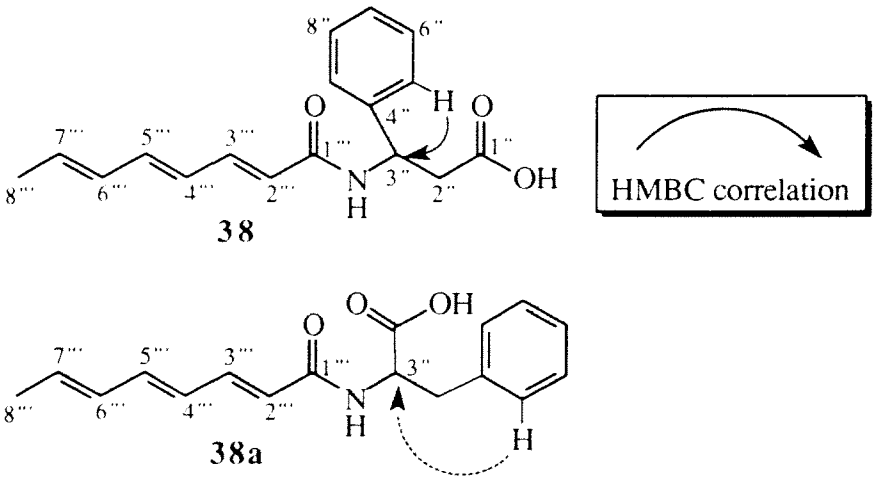

Figure 26. An HMBC correlation for moiramide A.

The configurations of the olefinic functionalities were determined by NOE difference experiments (Figure 27). Irradiation of the signal for H5''' resulted in enhancement of the H3''' and H7''' signals. This suggested an E configuration for the $\Delta^{4''',5'''}$ and $\Delta^{6''',7'''}$ double bonds. The signal for H4''' was enhanced by irradiation of the H2''' resonance suggesting an E configuration for the $\Delta^{2''',3'''}$ olefin.

The NMR data presented for moiramide A supports the proposed constitution for **38**. The absolute configuration of C3'' in **38** will be discussed in section 5.3.5.

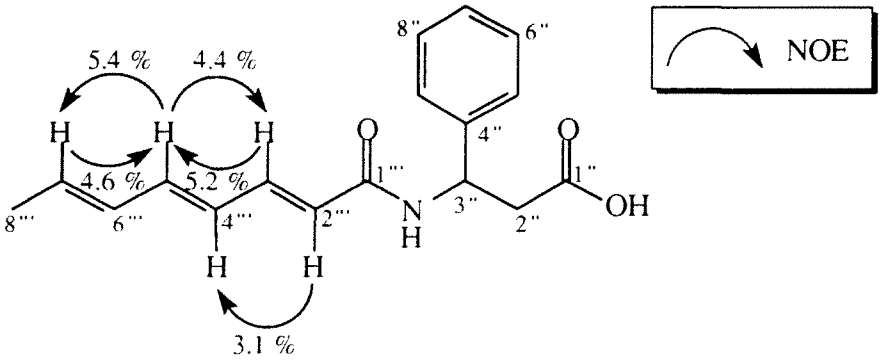

Figure 27. Results from selected NOE difference experiments on moiramide A.

5.3.2. Moiramide B

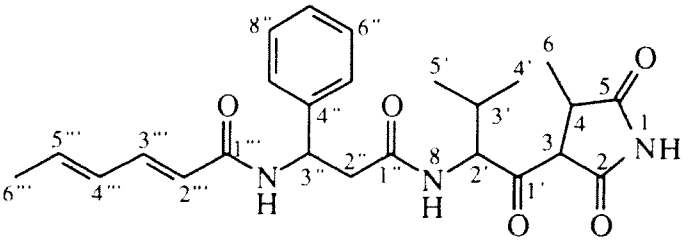

39

Moiramide B (**39**) was isolated as an amorphous white solid. The HREIMS spectrum showed a molecular ion at 453.2262 corresponding to a molecular formula of $C_{25}H_{31}N_3O_5$

(ΔM -0.1 mmu). This molecular formula indicated that **39** had twelve sites of unsaturation.

Examination of the NMR data, summarized in Table 6, suggested that moiramide B contained a β-phenylalanine moiety and an olefinic chain as depicted by fragment **A**. Four olefinic resonances in the ^{1}H NMR spectrum (Figure 28) at δ 5.92, 6.06, 6.19 and 6.95 and a methyl doublet at δ 1.78 suggested that moiramide B contained a hexadienoyl fragment in place of the octatrienoyl fragment present in moiramide A. No carboxylic acid proton was observed in the ^{1}H NMR spectrum of **39**.

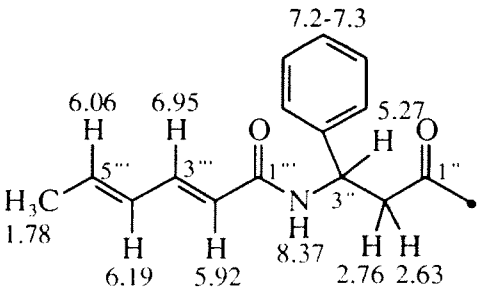

A

Moiramide B had a more complex structure than moiramide A since additional resonances in the ^{1}H NMR spectrum of **39** included three upfield methyl doublets, two methine signals at δ 3.91 and δ 4.61, a second amide proton at δ 8.08 and a broad singlet at δ 11.33.

The ^{13}C NMR spectrum of moiramide B (Figure 29) showed twenty-three resolved resonances. The aromatic resonances at δ 126.4 and δ 128.2 accounted for two carbons each so that the ^{13}C NMR spectrum confirmed the presence of twenty-five carbons. An APT experiment (Figure 29) indicated four methyls, one methylene and fourteen methine groups accounting for twenty-eight of the thirty-one protons in the molecule. The deshielded ^{13}C NMR resonances at δ 164.4, 169.8, 173.7, 180.0 and 203.3 suggested that **39** contained five carbonyl functionalities and these accounted for the five oxygen atoms in the molecule. Fragment **A** accounted for eight of the twelve sites of unsaturation in moiramide B. Three sites of unsaturation are accounted for by the three unassigned carbonyl functionalities and the remaining site of unsaturation had to be a ring.

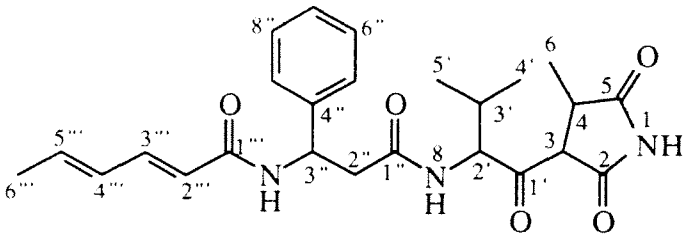

39

Table 6. ^{1}H and ^{13}C NMR data for moiramide B (**39**).

C#	$^{13}C^{a}$	$^{13}H^{b}$	COSY	HMBC[c]
1-NH	—	11.33,bs	—	—
2	173.7	—	—	H3
3	57.8	3.91,d(5.5)	H4	H1,H4,H6
4	38.9	2.90,dq(7.3,5.5)	H3,H6	H1,H3,H6
5	180.0	—	—	H4,H6
6	14.5	1.07,d(7.3)	H4	H3,H4
1'	203.3	—	—	H3,H4,H2'
2'	63.0	4.61,dd(8.4,5.4)	2'-NH,H3'	2'-NH,H4',H5'
3'	28.1	2.28,m	H2',H4',H5'	H2',H4',H5'
4'	17.2	0.74,d(6.7)	H3'	H3',H5'
5'	19.4	0.79,d(6.7)	H3'	H4'
2'-NH	—	8.08,d(8.4)	H2'	—
1"	169.8	—	—	H2',H2'-NH,H2a",H2b",H3"
2a"	41.9	2.63,dd(14.3,6.0)	H2b"	H3",H3"-NH
2b"	—	2.76,dd(14.3,8.6)	H2a",H3"	—
3"	49.8	5.27,m	H2b",3"-NH	H2a",H2b", H3"-NH
4"	142.8	—	—	H2a",H2b", H3"
5"	126.4	7.3	—	—
6"	128.2	7.3	—	—
7"	126.8	7.20,m	—	—
8"	128.2	7.3	—	—
9"	126.4	7.3	—	—
3"-NH	—	8.37,d,(8.4)	H3"	—
1"'	164.4	—	—	H3",3"-NH,H2"',H3"'
2"'	122.9	5.92,d(15.1)	H3"'	—
3"'	139.4	6.95,dd(15.1,10.8)	H2"',H4"'	H2"',H4"',H5"'
4"'	129.9	6.19,dd(15.0,10.8)	H3"',H5"'	H2"',H6"'
5"'	136.6	6.06,m	H4"',H6"'	H3"',H4"',H6"'
6"'	18.2	1.78,d(6.5)	H5"'	H4"',H5"'

[a] Recorded in DMSO-d_6 at 125 MHz. Chemical shifts in ppm relative to solvent.
[b] Recorded in DMSO-d_6 at 400 MHz. Chemical shifts in ppm relative to solvent.
[c] Carbons in the carbon # column are correlated to the listed proton resonances.

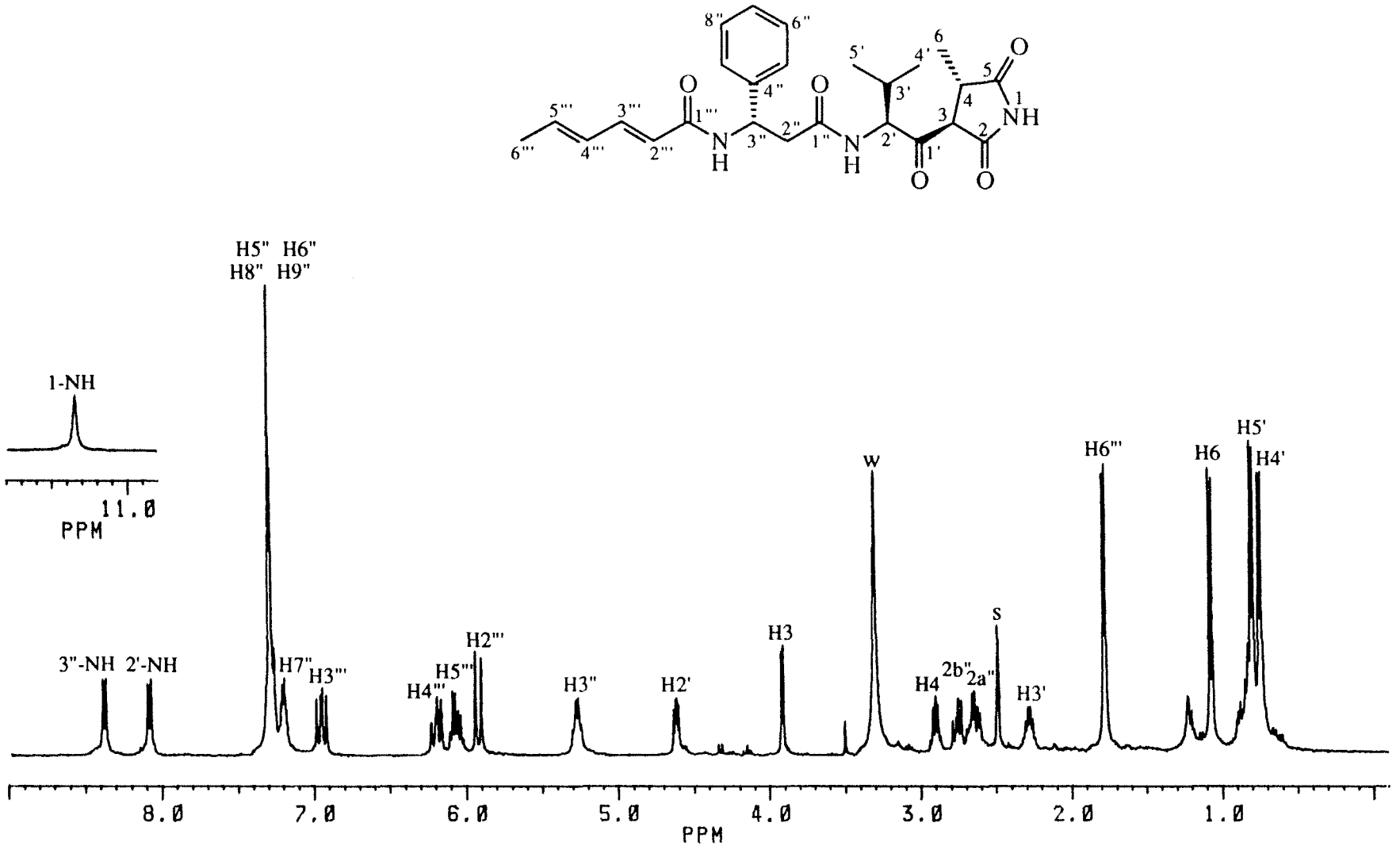

Figure 28. ^{1}H NMR spectrum of moiramide B (**39**) (400 MHz, DMSO-d_6).

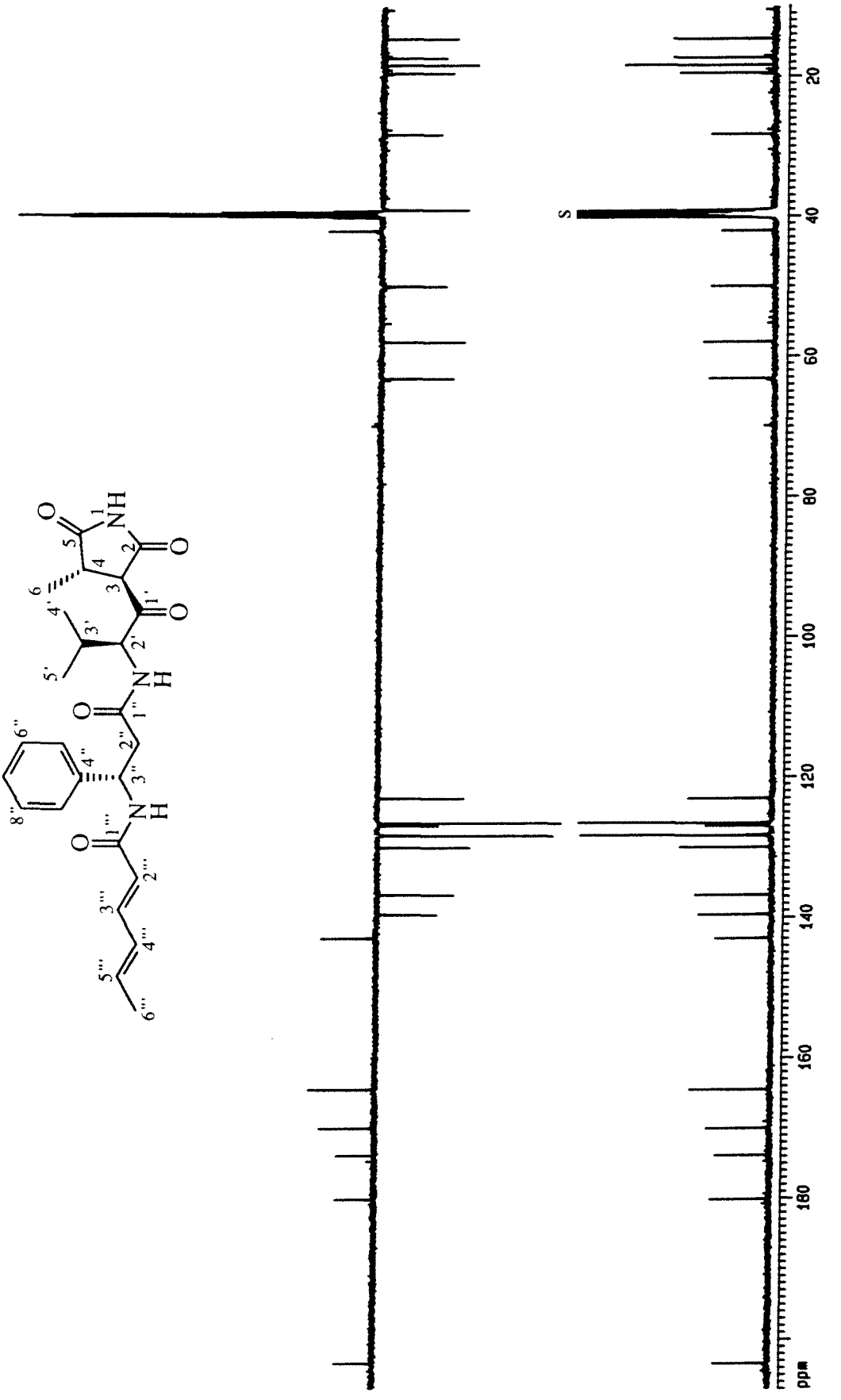

Figure 29. ^{13}C and APT NMR spectra of moiramide B (**39**) (125 MHz, DMSO-d_6).

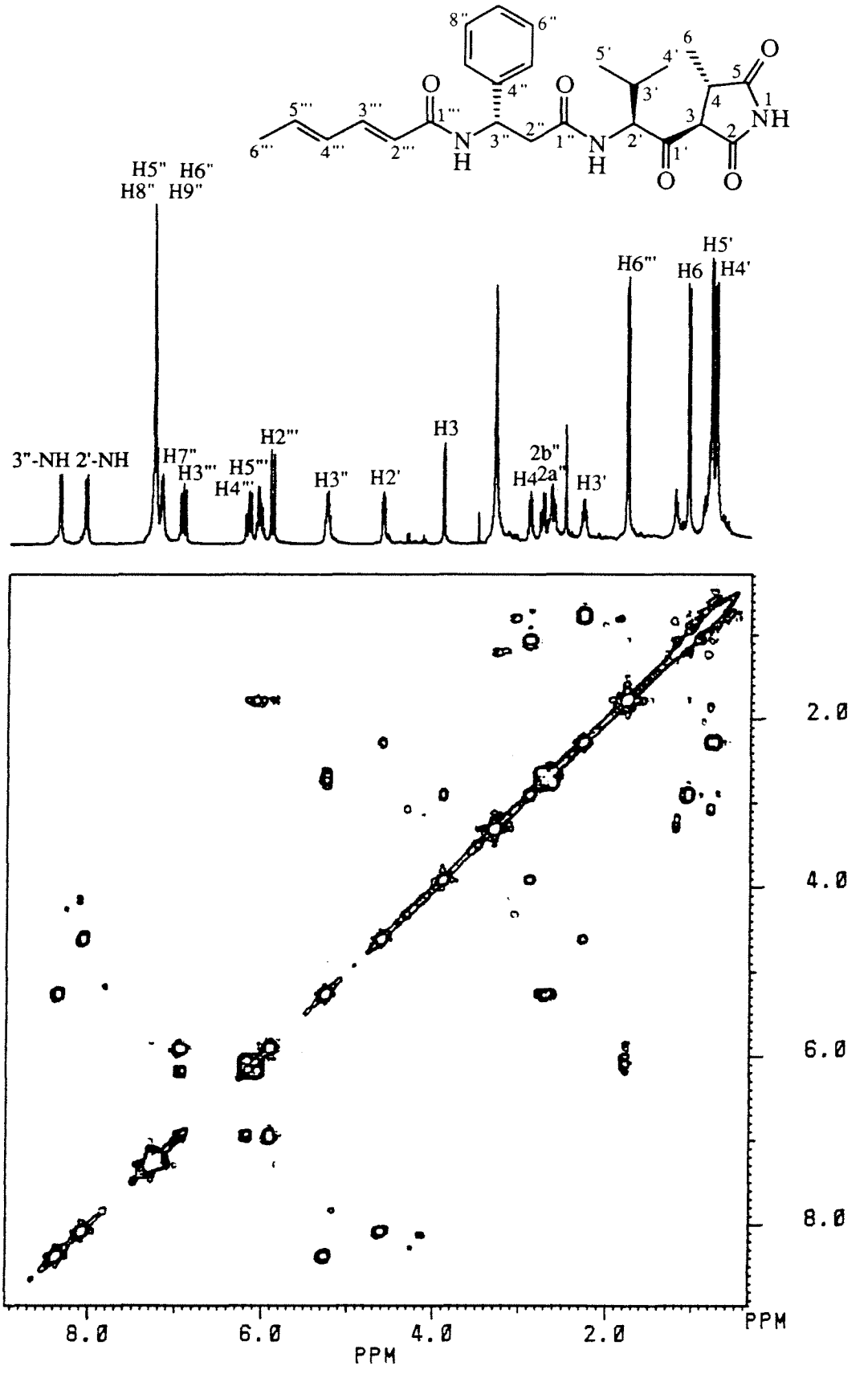

Figure 30. ^{1}H COSY NMR spectrum of moiramide B (**39**) (400 MHz, DMSO-d_6).

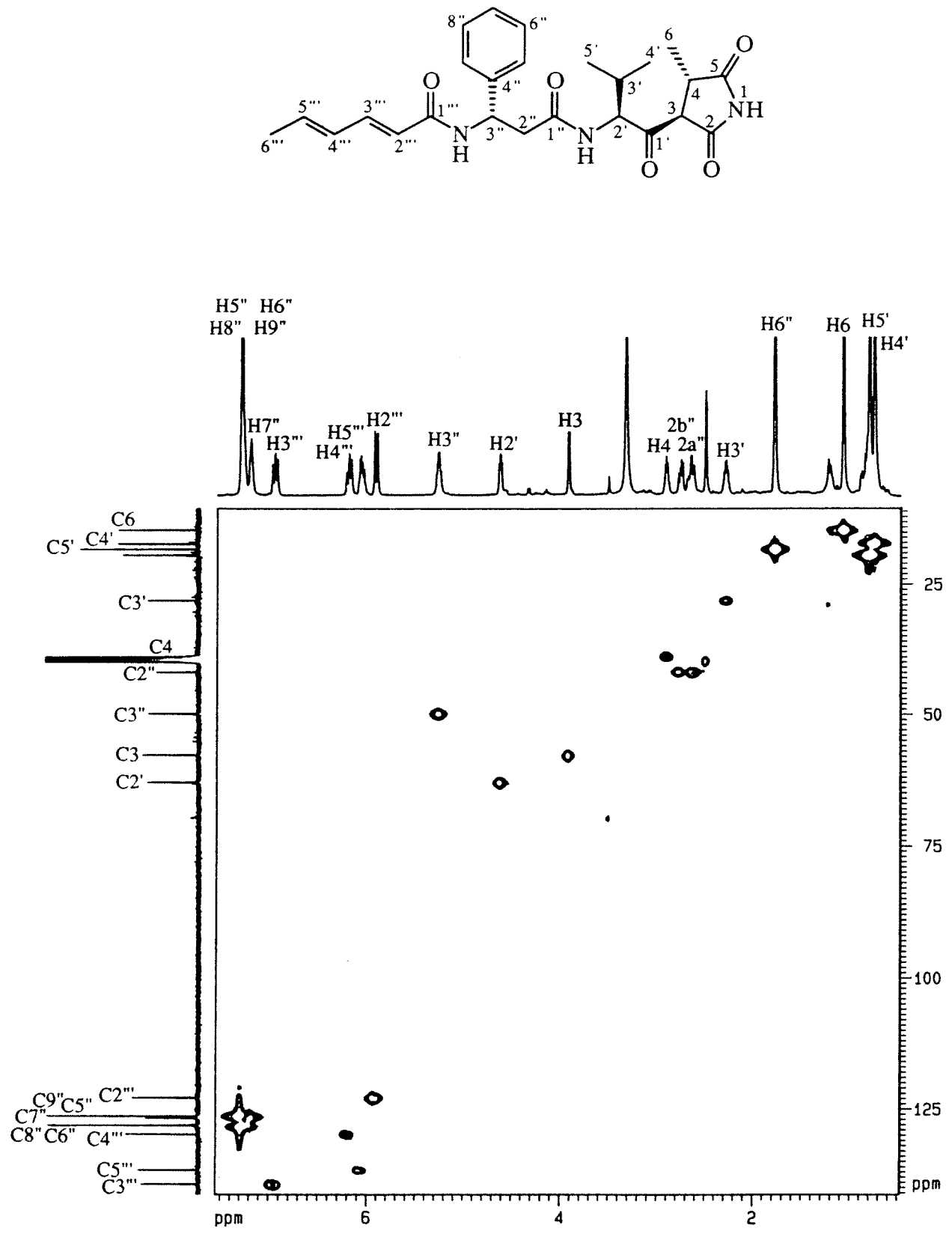

Figure 31. HMQC NMR spectrum of moiramide B (**39**) (500 MHz ^{1}H NMR, DMSO-d_6).

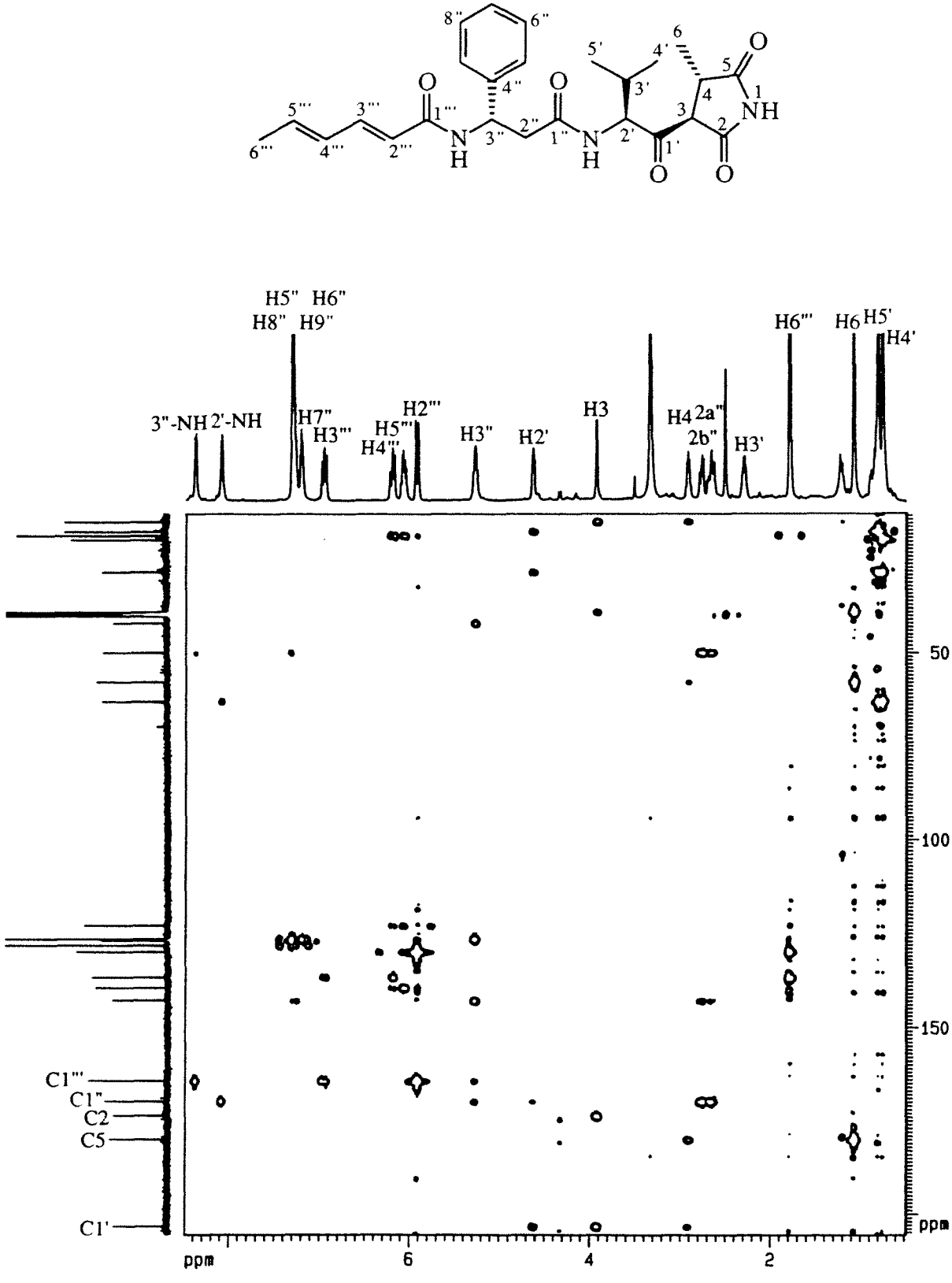

Figure 32. HMBC NMR spectrum of moiramide B (**39**) (500 MHz ^{1}H NMR, DMSO-d_6).

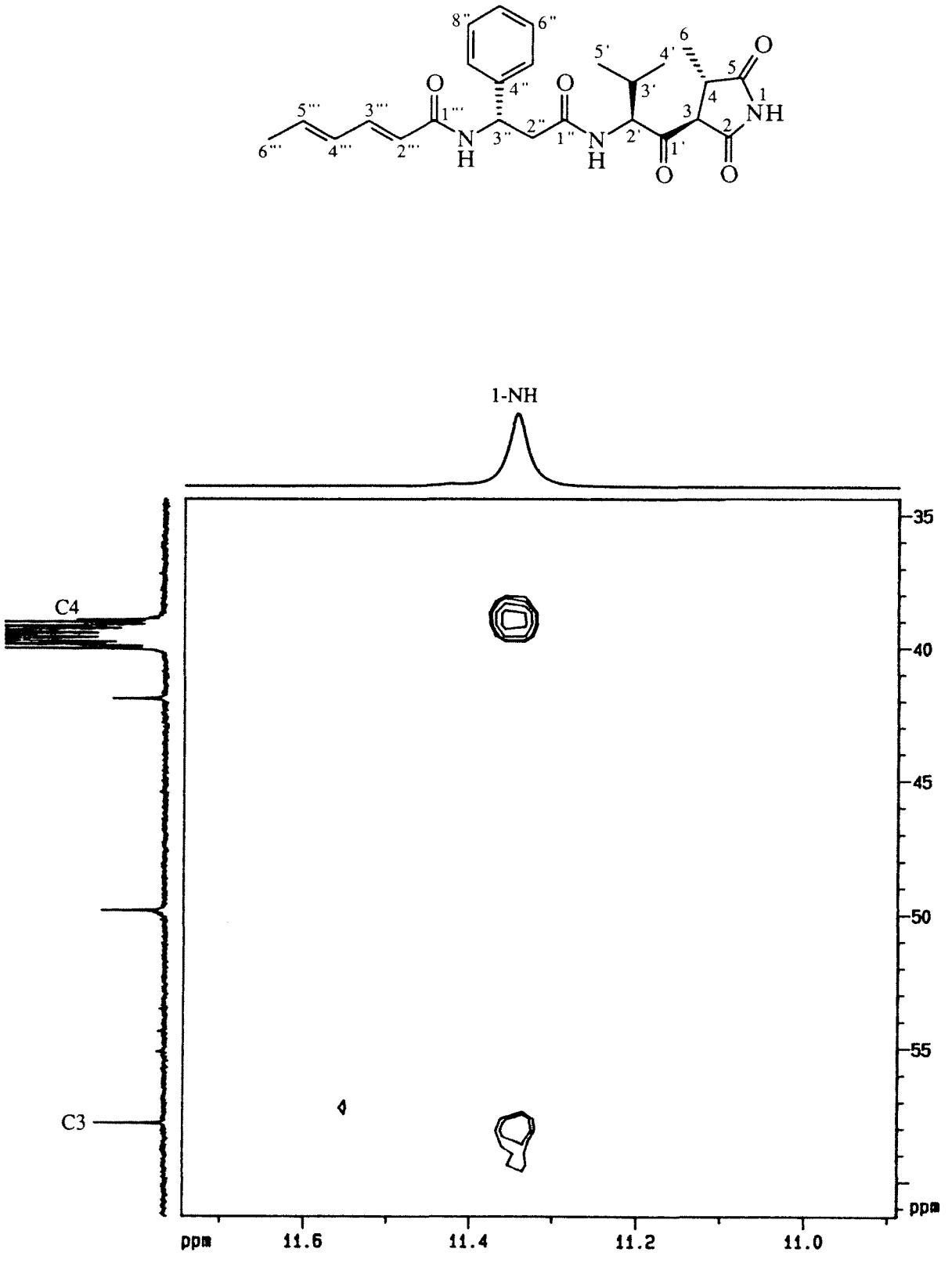

Figure 33. HMBC NMR spectrum of moiramide B (**39**) (500 MHz ^{1}H NMR, DMSO-d_6).

Analysis of the ^{1}H, COSY (Figure 30) and HMQC (Figure 31) NMR data for moiramide B identified two additional fragments, **B** and **C**. In fragment **B** two methyl doublets at δ 0.74 (H4') and δ 0.79 (H5') showed COSY correlations to a methine proton at δ 2.28 (H3') which in turn was coupled to a doublet of doublets, integrating for one proton, at δ 4.61 (H2'). The H2' proton showed a correlation to a doublet which integrated for one proton at δ 8.08 (2'-NH). This proton at δ 8.08 had no proton-carbon correlation in the HMQC spectrum and was therefore assigned to an amide proton. The downfield chemical shift of the methine proton H2' and a ^{13}C chemical shift of 63.0 ppm for its attached carbon suggested that C2' was attached to a nitrogen atom. In fragment **C** a methyl doublet at δ 1.07 (H6) showed a COSY correlation to a methine proton at δ 2.90 (H4) which in turn was coupled to a methine doublet at δ 3.91 (H3).

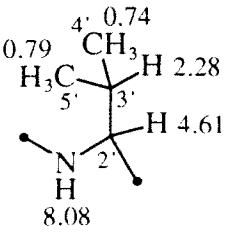

B

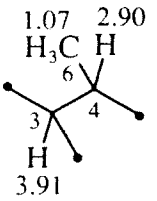

C

The ^{1}H, COSY, ^{13}C and HMQC NMR data identified fragments **A**, **B**, and **C**, together accounting for thirty protons, twenty-three carbons, two nitrogens and two oxygen atoms in the molecule and eight of the twelve sites of unsaturation.

An HMBC experiment (Figure 32) assigned the three remaining carbonyl groups and the proton at δ 11.33. This downfield proton had no attached carbon. HMBC correlations between the carbon resonance at δ 169.8 (C1") and the protons at δ 4.61 (H2') and δ 8.08 (2'-NH) connected fragments **A** and **B** by an amide bond. The carbonyl at C1' was positioned between C2' and C3 by HMBC correlations from the protons at δ 2.90 (H4), δ 3.91 (H3) and δ 4.61 (H2') to the carbon at δ 203.3 (C1'). HMBC correlations from the proton resonances at δ 2.90 (H4) and δ 1.07 (H6) to the carbonyl carbon at δ 180.0 (C5) assigned C5 adjacent to the

methine carbon C4. The final carbonyl was assigned from the HMBC correlation between the H3 proton at δ 3.91 and the carbon at δ 173.7 (C2). HMBC correlations from the H1 imide proton at δ 11.33 into the carbons at δ 57.8 (C3) and δ 38.9 (C4) (Figure 33) formed an acylsuccinimide ring. Selected results from the HMBC experiment are summarized in Figure 34.

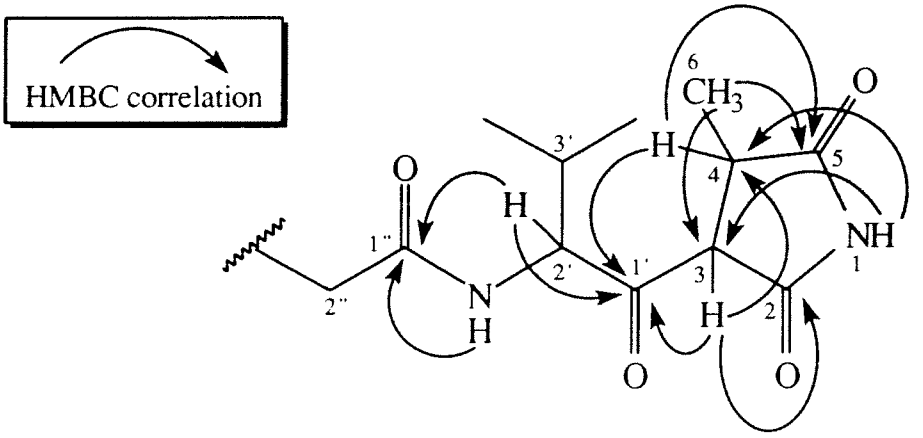

Figure 34. Selected HMBC correlations for moiramide B (**39**).

The configurations of the olefinic double bonds were determined by NOE difference experiments (Figure 35). Irradiation of the H3''' resonance at δ 6.95 resulted in the enhancement of the H5''' resonance at δ 6.06. This suggested an E configuration for the $\Delta^{4''',5'''}$ double bond. The signal for H2''' was enhanced by irradiation of the H4''' resonance, demonstrating an E configuration for the $\Delta^{2''',3'''}$ olefin.

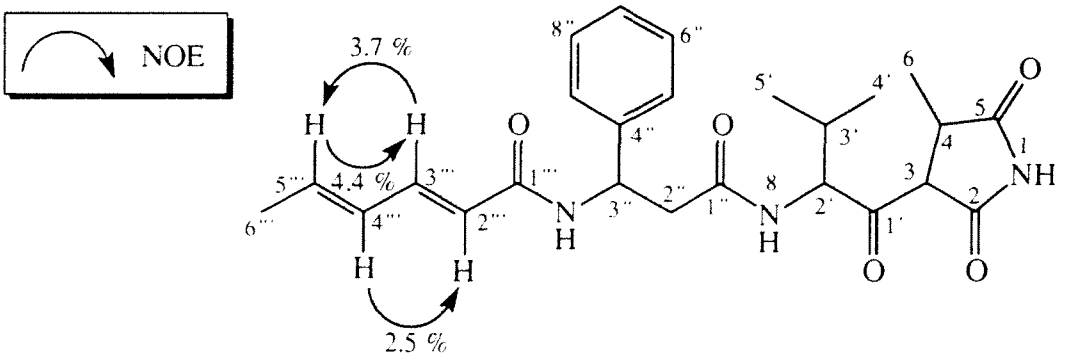

Figure 35. Results from selected NOE difference experiments on moiramide B (**39**).

From the NMR data it was not possible to determine the relative configurations at C3, C4, C2' and C3". The stereochemistry of the chiral centers in moiramide B will be discussed in section 5.3.5.

5.3.3. Moiramide C (40)

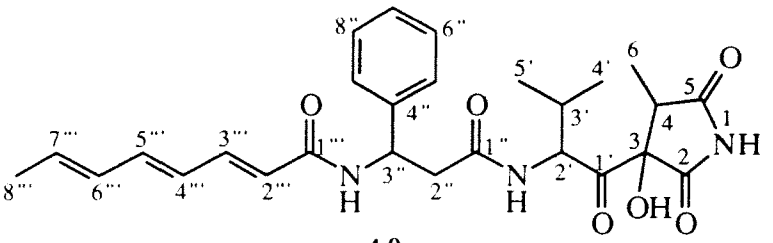

40

Moiramide C (**40**) was isolated as an amorphous white solid. A molecular ion in the HREIMS at m/z 495.2379 corresponded to a molecular formula of $C_{27}H_{33}N_3O_6$ (ΔM +0.9 mmu).The molecular formula of **40** indicated that the molecule had thirteen sites of unsaturation. Examination of the ^{1}H and ^{13}C NMR data for moiramide C (Table 7) revealed that it contained the octatrienoyl and β-phenylalanine fragments present in moiramide A and the valine moiety present in moiramide B (**39**).

The acylsuccinimide portion of moiramide C seemed to be different from that in moiramide B. From the ^{1}H NMR spectrum of moiramide C (Figure 36) it was apparent that the resonance assigned to H3 in moiramide B was absent in moiramide C and the proton resonance at δ 2.89 (H4) in moiramide C was simplified to a quartet. These data together with the appearance of a sharp singlet at δ 6.99 in the ^{1}H NMR spectrum of moiramide C suggested the presence of a hydroxyl functionality at C3. Further support for the hydroxyl functionality came from the presence of a resonance at δ 86.8 (C3) in the ^{13}C NMR spectrum (Figure 37) that had no HMQC correlation (Figure 38) but was correlated to the hydroxyl proton at δ 6.99 and to the H1 imide proton at δ 11.41 in the HMBC spectrum (Figure 39).

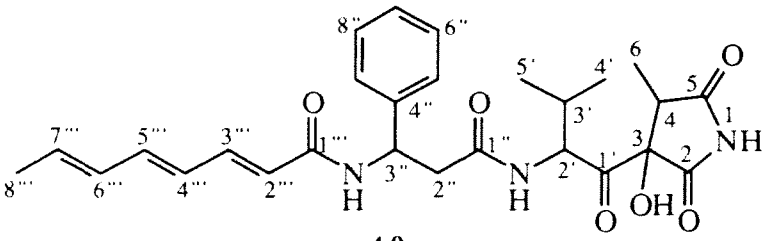

40

Table 7. ^{1}H and ^{13}C NMR data for moiramide C (**40**).

C#	$\delta^{13}C$[a]	$\delta^{13}H$[b]	COSY	HMBC[c]
1	—	11.41,bs	—	—
2	174.8	—	—	—
3	86.8	—	—	H1,3-OH
4	48.6	2.89,q(7.1)	H6	H1,H6
5	176.6	—	—	H4,H6
6	7.7	0.71,d(7.1)	H4	H4
3-OH	—	6.99,s	—	—
1'	208.6	—	—	H4,H2',3-OH
2'	58.0	5.18,dd(9.4,3.4)	2'-NH,H3'	H4',H5'
3'	27.4	2.50,m	H2',H4',H5'	H2',H5',H5'
4'	15.9	0.61,d(6.8)	H3'	H2',H5'
5'	19.7	0.81,d(6.8)	H3'	H4'
2"-NH	—	7.83d(9.4)	H2'	—
1"	169.5	—	—	2'-NH,H2",H3"
2"	41.8	2.66,d(7.4)	H3"	H3"
3"	49.9	5.25,m	H2",3"-NH	H2"
4"	142.7	—	—	H2", H3"
5"	126.3	7.3	—	—
6"	128.0	7.3	—	—
7"	126.7	7.19,m	—	—
8"	128.0	7.3	—	—
9"	126.3	7.3	—	—
3"-NH	—	8.33,d,(8.5)	H3"	—
1"'	164.1	—	—	3"-NH,H2"'
2"'	124.2	5.99,d(15.1)	H3"'	—
3"'	139.2	6.98,dd(15.1,11.4)	H2"',H4"'	H5"'
4"'	128.0	6.24,dd(15.0,11.4)	H3"',H5"'	—
5"'	138.8	6.53,dd(15.0,10.9)	H4"',H6"'	—
6"'	131.4	6.18,ddd(15.0,10.9,1.5)	H5"',H7"'	H4"',H8"'
7"'	133.2	5.90,m	H6"',H8"'	H5"',H8"'
8"'	18.2	1.76,d(6.4)	H7"'	—

[a] Recorded in DMSO-d_6 at 125 MHz. Chemical shifts in ppm relative to solvent.
[b] Recorded in DMSO-d_6 at 400 MHz. Chemical shifts in ppm relative to solvent.
[c] Carbons in the carbon # column are correlated to the listed proton resonances.

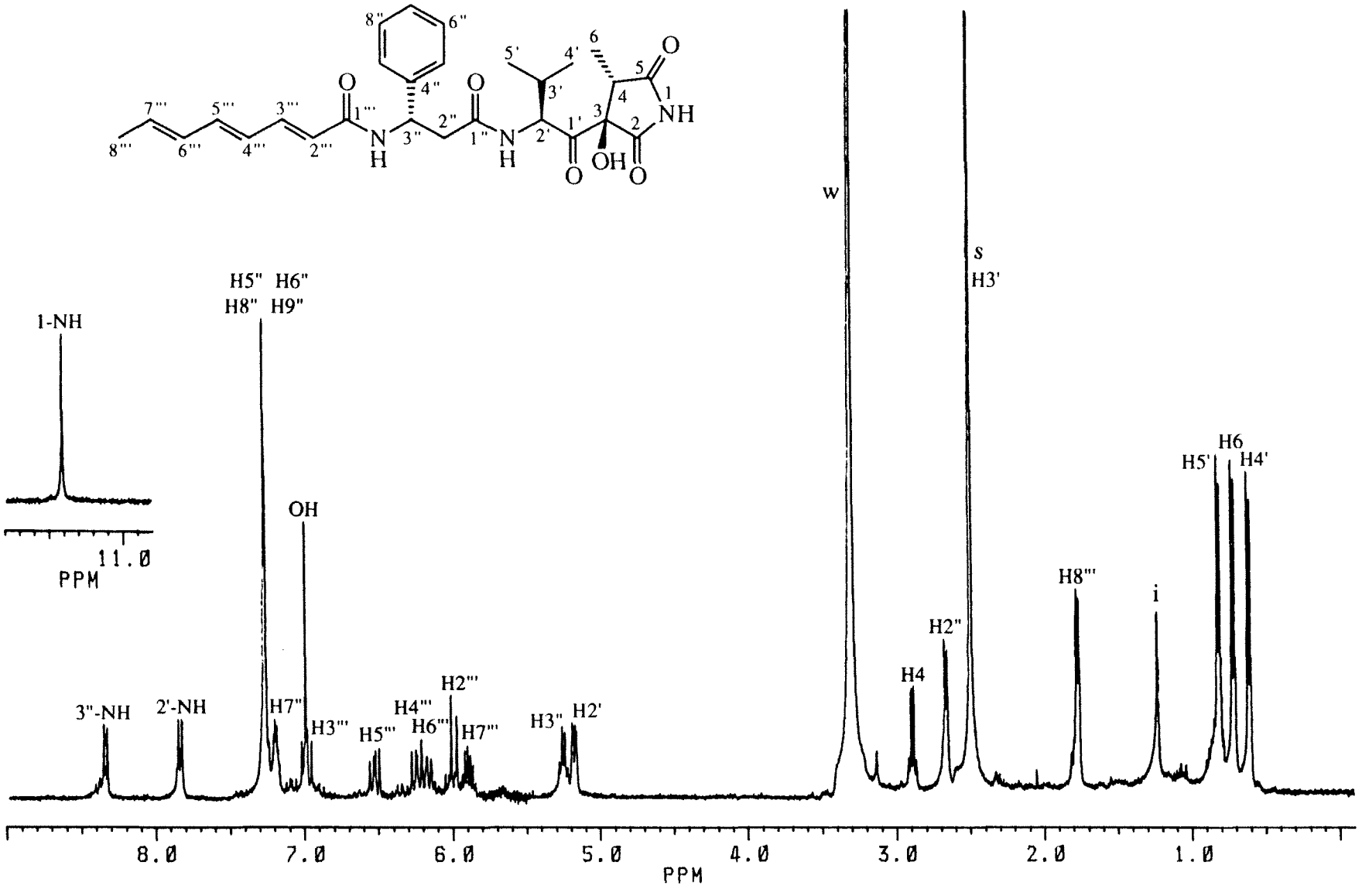

Figure 36. ^{1}H NMR spectrum of moiramide C (**40**) (400 MHz, DMSO-d_6).

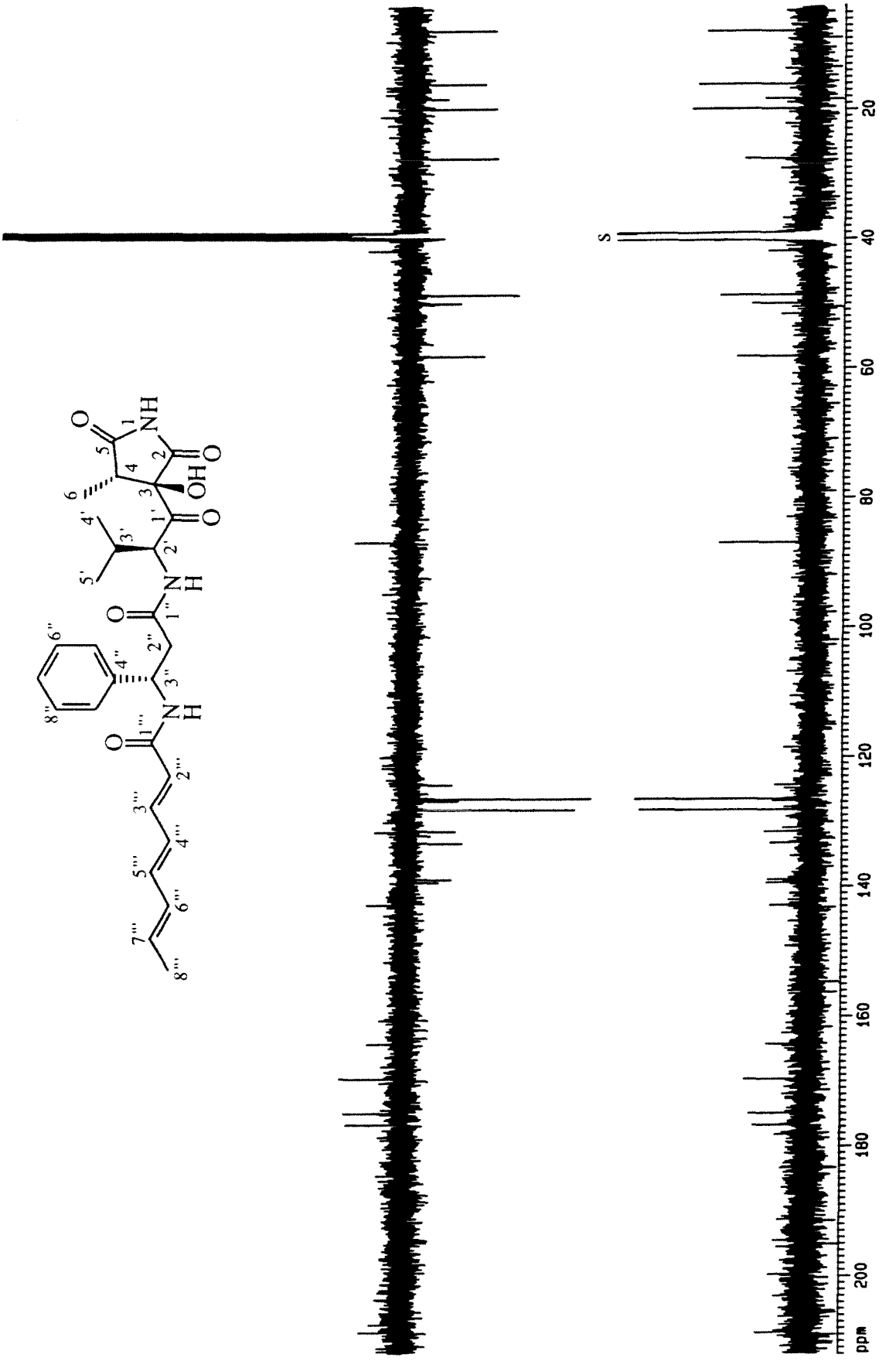

Figure 37. ^{13}C and APT NMR spectra of moiramide C (**40**) (125 MHz, DMSO-d_6).

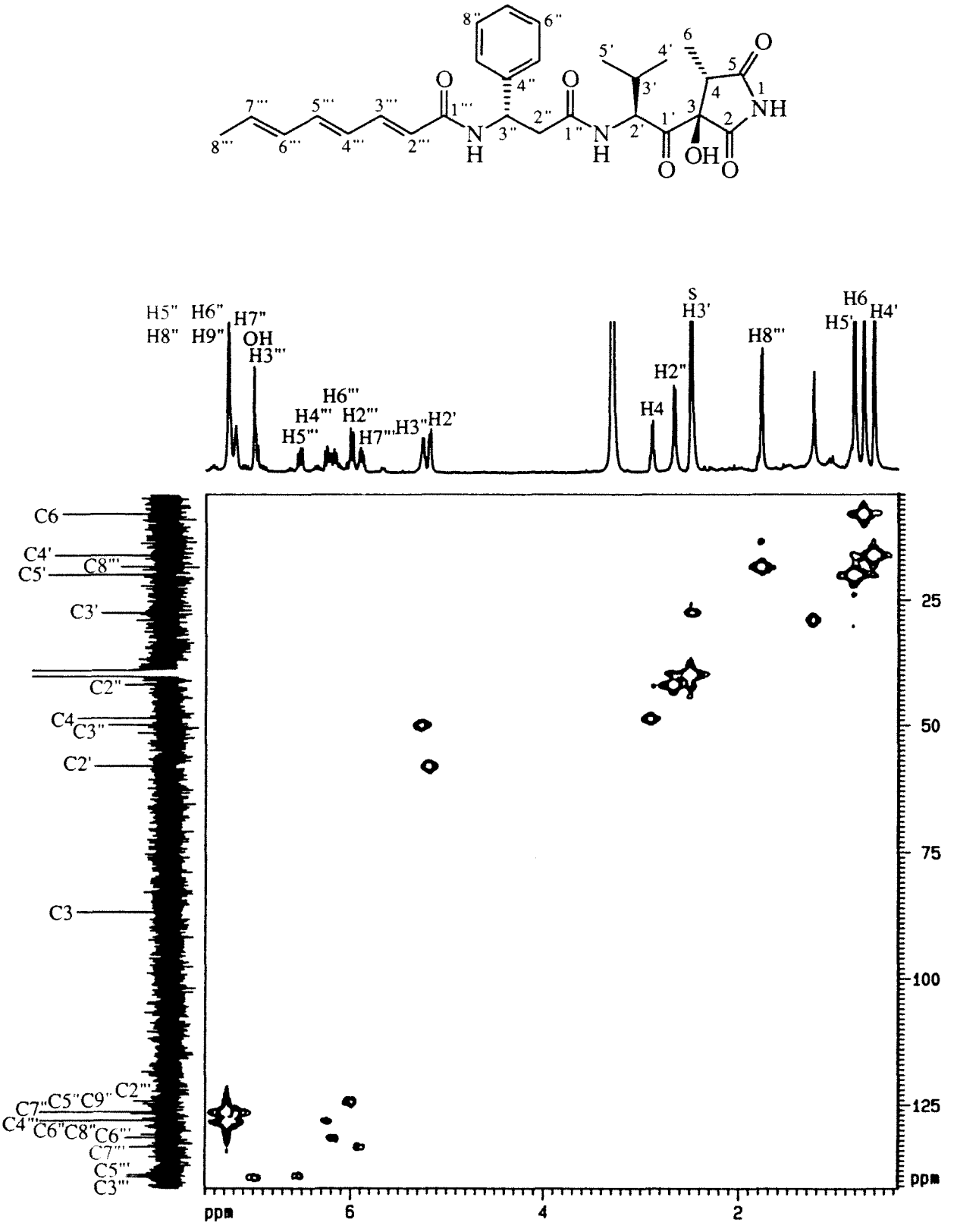

Figure 38. HMQC NMR spectrum of moiramide C (**40**) (500 MHz ^{1}H NMR, DMSO-d_6).

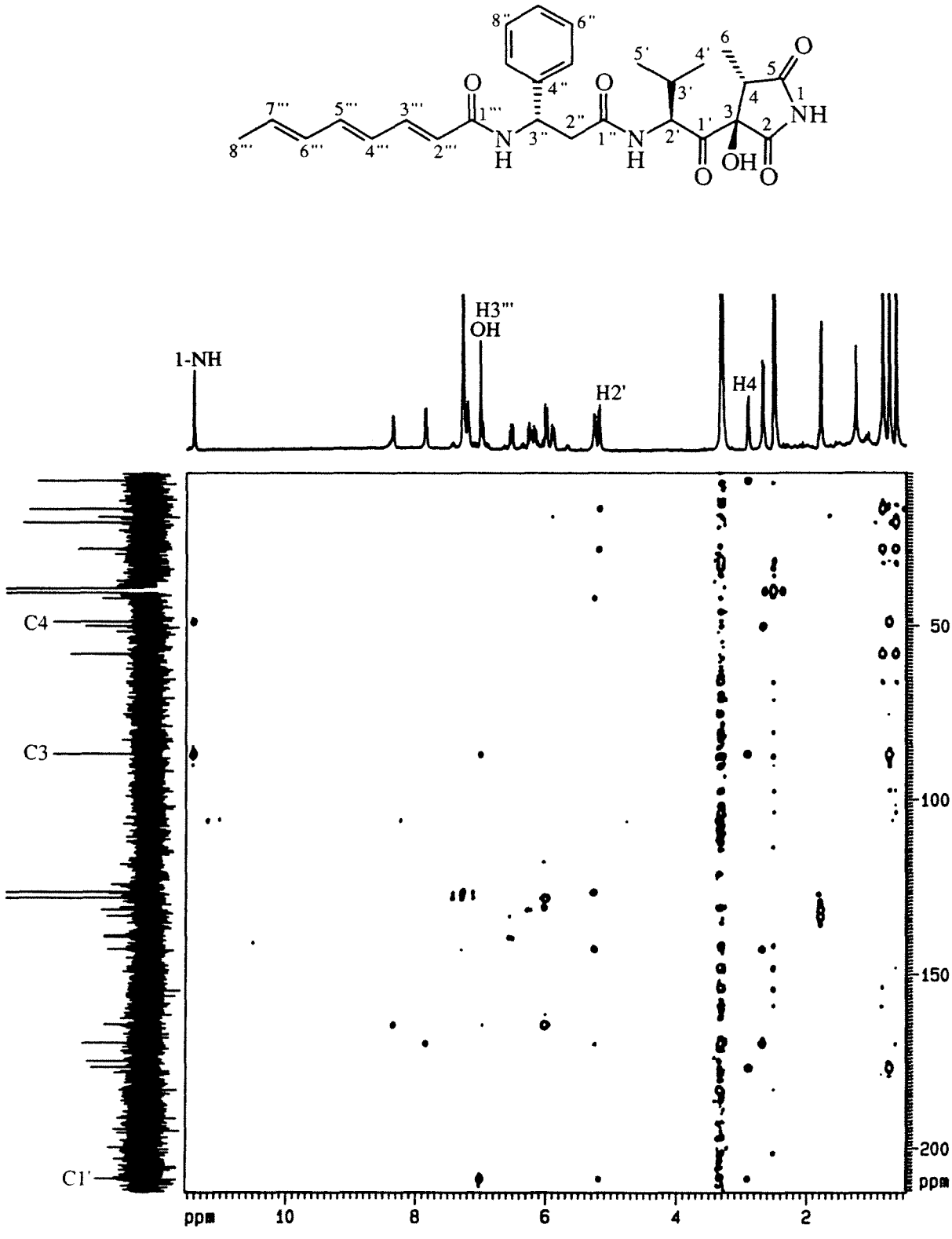

Figure 39. HMBC NMR spectrum of moiramide C (**40**) (500 MHz ^{1}H NMR, DMSO-d_6).

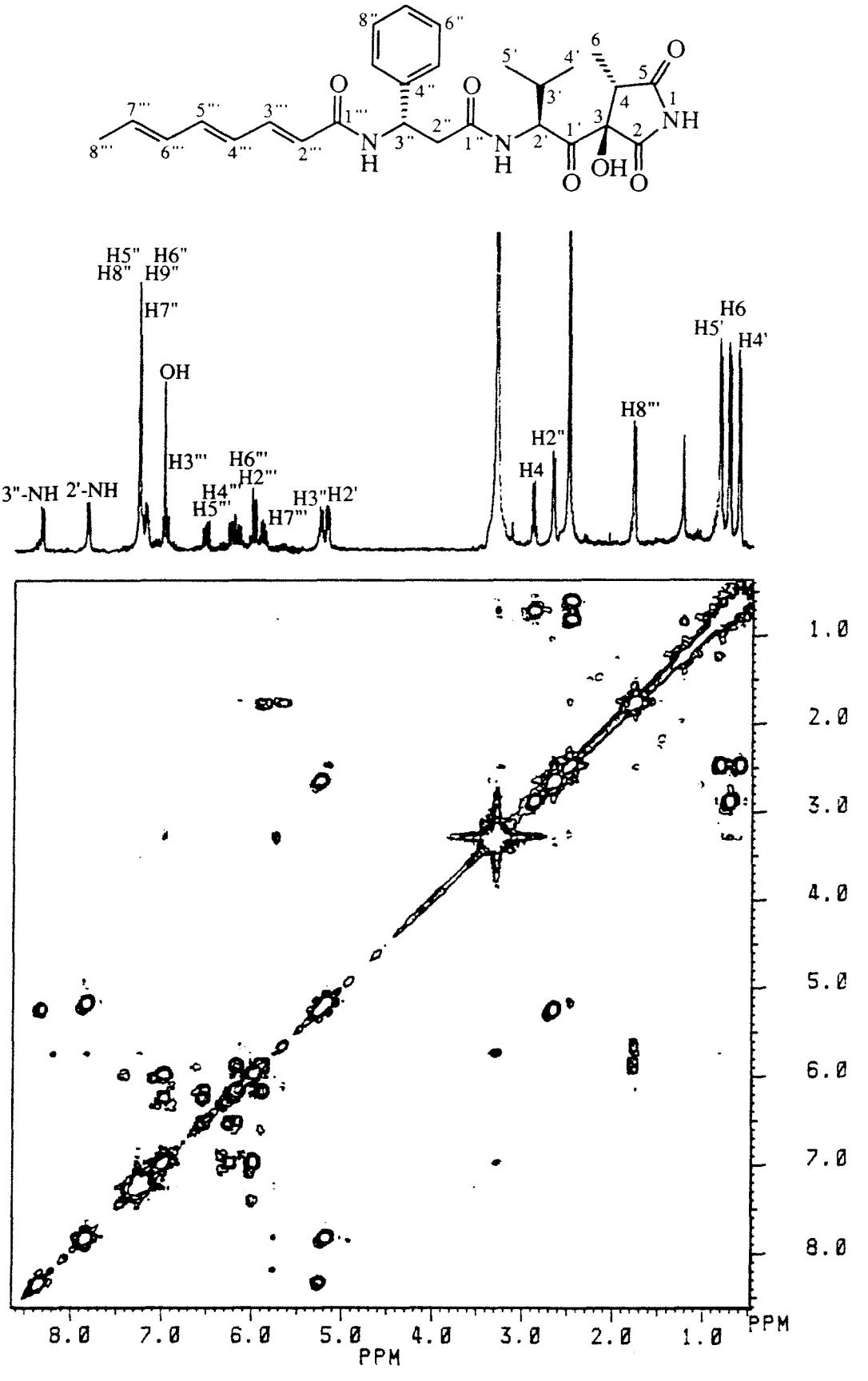

Figure 40. ^{1}H COSY NMR spectrum of moiramide C (**40**) (400 MHz, DMSO-d_6).

The hydroxyl proton at δ 6.99 (3-OH) also gave an HMBC correlation to the carbonyl resonance at δ208.6 (C1'). The COSY NMR data (Figure 40) supported the proposed connectivities in moiramide C (**40**).

Comparison of the ^{1}H NMR data for moiramide C with the NMR data of the octatrienoyl fragment of moiramide A suggested an all E configuration for the olefinic double bonds. NOE difference experiments (Figure 41) established a trans relative stereochemistry of the methyl and hydroxyl substituents on the acylsuccinimide ring. Irradiation of the signal for H4 resulted in the enhancement of the hydroxyl proton (3-OH) signal, and the H4 signal was enhanced by the irradiation of the hydroxyl proton resonance at δ 6.99.

The NMR data for moiramide C did not provide any information about the relative stereochemistry at C2' or C3", however, the data supported the proposed constitution of **40**. The stereochemistry of the chiral centers in moiramide C will be discussed in section 5.3.5.

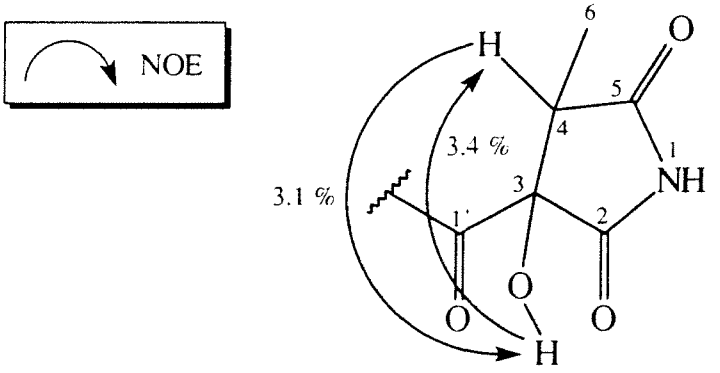

Figure 41. Results from selected NOE difference experiments on moiramide C.

5.3.4. Known compounds from *Pseudomonas fluorescens*

Two known compounds andrimid (**41**)[51] and prodigiosin (**33**)[34] were isolated from the ethyl acetate extract of a *P. fluorescens* culture. Andrimid was isolated as an amorphous white solid. Its structure was determined by the comparison of its ^{1}H and ^{13}C NMR data (see experimental) with published results.[51a] A molecular ion in the HREIMS at m/z 479.2416 confirmed the molecular formula $C_{27}H_{33}N_3O_5$ (ΔM -0.4 mmu).

Andrimid was initially isolated from cultures of *Enterobacter* sp. that is found as an intracellular symbiont of the brown planthopper *Nilaparvata lugens*. Andrimid exhibits potent antibiotic activity against *Xanthomonas campestris* pv. *orzae*, the pathogen that causes bacterial blight in rice plants.

Prodigiosin, isolated as a red powder, was identified by the comparison of its ^{1}H NMR and MS data with literature values.[34p] A molecular ion at 323.2006 in the HREIMS corresponded to a molecular formula of $C_{20}H_{28}N_3O$ (ΔM +0.8 mmu). This pigment was isolated from liquid cultures of *Serratia odorifera* discussed previously in this thesis.

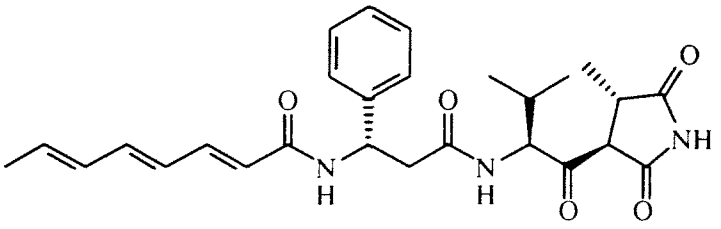

41 Andrimid

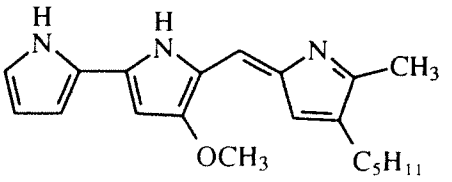

33 Prodigiosin

5.3.5. The absolute stereochemistry of moiramides A, B and C

The absolute configuration of the four chiral centers in andrimid (**41**), originally isolated from cultures of an *Enterobacter* sp., were determined to be (3R,4S,2'S,3"S) by amino acid analysis[51a] and stereocontrolled synthesis.[51b] There is no circular dichroism or rotation information in the literature for this sample that would provide a quick method for confirming the absolute configuration of the andrimid isolated from *P. fluorescens*. However, it has been assumed that the andrimid isolated from *P. fluorescens* is identical to the sample originally isolated from the bacterium *Enterobacter* sp.. Families of related natural products generally have the same absolute configurations. It has also been assumed that the absolute configuration of the chiral centers in moiramides A and B are the same as those in andrimid based upon their structural similarity.

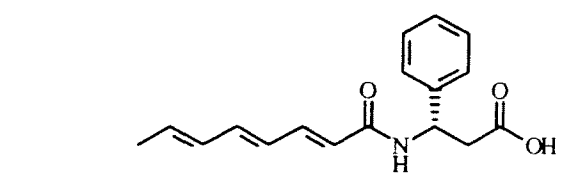

38 Moiramide A

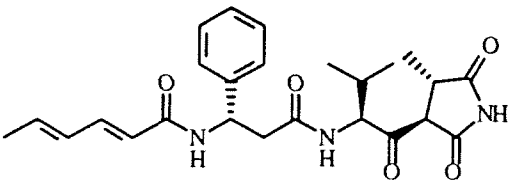

39 Moiramide B

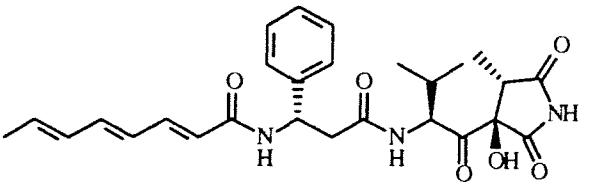

40 Moiramide C

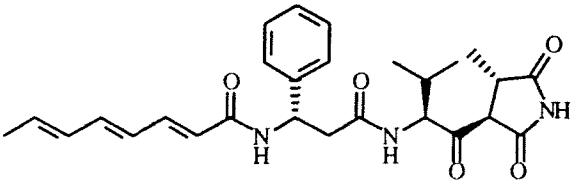

41 Andrimid

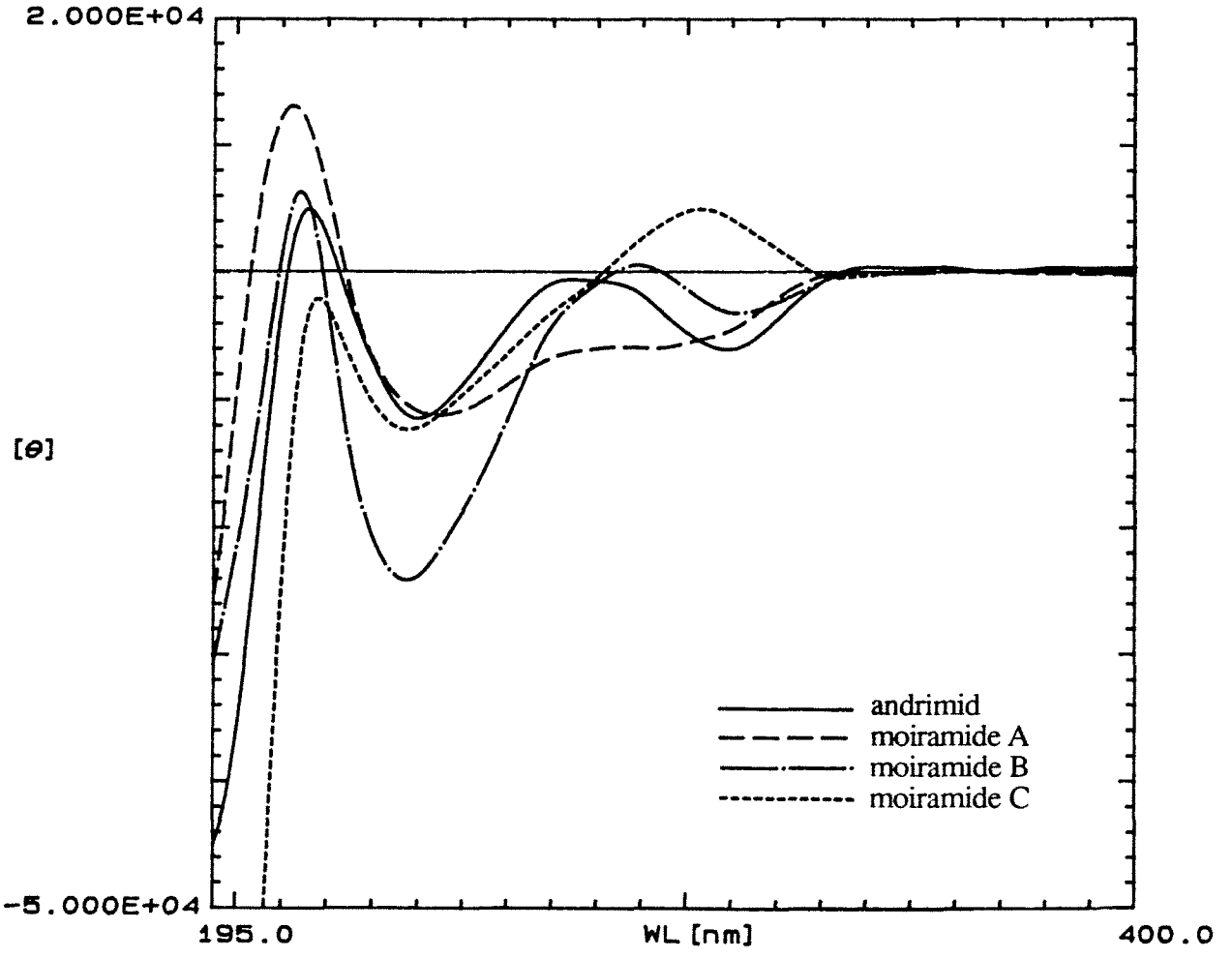

Figure 42. Circular Dichroism spectra of andrimid (**41**) and moiramides A (**38**), B (**39**) and C(**40**) (recorded in methanol).

In an attempt to verify the configurations of moiramides A (**38**), B (**39**) and C (**40**) circular dichroism (CD) spectra of andrimid (**41**) and compounds **38**, **39**, and **40** were recorded in methanol (Figure 42).

The major Cotton effect observed for moiramide A (**38**) at 245 nm had the same sign as that observed for andrimid. This suggested that C3" in moiramide A had the same configuration as in andrimid. This band, also seen in moiramides B and C, as are well as in andrimid can be tentatively assigned to the β-phenylalanine moiety present in all four compounds.

The CD spectrum of moiramide B is similar to that for andrimid suggesting that the configurations of the four chiral centers in moiramide B (**39**) are identical to those in andrimid. Further evidence for this assignment was provided by the NMR data. The NMR data for moiramide B was nearly identical to that for andrimid except for the resonances assigned to the polyene fragment.

A trans relative stereochemistry of the methyl and hydroxyl substituents on the acylsuccinimide ring in moiramide C was established by NOE difference experiments. If the configuration at C4 in moiramide C (**40**) is assumed to be identical to the configuration in andrimid then the stereochemistry of this compound is as depicted in structure **40** (Figure 42).

5.3.6. Antimicrobial activity of andrimid and moiramides A, B and C

The ethyl acetate extract from the solid culture of *P. fluorescens* had shown antibacterial activity against *Staphylococcus aureus* and methicillin-resistant *S. aureus*. Moiramides A to C and andrimid were tested for antimicrobial activity against a variety of microorganisms. Moiramides A and C were found to be inactive against the test organisms. The in vivo antimicrobial activities of moiramide B and andrimid are listed in Table 8 along with the results from the known antibiotic ciprofloxacin. The antibiotic activities are recorded as minimum inhibitory concentrations (MIC), that is, the smallest amount of compound needed to inhibit the growth of the test organism.

Table 8. Antimicrobial activities of moiramide B (**39**), andrimid (**41**) and ciprofloxacin.

	Minimum inhibitory concentration μg/mL		
Test Organism	Moiramide B	Andrimid	Ciprofloxacin
Staphylococcus aureus	2	4	0.25
S. aureus (methicillin-resistant)	0.5	2	0.25
S. aureus (oxacillin-resistant)	1	8	
S. aureus (oxacillin, gentamicin, ciprofloxacin-resistant	0.5	2	
Enterococcus faecium (vancomycin-resistant)	4	32	0.12
Escherichia coli (permeability mutant)	0.25	2	≤0.015
Escherichia coli	16	64	0.03
Pseudomonas aeruginosa	>128	>128	0.50
Candida albicans	>128	>128	≤0.06

Moiramide B (**39**) and andrimid (**41**) both showed significant antibacterial activity against the test organisms. Both compounds exhibited activity only against Gram-positive bacteria. They did not show significant activity against the Gram-negative bacterium *Pseudomonas aeruginosa* or the yeast *Candida albicans*. In contrast, the known antibiotic ciprofloxacin exhibited a broad spectrum of activity against both Gram-positive and Gram-negative bacteria as well as the yeast *Candida albicans*. Moiramide B and andrimid exhibited potent antibacterial activity against drug-resistant strains of the human pathogen *Staphylococcus aureus*. Andrimid was found to have only weak in vivo antibacterial activity against *S. aureus* in mice ($ED_{50} \geq 16$ mg/kg) and was found not to be cytotoxic.

McWhorter et al. observed a strict requirement for the methyl group and stereochemistry at the C3 and C4 positions of the acylsuccinimide ring for antimicrobial activity in andrimid (**50**).[51b] This observation was reinforced by the observed antimicrobial activities of moiramides A to C. Moiramide A with no acylsuccinimide ring and moiramide C with the presence of a 3R hydroxyl functionality both showed no antibacterial activity. Only moiramide B and andrimid with a 4S-methyl group were biologically active.

5.4. Conclusion

Examination of the ethyl acetate extracts of a solid culture of *Pseudomonas fluorescens* obtained from an unidentified tunicate in Moira Sound, Alaska, led to the isolation of moiramides A (**38**), B (**39**) and C (**40**). The known compounds andrimid (**41**) and prodigiosin (**33**) were also isolated from this extract.

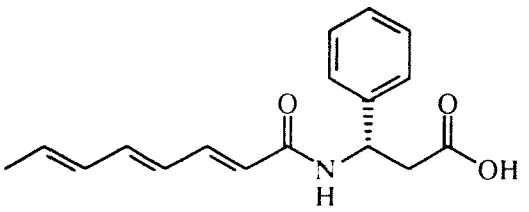

38 Moiramide A

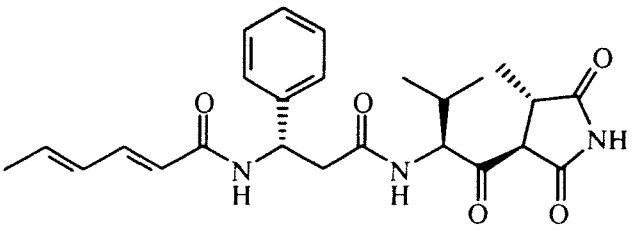

39 Moiramide B

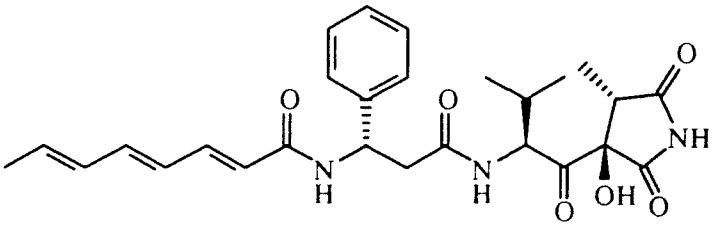

40 Moiramide C

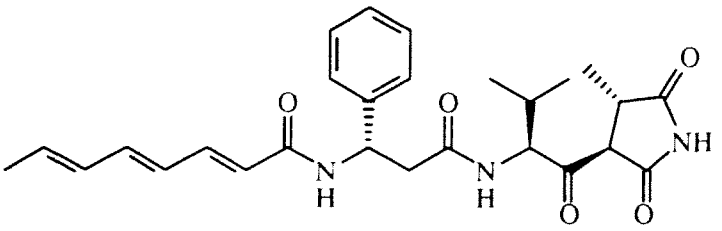

41 Andrimid

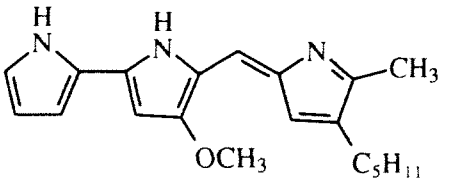

33 Prodigiosin

The crude extract showed antimicrobial activity against *Staphylococcus aureus* and methicillin-resistant *S. aureus*. Moiramide B and andrimid proved to be the compounds responsible for this activity.

6. BIOSYNTHESIS OF ANDRIMID

6.1. Biogenesis

The biogenetic origin of the 3-acyl-4-methylsuccinimide fragment in andrimid (**41**) and moiramides B (**39**) and C (**40**) was not immediately obvious from their structures and a search of the literature failed to provide any clear precedent for the biogenetic origin of this fragment. Four alternative biogenetic origins (**A**, **B**, **C**, **D**) for the acylsuccinimide ring in andrimid that seemed reasonable possibilities at the outset of this study are depicted in Figure 43. The four pathways all start with linear fragment R corresponding to moiramide A (**38**).

In pathway **A** four of the succinimide ring carbons are derived from glutamic acid. Nucleophilic addition of glutamic acid to fragment R followed by ring closure and loss of the glutamate C1 by decarboxylation provides the acylsuccinimide ring. Subsequent methylation, presumably from S-adenosylmethionine, at C4 of the succinimide ring leads to andrimid. This is an attractive pathway since the amine group of glutamic acid provides the nitrogen in the acylsuccinimide ring of the natural product. Precedent for the loss of C1 of glutamate is provided by the formation of the maleimide ring during the biosynthesis of showdomycin.[53]

Succinic acid provides the four succinimide ring carbons in pathway **B**. Nucleophilic addition of succinic acid to the carbonyl carbon of a valine moiety, the introduction of nitrogen, possibly from ammonia, and ring closure leads to the formation of the succinimide ring. Subsequent methylation, presumably from S-adenosylmethionine, would lead to the natural product. This is an attractive pathway since the correct oxidation state exists at C5.

Pathways **C** and **D** are based on a proposal put forward by McWhorter et al. during the stereocontrolled synthesis of the acylsuccinimide ring in andrimid.[51b] The synthesis was based on an expected biogenetic pathway in which a valine residue, accounting for C1' to C5', is homologated with an acetate unit presumably via malonyl-CoA.

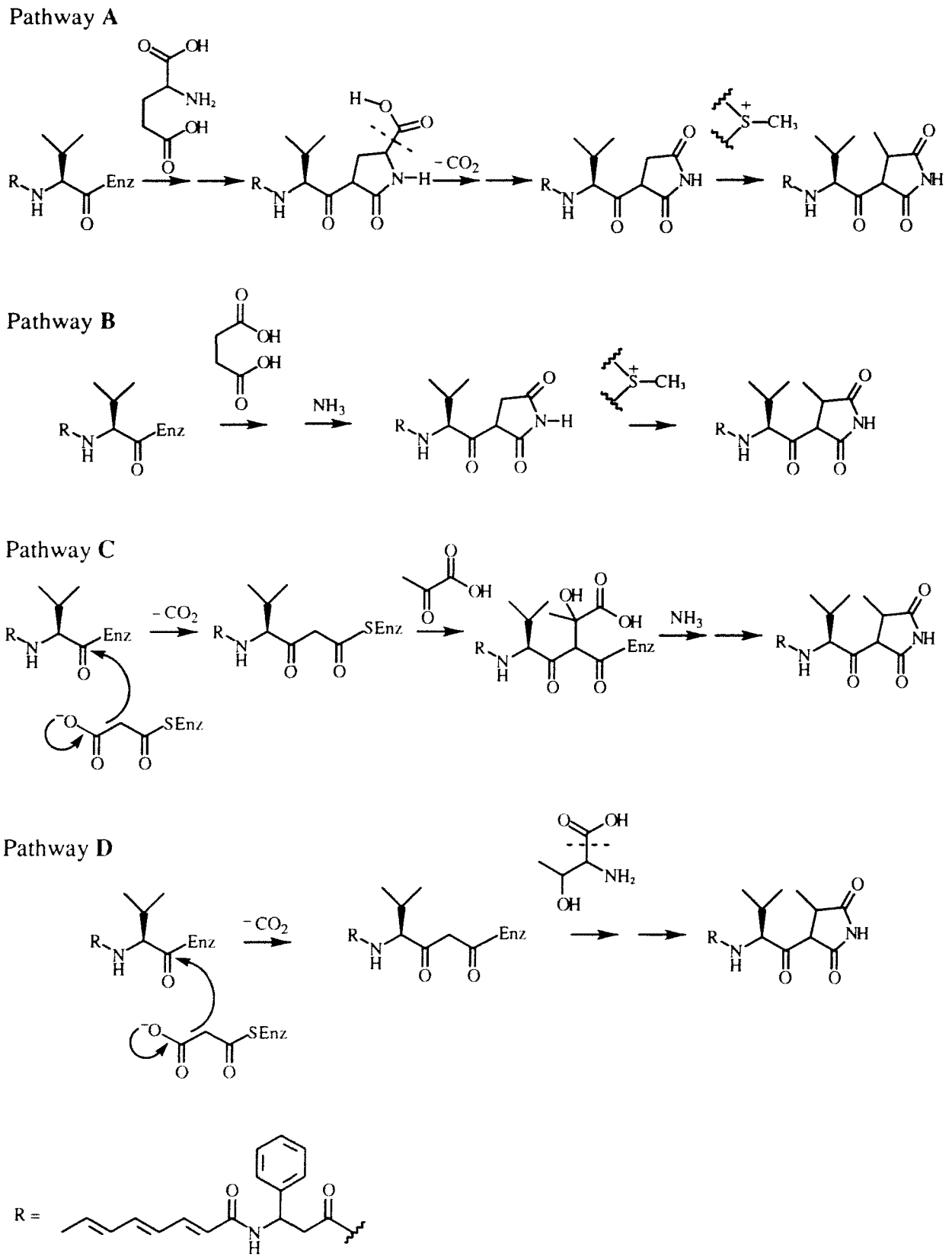

Figure 43. Alternative biogenetic origins of the acylsuccinimide ring in andrimid.

This acetate unit would account for C2 and C3 of the acylsuccinimide ring. McWhorter et al. did not propose a biogenetic origin for the carbons C4, C5 and C6 or the nitrogen of the acylsuccinimide ring.

Pathway **C** involves the homologation of the valine moiety of fragment R by an acetate unit to form a new γ-amino-β-keto acid. The C6 methyl group as well as C4 and C5 of the acylsuccinimide ring may originate from pyruvic acid. The introduction of nitrogen, possibly from ammonia, and ring closure leads to andrimid. This is an attractive pathway since the correct oxidation state exists at C5 of the acylsuccinimide ring and pyruvic acid provides the C4 methyl branch.

In the fourth proposal, pathway **D**, the valine moiety of fragment R is homologated by an acetate unit, presumably via malonyl-CoA. The C6 methyl branch as well as the C4, C5 and the nitrogen of the acylsuccinimide ring may originate from threonine. Loss of the threonine C1 by decarboxylation and ring closure would lead to the natural product. This is an attractive pathway since threonine provides the C4 methyl branch and the ring nitrogen.

A precedent for the homologation of an amino acid residue by an acetate unit is found in the biosynthesis of (3S,4R)-4-amino-3-hydroxy-6-methylheptanoic acid (AHMHA).[54a] In AHMHA an L-leucine residue is homologated by an acetate unit. This unusual amino acid is a component of the pepstatins (for example **42**)[54] and pepsidines.[55] Another unusual amino acid, 4-amino-3-hydroxy-5-phenylpentanoic acid (AHPPA), found in the aphatinins (for example **43**)[56] may be derived from the homologation of phenylalanine by acetate.

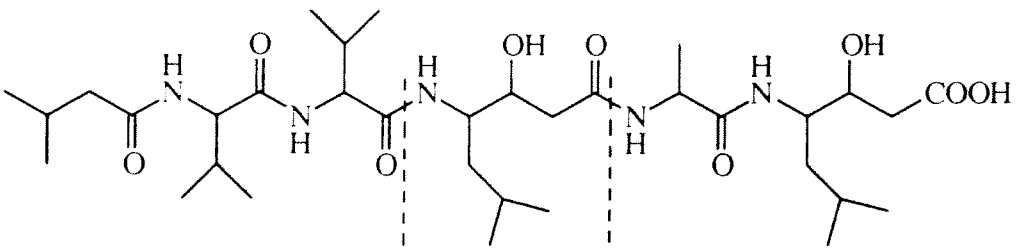

42 Pepstatin A

AHMHA

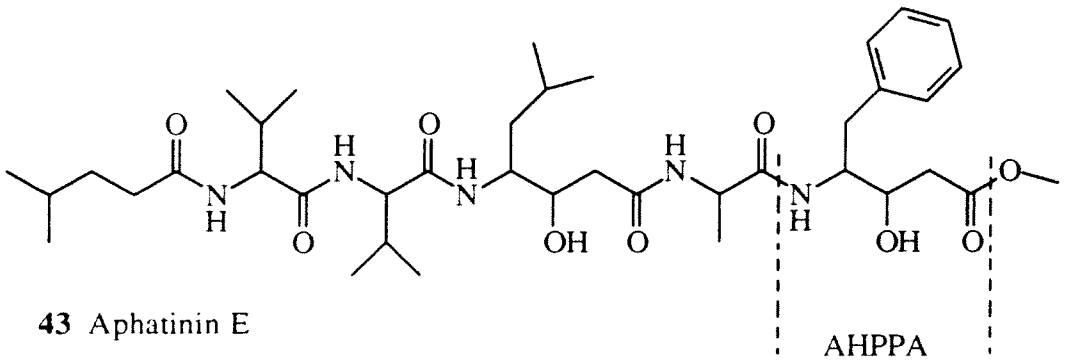

43 Aphatinin E

AHPPA

In an attempt to distinguish between the various possible biogenetic origins of the acylsuccinimide ring in andrimid depicted in Figure 43, the following series of stable isotope feeding experiments were proposed. 1) A feeding experiment using [1-^{13}C]valine would confirm that carbons C1' to C5' in pathways **A** to **D** are derived from valine. 2) Feeding [1-^{13}C]sodium acetate would distinguish between pathways **A/B** and **C/D**. If acetate was not incorporated into the C2 of the acylsuccinimide ring this would support pathways **A** and **B**. To distinguish between pathways **A** and **B** ^{13}C labelled glutamic acid and succinic acid would be fed in separate experiments. 3) Feeding [2-^{13}C,^{15}N]glutamic acid would determine if the carbons C2 to C4 and the ring nitrogen in pathway **A** are derived from glutamic acid. 4) Incorporation of [1,4-$^{13}C_2$]succinic acid into andrimid would support pathway **B** in which carbons C2 to C4 of the acylsuccinimide ring originate from succinic acid. 5) The origin of the C6 methyl group in pathways **A** and **B** can be probed by feeding [methyl-^{13}C]methionine. Incorporation of acetate into C2 of the acylsuccinimide ring in experiment 2 would support pathways **C** and **D**, and ^{13}C labelled pyruvic acid and threonine would be fed in separate experiments to distinguish between these two pathways. The incorporation of valine and acetate incorporation into C2 of the acylsuccinimide ring would provide evidence for the proposal by McWhorter et al. in which a valine residue is homologated by an acetate unit. 6) Feeding [1-^{13}C]sodium pyruvate would determine if the C6 methyl group as well as the C4 and C5 of the acylsuccinimide ring in pathway **C** originate from pyruvic acid. In this pathway the nitrogen may come from ammonia.

7) Feeding [2-^{13}C,^{15}N]threonine would determine if the C4 methyl branch as well as the C4, C5 and the nitrogen in pathway **D** are derived from threonine.

6.2. Results and Discussion

The labelled precursors [1-^{13}C: 0.5 g]valine, [1-^{13}C: 1 g]sodium acetate and [1,2-$^{13}C_2$: 0.5 g]sodium acetate were dissolved in water and filter sterilized before adding to the culture medium (4 x 500 mL tryptic soy broth, 1 % agar, 1 % sodium chloride) just before pouring the media into aluminium trays (23 x 33 x 5 cm) in separate experiments. The trays were each inoculated with 2 mL of an actively growing liquid culture of *Pseudomonas fluorescens* and incubated for 3 days at room temperature. After this time the cells were gently scraped off the solid media. The solid media was extracted with ethyl acetate to yield 0.65 g of a pungent dark red oil. The crude extract was chromatographed on a Sephadex LH-20 column eluted with ethyl acetate/methanol/water (8:2:1). The andrimid containing fractions were pooled and concentrated in vacuo to give a pink powder. Further purification by reversed-phase column chromatography and HPLC (eluent: 65:35 methanol/0.025 M phosphate buffer, pH 6.87) gave andrimid (50 mg). The incorporation of the labelled precursors into andrimid was determined by the comparison of the ^{13}C NMR spectrum of andrimid with that of a natural abundance spectrum run under identical conditions and the results are summarized in Table 9.

Andrimid, isolated from the feeding experiment with [1-^{13}C]valine displayed one enhanced peak in the ^{13}C NMR spectrum at δ 203.3 (Figure 44). A specific incorporation of 22.4 % at the carbonyl carbon of the valine moiety was observed thus supporting the proposal by McWhorter et al., and the pathways **A** to **D** (Figure 43).

The feeding experiment using [1-^{13}C]sodium acetate led to the isolation of andrimid that showed five enhanced peaks in the ^{13}C NMR spectrum (Figure 45) with enrichment at C2, C1''', C3''', C5''' and C7'''. This suggested that four molecules of acetate were used in the biosynthesis of the octatrienoyl fragment.

Table 10. Stable isotope incorporation data for andrimid (**41**).

		[1-^{13}C] valine	[1-^{13}C] acetate	[1,2-$^{13}C_2$]acetate			[1,2-$^{13}C_2$]glycine		[1,2-$^{13}C_2$,^{15}N]glycine				
C#	δ ^{13}C[a]	Specific Incorporation[b]		doublets[b,c]	singlets[b]	$^1J_{C,C}$ Hz	doublets[b,c]	singlets[b]	doublet of doublets[b,c]	doublets[b,c]	$^1J_{C,C}$ Hz	$^1J_{C,N}$ Hz	$^2J_{C,N}$ Hz
2	173.6	0.0	18.4	17.0	0.9	42.8	1.2	0.1					
3	57.8	-0.1	-0.2	16.2	1.1	42.8	0.3	0.7					
4	38.9	0.0	1.1		0.3		29.3	1.9	10.2		45.8		5.7
5	179.9	0.0	-0.1		-0.1		30.0	12.5	9.7	2.3	45.8	12.4	
6	14.5	0.0	0.0		17.0		1.1	1.0					
1'	203.3	22.4	0.1		-0.1			0.1					
2'	63.0	0.0	0.1		-0.1			0.1					
3'	28.1	0.0	0.0		-0.1			0.1					
4'	17.2	0.0	0.0		0.0			0.0					
5'	19.3	0.1	0.1		0.0			0.1					
1"	169.8	0.0	0.2		0.1			0.0					
2"	41.9	0.1	0.1		0.0			0.1					
3"	49.8	0.0	0.0		0.1			0.0					
4"	142.8	0.1	0.1		-0.1			0.0					
5"	126.4	0.0	-0.1		0.0			0.1					
6"	128.2	0.1	0.1		0.1			0.1					
7"	126.8	0.1	-0.1		0.0			0.0					
8"	128.2	0.1	0.1		0.1			0.1					
9"	126.4	0.0	-0.1		0.0			0.1					
1"'	164.2	0.1	21.7	24.9	1.7	64.4	1.3	2.5					
2"'	124.2	0.1	0.1	20.2	1.9	64.4	1.1	1.7					
3"'	139.4	0.1	17.7	17.7	1.9	56.3	1.1	2.5					
4"'	128.0	0.0	-0.3	14.5	2.1	56.2	0.9	1.6					
5"'	138.8	0.0	18.7	18.3	1.5	55.7	1.0	2.3					
6"'	131.4	0.1	-0.2	16.8	2.1	55.7	1.2	2.1					
7"'	133.3	0.1	17.2	19.0	1.6	43.0	1.0	2.5					
8"'	18.2	0.1	-0.1	18.9	1.1	43.0	1.4	2.1					

[a] Recorded in DMSO-d_6 at 125 MHz. Chemical shifts in ppm relative to solvent.

[b] Specific Incorporation = % enhancement above natural abundance = 1.1 % x ([integrated peak area of enriched signal - integrated peak area of natural abundance singlet] / integrated peak area of natural abundance singlet).[41]

[c] Integrated peak area of enriched signal = combined integrated area of the multiplet.

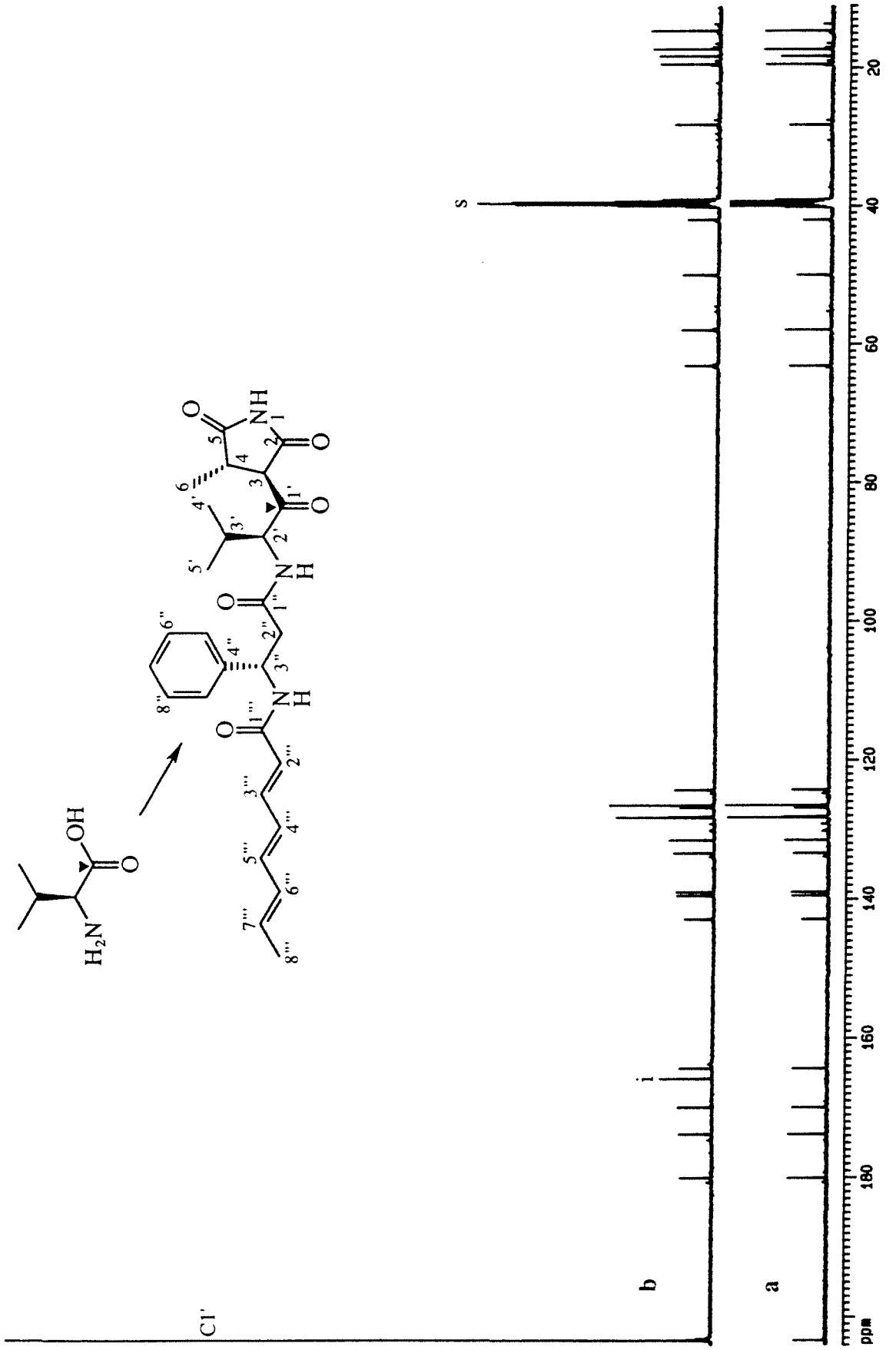

Figure 44. ^{13}C NMR spectra of a) andrimid (**41**) and b) **41** labelled by [1-^{13}C]valine (125 MHz, DMSO-d_6).

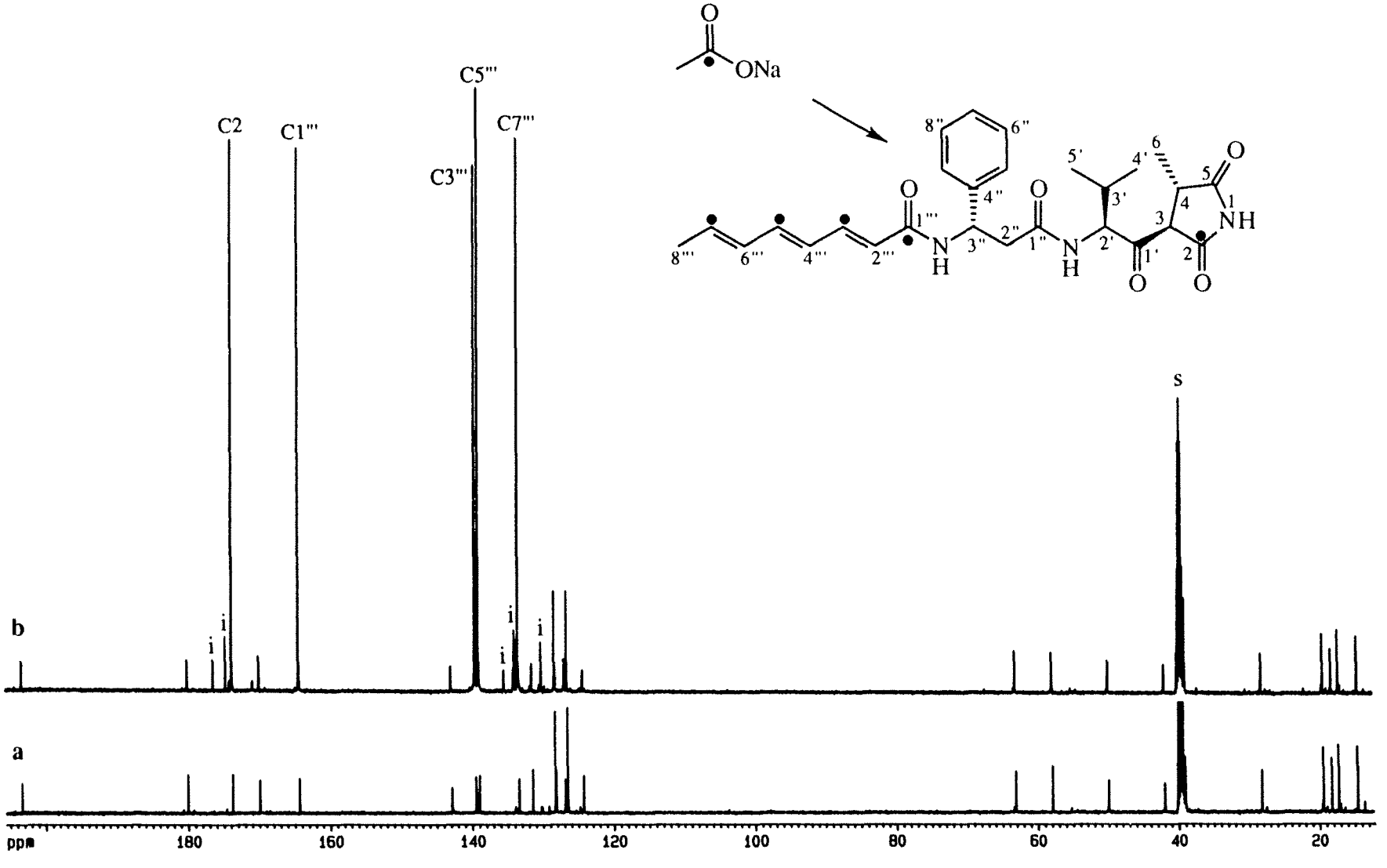

Figure 45. ^{13}C NMR spectra of a) andrimid (**41**) and b) **41** labelled by [1-^{13}C]sodium acetate (125 MHz, DMSO-d_6).

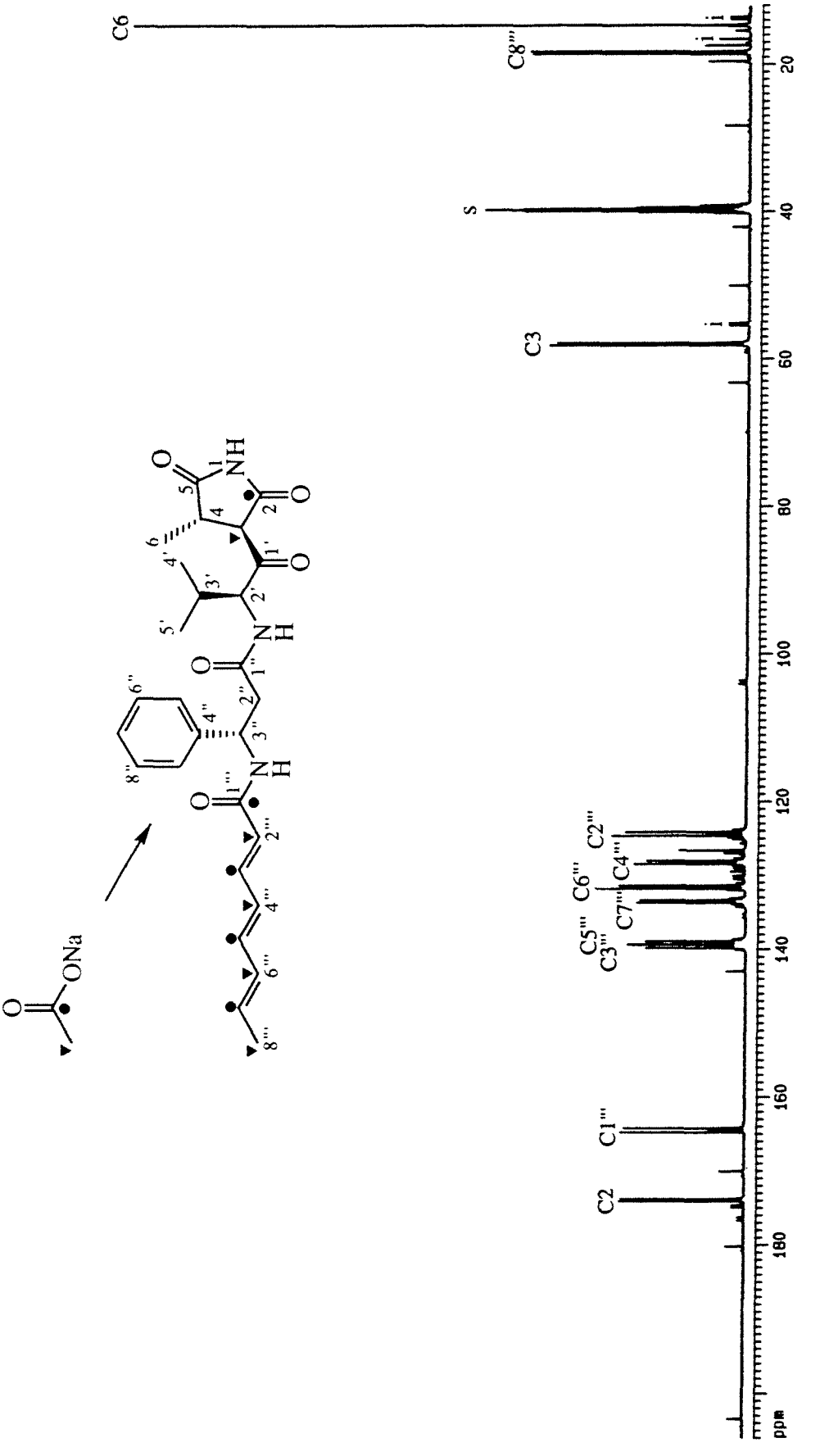

Figure 46. ^{13}C NMR spectrum of andrimid (**41**) labelled by [1,2-$^{13}C_2$]sodium acetate (125 MHz, DMSO-d_6).

Of greater interest was the efficient incorporation (18.4 % specific incorporation) of the labelled precursor into the carbonyl carbon, C2, of the acylsuccinimide ring. Again, this provided evidence for the proposal by McWhorter et al. in which a valine moiety is homologated with an acetate residue as depicted by pathways **C** and **D** in Figure 43. The observed labelling pattern ruled out the biogenetic pathways **A** and **B** in Figure 43 since C2 and C3 of the succinimide ring in these two pathways are not derived from acetate.

An incorporation study using [1,2-$^{13}C_2$]sodium acetate identified the intact acetate units. The proton decoupled ^{13}C NMR spectrum is provided in Figure 46. This experiment confirmed the incorporation of four acetate units into the octatrienoyl fragment. It also confirmed the incorporation of an intact acetate unit at C2/C3 of the acylsuccinimide ring. An interesting, though unexpected, result was provided by the enhancement of the C6 methyl resonance at δ 14.5 (17.0 % specific incorporation). This signal appeared as a singlet in the proton decoupled ^{13}C NMR spectrum suggesting that the methyl group was not incorporated as an intact acetate unit. The incorporation of intact acetate units lead to the appearance of doublets flanking a central singlet in the proton decoupled ^{13}C NMR spectrum. The central singlet is due to natural abundance ^{13}C in the unlabelled molecules and the doublet that is centered around the singlet is due to $^{13}C/^{13}C$ coupling in doubly labelled molecules. This enhancement of the C4 methyl group suggested that it was derived from the C2 of an acetate unit. The carbons C4 and C5 of the acylsuccinimide ring were not significantly enhanced by acetate. This experiment ruled out the biogenetic pathways **C** and **D** depicted in Figure 43. The C4 methyl branch in these two pathways is not derived from acetate.

The results from the acetate and valine feeding experiments provided evidence for the proposal by McWhorter et al. in which a valine moiety may be homologated with an acetate unit presumably via malonyl-CoA. The feeding experiments utilizing [1-^{13}C]valine and ^{13}C labelled acetate have not accounted for the carbons C4, C5 and the nitrogen of the succinimide ring. The unexpected labelling of the C6 methyl by C2 of acetate gave rise to the proposed pathway for the formation of the acylsuccinimide ring in andrimid utilizing valine, acetate and glycine that is depicted in Figure 47.

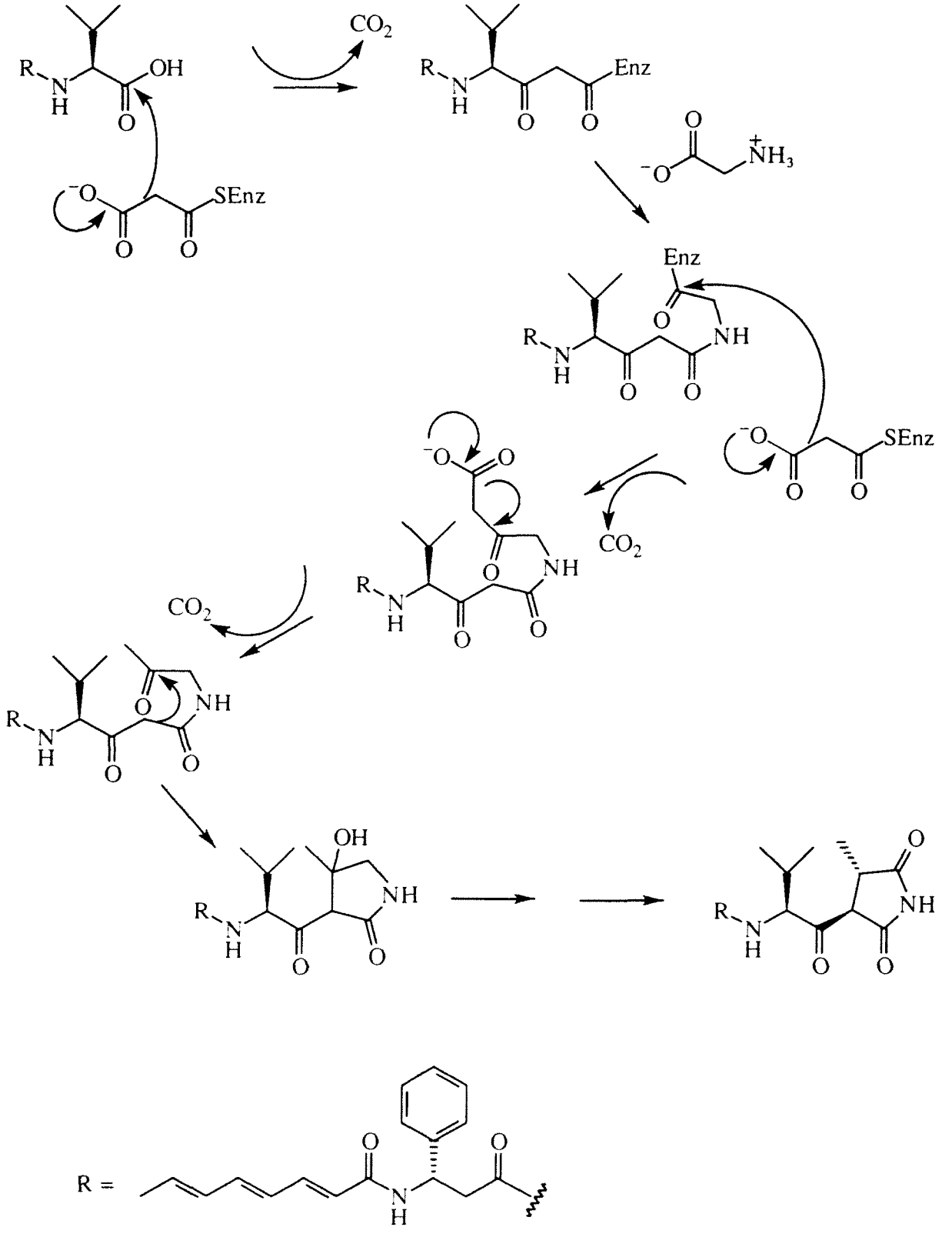

Figure 47. Proposed biogenesis of the acylsuccinimide ring in andrimid.

In this proposed pathway the valine moiety is homologated with an acetate unit via malonyl-CoA to give the new γ-amino-β-keto acid. This new amino acid would form a peptide bond with a molecule of glycine, which is in turn homologated to a second acetate unit. Decarboxylation at the terminal γ-amino-β-keto acid would lead to the methyl branch at C4. Ring closure followed by a change in oxidation state at C4 and C5 would lead to andrimid. To test this proposal a culture of *P. fluorescens* was fed both [1,2-$^{13}C_2$: 250 mg] and [1,2-$^{13}C_2$,^{15}N: 100 mg] labelled glycine in separate experiments using the same protocol used for the valine and acetate feeding experiments.

The ^{13}C NMR spectrum of andrimid resulting from the [1,2-$^{13}C_2$]glycine feeding experiment (Figure 48) showed significantly enhanced peaks for both the C4 and C5 resonances (29.3 % and 30.0 % specific incorporation). The C4 resonance at δ 38.9 appeared as a doublet ($^1J_{C4.C5}$ = 45.8 Hz) arising from $^{13}C/^{13}C$ coupling in doubly labelled molecules flanking a central singlet arising from the natural abundance ^{13}C of unlabelled andrimid. The carbonyl resonance at δ 179.9 also appeared as a doublet flanking a central singlet. The enriched doublet ($^1J_{C4.C5}$ = 45.8 Hz) from doubly labelled molecules was centered around a singlet that showed significant enhancement (12.5 % specific incorporation) above the natural abundance ^{13}C indicating the presence of molecules singly labelled at C5.

Examination of the ^{13}C NMR spectrum (Figure 49) from the [1,2-$^{13}C_2$,^{15}N]glycine feeding experiment showed that the nitrogen of the acylsuccinimide ring was also derived from glycine. The C4 resonance now appeared as a doublet of doublets ($^1J_{C4.C5}$ = 45.8 Hz, $^2J_{C4.N1}$ = 5.7 Hz), due to one bond $^{13}C/^{13}C$ and two bond $^{13}C/^{15}N$ coupling in triply labelled molecules, around a central singlet arising from natural abundance ^{13}C in unlabelled molecules (Figure 50). The C5 resonance also gave a doublet of doublets ($^1J_{C4.C5}$ = 45.8 Hz, $^1J_{C4.N1}$ = 12.4 Hz), due to one bond $^{13}C/^{13}C$ and $^{13}C/^{15}N$ coupling in triply labelled molecules centered around a doublet ($^1J_{C4.N1}$ = 12.4 Hz), due to one bond $^{13}C/^{15}N$ coupling in doubly labelled molecules, and a singlet due to the natural abundance ^{13}C in unlabelled molecules of andrimid (Figure 50). These results provide evidence for the incorporation of glycine into the acylsuccinimide ring of andrimid.

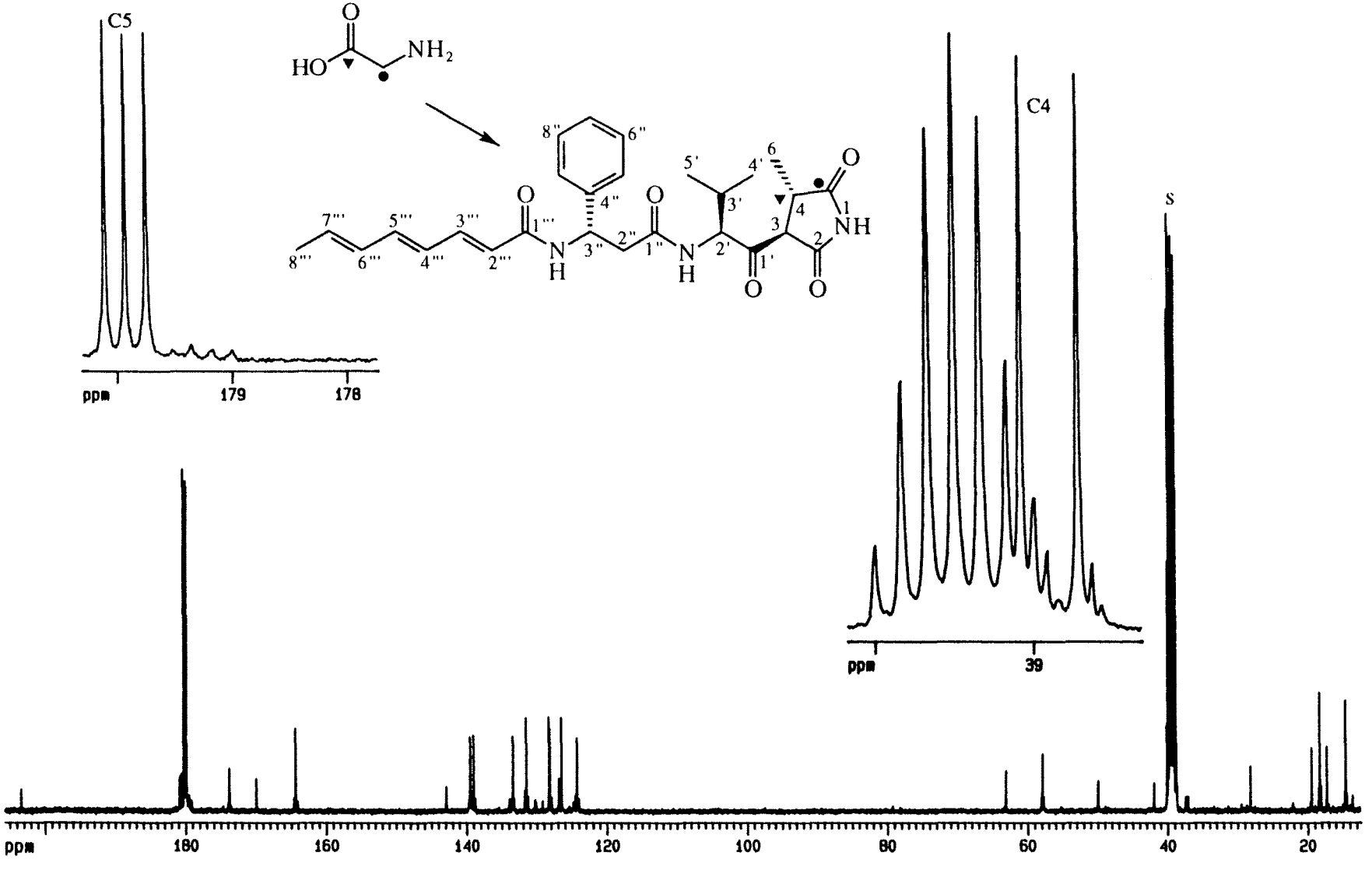

Figure 48. ^{13}C NMR spectrum of andrimid (**41**) labelled by [1,2-$^{13}C_2$]glycine (125 MHz, DMSO-d_6).

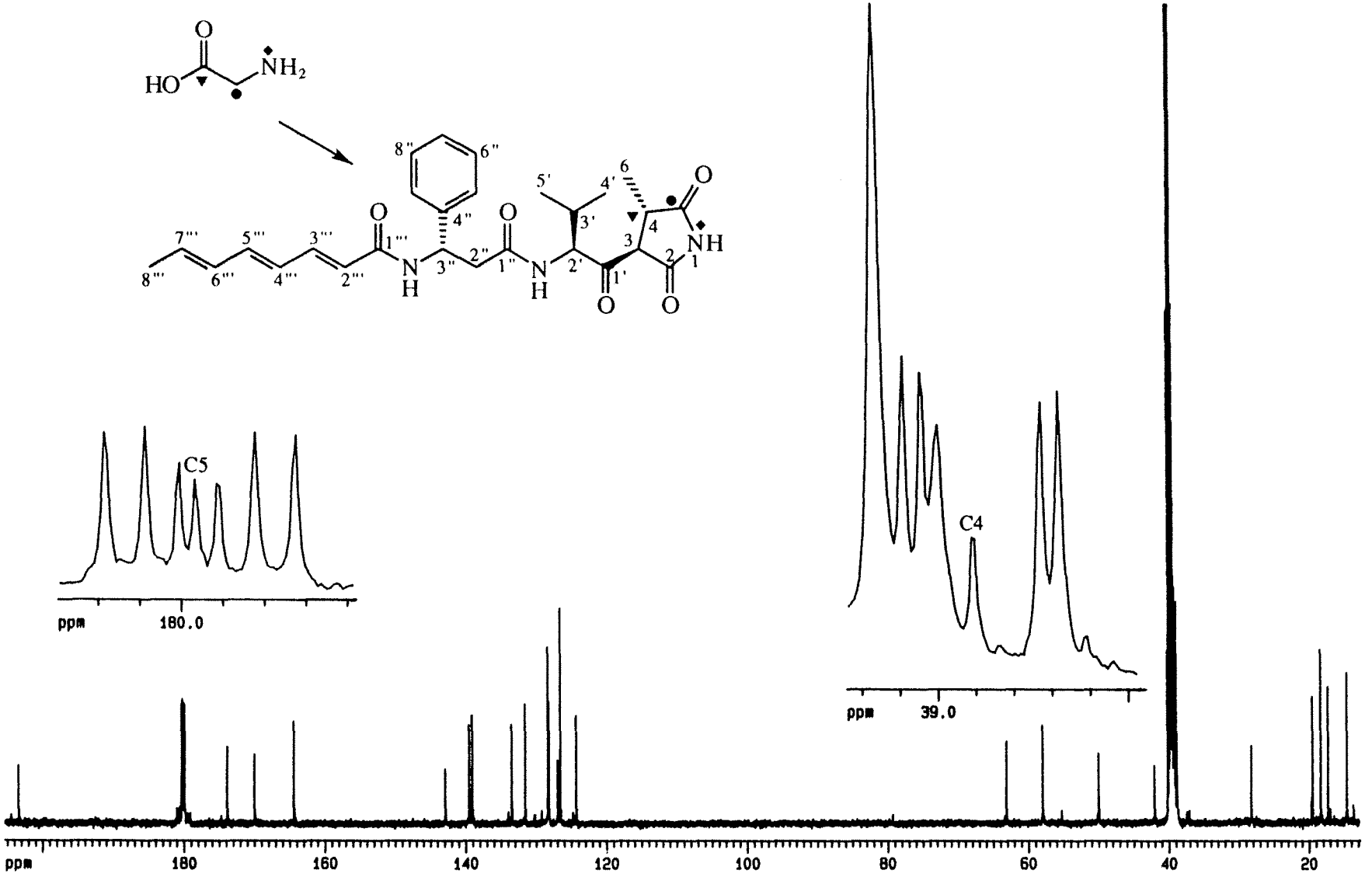

Figure 49. ^{13}C NMR spectrum of andrimid (**41**) labelled by [1,2-$^{13}C_2$,^{15}N]glycine (125 MHz, DMSO-d_6).

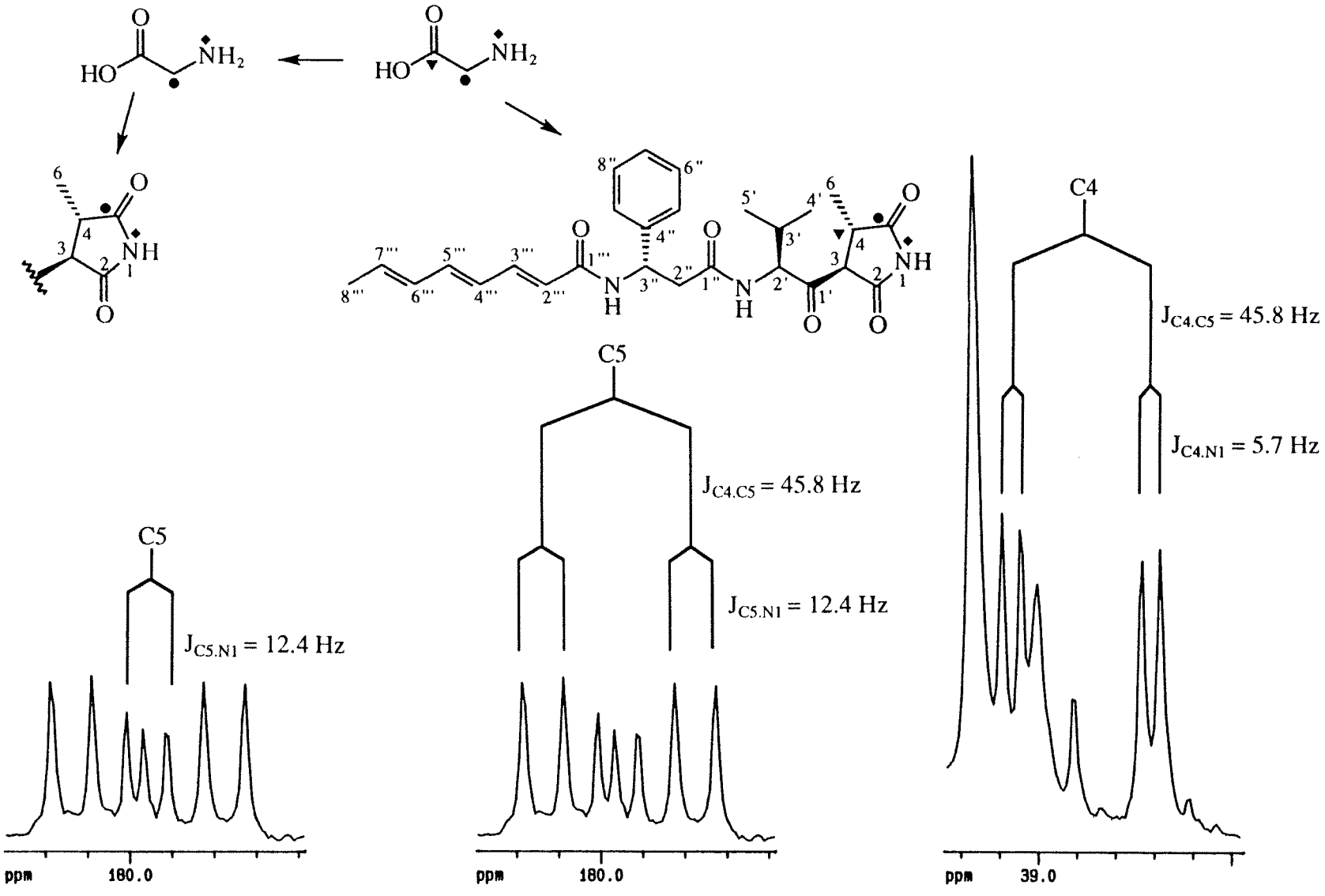

Figure 50. $^{13}C/^{13}C$ and $^{13}C/^{15}N$ coupling constants for the C4 and C5 resonances of andrimid (**41**) labelled by [1,2-$^{13}C_2$,^{15}N]glycine.

The feeding experiments using [1,2-$^{13}C_2$] and [1,2-$^{13}C_2$,^{15}N] labelled glycine also provided evidence for the incorporation of only the nitrogen atom and the C2 atom of the original glycine into the nitrogen and C5 of the acylsuccinimide ring. In the [1,2-$^{13}C_2$]glycine experiment the central singlet for the C5 resonance in the ^{13}C NMR spectrum was enhanced suggesting the incorporation of a singly labelled precursor. In addition, the [1,2-$^{13}C_2$,^{15}N]glycine feeding experiment led to the isolation of andrimid that showed a doublet ($^1J_{C4,N1}$ = 12.4 Hz) in the ^{13}C NMR spectrum arising from the incorporation of doubly labelled molecules as well as a doublet of doublets around a central singlet. These results suggest that a pathway exists for the loss and replacement of the carboxyl carbon atom (C1) of glycine. In an experiment using [1-^{14}C]glycine Klein and Sagers demonstrated the exchange of the carboxyl group of glycine with bicarbonate from the culture of *Peptococcus glycinophilus*.[57] A similar reaction in *P. fluorescens* would account for the incorporation of only the nitrogen and C2 carbon of glycine observed in the biosynthesis of andrimid.

Low level incorporation of ^{13}C into the carbons derived from acetate was observed in the ^{13}C NMR spectrum of andrimid arising from the [1,2-$^{13}C_2$]glycine experiment. Small doublets from doubly labelled molecules were observed around a central singlet that was enhanced above the natural abundance ^{13}C arising from singly labelled molecules. These results support the metabolism of [1,2-$^{14}C_2$]glycine into acetate as previously observed in cultures of *Diplococcus glycinophilus*.[58]

6.3. Conclusion

Stable isotope studies on andrimid have shown that the acylsuccinimide fragment is derived from valine, glycine and acetate. The results are consistent with the proposed biogenesis depicted in Figure 47. This pathway involves the homologation of amino acids with acetate, presumably via malonyl-CoA, as in the biosynthesis of 4-amino-3-hydroxy-6-methylheptanoic acid.[54a] In andrimid biosynthesis a valine moiety is homologated with an acetate unit to form the

new γ-amino-β-keto acid 4-amino-3-keto-5-methylhexanoic acid. A second new γ-amino-β-keto acid, 4-amino-3-ketobutanoic acid, is formed by the homologation of glycine with acetate. The proposed biogenesis proceeds through a dipeptide-like intermediate formed between these two γ-amino-β-keto acids.

The isolation of moiramide A from cultures of *P. fluorescens* suggest that it may be an intermediate in the biosynthesis of andrimid. Although the mechanism for the biosynthesis of andrimid is not known, three possibilities for the assembly of the building blocks in andrimid can be postulated. In the first pathway the octatrienoyl fragment is derived from polyketide biosynthesis onto which the β-phenylalanine and the γ-amino-β-keto acids are assembled in a linear process similar to polyketide biosynthesis. Another possibility involves the linear build up of andrimid from the 4-amino-3-keto-5-methylhexanoic acid terminus. Andrimid may also be formed by a convergent mechanism. This would involve bringing together two fragments made independently, such as moiramide A and a dipeptide-like intermediate resulting from the condensation of the two unusual γ-amino-β-keto acids. The stable isotope feeding experiments carried out in this study provide information about the building blocks in andrimid but they do not provide any information about the timing of assembly and further studies are required.

7. SECONDARY METABOLITES FROM *PSEUDOMONAS* SP. (91V47)

7.1. Introduction

The bacterial isolate 91V47, obtained from an abalone collected off Cortez Island in Georgia Strait, British Columbia, was identified as a Gram-negative *Pseudomonas* sp.. Preliminary studies showed that extracts of liquid shake cultures of this *Pseudomonas* sp. 91V47 had potent in vitro cytotoxicity against P388 murine leukemia (ED_{50} = 0.0287 μg/mL) as well as antimicrobial activity against methicillin-resistant *Staphylococcus aureus*. This bacterium was grown in moderate scale culture in order to obtain sufficient quantities of the cytotoxic and antimicrobial metabolites for structure determination.

7.2. Results and Discussion

Pseudomonas sp. 91V47 was grown in liquid shake culture at room temperature. Thirty-six one liter Erlenmeyer flasks containing 500 mL of tryptic soy broth medium and 1 % sodium chloride were each inoculated with 2 mL of an actively growing culture of *Pseudomonas* sp. 91V47 and the cultures were harvested by filtration five days after inoculation. The supernatant was passed over a column of XAD-4 resin and the adsorbed organic material was eluted with methanol. The crude residue was partitioned between water and ethyl acetate. Fractionation of the organic soluble materials by Sephadex LH-20 (eluent: 3:1 methanol/dichloromethane) yielded thirteen fractions. An early eluting fraction was found to be cytotoxic. The more polar constituents of this fraction were purified by reversed-phase HPLC (eluent: methanol/0.025 M phosphate buffer, pH 6.78) and yielded the new natural products **44** (15 mg), **45** (12 mg) and **46** (8 mg).

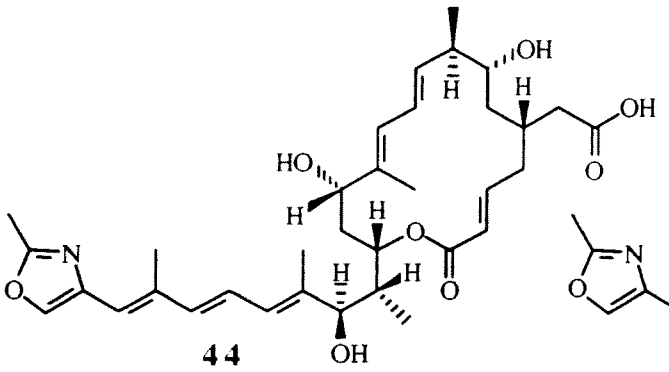

44

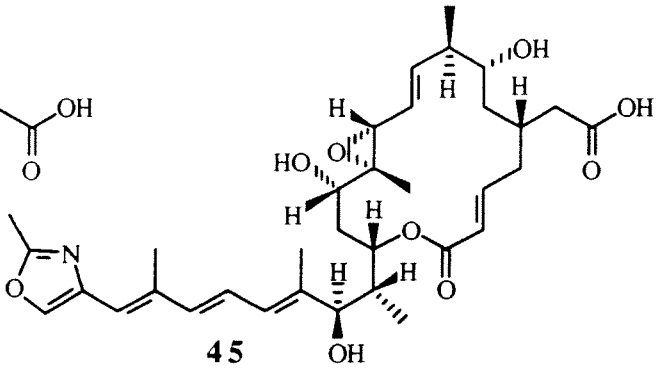

45

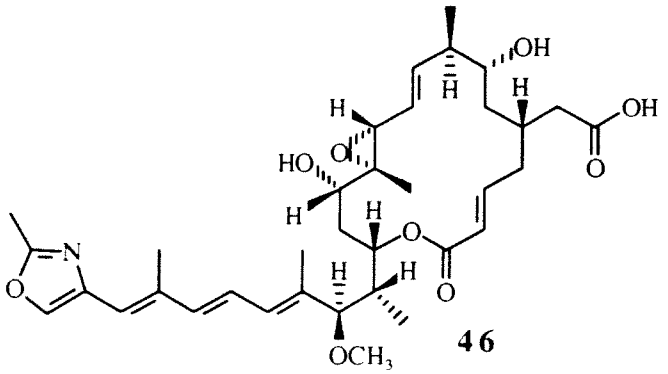

46

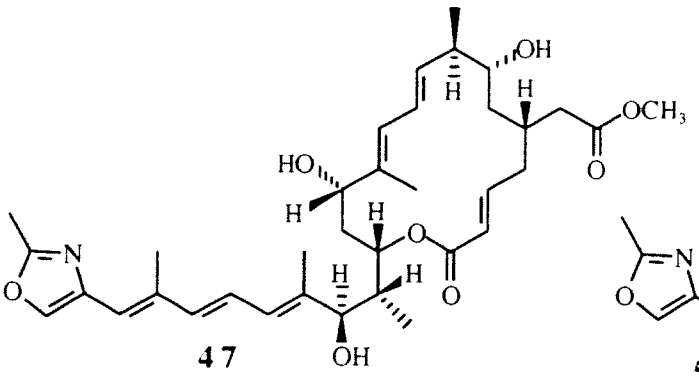

47

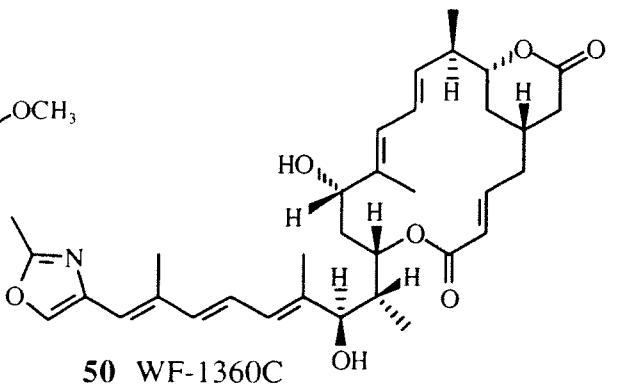

50 WF-1360C

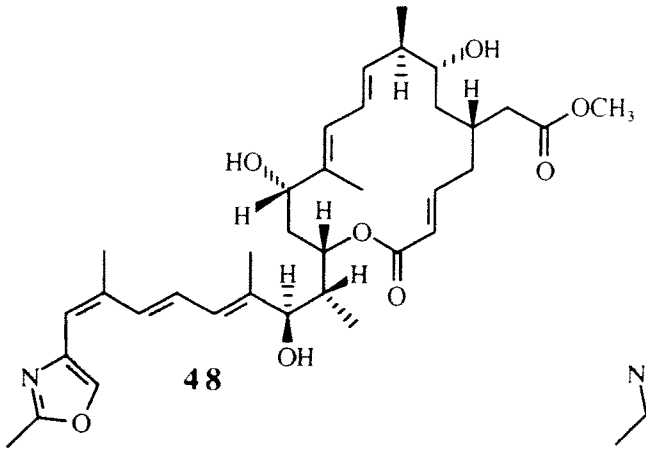

48

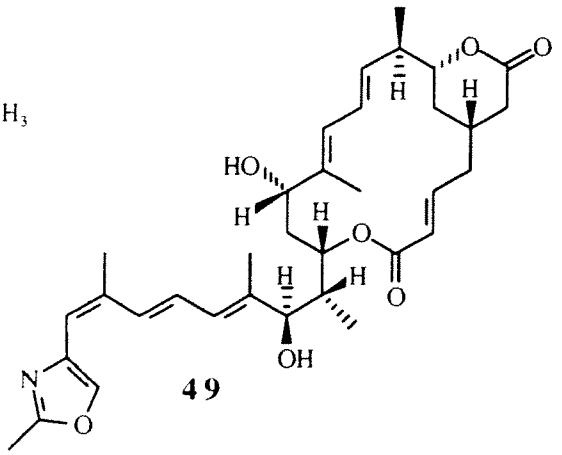

49

Purification of the less polar compounds by normal phase silica flash column chromatography and HPLC (eluent: ethyl acetate/ hexane) yielded **47** (8 mg), **48** (≈1 mg) and **49** (2 mg) as well as the known compound WF-1360C (**50**) (9 mg).[59]

7.2.1. WF-1360C (50)

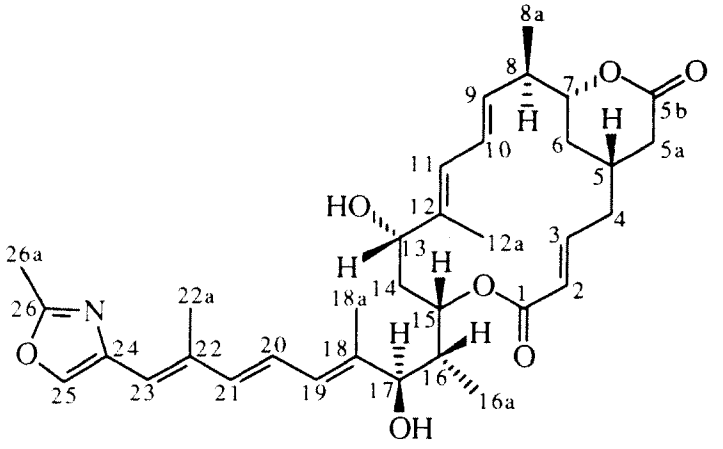

WF-1360C (**50**) was obtained as a white amorphous solid. The structure of WF-1360C was elucidated by comparison of its MS and NMR data with literature values[59] (Table 10). A molecular ion in the HREIMS at m/z 579.3202 was consistent with a molecular formula of $C_{34}H_{45}NO_7$ (ΔM +0.6 mmu). The IR spectrum contained absorption bands at 3418 and 1715 cm^{-1} that were assigned to hydroxy and carbonyl functionalities, respectively. The ^1H NMR spectrum of WF-1360C (**50**) is provided in Figure 51. Several discrepancies in the ^{13}C NMR data of **50** (Figure 52) and the literature assignments for the carbon resonances at C10, C11, C12a, C13, C17 and C18a were resolved by the analysis of the COSY, HMQC and HMBC data (Table 10). No two-dimensional data has been reported in the literature for WF-1360C.

Table 10. ^{1}H and ^{13}C NMR data for WF-1360C (**50**).

	WF-1360C		WF-1360C isolated from 91V47			
C#	δ ^{13}C[a]	δ ^{1}H[b]	δ ^{13}C[c]	δ ^{1}H[d]	COSY	HMBC[e]
1	166.2	—	166.2	—	—	H2
2	124.5	5.63	124.2	5.63,d(15.7)	H3	—
3	146.7	6.79	146.8	6.80,m	H2,H4,H4'	—
4	38.3	1.75	38.3	1.75,m	H3,H4'	H2,H5a
4'	—	2.55	—	2.55,m	H3,H4	—
5	29.7	1.80	29.6	1.80,m	H5a,H5a',H6	H4,H5a
5a	36.9	2.10	36.8	2.08,m	H5,H5a'	H6'
5a'	—	2.77	—	2.77,dm(14.9)	H5,H5a	—
5b	170.3	—	170.3	—	—	H5a
6	34.6	0.70	34.6	0.70,m	H5,H6',H7	—
6'	—	1.97	—	1.97,m	H6,H7	—
7	83.2	3.70	83.2	3.70,m	H6,H6',H8	H6,H8H8a
8	45.3	2.29	45.2	2.29,m	H7,H8a,H9	H8a,H9
8a	16.6	1.20	16.5	1.22,d(6.6)	H8	H9
9	134.6	5.18	134.7	5.19,dd(15.2,9.6)	H8,H10	H8a,H11
10	126.1*	6.24	129.7	6.25,dd(15.2,10.9)	H9,H11	H11
11	129.8*	5.79	126.3	5.85,d(10.9)	H10,H12a	H9,H12a,H13
12	139.3	—	139.2	—	—	H12a
12a	12.8	1.81	11.0	1.81,s	H11	H11,H13
13	77.9	3.99	78.3	4.00,dd(10.6,2.6)	H14,H14'	H11,H12a
14	33.5	1.83	33.5	1.90,m	H13,H14'	—
14'	—	2.16	—	2.15,m	H13,H14,H15	—
15	74.9	4.69	74.8	4.70,dd(10.6,5.1)	H14'	H16a
16	40.0	2.12	40.0	2.12,m	H16a,H17	H16a,H17
16a	9.6	0.97	9.7	0.97,d(6.9)	H16	H17
17	78.3	3.89	77.6	3.90,d(6.3)	H16	H16a,H18a
18	138.7	—	138.3	—	—	H18a
18a	11.0	1.88	12.8	1.89,s	H19	H17
19	126.7*	6.21	126.7	6.21,d(10.9)	H18a,H20	H17,H18a,H21
20	124.2	6.58	124.4	6.58,dd(15.2,10.9)	H19,H21	H21
21	137.3	6.40	137.4	6.40,d(15.2)	H20	—
22	137.1	—	137.0	—	—	H20,H22a
22a	14.4	2.13	14.4	2.14,s	H23	H21
23	120.4	6.25	120.4	6.25,s	H22a	H21,H22a
24	138.7	—	138.7	—	—	H25
25	135.8	7.54	135.9	7.53,s	—	—
26	161.0	—	160.9	—	—	H25,H26a
26a	13.8	2.46	13.8	2.46,s	—	—
17-OCH_3						

[a] Recorded in $CDCl_3$ at 67.5 MHz.[59b] Chemical shifts in ppm relative to TMS. * Interchangeable assignments.

[b] Recorded in $CDCl_3$.[59a]

[c] Recorded in $CDCl_3$ at 125 MHz. Chemical shifts in ppm relative to solvent.

[d] Recorded in $CDCl_3$ at 400 MHz. Chemical shifts in ppm relative to TMS.

[e] Carbons in the carbon # column are correlated to the listed proton resonances.

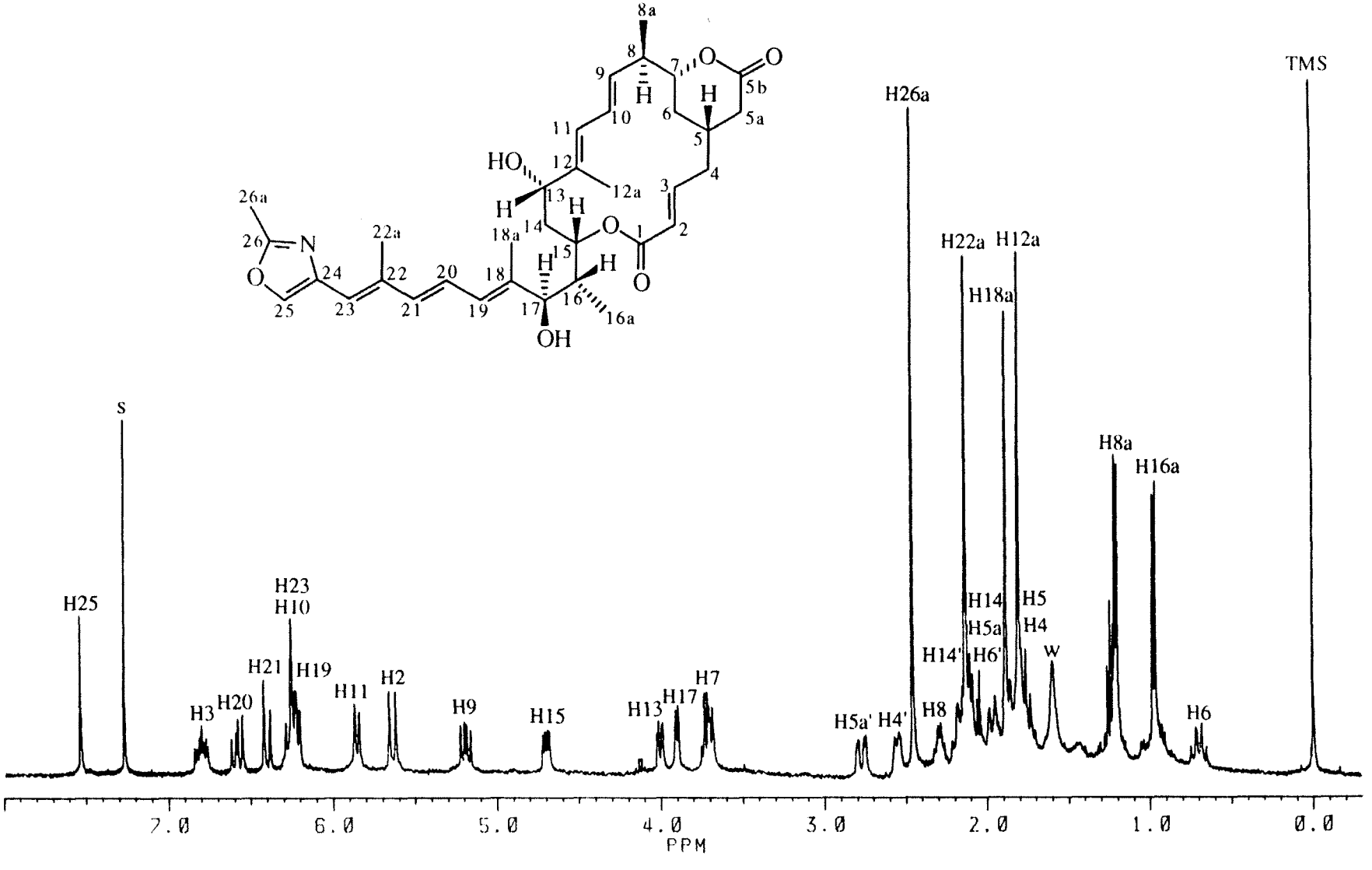

Figure 51. ^{1}H NMR spectrum of WF-1360C (**50**) (400 MHz, $CDCl_3$).

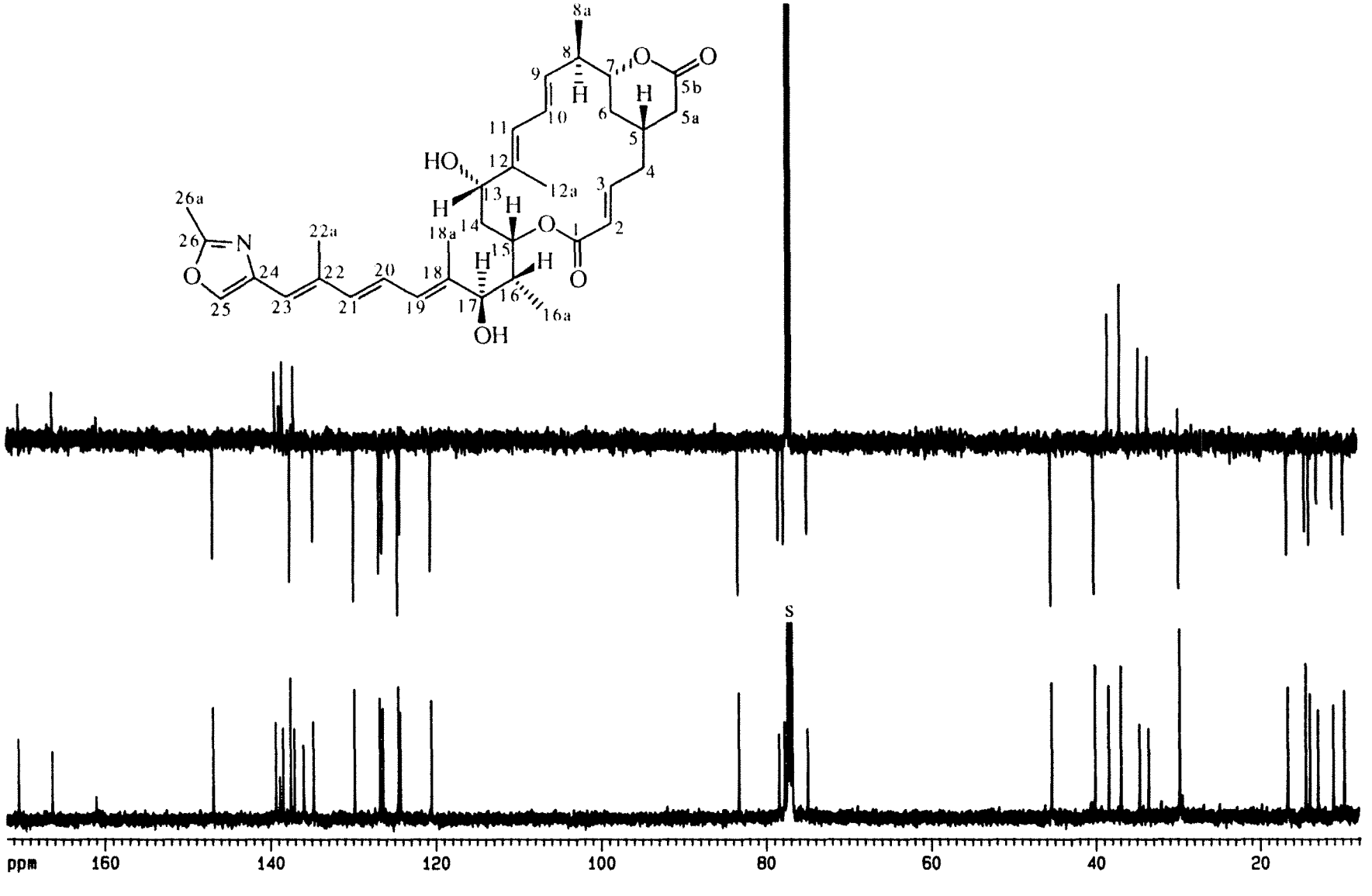

Figure 52. ^{13}C and APT NMR spectra of WF-1360C (**50**) (125 MHz, $CDCl_3$).

WF-1360C is a rhizoxin analog that was originally isolated from the fungi *Rhizopus chinensis*,[59a] the pathogen responsible for rice seedling blight, and *Rhizopus* sp. No. F-1360.[59b] Other rhizoxin analogs have also been reported in the literature.[59] Rhizoxin (**53**),[60] originally isolated from the fungus *Rhizopus chinensis* is a 16-membered macrolide that exhibits potent antifungal and antitumour activity.[61]

Three new natural products **44**, **45** and **46** have been isolated from liquid cultures of *Pseudomonas* sp. 91V47. These compounds are rhizoxin analogs containing a δ-hydroxy acid functionality in place of the δ-lactone. Compounds **44** to **46** are δ-hydroxy acids of the previously isolated δ-lactone rhizoxin analogs **50** to **52**.[59] The δ-hydroxy acids **44** to **46** have not been found as natural products but they have been claimed in the Patent literature[62] as semi-synthetic derivatives of **50** to **52**. No spectroscopic data has been reported for these compounds.

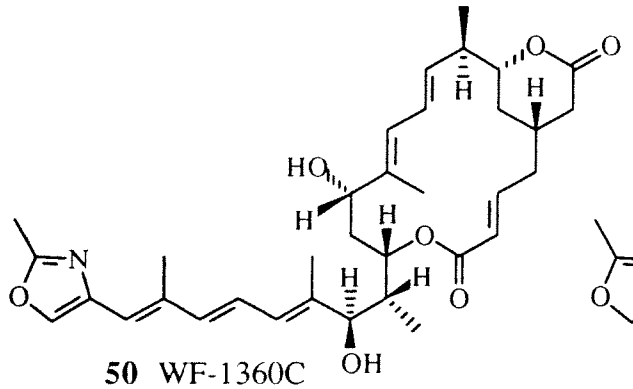

50 WF-1360C

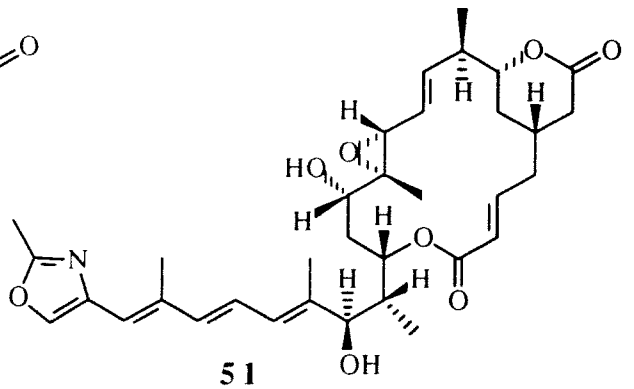

51

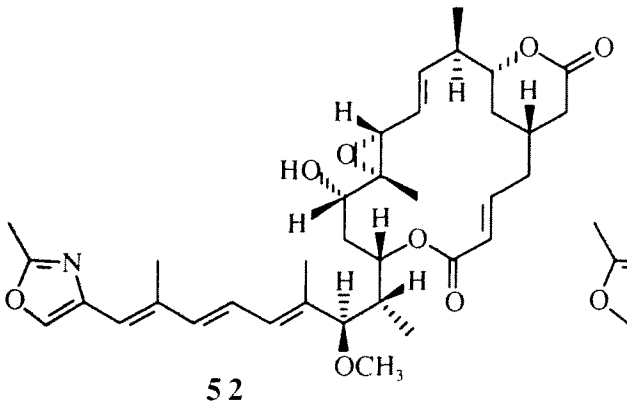

52

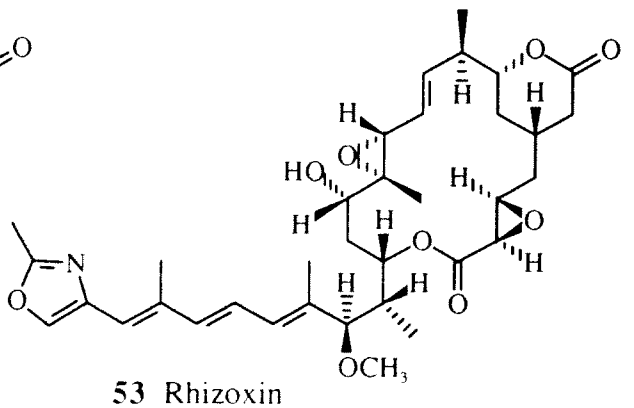

53 Rhizoxin

7.2.2. Compound 44

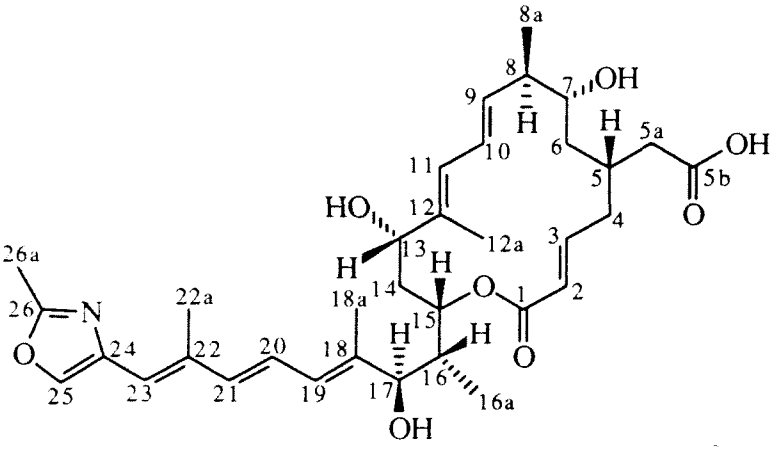

Compound **44** was isolated as an unstable white solid. The HRLSIMS showed a peak at m/z 598.33982 ($C_{34}H_{48}NO_8$ ΔM +1.83 mmu) corresponding to (M + H). The IR spectrum contained absorption bands at 3400 and 1710 cm^{-1} consistent with hydroxy and carbonyl functionalities. Inspection of the ^1H NMR spectrum (Figure 53) identified **44** as a rhizoxin analog with a similar structure to WF-1360C (**50**). A δ-hydroxy acid moiety in **44** replaced the δ-lactone in WF-1360C. Evidence for the δ-hydroxy acid moiety was provided by the ^1H and COSY NMR data. The ^1H NMR spectrum of **44** contained a downfield proton resonance at δ 11.98 that had no attached carbon and was assigned to a carboxylic acid proton. The 7-OH proton at δ 4.51 showed a COSY correlation (Figure 54) to the H7 proton at δ 2.83. The ^{13}C NMR (Figure 55), HMQC (Figure 56) and HMBC (Figure 57) data are summarized in Table 11.

One of the structural differences between compound **44** and rhizoxin (**53**) was the presence of $\Delta^{2,3}$ and $\Delta^{11,12}$ double bonds instead of epoxy groups. A large coupling constant for the H2 doublet ($^1J_{H2,H3}$ = 15.6 Hz) suggested an E configuration for the $\Delta^{2,3}$ double bond. An NOE experiment assigned the configuration at the $\Delta^{11,12}$ olefin. Irradiation of the H12a methyl resonance at δ 1.61 induced an NOE (-5.8 %) at δ 6.05 (H10) indicating an E configuration.

Table 11. ^{1}H and ^{13}C NMR data for compound **44**.

C#	δ $^{13}C^{a}$	δ $^{1}H^{b}$	COSY	HMBC[c]
1	165.0	—	—	H2
2	123.3	5.58,d(15.6)	H3	H4
3	147.8	6.55,m	H2,H4,H4'	H4
4	37.6	1.82,m	H3,H4'	H2,H5a,H5a',H6'
4'	—	2.25,m	H3,H4	—
5	34.2	1.75,m	H5a	H4,H5a,H5a'
5a	40.1	2.04,dd(16.2,4.9)	H5,H5a'	H6'
5a'	—	2.90,dd(16.2,3.2)	H5a	—
5b	174.0	—	—	H5a,H5a'
6	36.4	0.78,m	H6',H7	—
6'	—	1.82,m	H6	—
7	75.7	2.83,m	H6,H7-0H,H8	H6,H6',H8a
8	45.8	1.88,m	H7,H8a,H9	H8a,H9,H10
8a	17.0	0.90,d(7.3)	H8	H9
9	136.9	5.10,dd(15.2,9.6)	H8,H10	H8a,H11
10	127.6	6.05,dd(15.2,10.8)	H9,H11	H11
11	124.2	5.53,d(11.0)	H10,H12a	H9,H12a,H13
12	138.6	—	—	H12a
12a	10.6	1.61,s	H11	H11,H13
13	77.0	3.68,m	H13-OH,H14	H11,H12a
14	33.0	1.64,m	H13,H14'	H15
14'	—	1.85,m	H14,H15	—
15	73.1	4.62,dd(9.7,3.2)	H14',H16	H16a
16	40.0	1.81,m	H15,H16a,H17	H16a,H17-OH
16a	9.8	0.84,d(6.7)	H16	H15
17	77.4	3.70,m	H16,H17-OH	H16a,H18a,H19
18	140.6	—	—	H18a
18a	12.1	1.78,s	H19	H19
19	125.5	6.08,d(10.0)	H18a,H20	H18a,H21
20	124.6	6.60,m	H19,H21	H18a
21	136.4	6.39,d(15.1)	H20	H19,H23
22	136.2	—	—	H20
22a	14.0	2.15,s	H23	H21,H23
23	119.6	6.23,s	H22a	H21,H22a
24	138.2	—	—	H25
25	137.1	8.01,s	—	—
26	160.4	—	—	H25,H26a
26a	13.3	2.39,s	—	—
5b-OH	—	11.98,s	—	—
7-OH	—	4.51,d(6.1)	H7	—
13-OH	—	4.67,(3.0)	H13	—
17-OH	—	4.83,d(4.5)	H17	—
17-OCH_3				

[a] Recorded in DMSO-d_6 at 125 MHz. Chemical shifts in ppm relative to solvent.
[b] Recorded in DMSO-d_6 at 400 MHz. Chemical shifts in ppm relative to TMS.
[c] Carbons in the carbon # column are correlated to the listed proton resonances.

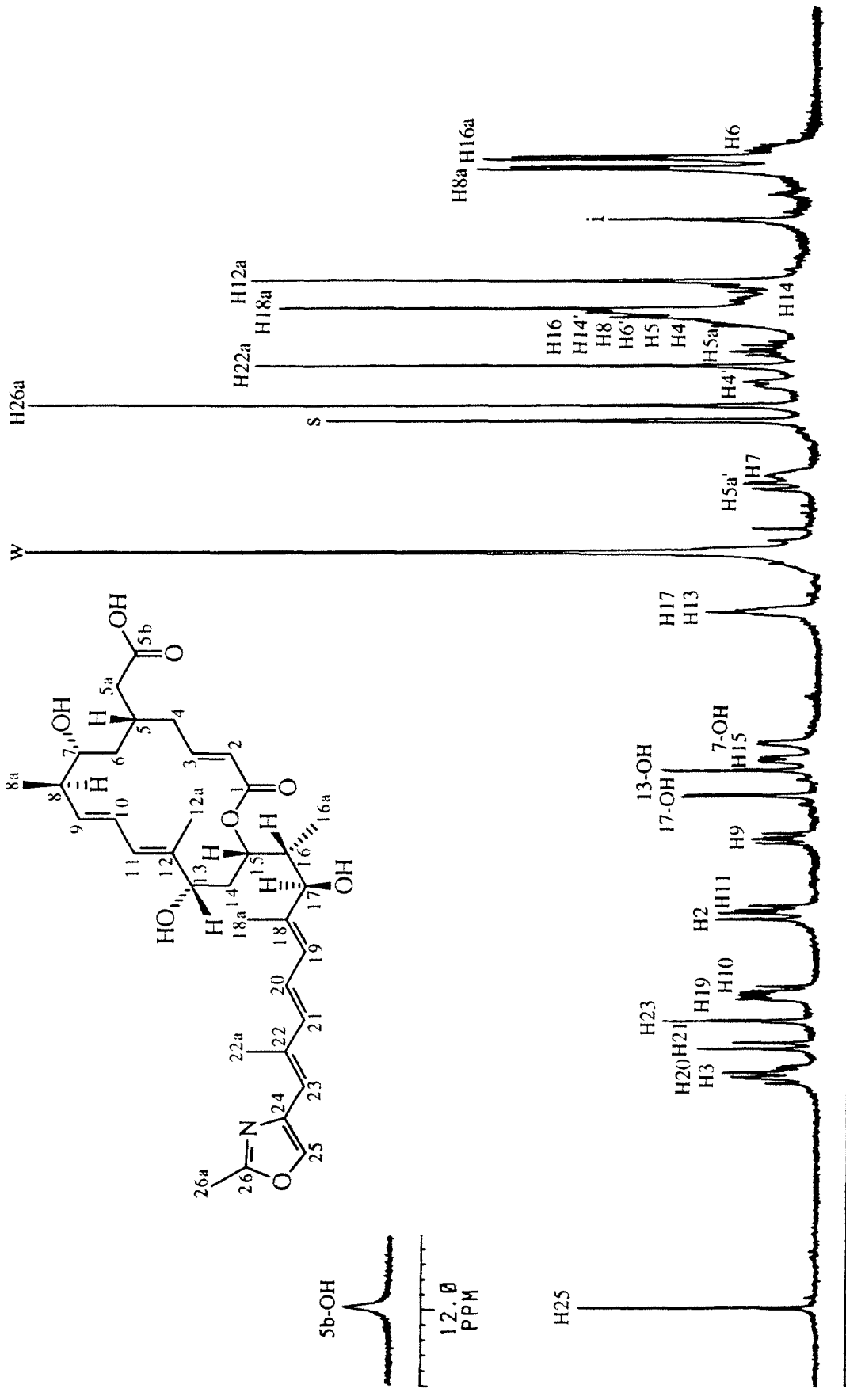

Figure 53. ^{1}H NMR spectrum of compound **44** (400 MHz, DMSO-d_6).

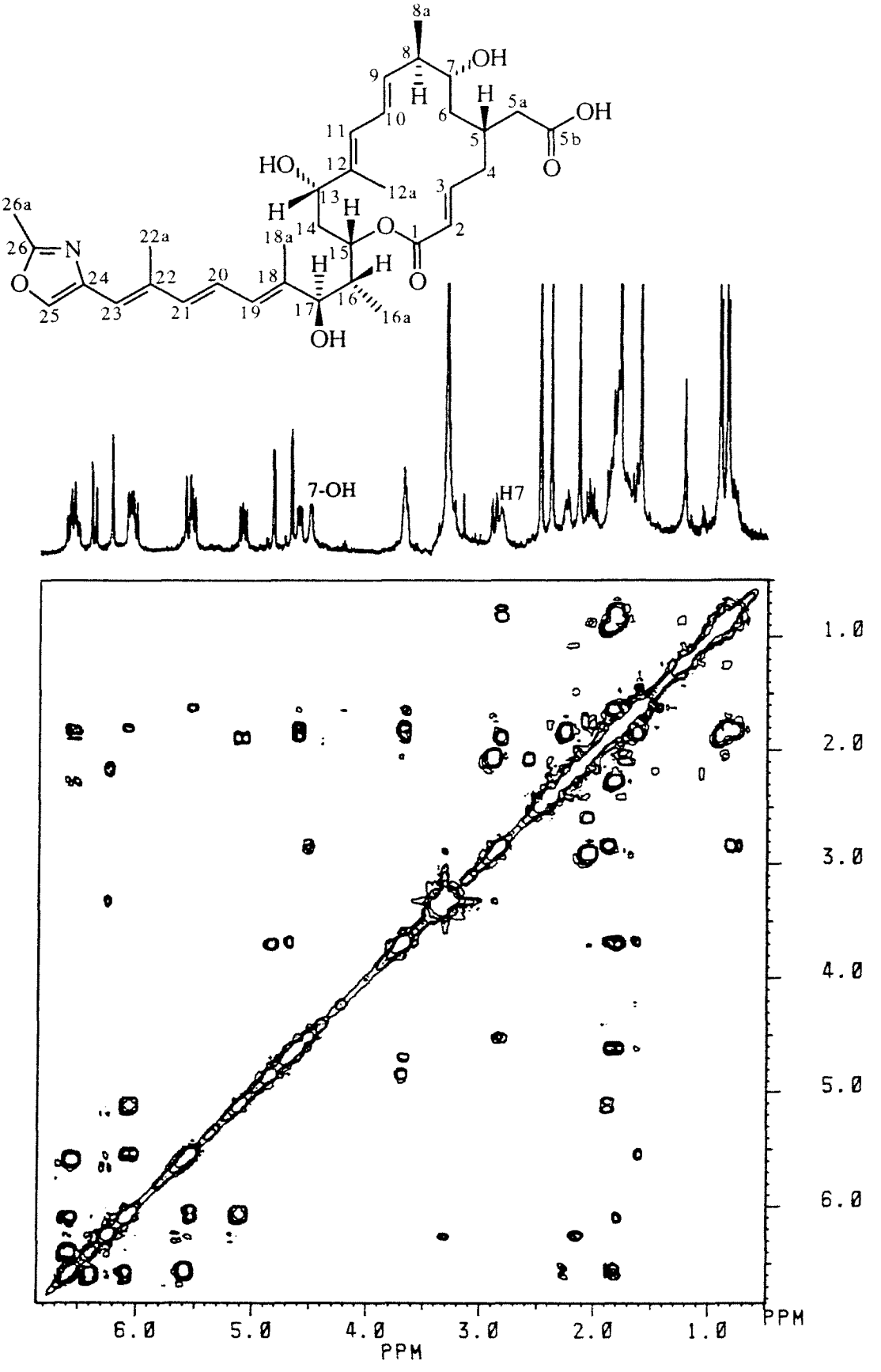

Figure 54. ^{1}H COSY NMR spectrum of compound **44** (400 MHz, DMSO-d_6).

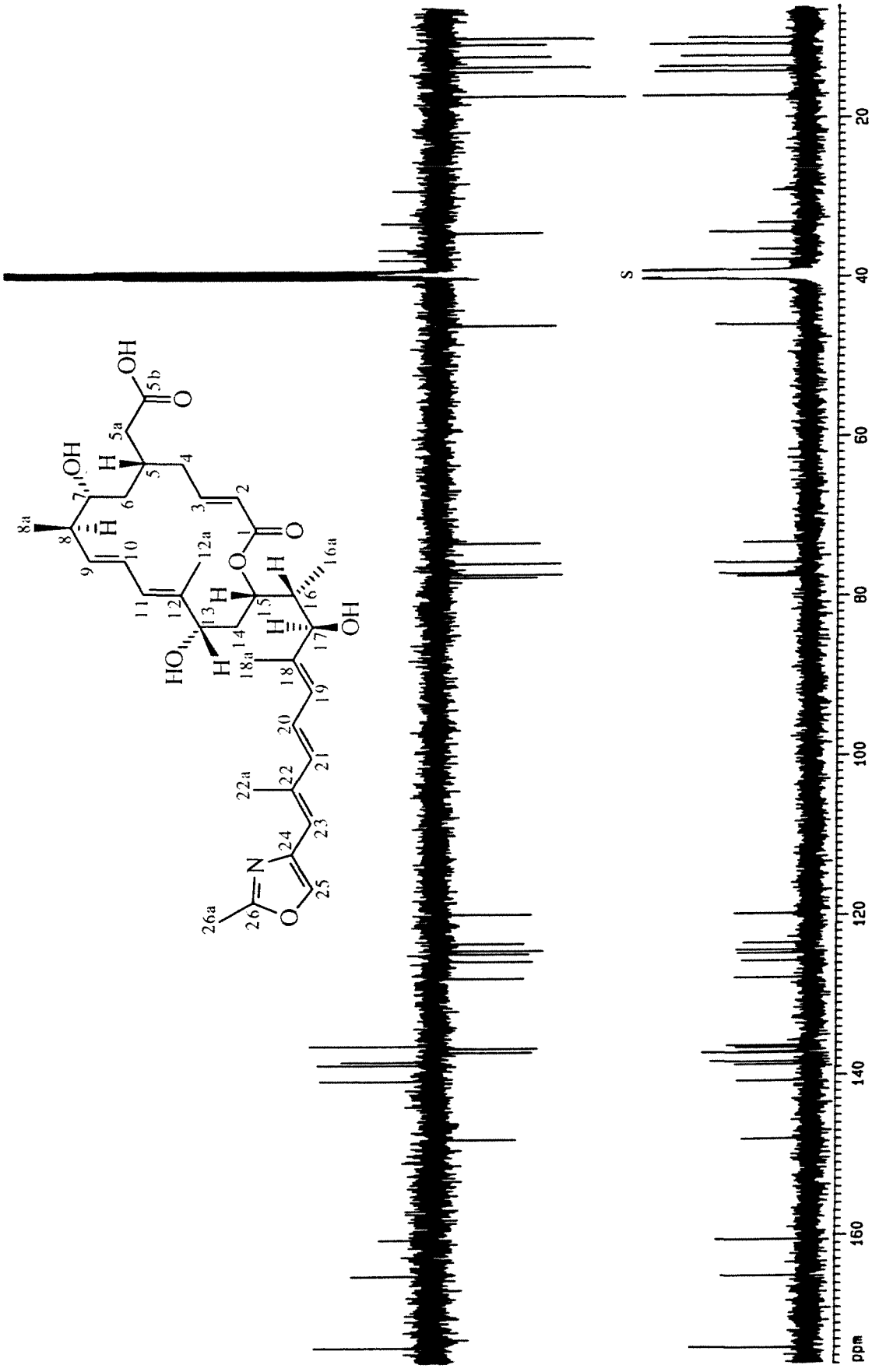

Figure 55. ^{13}C and APT NMR spectra of compound **44** (125 MHz, DMSO-d_6).

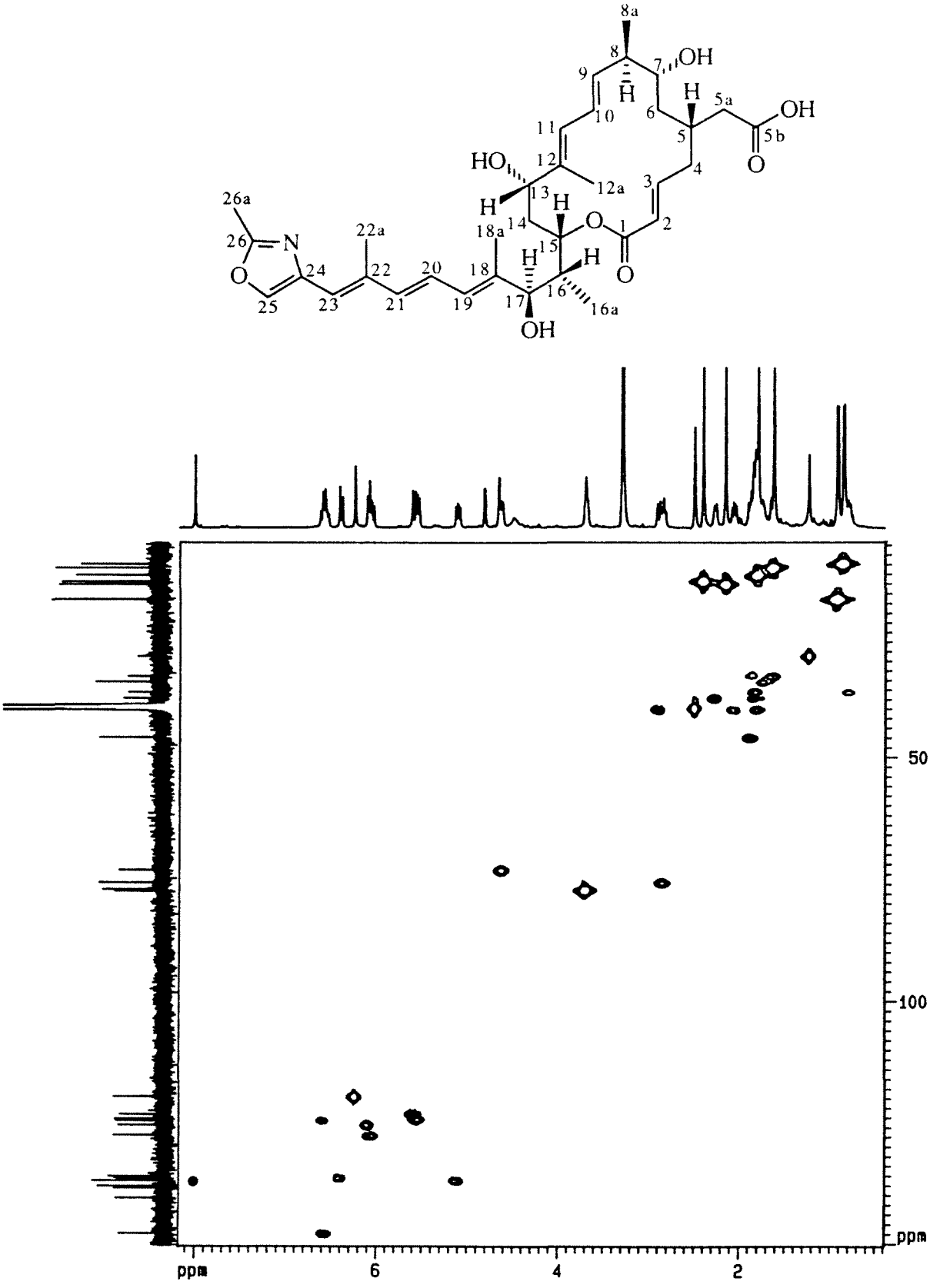

Figure 56. HMQC NMR spectrum of compound **44** (500 MHz ^{1}H NMR, DMSO-d_6).

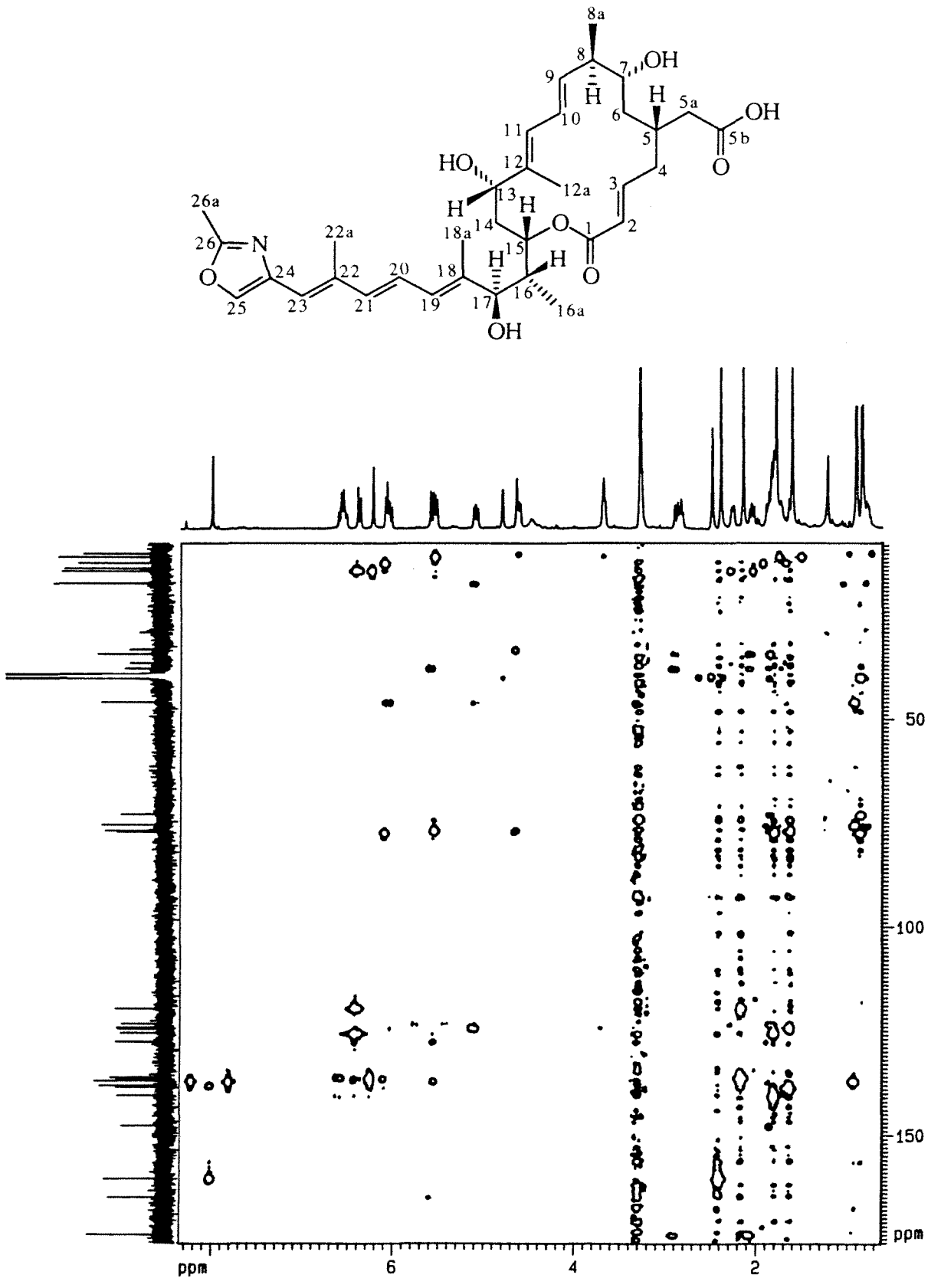

Figure 57. HMBC NMR spectrum of compound **44** (500 MHz ^{1}H NMR, DMSO-d_6).

The absolute configuration of rhizoxin (**53**) has been determined by interrelation to a related compound whose structure was established by X-ray crystallography, and by hydrolytic cleavage of the C2/C3 epoxide in rhizoxin using $H_2{}^{18}O$ and subsequent acetylation to give the ring opened ^{18}O-labelled seco-rhizoxin acetate.[63] The absolute stereochemistry of **44** was assumed to be as shown in structure **44** due to the similarity of this compound with rhizoxin (**53**).[60]

The ^1H NMR spectrum of compound **44** was originally obtained in chloroform-d. However, compound **44** readily cyclized to WF-1360C (**50**) during an overnight NMR experiment. Evidence for this cyclization was the appearance of a proton resonance at 0.70 ppm in the ^1H NMR spectrum (chloroform-d). This proton resonance was assigned to the H6 proton in WF-1360C (**50**). The ^1H chemical shift of the H6 proton observed for compound **44** obtained in chloroform-d was 0.98 ppm. Therefore, this upfield chemical shift of the H6 proton resonance was diagnostic for δ-lactone formation. Purification of the mixture of compounds **44** and **50** by reversed-phase HPLC (eluent: methanol/0.025 M phosphate buffer, pH 6.78) led to the partial recovery of compound **44** as well as WF-1360C (**50**) and the methyl ester of **44**, compound **47**. Subsequent attempts to repeat the cyclization of the δ-hydroxy acid compounds failed and resulted in a mixture of decomposition products.

7.2.3. Compound 45

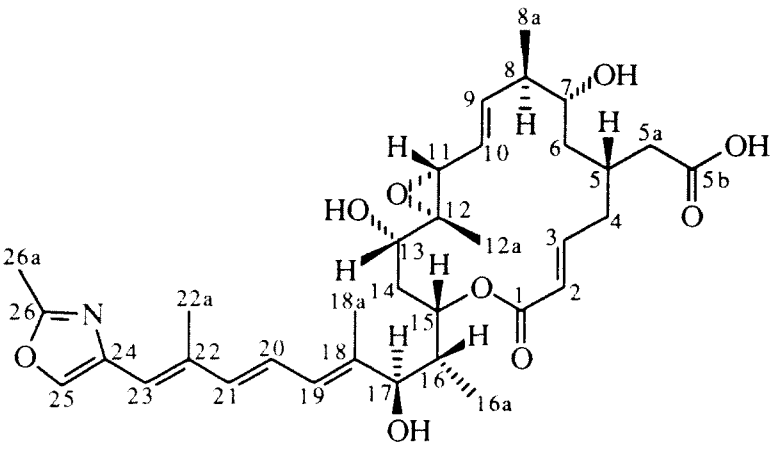

Compound **45** was isolated as an unstable white solid. A peak in the HRLSIMS at m/z 614.33214 ($C_{34}H_{48}NO_9$, ΔM -0.77 mmu) was appropriate for (M + H). Absorption bands at 3420 and 1714 cm^{-1} in the IR spectrum of **45** were consistent with hydroxy and carbonyl functionalities. Analysis of the NMR data (Table 12) identified **45** as a rhizoxin analog. Compound **45** contained a δ-hydroxy acid moiety as indicated by the presence of a 7-OH proton at δ 4.46 and a carboxylic acid proton at δ 12.06 in the ^1H NMR spectrum (Figure 58). Compound **45** differed from **44** at the C11/C12 bond. Two epoxy carbon signals were observed at δ 60.7 (C11) and δ 64.7 (C12) in the ^{13}C NMR spectrum (Figure 59) of **45** in place of the two olefinic signals C11 and C12 in **44** suggesting that **45** contained an epoxide. This was corroborated by the appearance of a resonance at δ 2.84 (H11) in the ^1H NMR spectrum. The COSY (Figure 60), HMQC (Figure 61) and HMBC (Figure 62) data summarized in Table 12 confirmed the proposed constitution of **45**. The absolute stereochemistry shown in structure **45** was proposed on the basis of its similarity to rhizoxin.[60]

Table 12. ^{1}H and ^{13}C NMR data for compound **45**.

C#	^{13}C[a]	^{1}H[b]	COSY	HMBC[c]
1	164.6	—	—	H2,H3
2	124.9	5.74,d(15.6)	H3	—
3	145.5	6.67,m	H2,H4,H4'	—
4	34.6	2.10,m	H3,H4'	H2,H5a'
4'	—	2.40,m	H3,H4	—
5	30.6	2.15,m	H6,H6'	H5a,H5a'
5a	40.0	2.20,m	—	H4'
5a'	—	2.30,m	—	—
5b	173.7	—	—	H5a,H5a'
6	37.8	0.95,m	H5,H6',H7	H5a'
6'	—	1.52,m	H5,H6	—
7	70.7	2.98,m	H6,H7-OH,H8	H8a
8	44.9	1.90,m	H7,H8a,H9	H8a,H10
8a	17.4	0.94,d(6.6)	H8	—
9	140.2	5.32,dd((15.6,9.2)	H8,H10	H8a,H11
10	125.8	5.08,dd(15.6,8.1)	H9,H11	H11
11	60.7	2.84,d(8.1)	H10	H9,H12a
12	64.7	—	—	H12a
12a	10.8	1.17,s	—	—
13	76.9	2.78,dd(10.5,2.5)	H14,H14'	H12a,H15
14	33.4	1.75,m	H13,H14',H15	—
14'	—	1.85,m	H13,H14,H15	—
15	73.8	4.64,dd(9.7,3.6)	H14,H14',H16	H16a
16	39.7	1.85,m	H15,H16a,H17	H16a
16a	9.6	0.86,d(6.8)	H16	—
17	77.5	3.69,d(7.6)	H16	H16a,H18a,H19
18	140.5	—	—	H18a
18a	12.0	1.78,s	H19	H19
19	125.6	6.05,d(11.0)	H18a,H20	H18a,H21
20	124.5	6.57,dd(15.2,11.0)	H19,H21	—
21	136.6	6.35,d(15.2)	H20	H19,H22a,H23
22	136.2	—	—	H20,H21
22a	14.0	2.13,s	H23	H21,H23
23	119.7	6.22,s	H22a	H21,H22a
24	138.2	—	—	H23,H25
25	137.1	8.00,s	—	—
26	160.5	—	—	H25,H26a
26a	13.4	2.39,s	—	—
5b-OH	—	12.06,s	—	—
7-OH	—	4.46,d(6.6)	H7	—
13-OH	—	5.01,d(3.8)	—	—
17-OH	—	4.87,d(4.5)	H17	—

[a] Recorded in DMSO-d_6 at 125 MHz. Chemical shifts are referenced to solvent.
[b] Recorded in DMSO-d_6 at 400 MHz. Chemical shifts in ppm relative to TMS.
[c] Carbons in the carbon # column are correlated to the listed proton resonances.

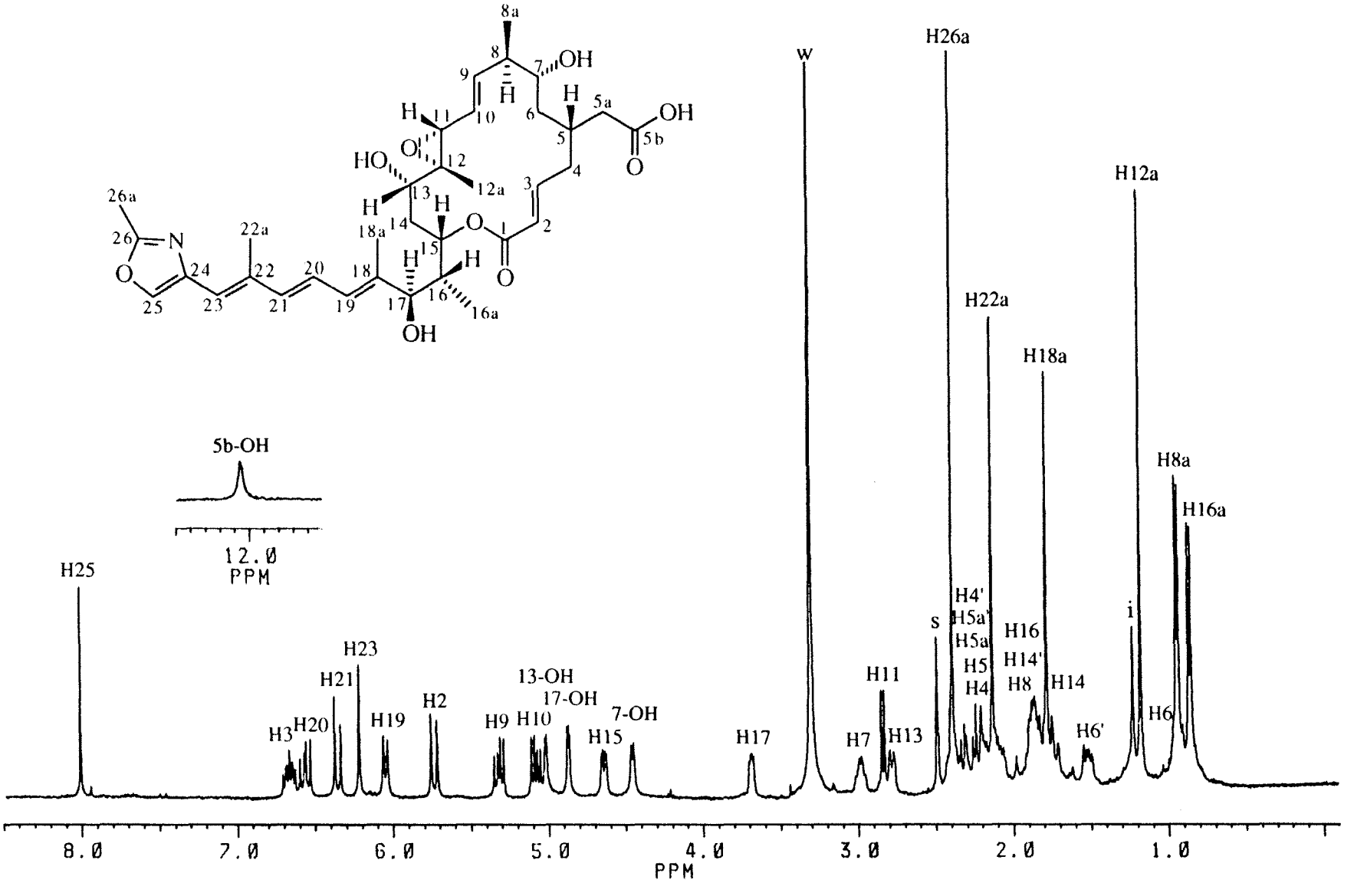

Figure 58. ^{1}H NMR spectrum of compound **45** (400 MHz, DMSO-d_6).

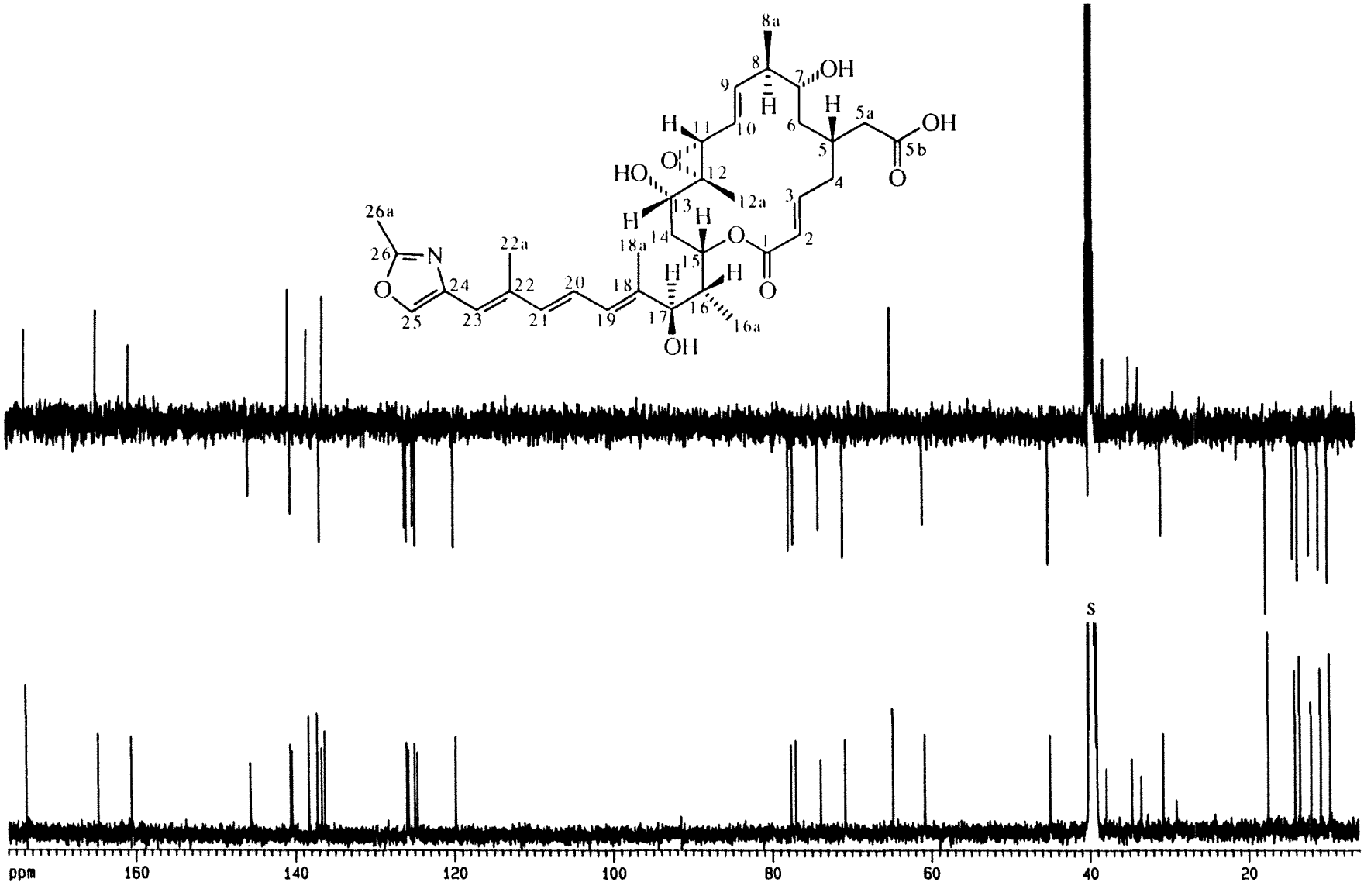

Figure 59. ^{13}C and APT NMR spectra of compound **45** (125 MHz, DMSO-d_6).

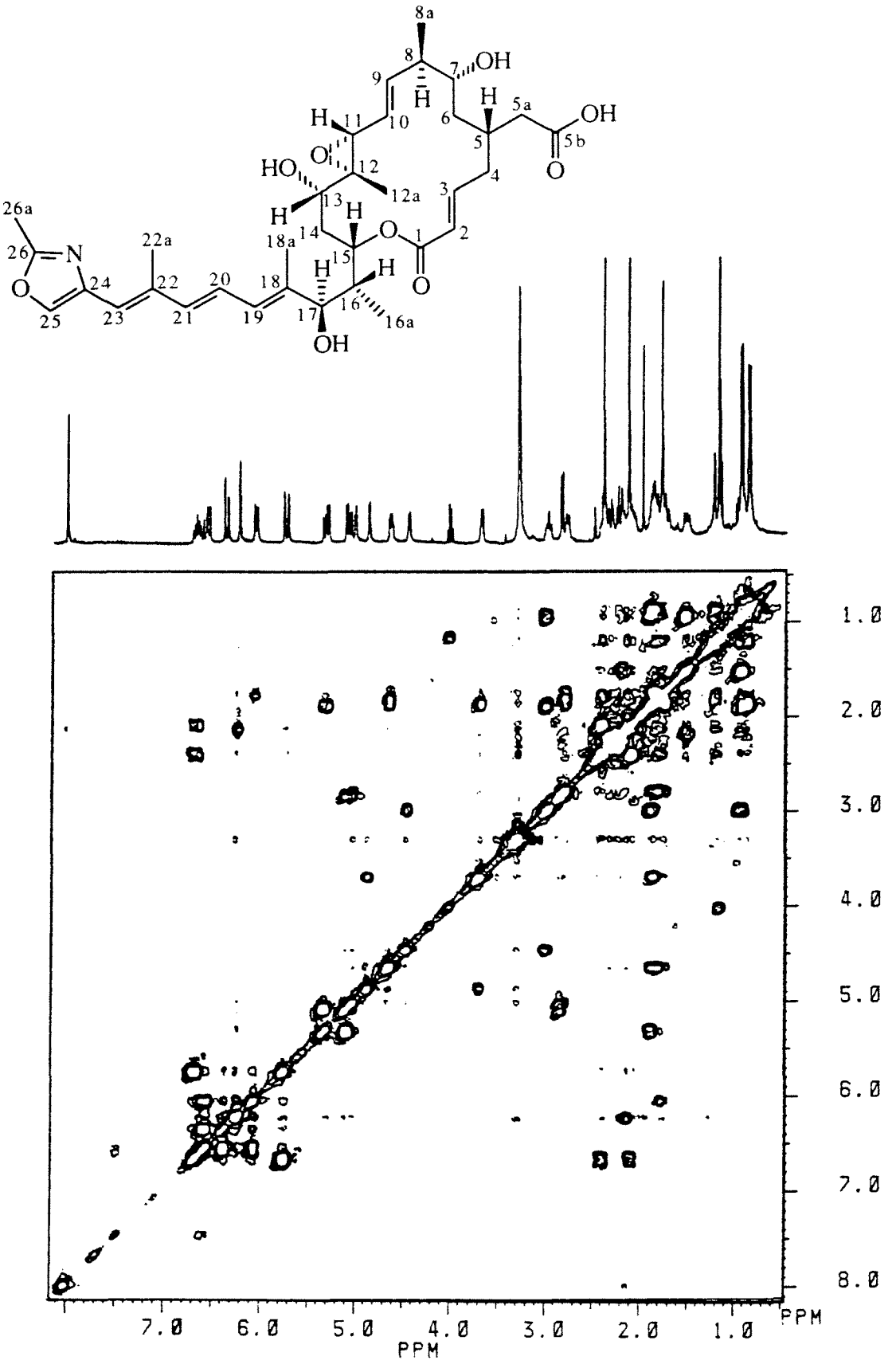

Figure 60. ^{1}H COSY NMR spectrum of compound **45** (400 MHz, DMSO-d_6).

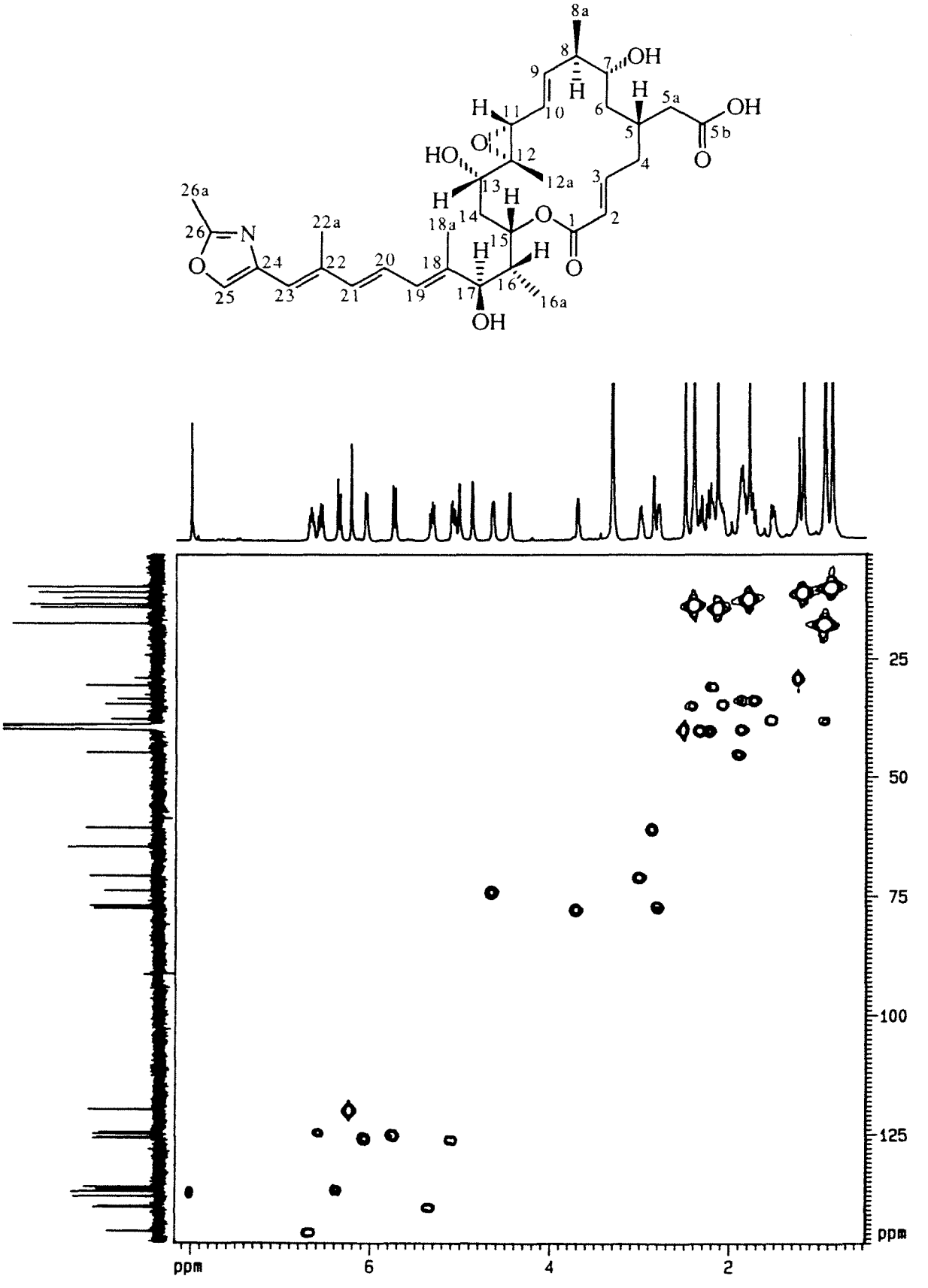

Figure 61. HMQC NMR spectrum of compound **45** (500 MHz ^{1}H NMR, DMSO-d_6).

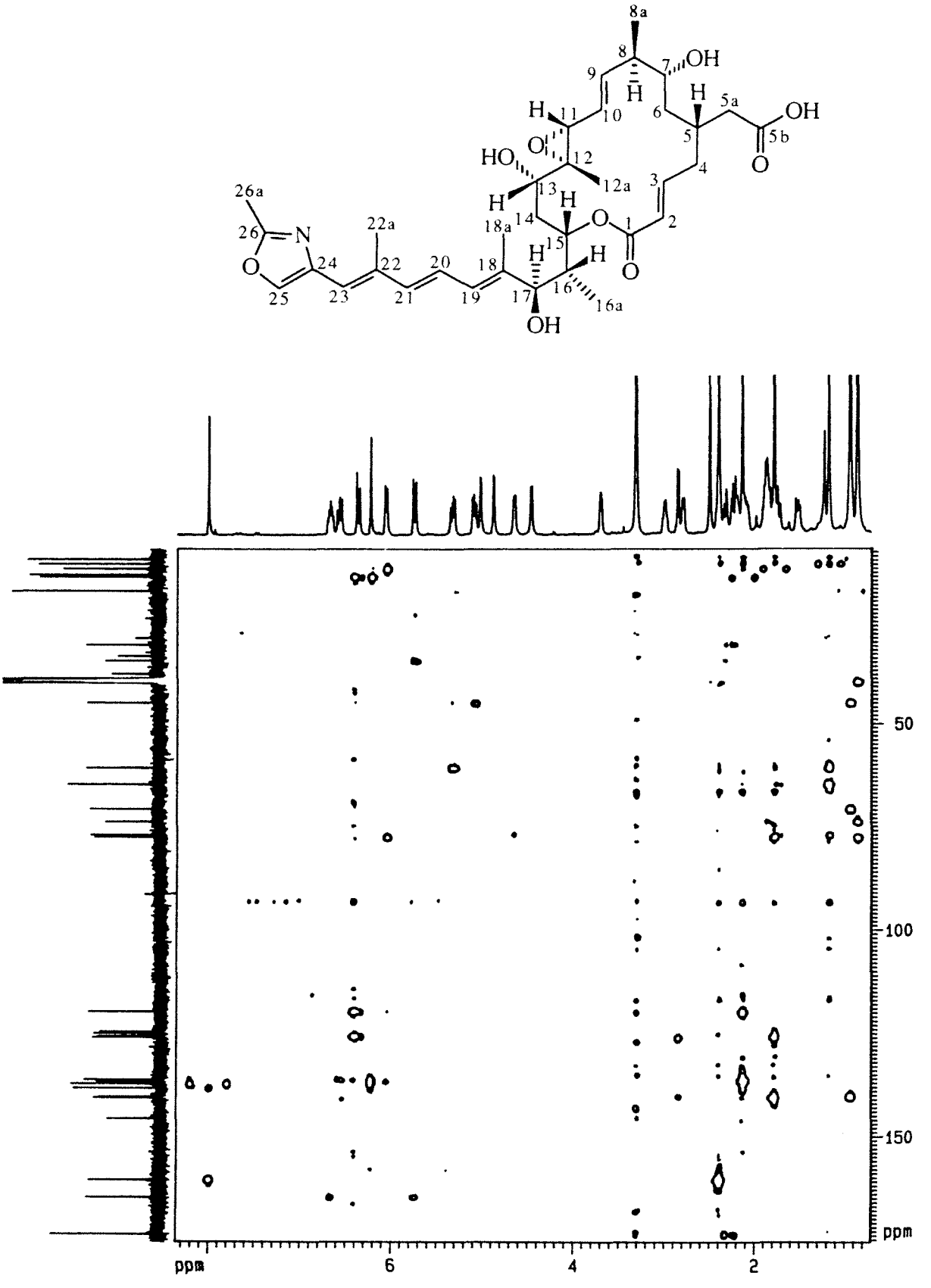

Figure 62. HMBC NMR spectrum of compound **45** (500 MHz ^{1}H NMR, DMSO-d_6).

7.2.4. Compound 46

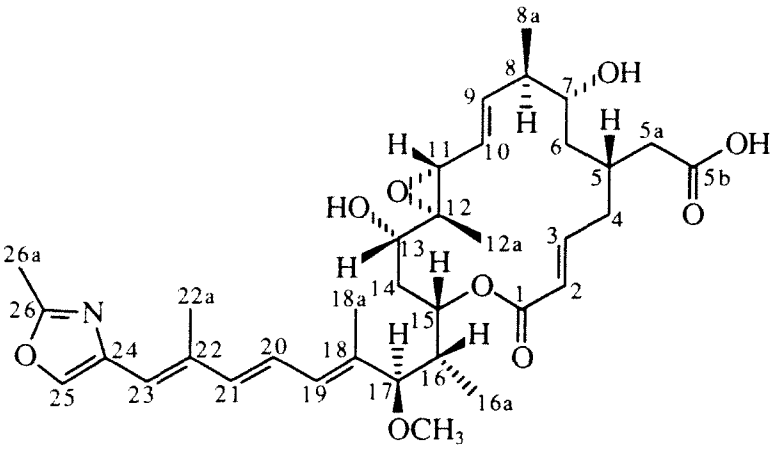

Compound **46** was isolated as an unstable white solid. The HRLSIMS showed a peak at m/z 628.34436 ($C_{35}H_{50}NO_9$, ΔM -4.20) corresponding to (M + H). Absorption bands at 3428 and 1713 cm^{-1} were consistent with hydroxy and carbonyl functionalities. Analysis of the NMR data (Table 13) identified **46** as a rhizoxin analog. The structure of **46** was disclosed by comparison of its NMR data with those of **45**. A new signal in the ^1H NMR spectrum (Figure 63) at δ 3.08, a singlet integrating for three protons, and a new carbon signal at δ 55.6 in the ^{13}C NMR spectrum (Figure 64) demonstrated that **46** contained a methoxy group. This was corroborated by an HMBC correlation from the methyl resonance at δ 3.08 (17-OCH_3) to the carbon resonance at δ 88.2 (C17). COSY (Figure 65), HMQC (Figure 66) and HMBC (Figure 67) experiments confirmed the proposed constitution for **46**. The absolute configuration was assumed to be as shown in structure **46** due to the similarity of this compound with rhizoxin.[60]

Table 13. ^{1}H and ^{13}C NMR data for compound **46**.

C#	δ ^{13}C[a]	δ ^{1}H[b]	COSY	HMBC[c]
1	164.6	—	—	H2,H3
2	124.7	5.76,d(15.5)	H3	—
3	145.8	6.69,m	H2,H4,H4'	—
4	34.6	2.08,m	H3,H4'	H2,H5a'
4'		2.42,m	H3,H4	—
5	30.6	2.20,m	H6'	H5a'
5a	40.0	2.23,m	—	H4'
5a'		2.33,m	—	—
5b	173.7	—	—	H5a,H5a'
6	37.8	0.95,m	H6',H7	—
6'	—	1.52,m	H5,H6	—
7	70.7	3.00,m	H6,H7-0H,H8	H8a
8	44.9	1.88,m	H7,H8a,H9	H8a,H9,H10
8a	17.4	0.94,d(6.6)	H8	H9
9	140.2	5.33,dd(15.6,9.2)	H8,H10	H8a
10	125.8	5.07,dd(15.6,8.0)	H9,H11	H11
11	60.6	2.84,d(8.0)	H10	H9,H12a
12	64.6	—	—	H12a,H14
12a	10.7	1.19,s	—	—
13	76.9	2.77,dm(10.1)	H13-OH,H14,H14'	H12a,H14,H14',H15
14	33.2	1.65,m	H13,H14'	H13-OH
14'		1.85,m	H13,H14,H15	—
15	72.9	4.63,dd(9.6,3.2)	H14'	H14'H16a
16	38.9	1.93,m	H16a,H17	H16a
16a	10.1	0.91,d(6.7)	H16	H15
17	88.2	3.28,d(8.8)	H16	H16a,H17-0CH_3,H18a,H19
17-OCH_3	55.6	3.08,s	—	—
18	136.0[d]	—	—	H18a
18a	11.3	1.76,s	H19	H19
19	128.8	6.13,d(11.0)	H18a,H20	H18a,H21
20	124.0	6.63,dd(15.1,11.0)	H19,H21	—
21	137.5	6.42,d(15.1)	H20	H19,H23
22	136.1[d]	—	—	H20,H22a
22a	14.0	2.16,s	H23	H21,H23
23	120.3	6.27,s	H22a	H21,H22a
24	138.1	—	—	H25
25	137.3	8.04,s	—	—
26	160.5	—	—	H25,H26a
26a	13.4	2.41,s	—	—
5b-OH	—	12.07,s	—	—
7-OH	—	4.47,d(6.5)	H7	—
13-OH	—	5.07,d(3.9)	H13	—

[a] Recorded in DMSO-d_6 at 125 MHz. Chemical shifts are referenced to solvent.
[b] Recorded in DMSO-d_6 at 400 MHz. Chemical shifts in ppm relative to TMS.
[c] Carbons in the carbon # column are correlated to the listed proton resonances.
[d] May be interchanged.

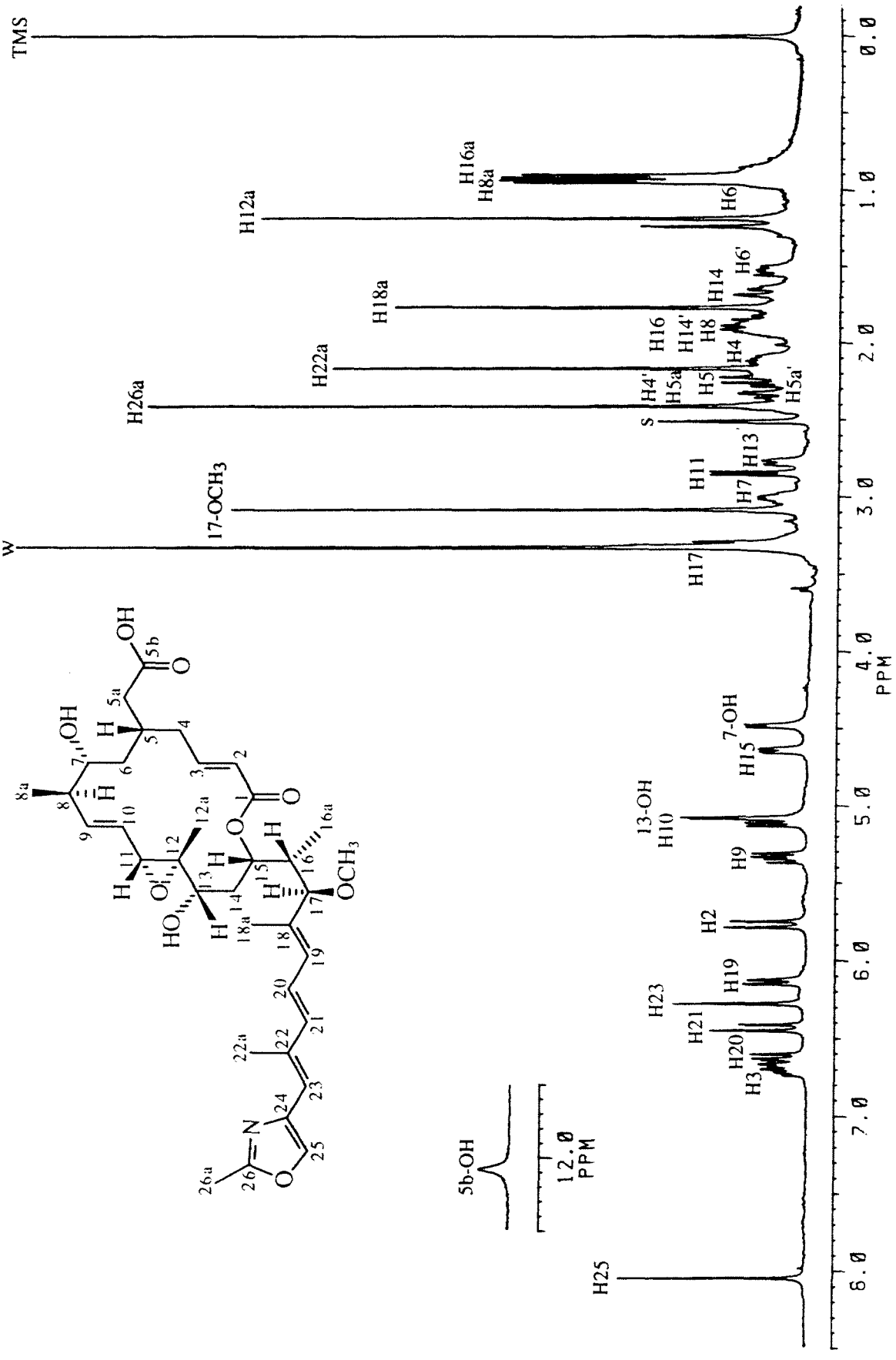

Figure 63. ^{1}H NMR spectrum of compound **46** (400 MHz, DMSO-d_6).

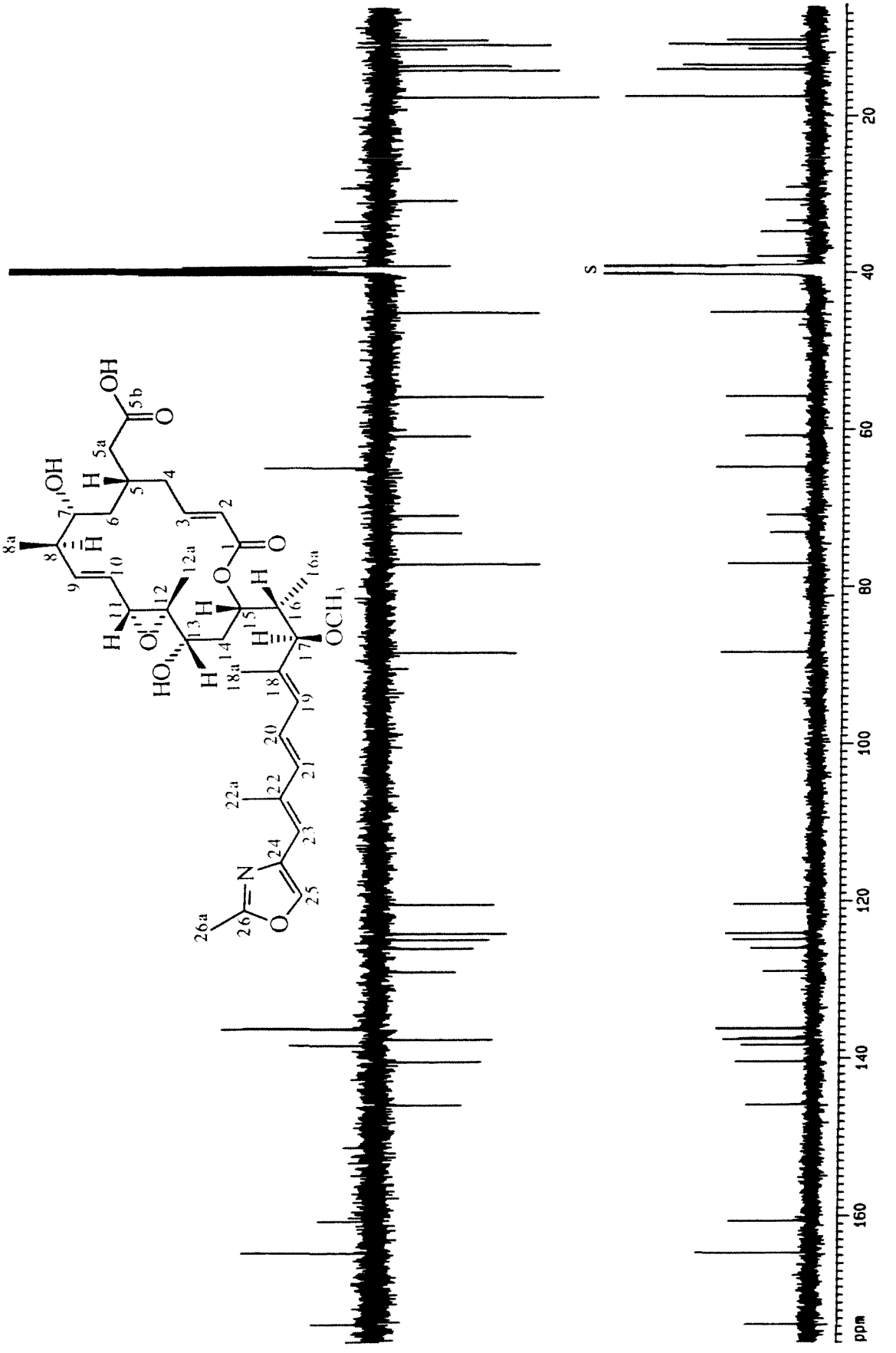

Figure 64. ^{13}C and APT NMR spectra of compound **46** (125 MHz, DMSO-d_6).

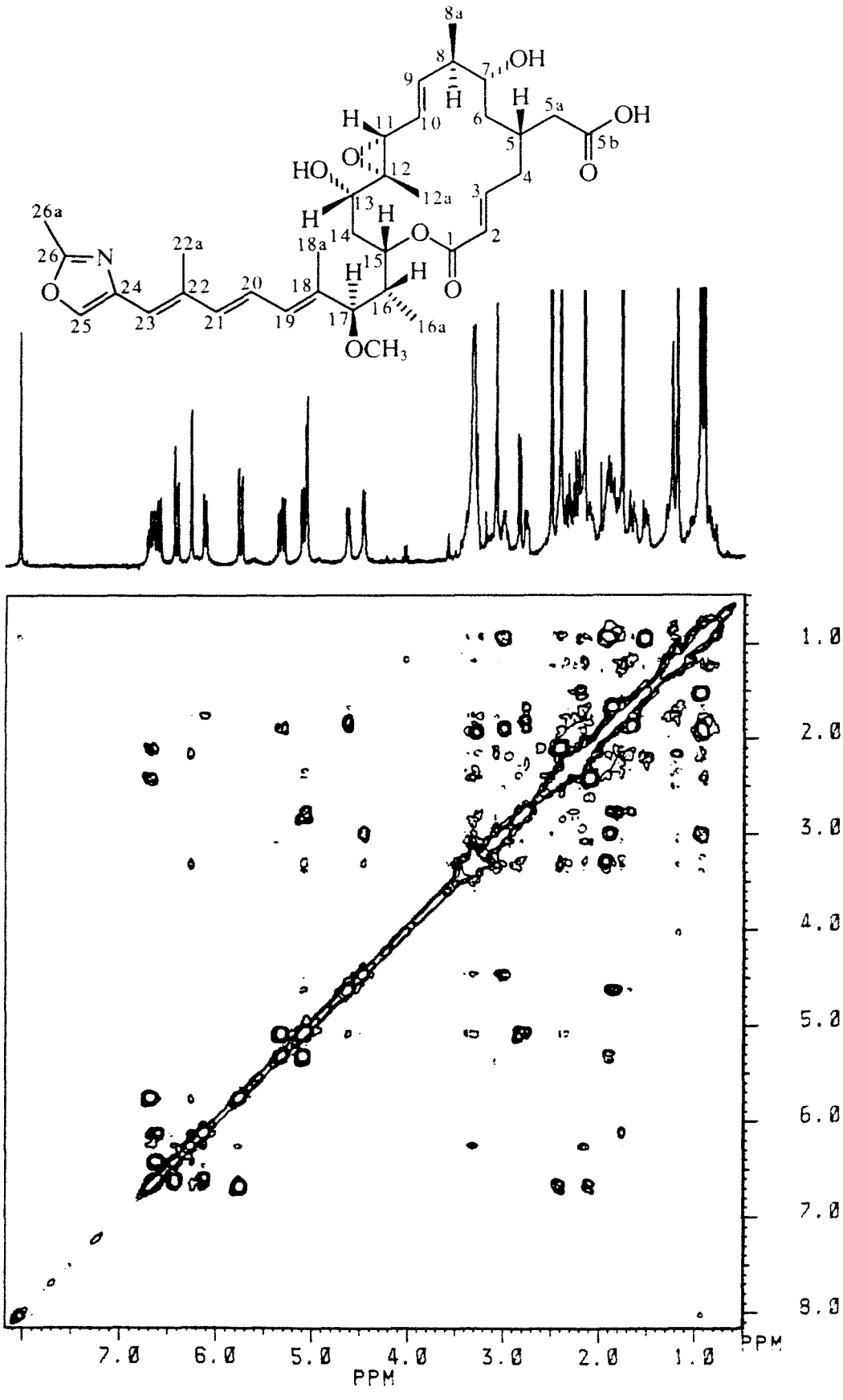

Figure 65. ^{1}H COSY NMR spectrum of compound **46** (400 MHz, DMSO-d_6).

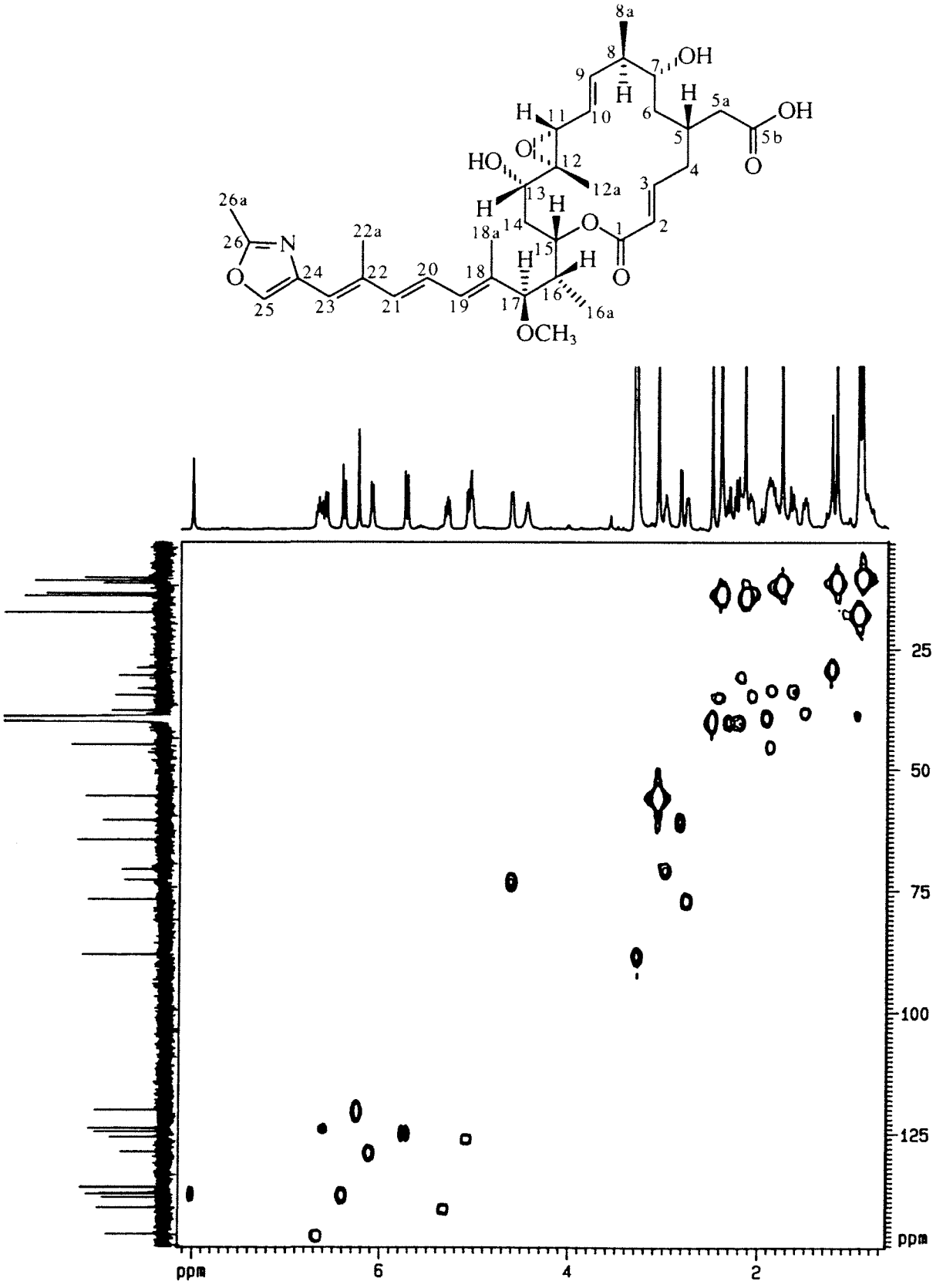

Figure 66. HMQC NMR spectrum of compound **46** (500 MHz ^{1}H NMR, DMSO-d_6).

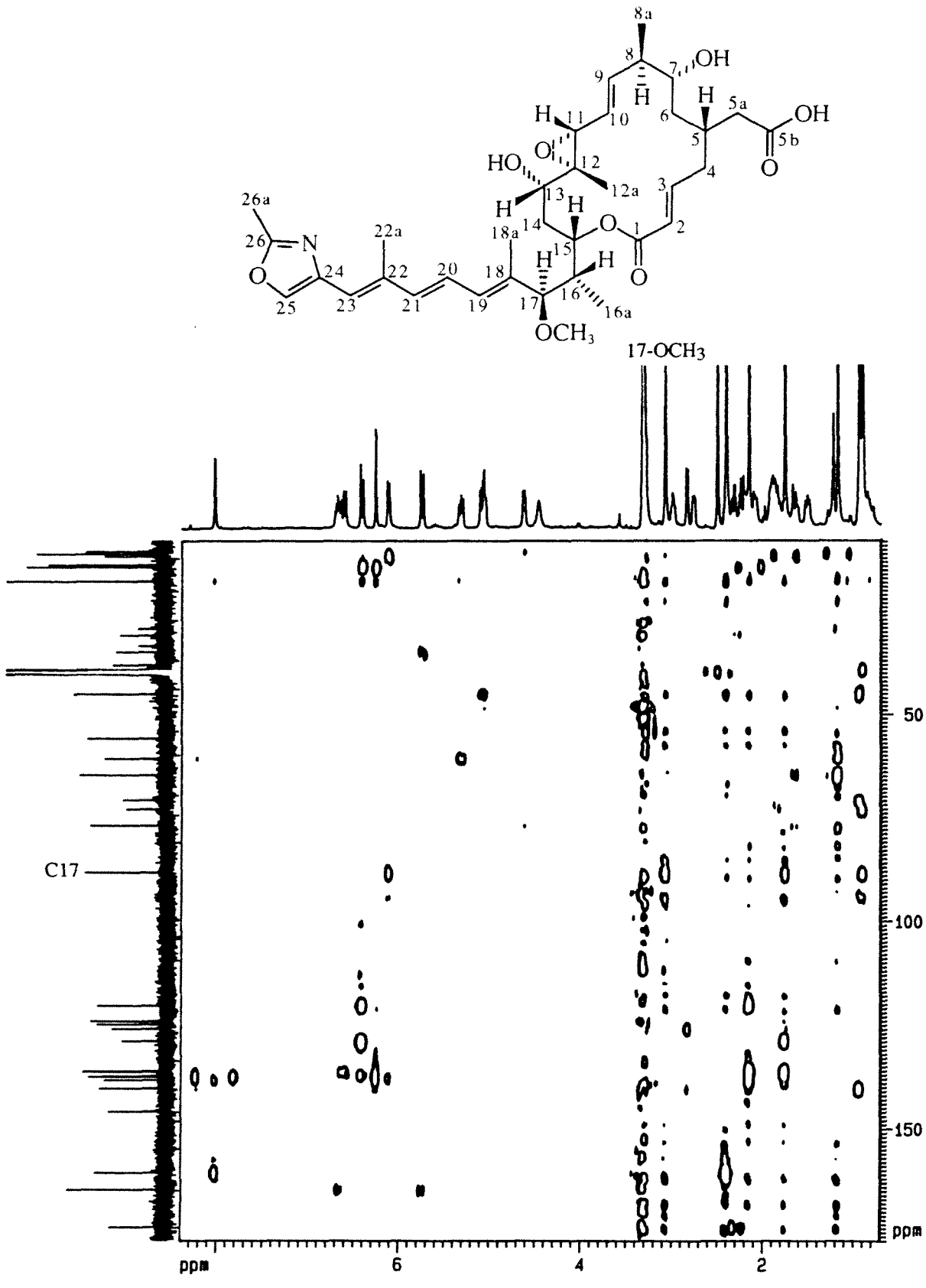

Figure 67. HMBC NMR spectrum of compound **46** (500 MHz ^{1}H NMR, DMSO-d_6).

7.2.5. Compound 47

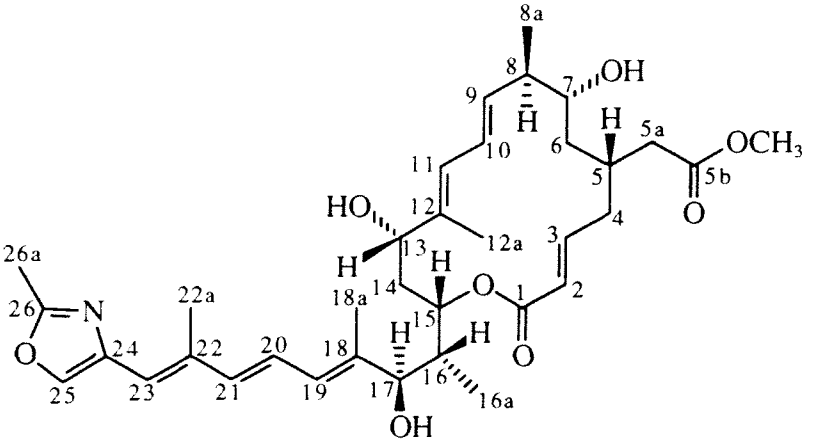

Compound **47** was isolated as an amorphous white solid. A molecular ion in the HREIMS at m/z 611.3449 (ΔM -0.9 mmu) corresponded to a molecular formula of $C_{35}H_{49}NO_8$. The IR spectrum contained absorption bands at 3412 and 1715 cm^{-1} indicating the presence of hydroxy and carbonyl functionalities. Comparison of the NMR data for **47** (Table 14) with those for WF-1360C (**50**) identified a δ-hydroxy methyl ester functionality for **47** in place of the δ-lactone in WF-1360C (**50**). A new signal in the ^1H NMR spectrum (Figure 68) at δ 3.68 (5b-OCH_3) and a new carbon signal at δ 51.6 (5b-OCH_3) in the ^{13}C NMR spectrum (Figure 69) demonstrated the presence of a methyl ester group. Upfield chemical shifts in the H7 proton (**47**: δ 3.11, WF-1360C (**50**): δ 3.70) and C7 carbon (**47**: δ 77.2, WF-1360C (**50**): δ 83.2) of **47** suggested a change in the δ-lactone ring of WF-1360C. Further evidence for the δ-hydroxy methyl ester was provided by an HMBC experiment. The methyl resonance at δ 3.68 (5b-OCH_3) showed an HMBC correlation to the carbonyl carbon at δ 173.8 (C5b). These data support the constitution depicted in **47**. The absolute stereochemistry was proposed to be as shown in structure **47** on the basis of its similarity to rhizoxin.[60] This compound is probably an artifact due to the use of methanol in the isolation procedure.

Table 14. ^{1}H and ^{13}C NMR data for compound **47**.

C#	δ ^{13}C[a]	δ ^{1}H[b]	COSY	HMBC[c]
1	166.7	—	—	H2
2	123.0	5.61,dd(15.4,1.6)	H3	—
3	149.3	6.80,m	H2,H4,H4'	—
4	39.2	1.95,m	H3,H4'	H2,H5,H5a,H5a'
4'	—	2.35,m	H3,H4	—
5	34.5	1.97,m	H5a,H5a'	H5a
5a	40.5	2.40,m	H5,H5a'	H5
5a'	—	2.81,dd(15.6,4.4)	H5,H5a	—
5b	173.8	—	—	H5a,5b-OMe
5b-OMe	51.6	3.68,s	—	—
6	37.1	0.96,m	H6',H7	—
6'	—	2.02,m	H6	—
7	77.2	3.11,m	H6,H8	H8a
8	46.1	2.04,m	H7,H8a,H9	H8a,H10
8a	16.6	1.05,d(6.5)	H8	H9
9	137.8	5.25,dd(15.1,9.6)	H8,H10	H8a,H11
10	128.1	6.13,dd(15.1,10.8)	H9,H11	—
11	126.6	5.81,d(10.8)	H10,H12a	H9,H12a
12	138.1[d]	—	—	H12a
12a	10.5	1.76,s	H11	H11
13	78.7	4.06,bd(10.6)	H14,H14'	H11,H12a
14	34.3	1.90,m	H13,H14'	—
14'	—	2.10,m	H13,H14,H15	—
15	73.8	4.90,dd(10.3,6.8)	H14'	H16a
16	40.6	1.90,m	H16a,H17	H16a
16a	9.7	0.92,d(6.9)	H16	H15
17	75.7	3.91,bs	H16	H16a,H18a,H19
18	138.3[d]	—	—	H18a
18a	13.6	1.81,s	H19	H19
19	126.0	6.26,d(11.0)	H18a,H20	H18a,H21
20	124.5	6.57,dd(15.1,11.0)	H19,H21	—
21	137.1	6.39,d(15.1)	H20	H20,H22a
22	137.9[d]	—	—	—
22a	14.4	2.13,s	H23	H21,H23
23	120.2	6.24,s	H22a	H21,H22a
24	138.8	—	—	H25
25	135.8	7.52,s	—	H23
26	160.8	—	—	H25,H26a
26a	13.8	2.46,s	—	—

[a] Recorded in $CDCl_3$ at 125 MHz. Chemical shifts are referenced to solvent.
[b] Recorded in $CDCl_3$ at 400 MHz. Chemical shifts in ppm relative to TMS.
[c] Carbons in the carbon # column are correlated to the listed proton resonances.
[d] May be interchanged.

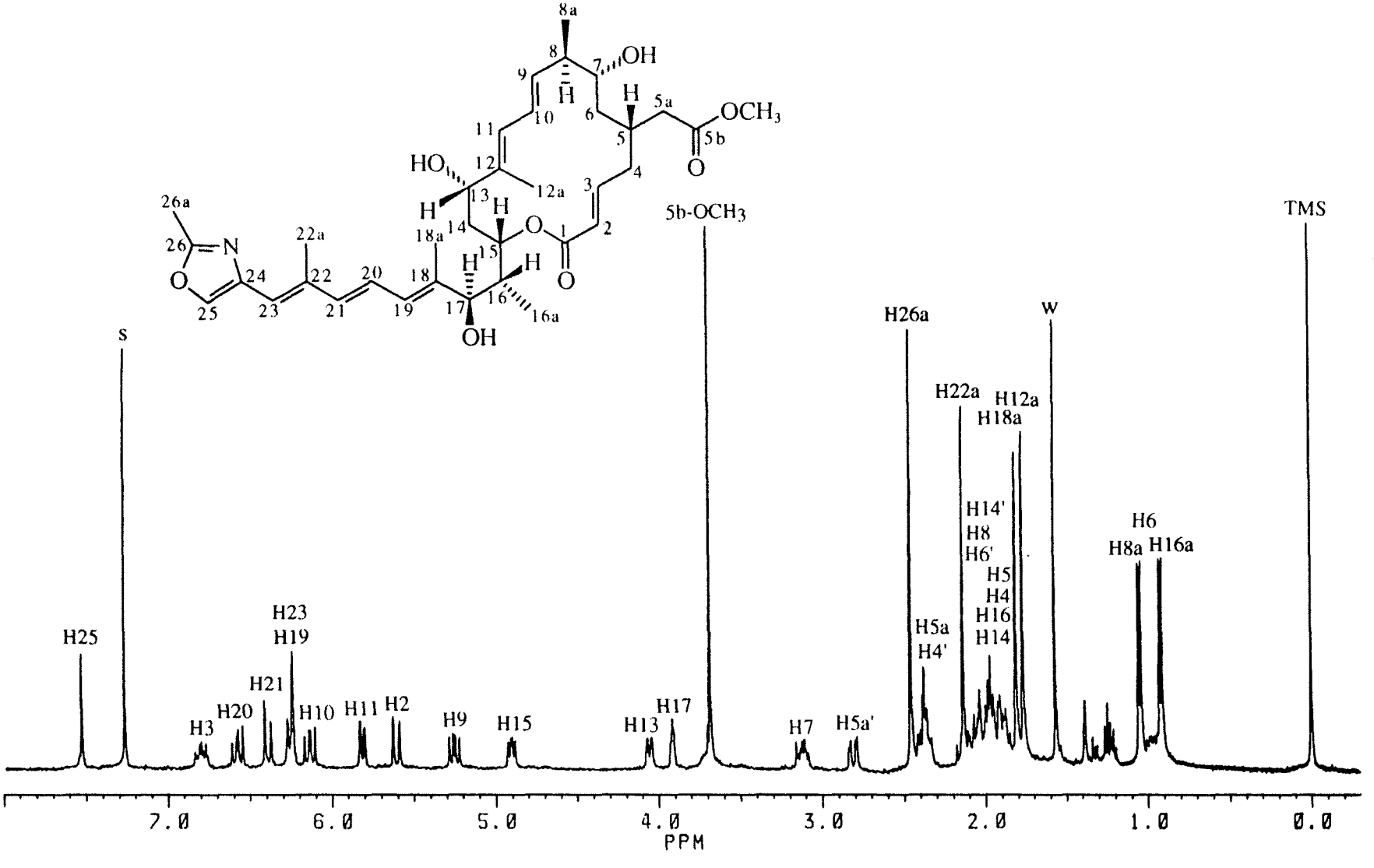

Figure 68. ^{1}H NMR spectrum of compound **47** (400 MHz, $CDCl_3$).

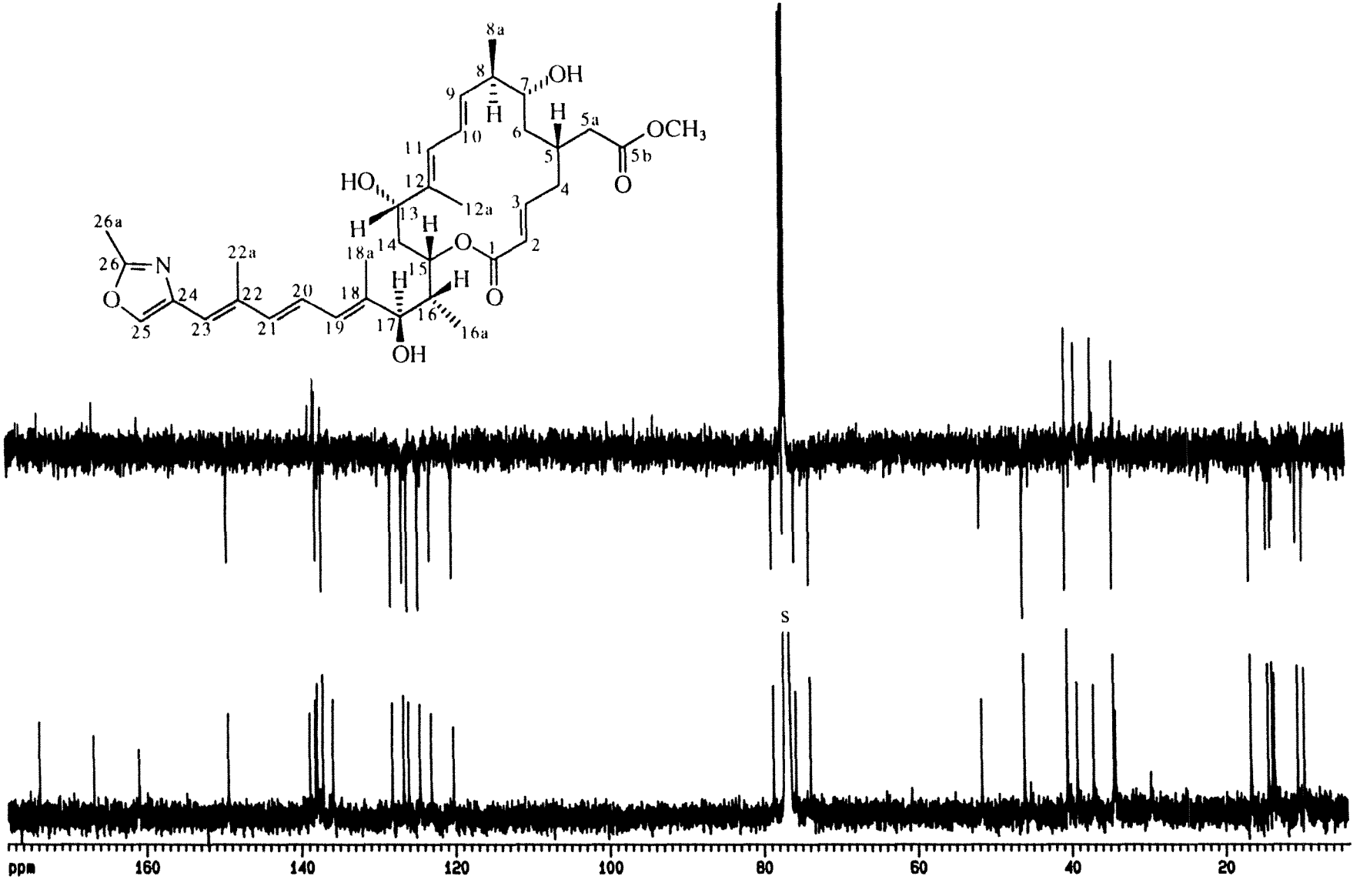

Figure 69. ^{13}C and APT NMR spectra of compound **47** (125 MHz, $CDCl_3$).

7.2.6. Compound 48

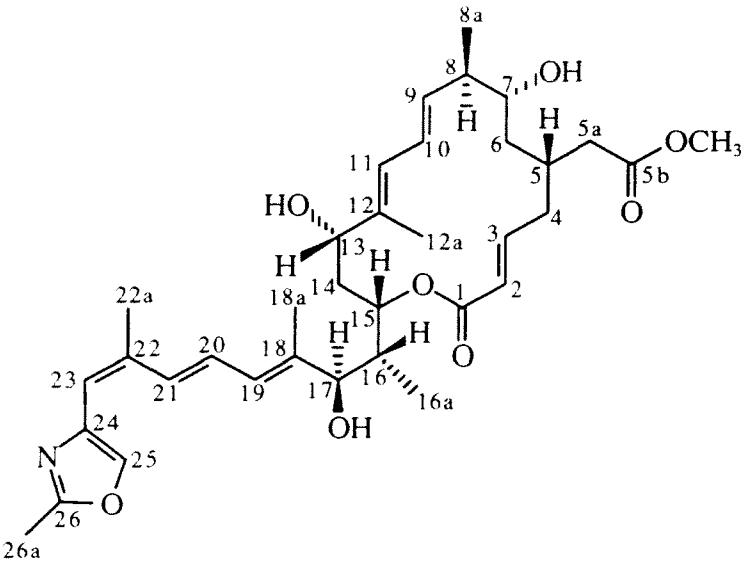

Compound **48** was obtained as a white solid. A molecular ion in the HREIMS at m/z 611.3463 (ΔM +0.5 mmu) was appropriate for a molecular formula of $C_{35}H_{49}NO_8$. Absorption bands at 3404 and 1715 cm^{-1} in the IR spectrum indicated the presence of hydroxy and carbonyl functionalities. Analysis of the ^1H (Figure 70) and ^{13}C NMR (Figure 71) data summarized in Table 15 identified **48** as a rhizoxin analog. Compound **48** was identified as the (22Z)-isomer of compound **47** on the basis of an NOE experiment. Irradiation of the methyl resonance at δ 2.03 (H22a) induced enhancements of the signals for H20 (19.2 %) and H23 (12.5 %). The absolute stereochemistry of **48** was proposed based on the structure of rhizoxin (**53**).[60] The (22Z)-isomer was probably an artifact due to the exposure of **47** to light. It has been shown that (22Z)-rhizoxin is a photoisomerization product obtained when rhizoxin was irradiated by a UV-Auto-Fade meter.[61g]

Table 15. ^{1}H and ^{13}C NMR data for compound **48**.

C#	δ ^{13}C[a]	δ ^{1}H[b]	COSY	HMBC[c]
1	166.8	—	—	—
2	123.1	5.61,dd(15.7,1)	H3	—
3	149.3	6.80,m	H2,H4,H4'	—
4	39.2	1.95,m	H3,H4'	H2,H5a
4'	—	2.35,m	H3,H4	—
5	34.4	1.95,m	H5a,H5a'	H5a
5a	40.5	2.40,m	H5,H5a'	—
5a'	—	2.81,dd(15.6,4.0)	H5,H5a	—
5b	173.8	—	—	5b-OMe
5b-OMe	51.6	3.68,s	—	—
6	37.1	0.95,m	H6',H7	—
6'	—	2.00,m	H6	—
7	77.5	3.11,m	H6,H8	H8a
8	46.1	2.05,m	H7,H8a,H9	H8a,H10
8a	16.7	1.05,d(6.5)	H8	H9
9	137.7	5.24,dd(15.1,9.6)	H8,H10	H8a
10	128.1	6.13,dd(15.1,10.8)	H9,H11	—
11	126.5	5.80,d(10.8)	H10,H12a	H9,H12a
12	138.0	—	—	H11,H12a
12a	10.6	1.77,s	H11	H11
13	78.6	4.06,bd(10.7)	H14,H14'	H11,H12a
14	34.5	1.90,m	H13,H14'	—
14'	—	2.10,m	H13,H14,H15	—
15	74.0	4.89,dd(9.8,7.2)	H14'	H16a
16	40.6	1.90,m	H16a,H17	H16a
16a	9.8	0.92,d(6.9)	H16	H15
17	75.9	3.93,bs	H16	H16a,H18a,H19
18	138.3	—	—	H18a
18a	13.5	1.81,s	H19	H19
19	126.5	6.33,d(11.0)	H18a,H20	H18a,H21
20	126.7	6.62,dd(15.3,11.0)	H19,H21	H21
21	131.1	7.34,d(15.3)	H20	H19,H22a,H23
22	135.8	—	—	H21,H22a
22a	20.9	2.03,s	H23	H21,H23
23	117.6	6.06,s	H22a	H22a
24	138.6	—	—	H25
25	135.9	7.47,s	—	H23
26	161.5	—	—	H25,H26a
26a	13.9	2.45,s	—	—

[a] Recorded in $CDCl_3$ at 125 MHz. Chemical shifts are referenced to solvent.
[b] Recorded in $CDCl_3$ at 500 MHz. Chemical shifts in ppm relative to TMS.
[c] Carbons in the carbon # column are correlated to the listed proton resonances.

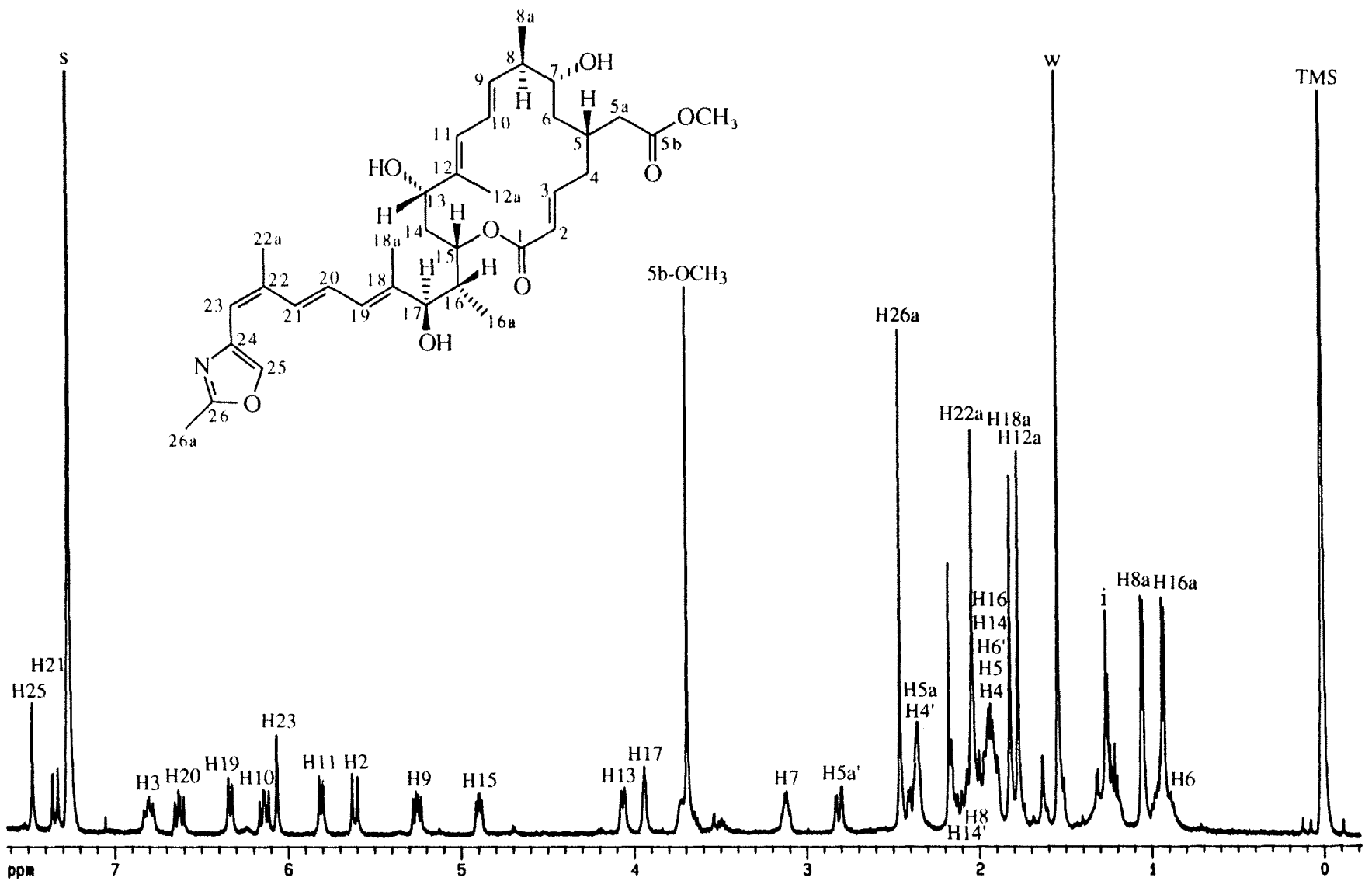

Figure 70. ^{1}H NMR spectrum of compound **48** (500 MHz, $CDCl_3$).

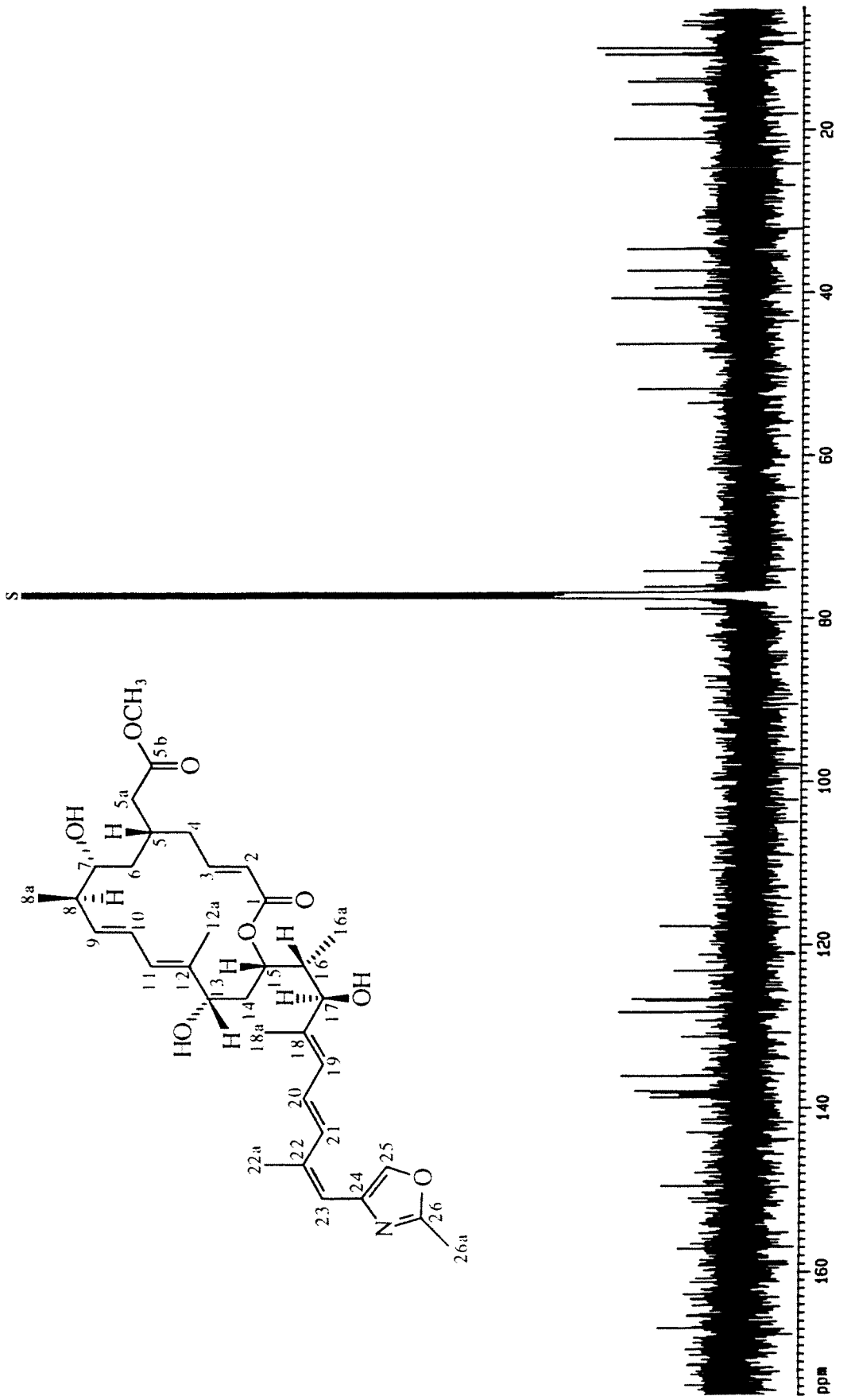

Figure 71. ^{13}C NMR spectrum of compound **48** (125 MHz, $CDCl_3$).

7.2.7. Compound 49

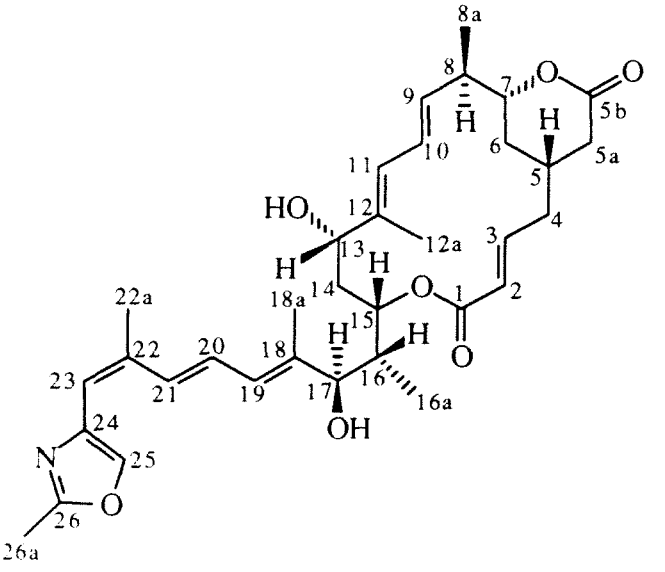

Compound **49** was obtained as a white solid. A molecular ion peak in the HREIMS at m/z 579.3188 was appropriate for the molecular formula $C_{34}H_{45}NO_7$ (ΔM -0.8 mmu). Hydroxy and carbonyl functionalities were indicated by the presence of absorption bands at 3415 and 1714 cm^{-1} in the IR spectrum. Analysis of the ^1H (Figure 72) and ^{13}C NMR (Figure 73) data summarized in Table 16 identified **49** as a rhizoxin analog. Compound **49** was identified as the (22Z)-isomer of WF-1360C (**50**) on the basis of an NOE experiment and is probably an artifact. Irradiation of the methyl resonance at δ 2.04 (H22a) induced enhancements of the signals for H20 (5.7 %) and H23 (7.5 %). The absolute stereochemistry of **49** was proposed based on its similarity to rhizoxin (**53**).[60]

Table 16. ^{1}H and ^{13}C NMR data for compound **49**.

C#	δ ^{13}C[a]	δ ^{1}H[b]	COSY	HMBC[c]
1	166.3	—	—	—
2	124.2	5.64,d(15.8)	H3	—
3	146.7	6.79,m	H2,H4,H4'	—
4	38.3	1.75,m	H3,H4'	H2,H5a
4'	—	2.55,m	H3,H4	—
5	29.7	1.80,m	H5a'	H5a
5a	36.8	2.10,m	H5a'	—
5a'	—	2.77,dd(18.1,3.1)	H5,H5a	—
5b	170.3	—	—	H5a
6	34.6	0.70,m	H6',H7	—
6'	—	1.97,m	H6	—
7	83.2	3.69,m	H6	H8a
8	45.3	2.30,m	H8a	H8a,H10
8a	16.6	1.20,d(6.4)	H8	—
9	134.6	5.18,dd(15.2,9.6)	H10	H8a,H11
10	129.7	6.25,dd(15.2,10.7)	H9,H11	—
11	126.0	5.83,d(10.7)	H10,H12a	H9,H12a
12	139.4	—	—	H11,H12a
12a	11.0	1.81,s	H11	H11
13	78.2	4.00,d(10.1)	H14,H14'	H11,H12a
14	33.9	1.88,m	H13,H14'	—
14'	—	2.15,m	H13,H14	—
15	75.1	4.68,dd(10.3,5.3)	—	H16a
16	40.1	2.15,m	H16a,H17	H16a
16a	9.7	0.98,d(6.7)	H16	—
17	78.0	3.92,bs	H16	H16a,H18a,H19
18	138.7	—	—	H18a
18a	12.7	1.89,s	H19	H19
19	127.3	6.29,d(11.2)	H18a,H20	H18a,H21
20	126.5	6.62,dd(15.3,11.2)	H19,H21	—
21	131.8	7.40,d(15.3)	H20	H19,H23
22	135.6	—	—	H20,H22a
22a	20.9	2.04,s	H23	H21,H23
23	117.6	6.07,s	H22a	H22a
24	138.3	—	—	—
25	136.1	7.47,s	—	H23
26	161.3	—	—	H25,H26a
26a	13.9	2.45,s	—	—

[a] Recorded in $CDCl_3$ at 125 MHz. Chemical shifts are referenced to solvent.
[b] Recorded in $CDCl_3$ at 500 MHz. Chemical shifts in ppm relative to TMS.
[c] Carbons in the carbon number # are correlated to the listed proton resonances.

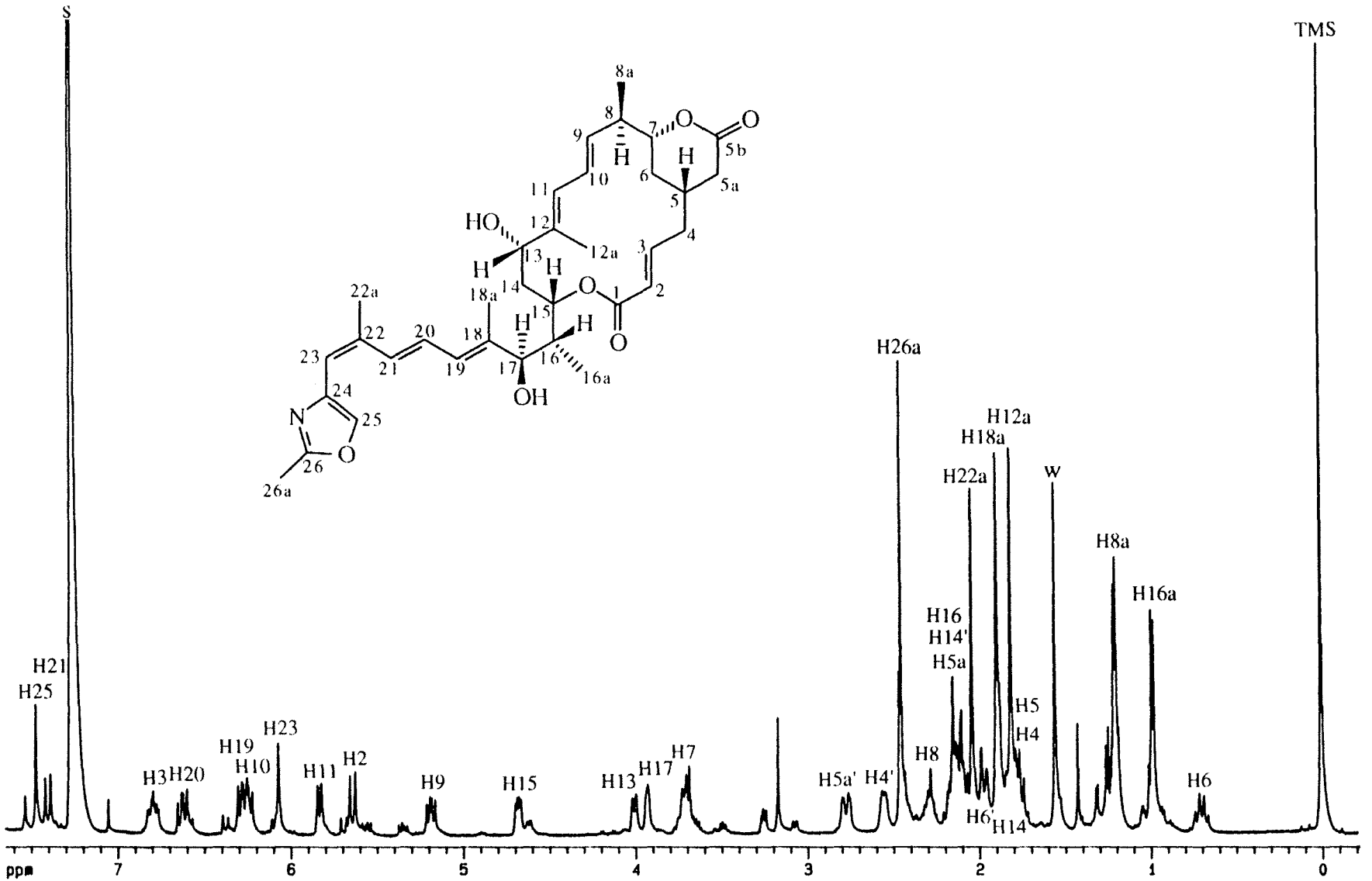

Figure 72. ^{1}H NMR spectrum of compound **49** (500 MHz, $CDCl_3$).

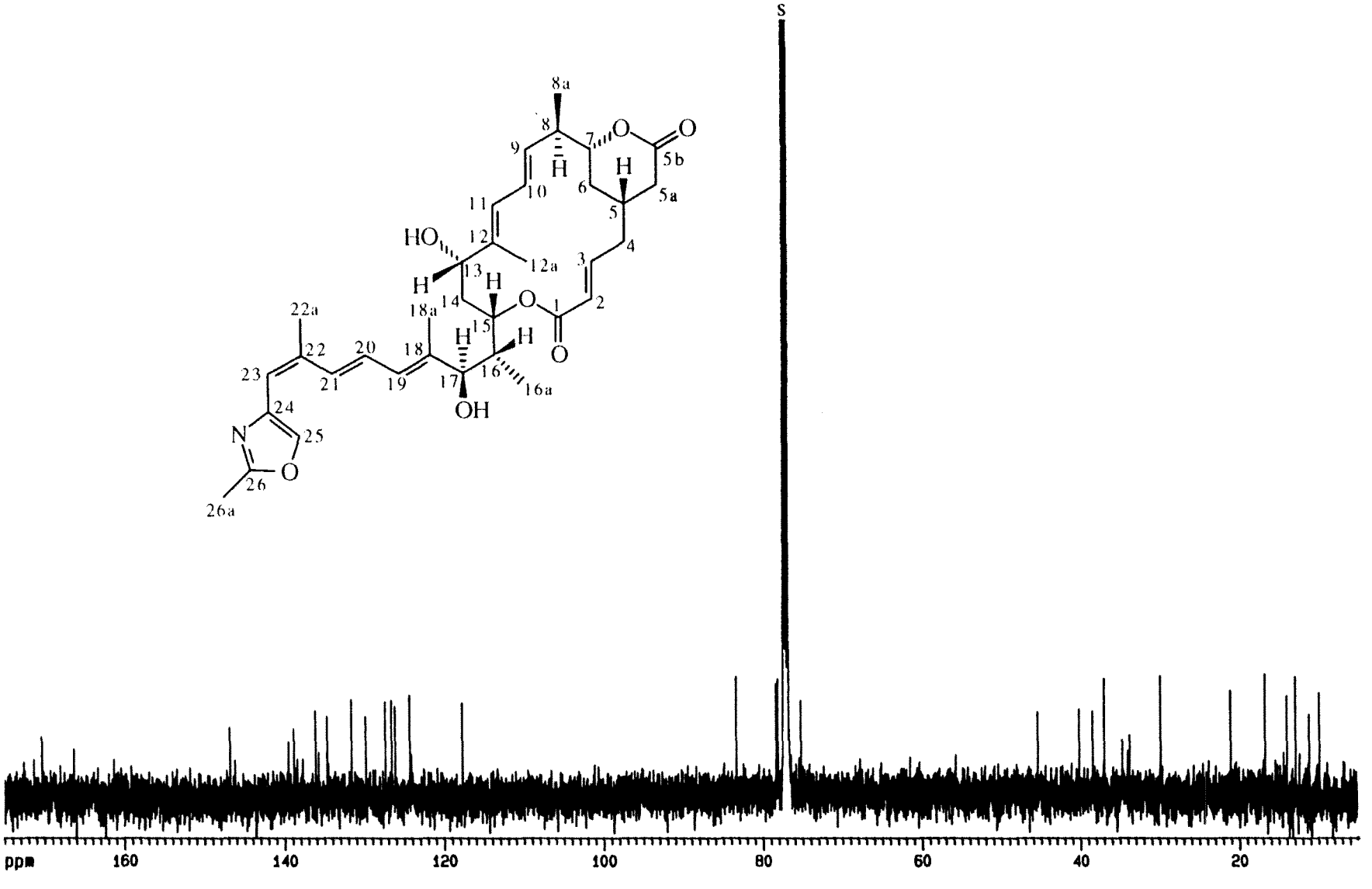

Figure 73. ^{13}C NMR spectrum of compound **49** (125 MHz, $CDCl_3$).

7.2.8. Biological activity of rhizoxin analogs 44 to 47 and 50

The crude extract obtained from cultures of *Pseudomonas* sp. (91V47) had shown potent in vitro cytotoxicity. The pure compounds **44** to **47** and compound **50** were tested against P388 murine leukemia and the results are presented in Table 17. The rhizoxin analogs **44** to **47** and **50** showed significant cytotoxicity against the P388 murine leukemia cell line. At concentrations of 100 μg/disc compounds **44** to **47** and **50** failed to show antibacterial activity against methicillin-resistant *Staphylococcus aureus*.

Table 17. Cytotoxic activity of the rhizoxin analogs **44** to **47** and **55**.

Compound	ED_{50} against P388 (μg/mL)
Crude extract	0.0287
Compound **44**	0.0230
Compound **45**	0.140
Compound **46**	0.008
Compound **47**	0.0613
Compound **50**	0.0586

7.3. Conclusion

A culture of the bacterium *Pseudomonas* sp. 91V47, isolated from an abalone collected off Cortez Island in Georgia Strait, British Columbia, resulted in the isolation and structure elucidation of the 16-membered macrolides **44** to **50**. Compounds **44** to **46** are new natural products containing a δ-hydroxy acid moiety in place of the δ-lactone in the previously reported rhizoxin analogs **50** to **52**.[59] Although compounds **44** to **46** have been claimed in the Patent literature[62] as semi-synthetic derivatives of **50** to **52**, no spectroscopic data has been published.

The new compounds **47** to **49** are presumed to be isolation artifacts. The rhizoxin analog WF-1360C (**50**) has been previously reported.[59]

The crude extract from cultures of *Pseudomonas* sp. 91V47 showed potent in vitro cytotoxic activity against the P388 murine leukemia cell line and antibacterial activity against methicillin-resistant *Staphylococcus aureus*. The rhizoxin analogs **44** to **47** and **50** proved to be responsible for the cytotoxic activity. However, the pure rhizoxin analogs did not exhibit antibacterial activity at concentrations of 100 μg/disc against methicillin-resistant *S. aureus*, therefore, the antibacterial constituents of the crude extract still need to be identified.

Rhizoxin (**53**) and the analogs **50** to **52** belong to a family of 16-membered ring macrolides originally isolated from the fungi *Rhizopus chinensis*, [59a] the pathogen responsible for rice seedling blight, and *Rhizopus* sp. F-1360.[59b] Rhizoxin and its analogs exhibit antifungal activity[59,60] and are promising lead compounds for antitumour drug development due to their in vitro and in vivo antitumour activity.[61] The mechanism of action is thought to be similar to that of the dimeric vinca alkaloids vincristine and vinblastine which inhibit mitosis by binding to tubulin.

Biosynthetic studies on rhizoxin have established a polyketide biosynthesis with O-acetyl-L-serine as a starter unit. The methyl substituents are derived from methionine.[64]

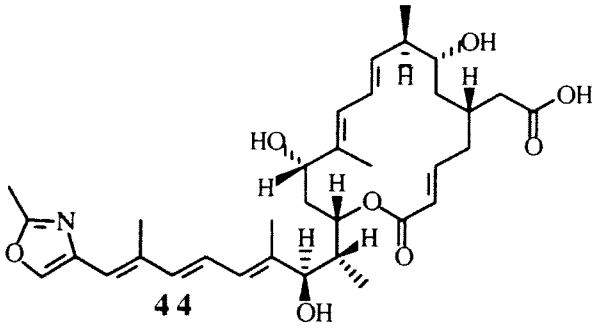

44

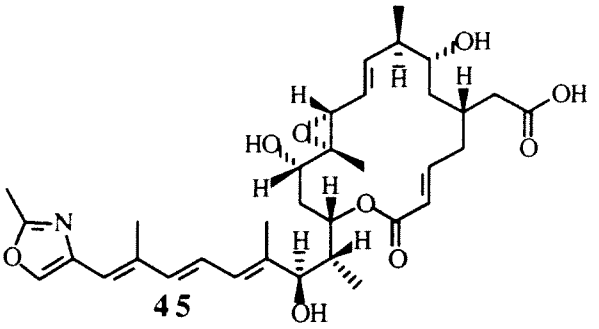

45

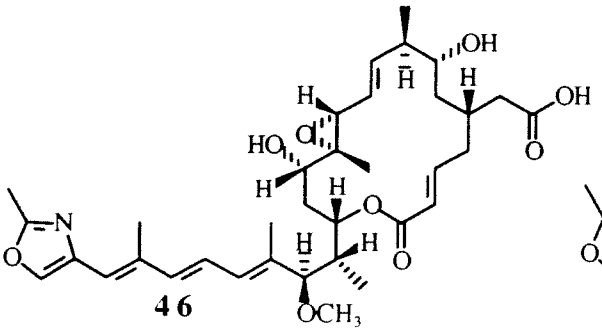

46

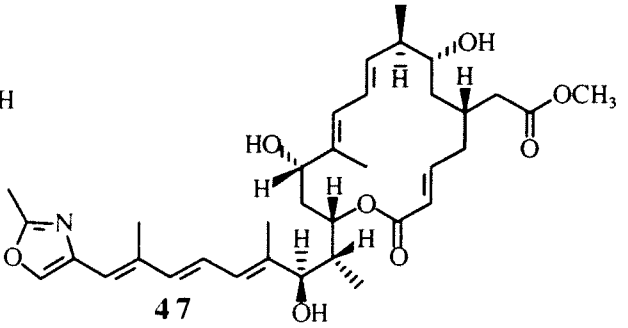

47

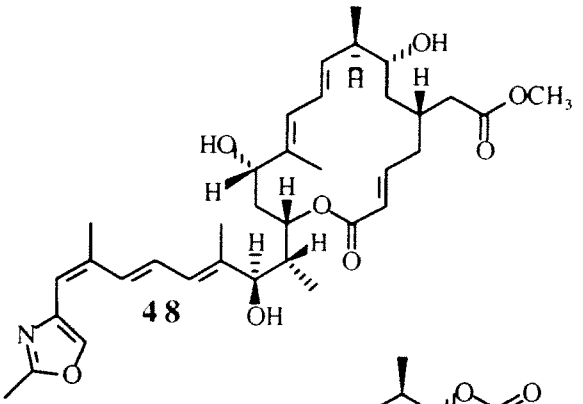

48

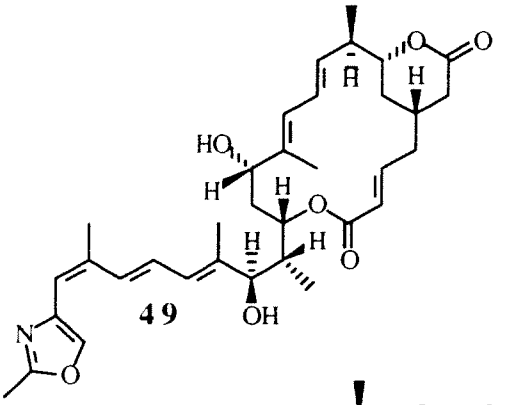

49

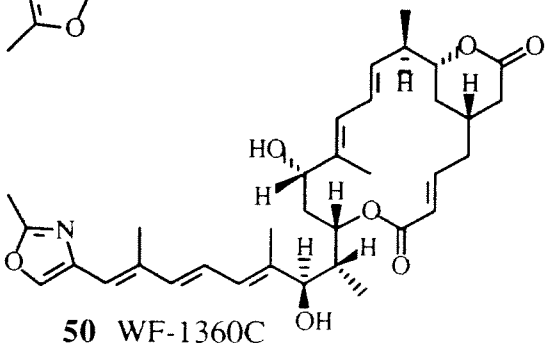

50 WF-1360C

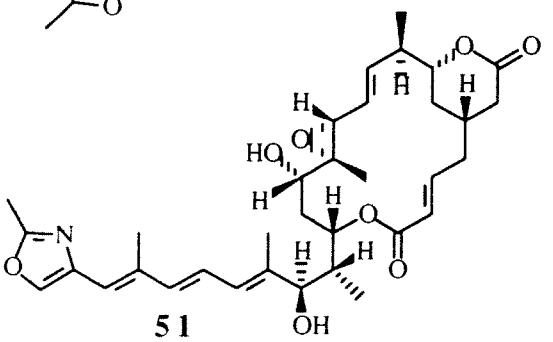

51

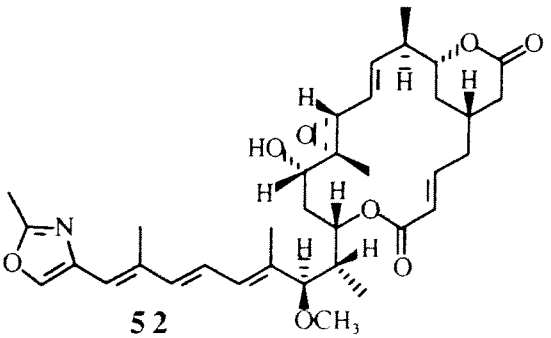

52

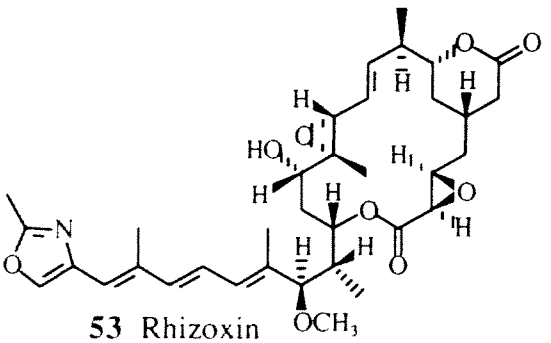

53 Rhizoxin

8. SECONDARY METABOLITES FROM *BACILLUS PUMILUS* (91Z50)

8.1. Introduction

A marine isolate of the bacterium *Bacillus pumilus* was obtained from a sediment sample collected in Georgia Strait, British Columbia. Preliminary studies showed that extracts of liquid shake cultures of *Bacillus pumilus* 91Z50 exhibited antimicrobial activity against *Staphylococcus aureus*, methicillin-resistant *S. aureus*, *S. saprophyticus* and *Enterococcus faecalis*. In order to obtain sufficient quantities of the antibacterial metabolites for structure elucidation *Bacillus pumilus* 91Z50 was grown in moderate scale liquid culture.

8.2. Results and Discussion

Bacillus pumilus 91Z50 was grown in liquid shake culture at room temperature in one liter Erlenmeyer flasks containing 500 mL of tryptic soy broth medium and 1 % sodium chloride. The cultures were harvested by filtration five days after inoculation and the supernatant was passed over a column of XAD-4 resin. Elution of the adsorbed organic material from the XAD-4 resin with methanol followed by evaporation of the methanol in vacuo gave a crude residue which exhibited antibacterial activity. The crude residue was partitioned between ethyl acetate and water and the antibacterial activity was found to reside in the organic extract. The ethyl acetate extract was fractionated by Sephadex LH-20 chromatography (eluent: 3:1 methanol/dichloromethane). An early eluting fraction contained an interesting purple TLC spot on spraying with ninhydrin (reversed-phase silica, R_f = 0.39, 4:1 methanol/water). Further purification by reversed-phase column chromatography and HPLC (eluent: methanol/water) yielded the known antimicrobial compound AI-77-B[65d] (**54**) (22 mg). Acetylation of AI-77-B gave the triacetate (**55**).[65d] A later LH-20 fraction showing antimicrobial activity was further

purified on Sephadex LH-20 (eluent: ethyl acetate/methanol/water 8:2:1) followed by normal phase TLC silica flash chromatography yielding the known compound AI-77-F (**56**)[65d] (6 mg) as well as the novel compound **57** (5 mg).

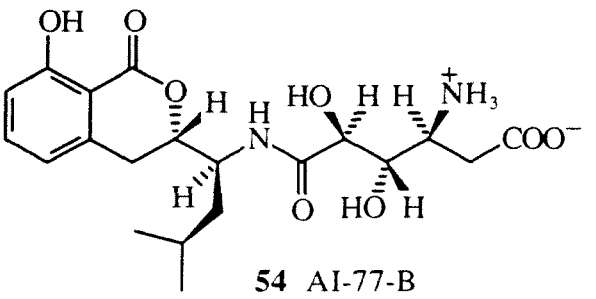

54 AI-77-B

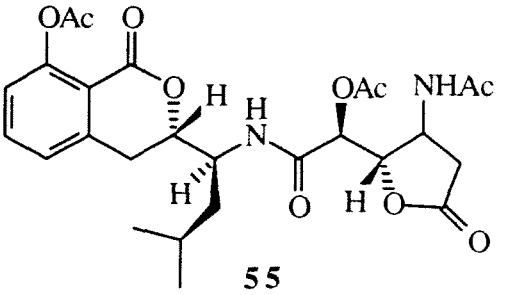

55

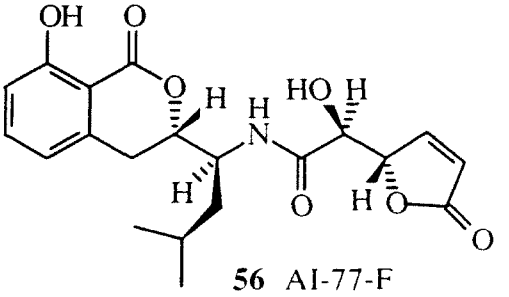

56 AI-77-F

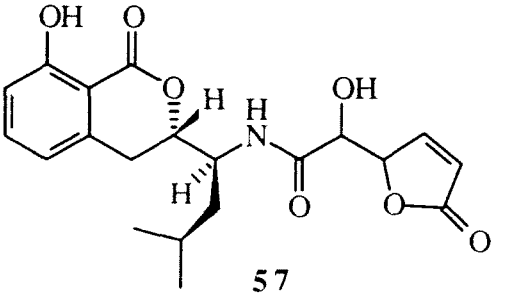

57

8.2.1. Known compounds from *Bacillus pumilus*

The major metabolite obtained from cultures of *Bacillus pumilus* was identified as AI-77-B (**54**) by comparing its MS and NMR data (see experimental) with literature values.[65d] ^{1}H (Figure 74) and ^{13}C (Figure 75) NMR spectra were obtained in methanol. A molecular ion peak was observed in the LRDCIMS at m/z 425 ($C_{20}H_{28}N_2O_8$ + H). The HREIMS did not show a molecular ion peak but a peak at m/z 406.1740 ($C_{20}H_{26}N_2O_7$, ΔM +0.0 mmu) corresponded to the molecular ion peak with the loss of water. At a concentration of 100 µg/disc AI-77-B showed antibacterial activity against *Staphylococcus aureus*, methicillin-resistant *S. aureus* and *S. saprophyticus*. This compound accounted for most of the antibacterial activity in the crude extract. AI-77-B, a gastroprotective substance, was originally isolated from a terrestrial isolate of the bacterium *Bacillus pumilus* obtained from a soil sample.[65]

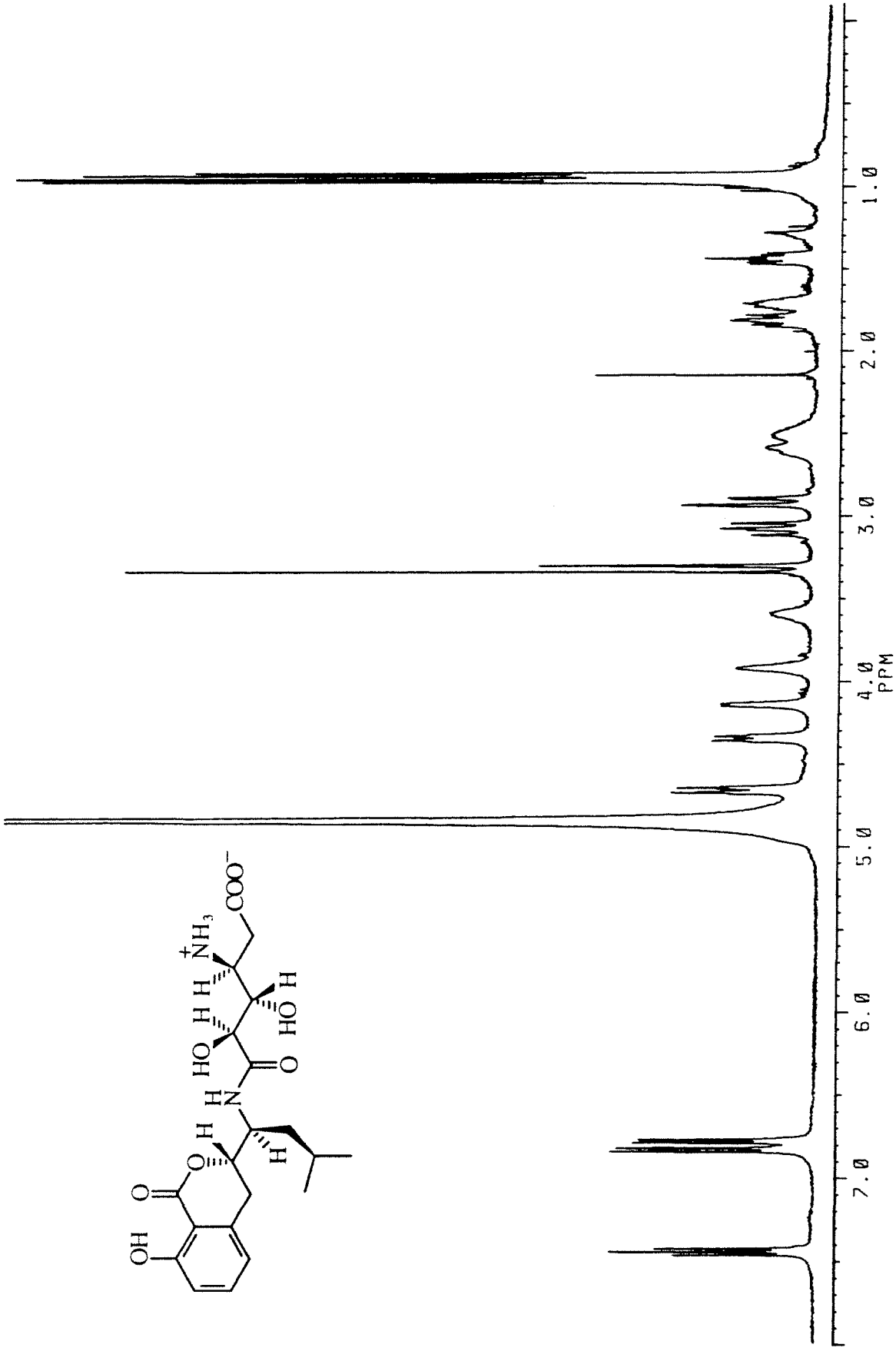

Figure 74. ^{1}H NMR spectrum of AI-77-B (**54**) (400 MHz, CD_3OD).

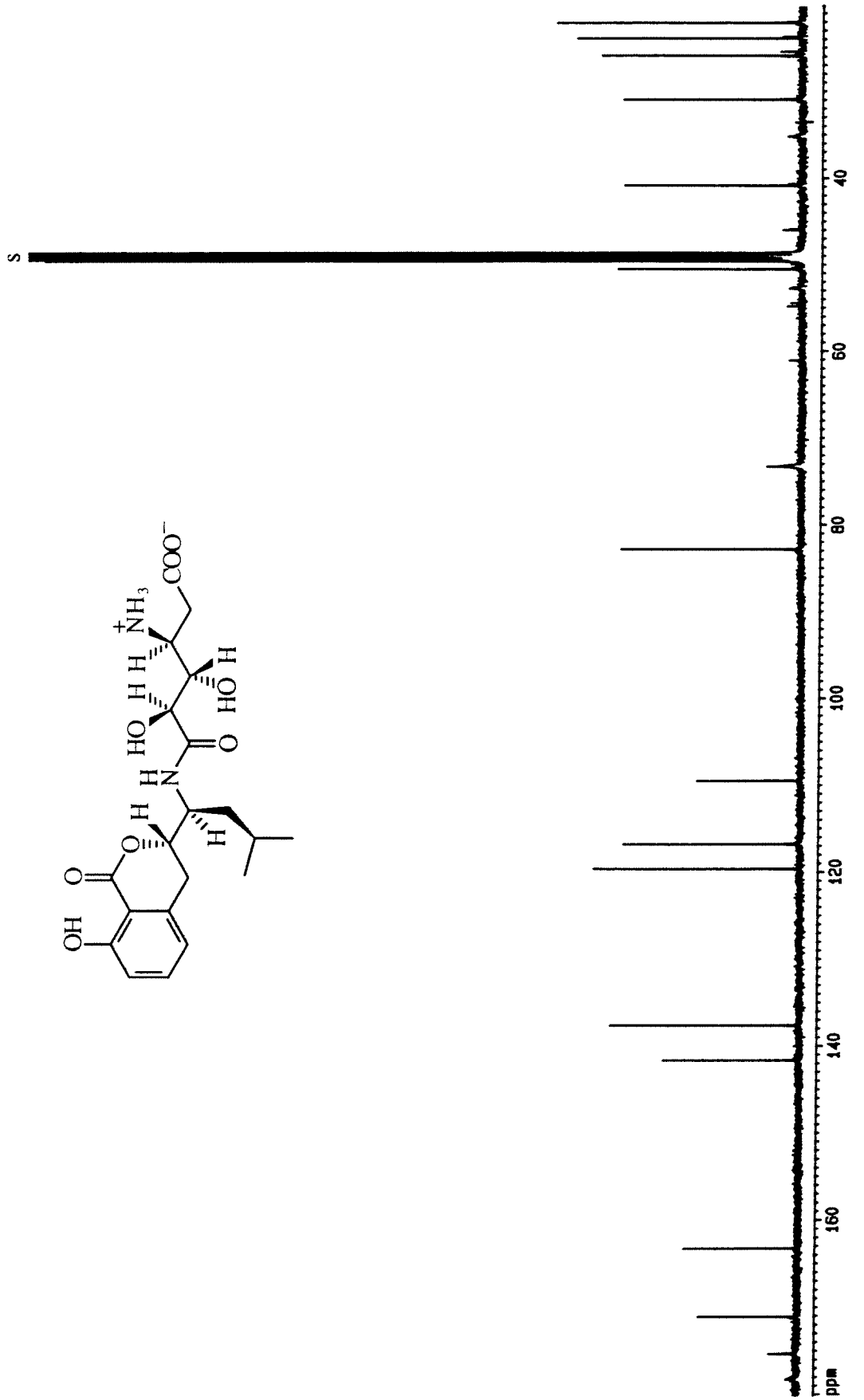

Figure 75. ^{13}C NMR spectrum of AI-77-B (**54**) (125 MHz, CD_3OD).

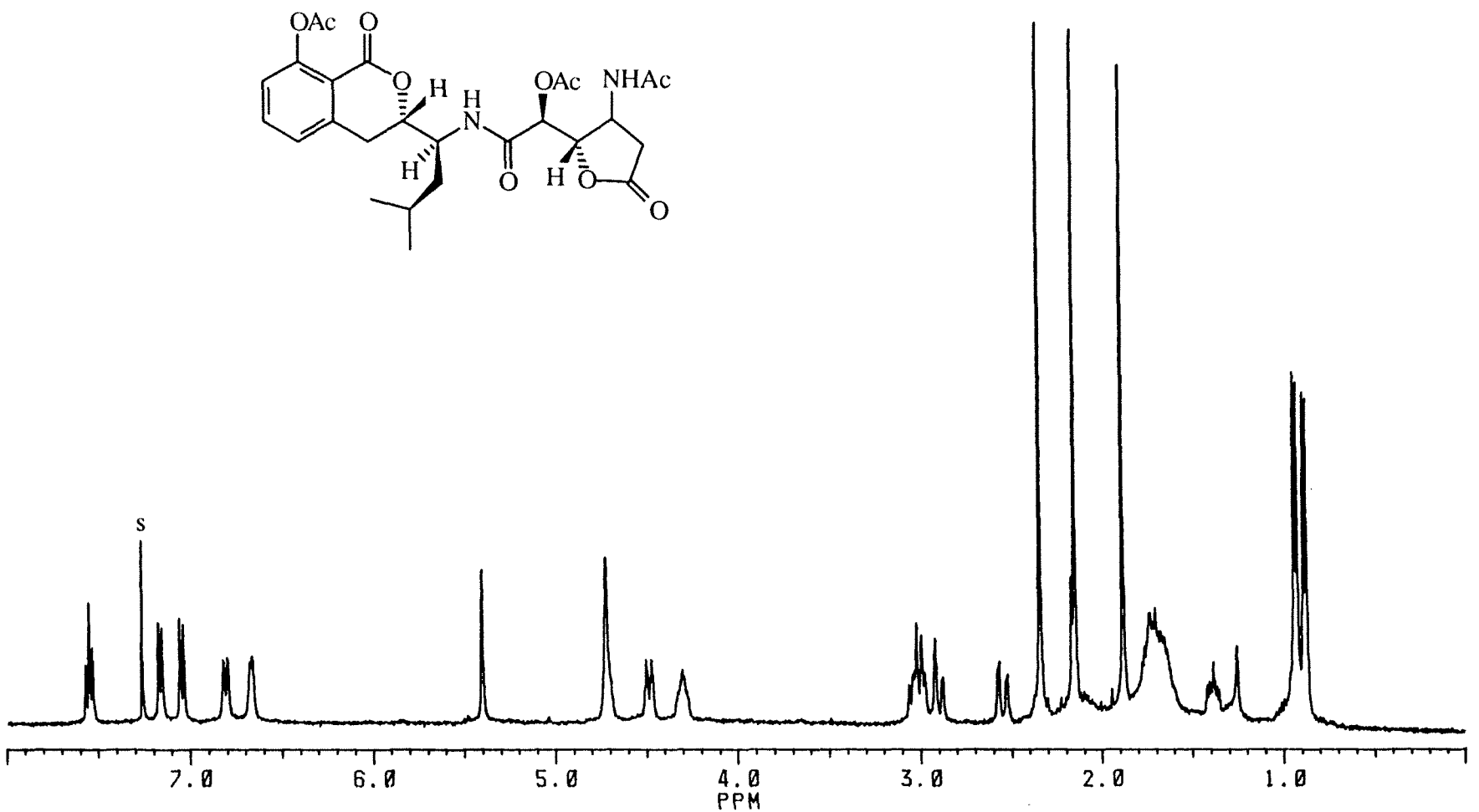

Figure 76. ^{1}H NMR spectrum of compound **55** (400 MHz, $CDCl_3$).

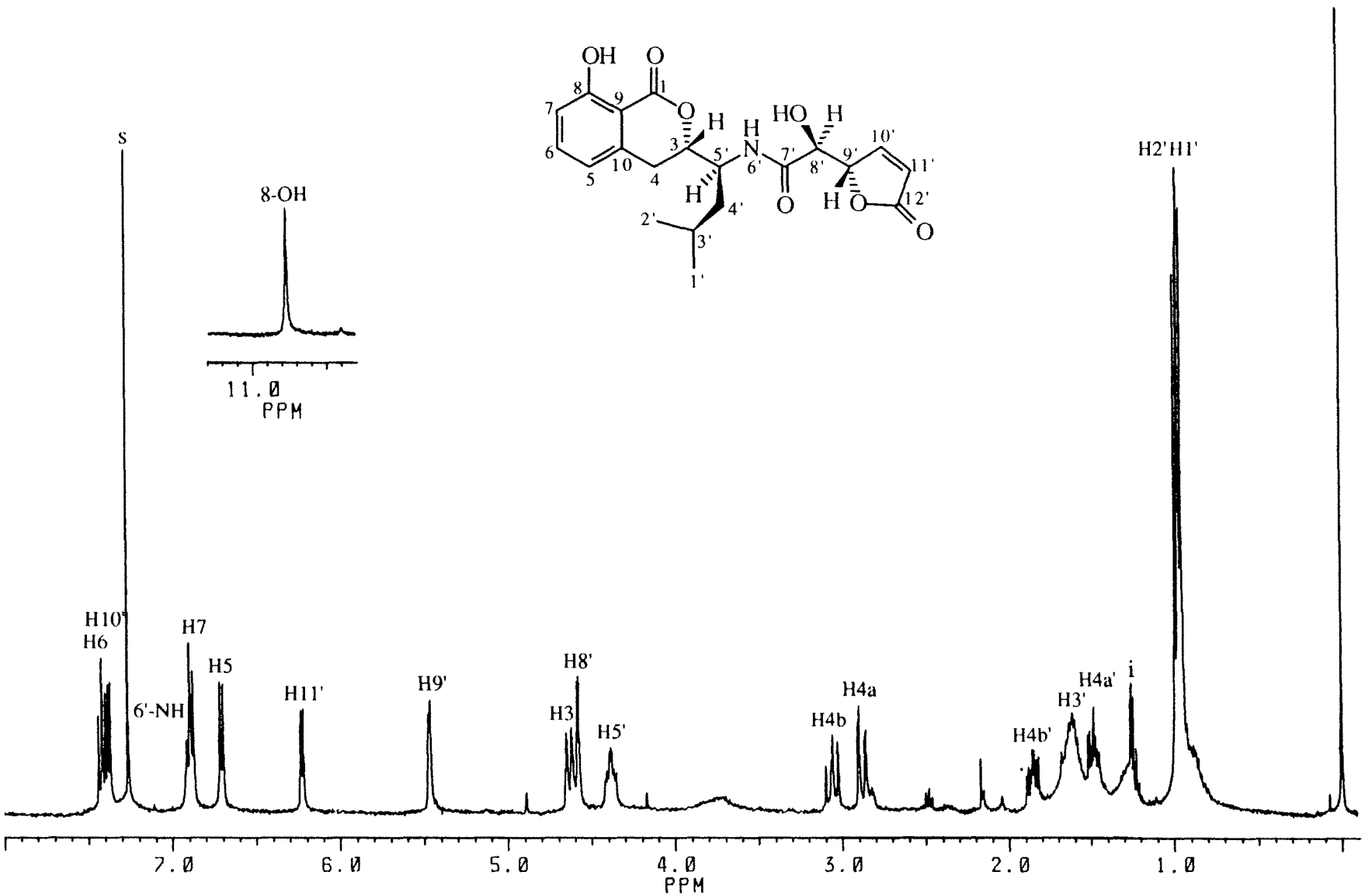

Figure 77. ^{1}H NMR spectrum of AI-77-F (**56**) (400 MHz, $CDCl_3$).

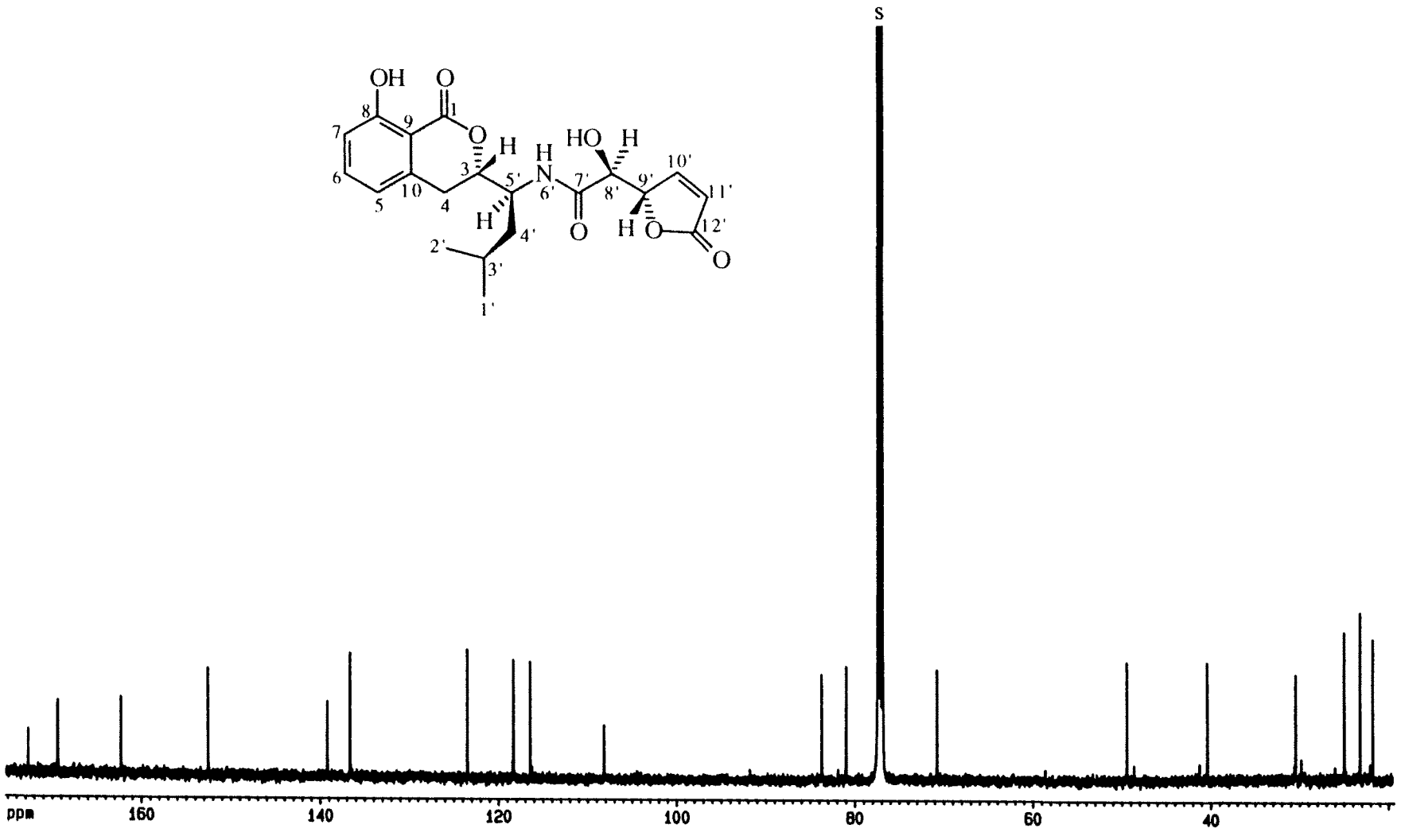

Figure 78. ^{13}C NMR spectrum of AI-77-F (**56**) (125 MHz, $CDCl_3$).

The structure of AI-77-B (**54**) was confirmed by acetylating a portion of the sample. The triacetate (**55**) gave a molecular ion at m/z 532.2060 (ΔM +0.3 mmu) in the HREIMS, appropriate for a molecular formula of $C_{26}H_{32}N_2O_{10}$. The structure of **55** was confirmed by comparison of its MS, ^1H NMR (Figure 76) and ^{13}C NMR data (see experimental) with published results.[65d]

A minor metabolite obtained from cultures of *Bacillus pumilus* 91Z50 was identified as AI-77-F by comparison of its MS and NMR data with literature values.[65d] AI-77-F (**56**) was isolated as a white amorphous solid. A molecular ion peak in the HREIMS at m/z 389.1478 (ΔM +0.3 mmu) corresponded to the molecular formula $C_{20}H_{23}NO_7$. The ^1H and ^{13}C NMR are shown in Figures 77 and 78, respectively. AI-77-F was originally isolated along with AI-77-B from a culture of *Bacillus pumilus*.

8.2.2. Compound 57

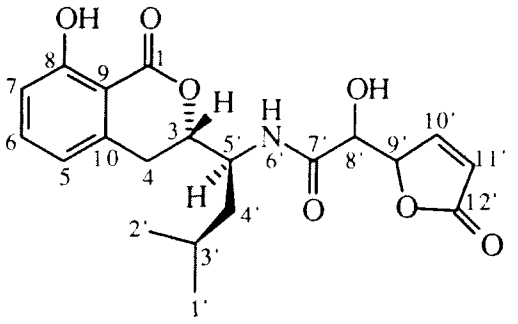

Compound **57**, a minor metabolite produced by liquid cultures of *Bacillus pumilus* 91Z50 was isolated as a white amorphous solid. A molecular ion in the HREIMS at m/z 389.1481 was appropriate for a molecular formula of $C_{20}H_{23}NO_7$ (ΔM +0.7 mmu). The IR spectrum of **57** contained a broad, shallow absorption band at 3327 cm^{-1} that was assigned to overlapping N-H and intramolecular bonded O-H stretching vibrations. A carbonyl absorption band at 1760 cm^{-1} in the IR spectrum was assigned to a butenolide carbonyl and the absorption

band at 1673 cm^{-1} corresponded to overlapping amide and αβ-unsaturated ester carbonyl groups. Comparison of the ^1H (Figure 79) and ^{13}C (Figure 80) NMR data obtained for **57** with the NMR data obtained for AI-77-F (**56**), summarized in Table 18, revealed that these two compounds were diastereomers.

The COSY (Figure 81), HMQC (Figure 82) and HMBC (Figure 83) data confirmed the proposed constitution for **57**. The ^1H and ^{13}C NMR data for AI-77-F and **57** differed at the butenolide moiety. An upfield chemical shift of the H8', H9' and H11' resonances as well as a downfield chemical shift of the H10' resonance were observed in the ^1H NMR spectrum of **57**. Comparison of the ^1H coupling constants for the two diastereomers suggested that the relative configuration at C3 and C5' were the same, however, a difference in the coupling constant for the H8' doublet (**57**: δ 4.33, d, $^1J_{H8',H9'}$ = 5.3 Hz; AI-77-F (**56**): δ 4.58, d, $^1J_{H8',H9'}$ = 4.4 Hz) suggested that the stereochemistry differed at the C8' or C9' position. If the stereochemistry of **57** at the C3 and C5' positions are assumed to be the same as in A I-77-F then **57** may have the absolute stereochemistry depicted by **57a** or **57b**. The $^1J_{H8',H9'}$ coupling constant for the diastereomer **57c** would be expected to be the same as that in **56**, therefore, **57c** was not considered as a possible structure for compound **57**.

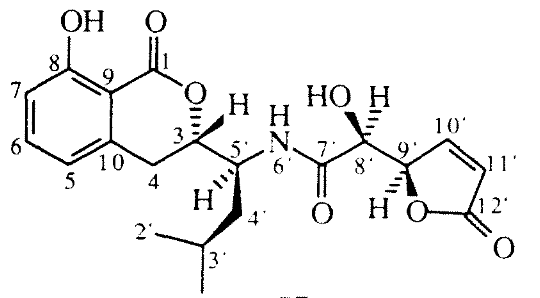
57a

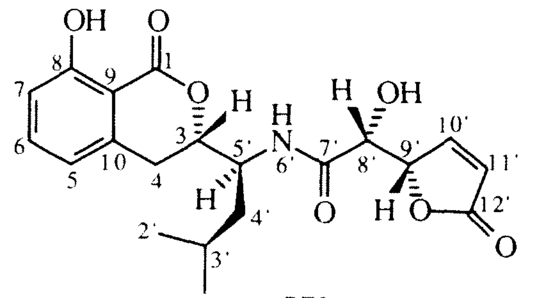
57b

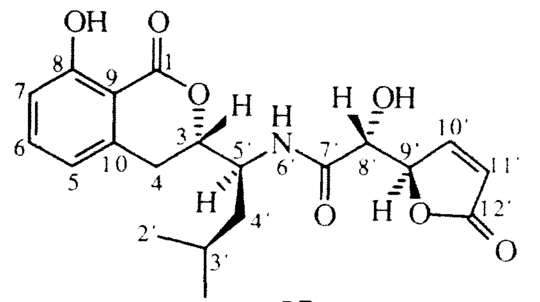
57c

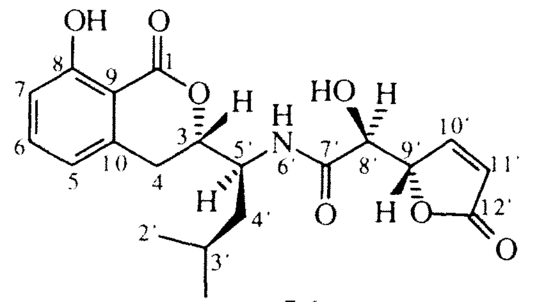
56

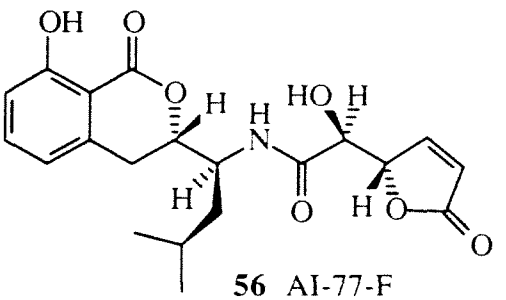

56 AI-77-F

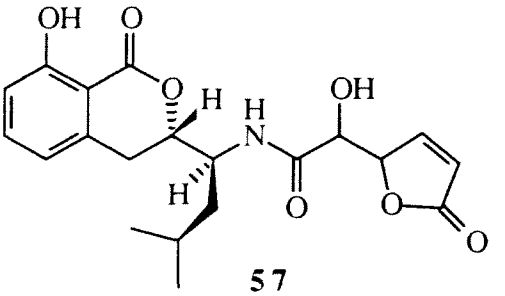

57

Table 18. ^{1}H and ^{13}C NMR data for AI-77-F (**56**) and compound **57**.

	AI-77-F (**56**)		Compound **57**			
C#	^{13}C[a]	^{1}H[b]	^{13}C[a]	^{1}H[b]	COSY	HMBC[c]
1	169.4[d]	—	169.4[d]	—	—	—
3	80.9	4.63,dt(12.3,2.5)	81.0	4.59,dt(12.5,2.5)	H4a,H4b	H4b
4a	30.3	2.88,dd(16.5,3.0)	30.3	2.84,dd(16.5,3.0)	H3,H4b	H5
4b	—	3.06,dd(16.5,12.3)	—	3.02,dd(16.5,12.5)	H3,H4a	—
5	118.2	6.71,d(7.4)	118.2	6.69,d(7.4)	H6	H4a,H7
6	136.5	7.42,dd(8.5,7.4)	136.5	7.40,dd(8.4,7.4)	H5,H7	—
7	116.3	6.88,d(8.5)	116.3	6.86,d(8.4)	H6	H5,8-OH
8	162.2	—	162.2	—	—	H6,H7,8-OH
9	108.1	—	108.0	—	—	H4a,H5,H7, 8-OH
10	139.1	—	139.1	—	—	H4a,H4b,H6
1'	21.6	0.96,d(6.5)	21.8	0.95,d(6.5)	H3'	—
2'	23.1	0.98,d(6.5)	23.1	0.97,d(6.5)	H3'	—
3'	24.9	1.61,m	24.7	1.67,m	H1',H2',H4a'	—
4'a	40.3	1.48,m	40.5	1.47,m	H3',H4b',H5'	—
4'b	—	1.85,m	—	1.83,m	H4a',H5'	—
5'	49.3	4.38,m	49.4	4.37,m	H4a',H4b',6'-NH	—
6'-NH	—	6.90,d(9.7)	—	6.91,d(9.7)	H5'	—
7'	169.3[d]	—	169.3[d]	—	—	—
8'	70.7	4.58,d(4.4)	72.0	4.33,d(5.3)	H8'-OH,H9'	—
9'	83.6	5.46,m	83.5	5.31,ddd(5.3,2.0,1.5)	H8',H10',H11',	H10'
10'	152.4	7.37,dd(5.7,1.2)	153.6	7.66,dd(5.8,1.5)	H9',H11'	H11'
11'	123.4	6.23,dd(5.7,1.8)	122.9	6.19,dd(5.8,2.0)	H9',H10'	H10,
12'	172.7	—	172.3	—	—	H10',H11'
8-OH	—	10.73,s	—	10.73,s	—	—
8'-OH	—	3.75,bs	—	3.73,bs	H8'	—

[a] Recorded in $CDCl_3$ at 400 MHz. Chemical shifts in ppm relative to TMS.
[b] Recorded in $CDCl_3$ at 125 MHz. Chemical shifts are referenced to solvent.
[c] Carbons in the carbon # column are correlated to the listed proton resonances.
[d] Carbons within the same column may be interchanged.

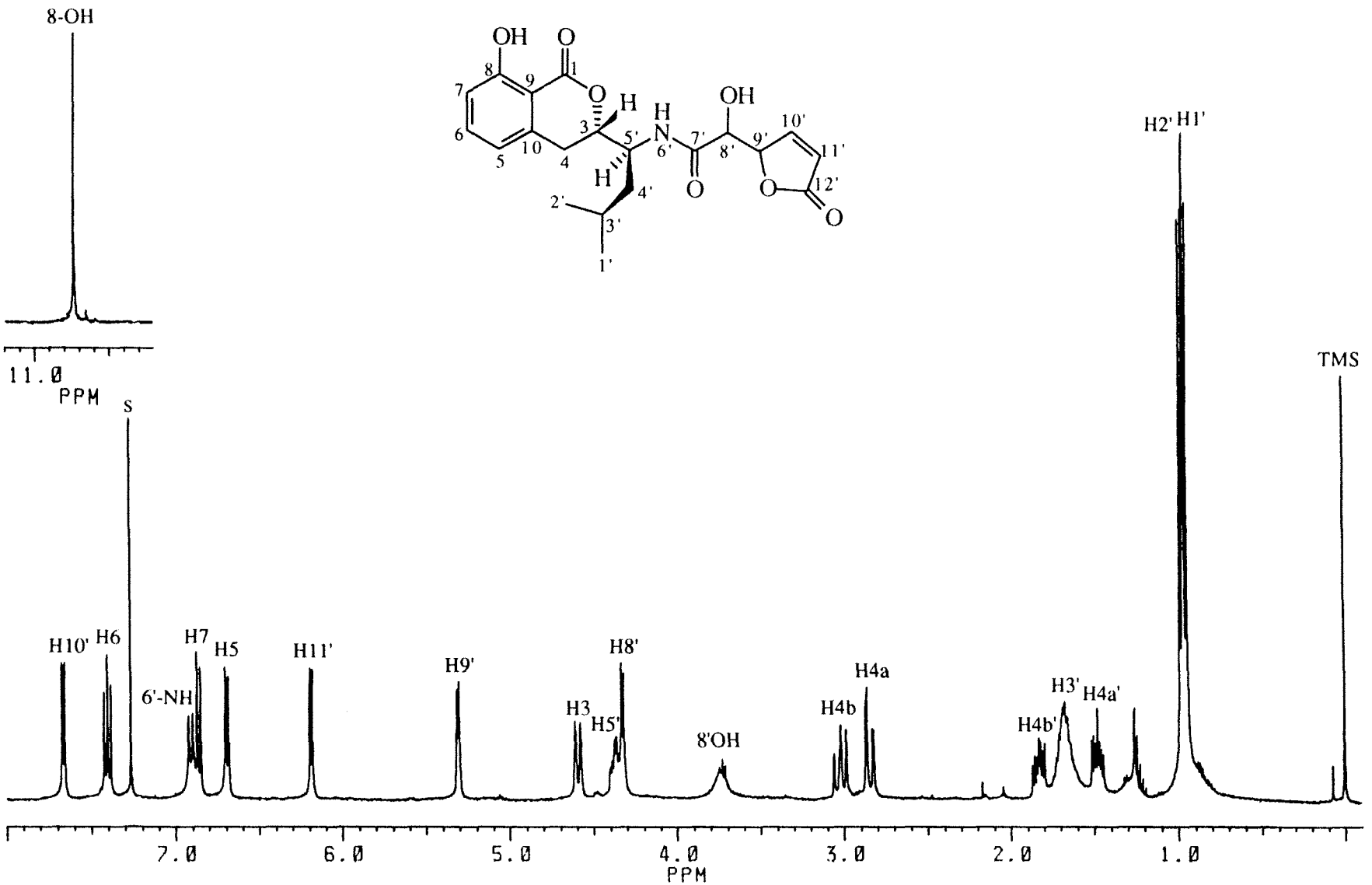

Figure 79. ^{1}H NMR spectrum of compound **57** (400 MHz, $CDCl_3$).

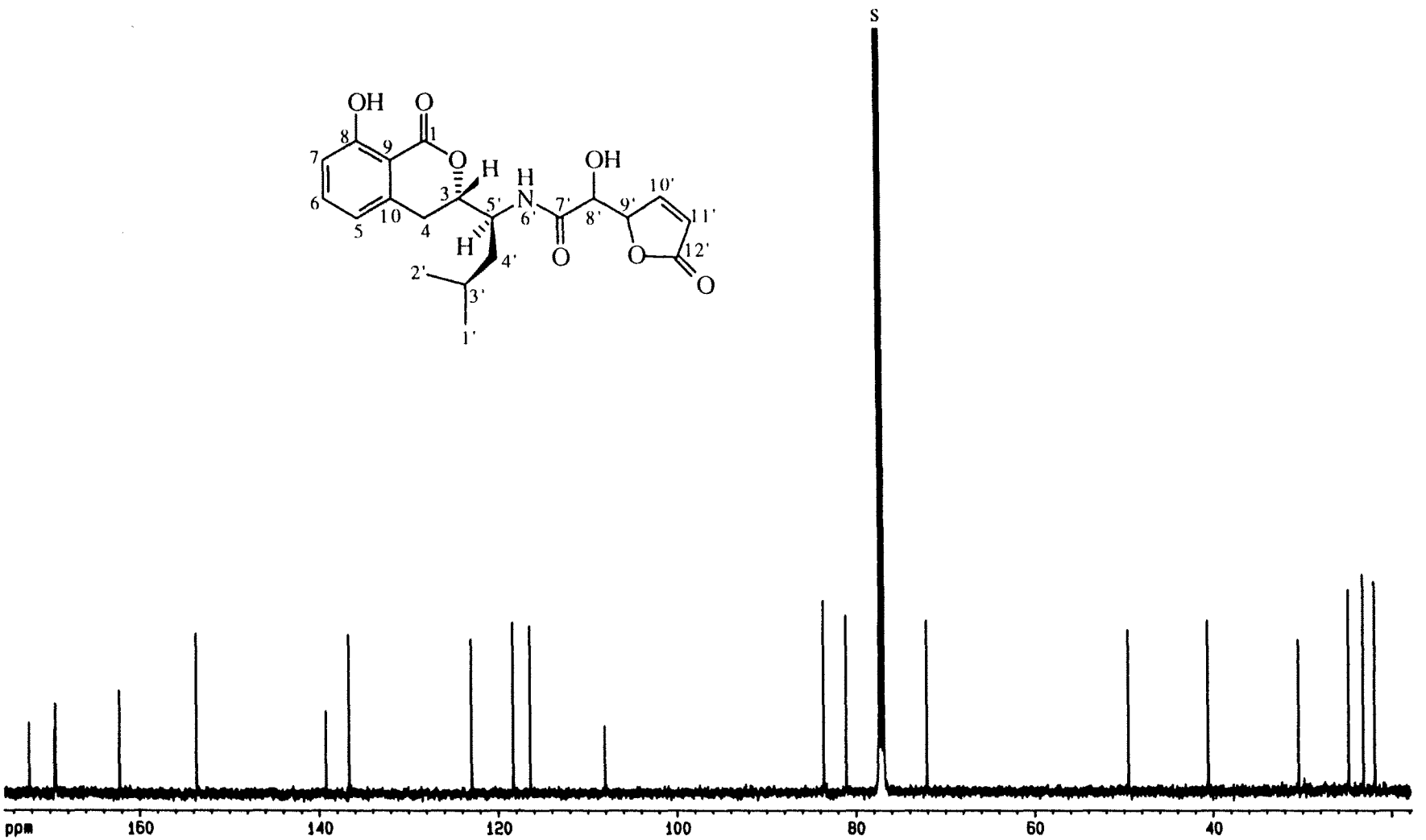

Figure 80. ^{13}C NMR spectrum of compound **57** (125 MHz, $CDCl_3$).

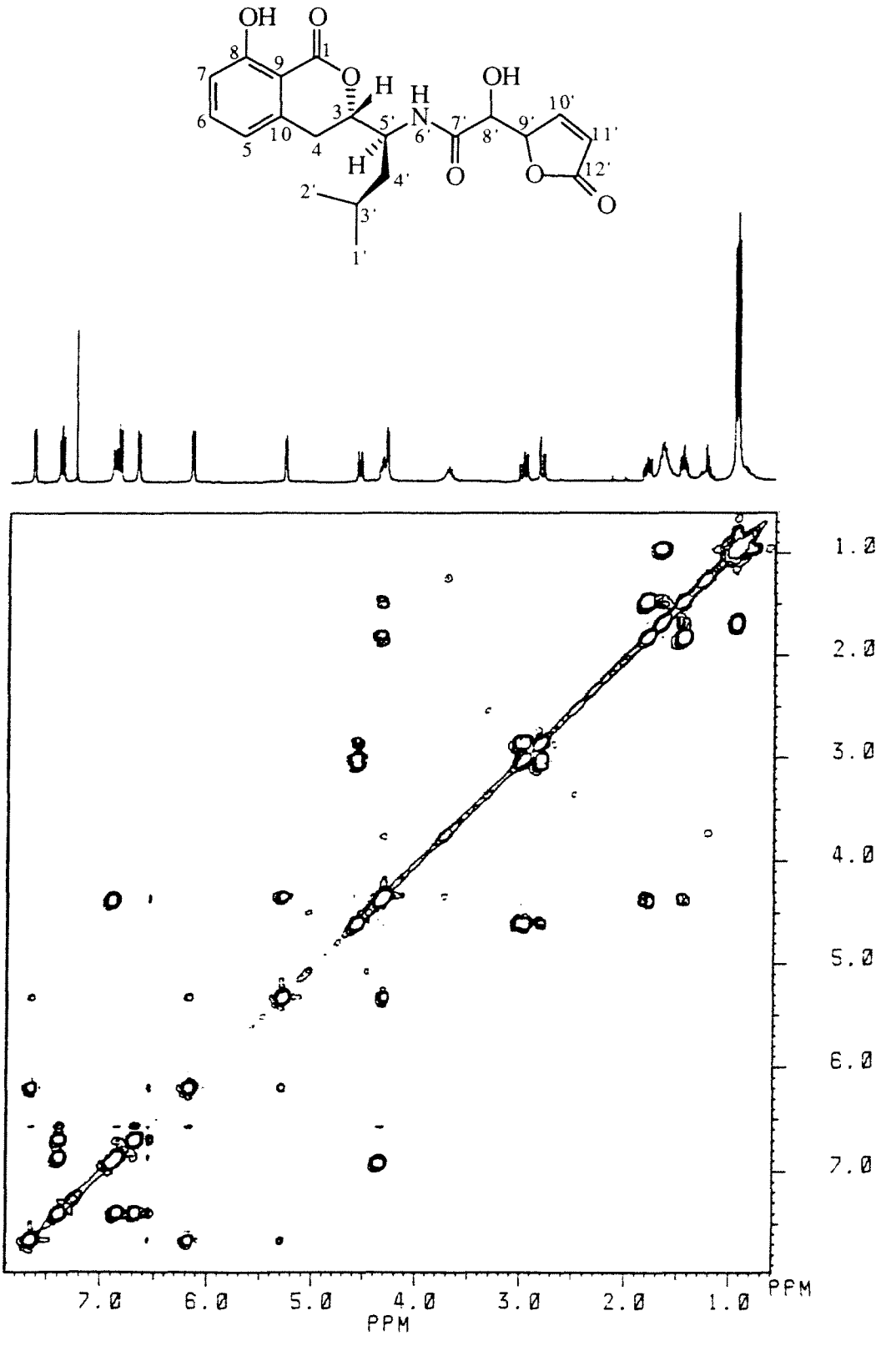

Figure 81. ^{1}H COSY NMR spectrum of compound **57** (400 MHz, $CDCl_3$).

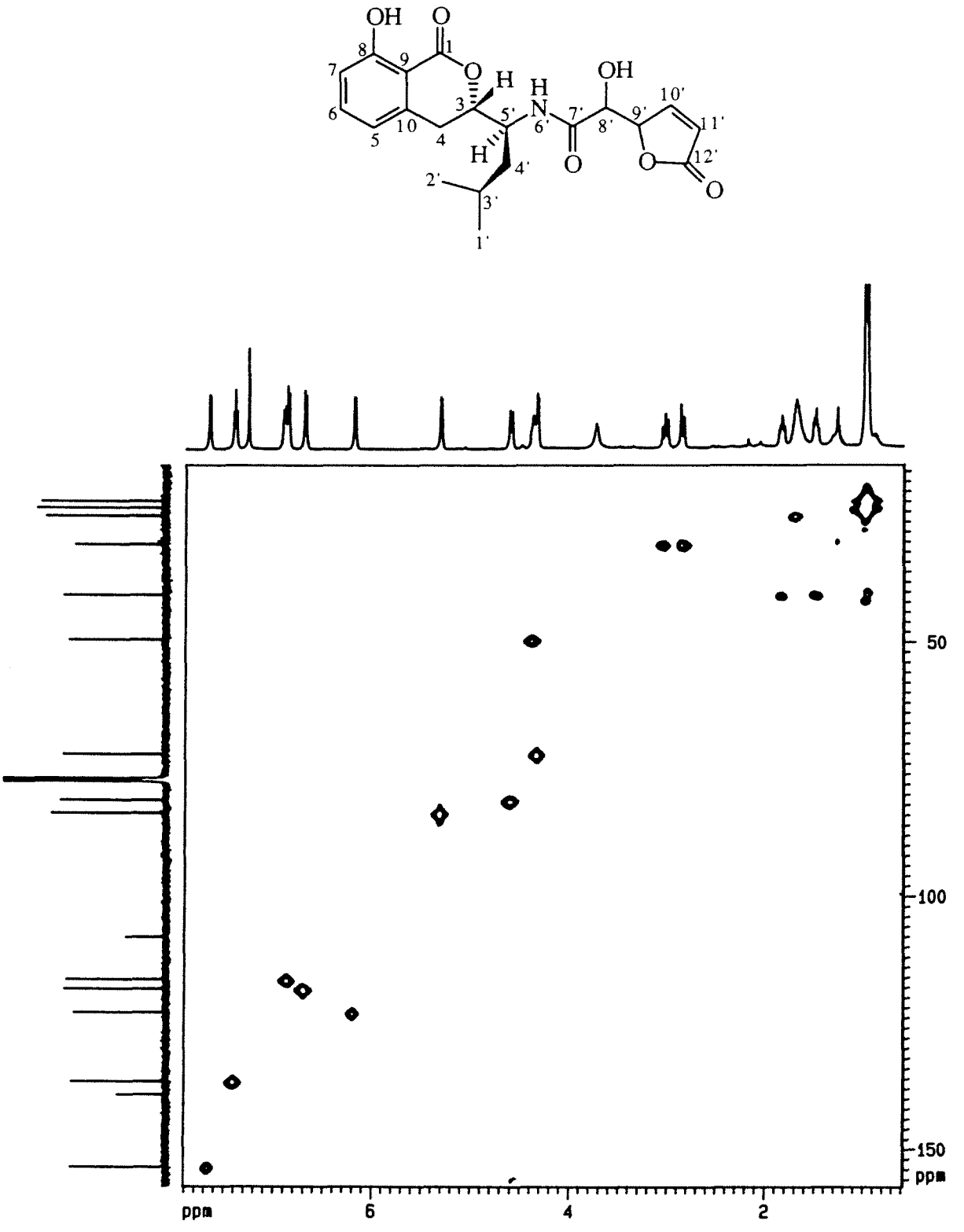

Figure 82. HMQC NMR spectrum of compound **57** (500 MHz ^{1}H NMR, $CDCl_3$).

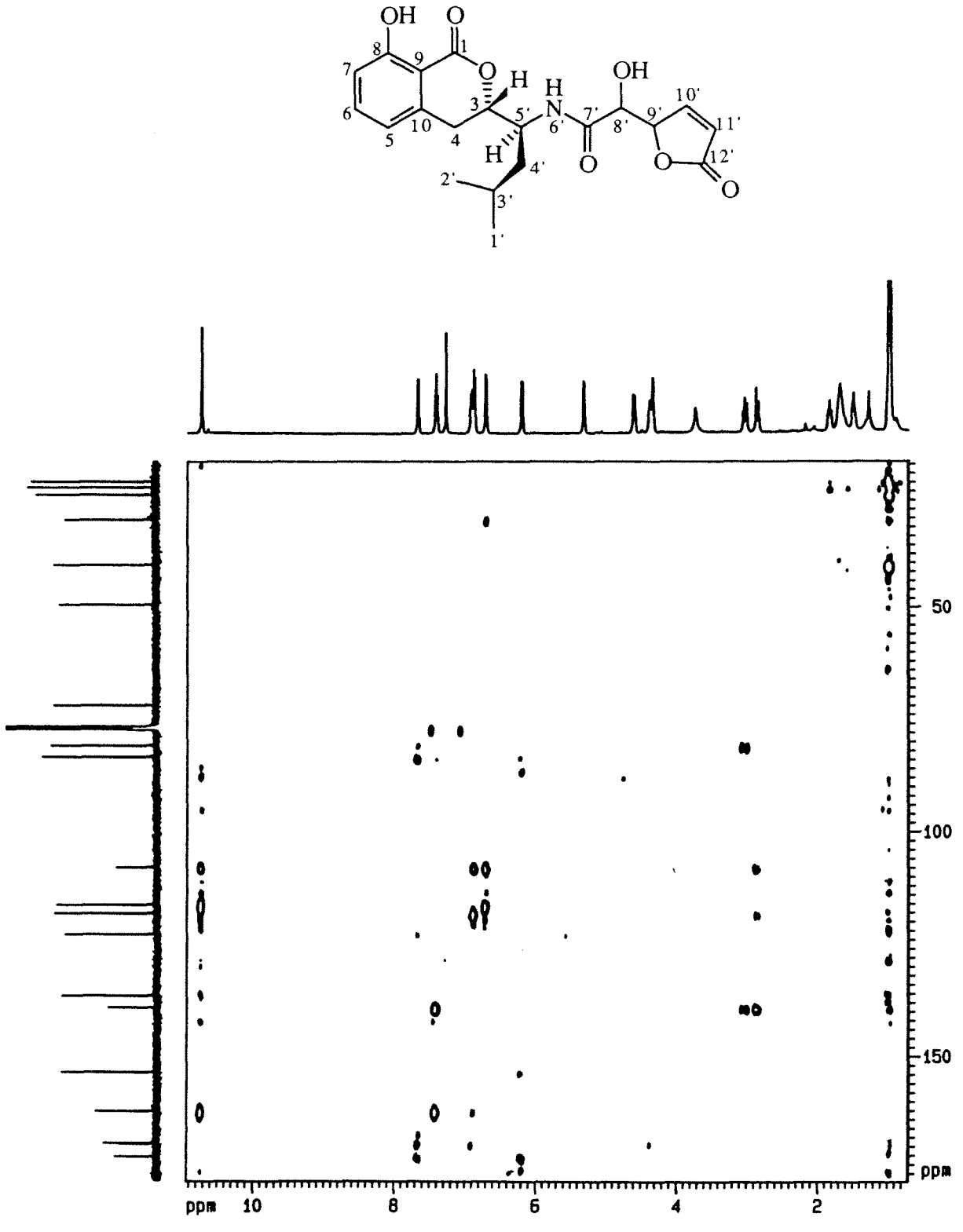

Figure 83. HMBC NMR spectrum of compound **57** (500 MHz ^{1}H NMR, $CDCl_3$).

8.2.3. Moshers ester

The Moshers method using 2-methoxy-2-phenyl-2-(trifluoromethyl) acetic acid (MPTA) esters[66] was investigated for the purpose of determining the absolute stereochemistry of the secondary alcohol in **57**. AI-77-F (**56**) was used as a model compound since its absolute configuration was known. S-(+)-MPTA-chloride, prepared according to the literature,[66a] was added to a solution of AI-77-F, triethylamine, $CDCl_3$ and a catalytic amount of dimethylaminopyridine.[67] After one hour the chloroform was evaporated and the residue was applied to a normal phase Sep-Pak (eluent: ethyl acetate/hexane). Further purification by normal phase HPLC (eluent: ethyl acetate/hexane) yielded the pure R-MPTA ester **58**.

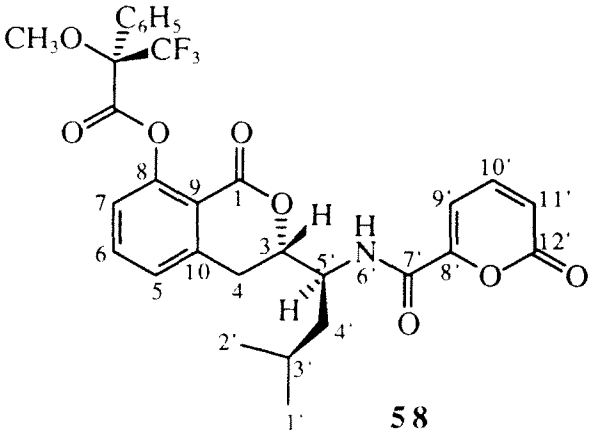

58

The Moshers ester **58** was isolated as a pale yellow film. A molecular ion in the HREIMS at m/z 587.1771 was appropriate for the molecular formula $C_{30}H_{28}NO_8F_3$ (ΔM +0.4 mmu). This molecular formula together with the appearance of a methyl singlet at δ 3.79, integrating for three protons, in the ^{1}H NMR spectrum of **58** (Figure 84) suggested that esterification occurred at only one of the alcohols. The ^{1}H NMR spectrum of **58** did not contain a signal that could be assigned to the H8' proton and no phenolic proton was observed. This

suggested that esterification occurred at the phenol. The absence of two oxygenated methine carbons for C8' and C9' in the ^{13}C NMR of **58** spectrum (Figure 85) suggested that the butenolide moiety present in **56** was absent in **58**. Carbon resonances at δ 158.9 (C8'), δ 103.8 (C9'), δ 142.6 (C10'), δ 123.7 (C11') and δ 167.7 (C12') as well as proton resonances at δ 5.79 (H9'), δ 8.50 (H10') and δ 6.41 (H11') indicated the presence of a substituted pyran-2-one ring.[68] COSY (Figure 86), HMQC (Figure 87) and HMBC (Figure 88) data supported the proposed constitution for **58**. The NMR data is summarized in Table 19.

Treatment of **56** with base would presumably result in the elimination of the H8' proton followed by ring opening to form a 5-keto acid derivative. Once the butenolide ring has been opened the unstable 5-keto acid derivative would readily cyclize to form a substituted pyran-2-one.

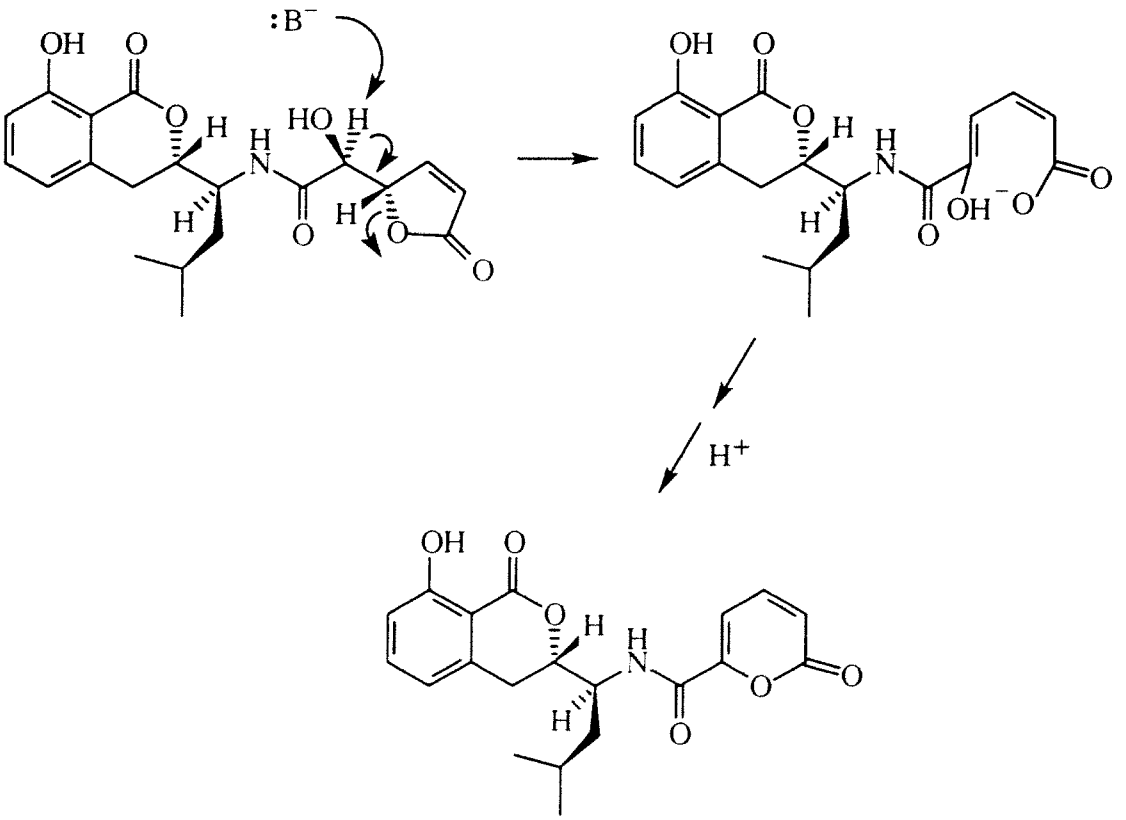

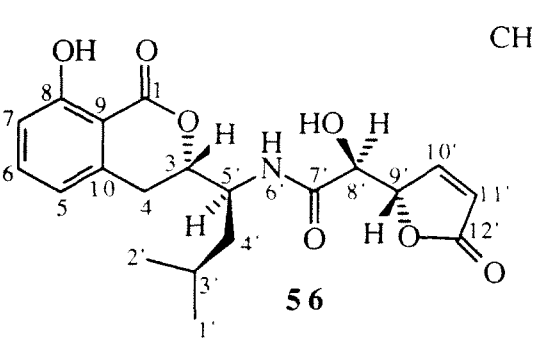

56

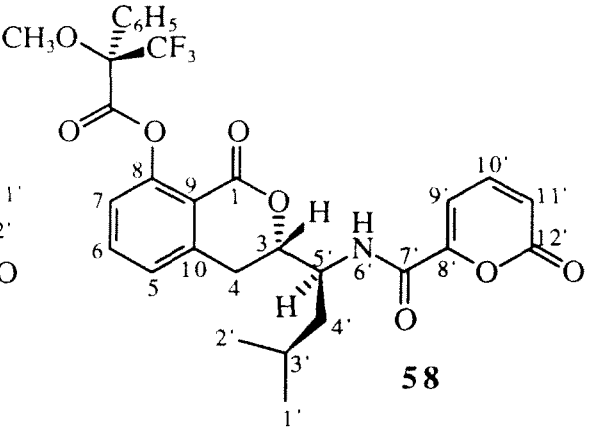

58

Table 19. ^{1}H and ^{13}C NMR data for AI-77-F (**56**)and **58**.

	AI-77-F (**56**)		Compound **58**			
C#	^{13}C[a]	^{1}H[b]	^{13}C[a]	^{1}H[b]	COSY	HMBC[c]
1	169.4[d]	—		—	—	—
3	80.9	4.63,dt(12.3,2.5)	79.8	4.62,m	H4a,H4b	H4b
4a	30.3	2.88,dd(16.5,3.0)	31.3	2.99,dd(16.4,3.3)	H3,H4b	—
4b	—	3.06,dd(16.5,12.3)	—	3.13,dd(16.4,11.3)	H3,H4a	—
5	118.2	6.71,d(7.4)	126.3	7.19,d(8.0)	H6	H7
6	136.5	7.42,dd(8.5,7.4)	134.8	7.51,t(8.0)	H5,H7	—
7	116.3	6.88,d(8.5)	122.1	6.94,d(8.0)	H6	H5
8	162.2	—	150.8	—	—	H6
9	108.1	—	118.1	—	—	H5,H7,
10	139.1	—	141.1	—	—	H6,H7
1'	21.6	0.96,d(6.5)	21.9	0.96,d(6.5)	H3'	—
2'	23.1	0.98,d(6.5)	23.0	0.96,d(6.5)	H3'	—
3'	24.9	1.61,m	24.8	1.65,m	H1',H2'	—
4'a	40.3	1.48,m	41.0	1.50,m	H4b',H5'	—
4'b	—	1.85,m	—	1.82,m	H4a',H5'	—
5'	49.3	4.38,m	49.5	4.45,m	H4a',H4b',6'-NH	—
6'-NH	—	6.90,d(9.7)	—	5.88,d(10.0)	H5'	—
7'	169.3[d]	—		—	—	—
8'	70.7	4.58,d(4.4)	158.9	—	—	H9',H10'
9'	83.6	5.46,m	103.8	5.79,s	H11'	—
10'	152.4	7.37,dd(5.7,1.2)	142.6	8.50,d(5.6)	H11'	H9'
11'	123.4	6.23,dd(5.7,1.8)	123.7	6.41,dd(5.6,1.7)	H9',H10'	—
12'	172.7	—	167.9	—	—	H11'
Ph	—	—	127.7(2C) 128.5(2C) 129.5	7.74,m 7.75,m 7.46-7.47 (3H)	—	—
OMe	—	—	56.0	3.79,s	—	—
C	—	—	85.5	—	—	—
CF_3	—	—		—	—	—
8-OH	—	10.73,s	—	—	—	—

[a] Recorded in $CDCl_3$ at 400 MHz. Chemical shifts in ppm relative to TMS.
[b] Recorded in $CDCl_3$ at 125 MHz. Chemical shifts are referenced to solvent.
[c] Carbons in the carbon #column are correlated to the listed proton resonances.
[d] May be interchanged.

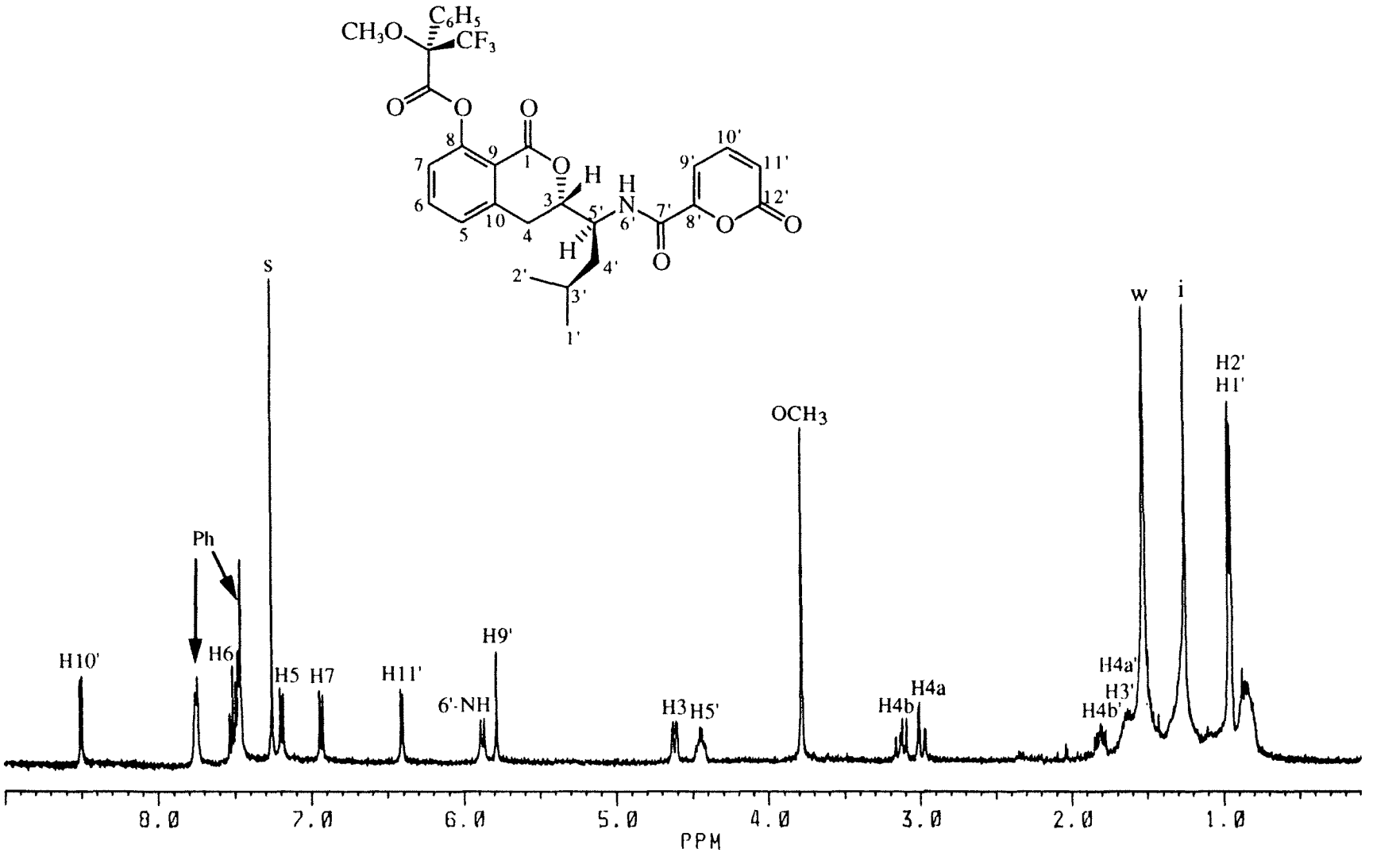

Figure 84. ^{1}H NMR spectrum of compound **58** (400 MHz, $CDCl_3$).

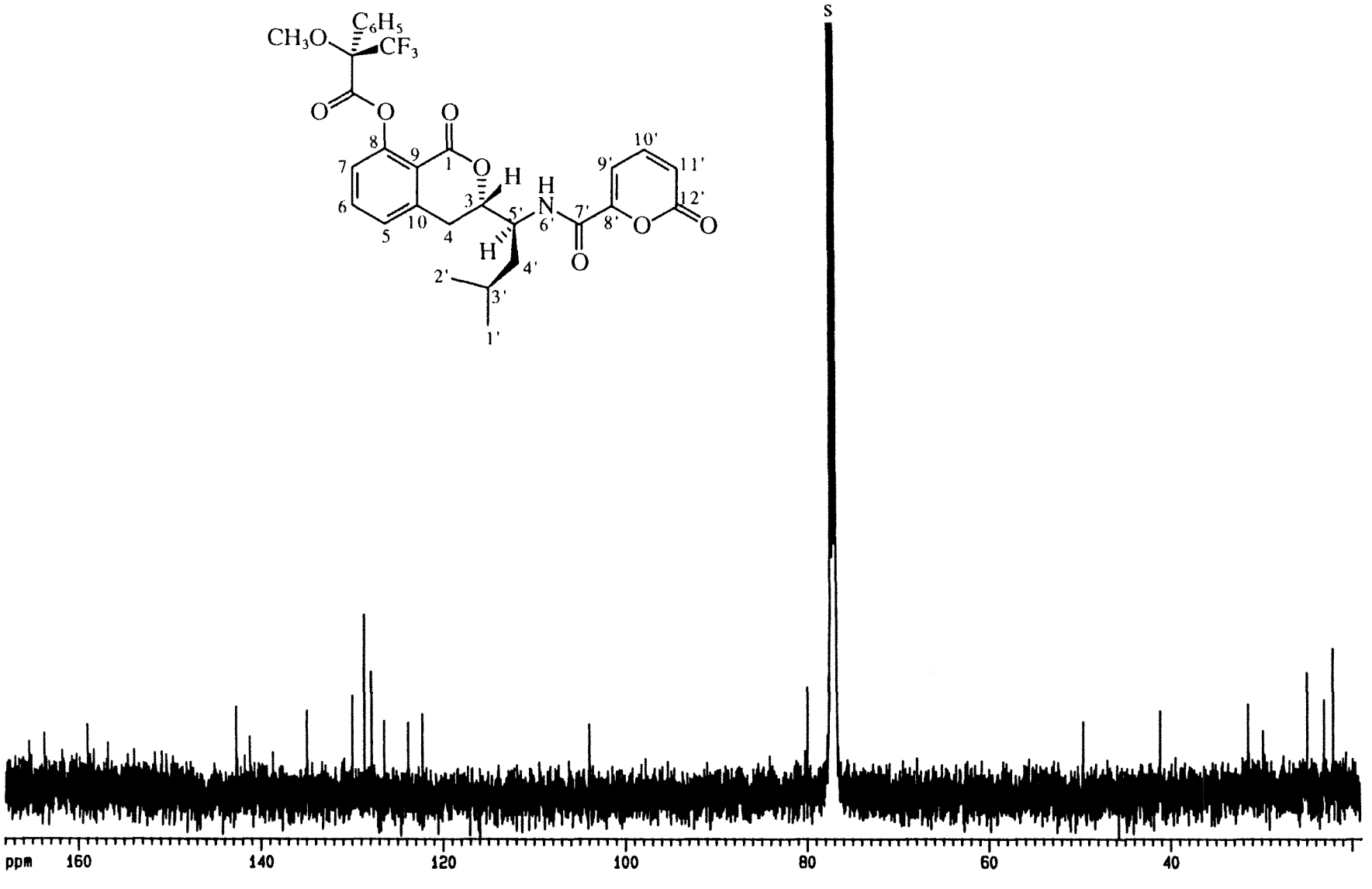

Figure 85. ^{13}C NMR spectrum of compound **58** (125 MHz, $CDCl_3$).

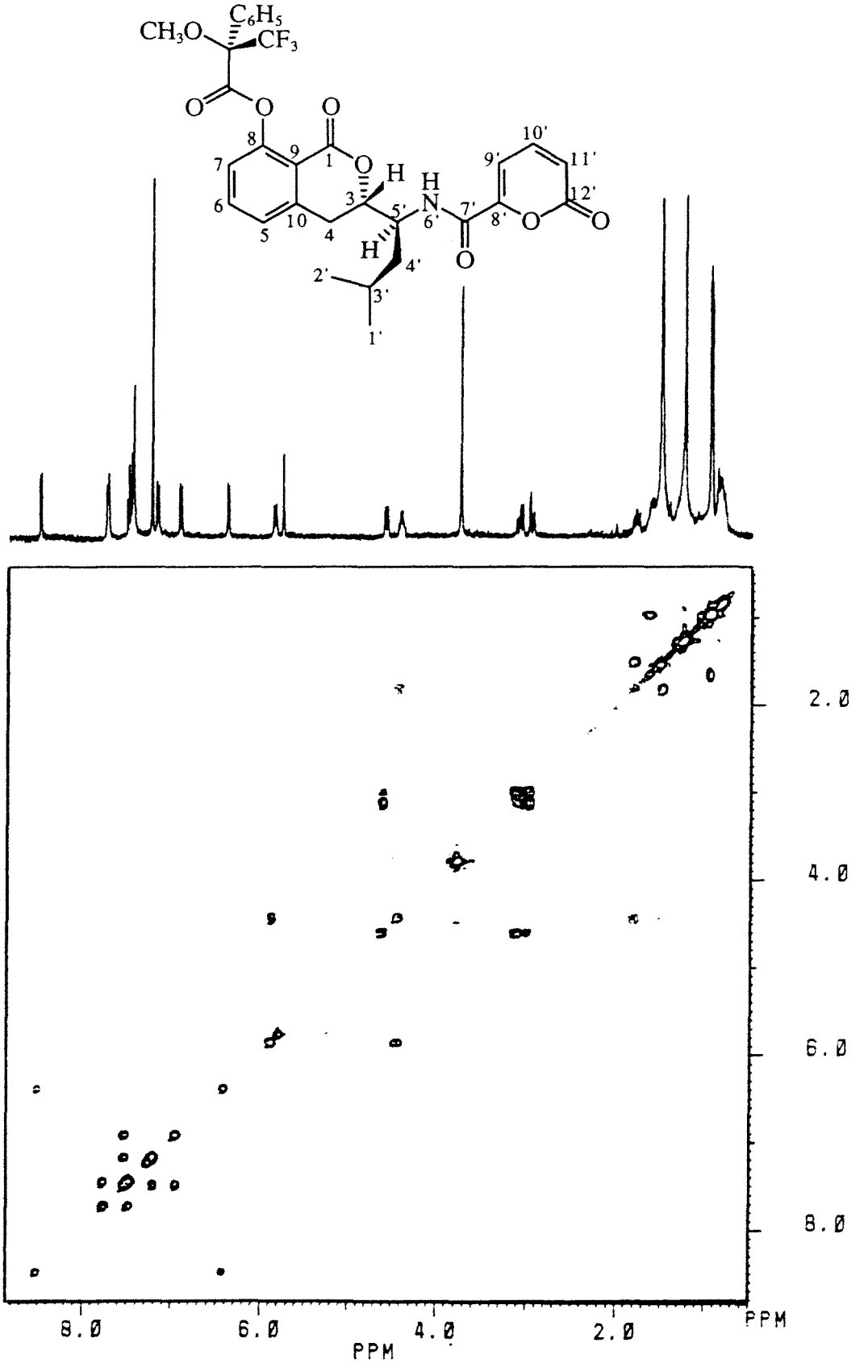

Figure 86. ^{1}H COSY NMR spectrum of compound **58** (400 MHz, $CDCl_3$).

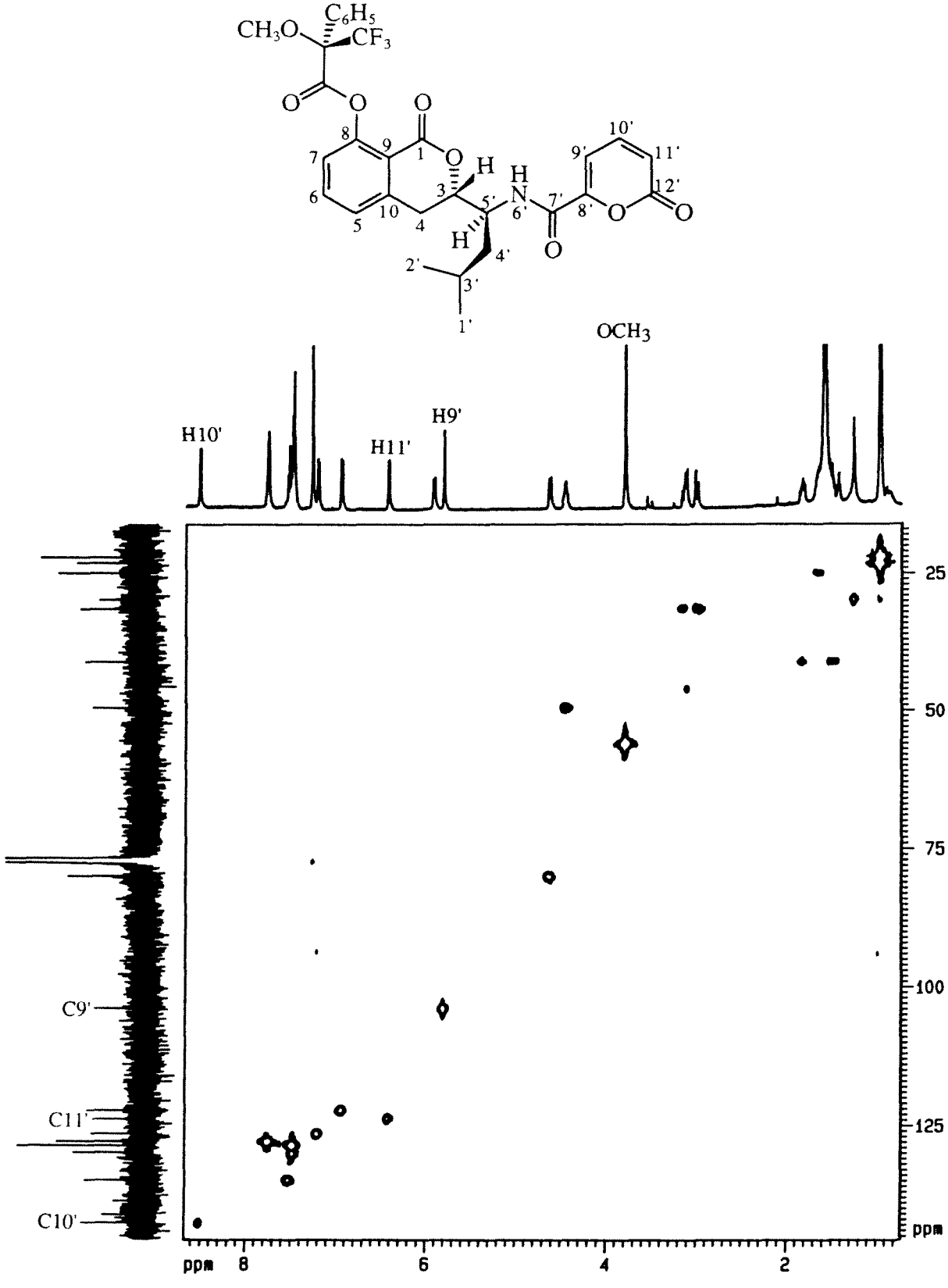

Figure 87. HMQC NMR spectrum of compound **58** (500 MHz ^{1}H NMR, $CDCl_3$).

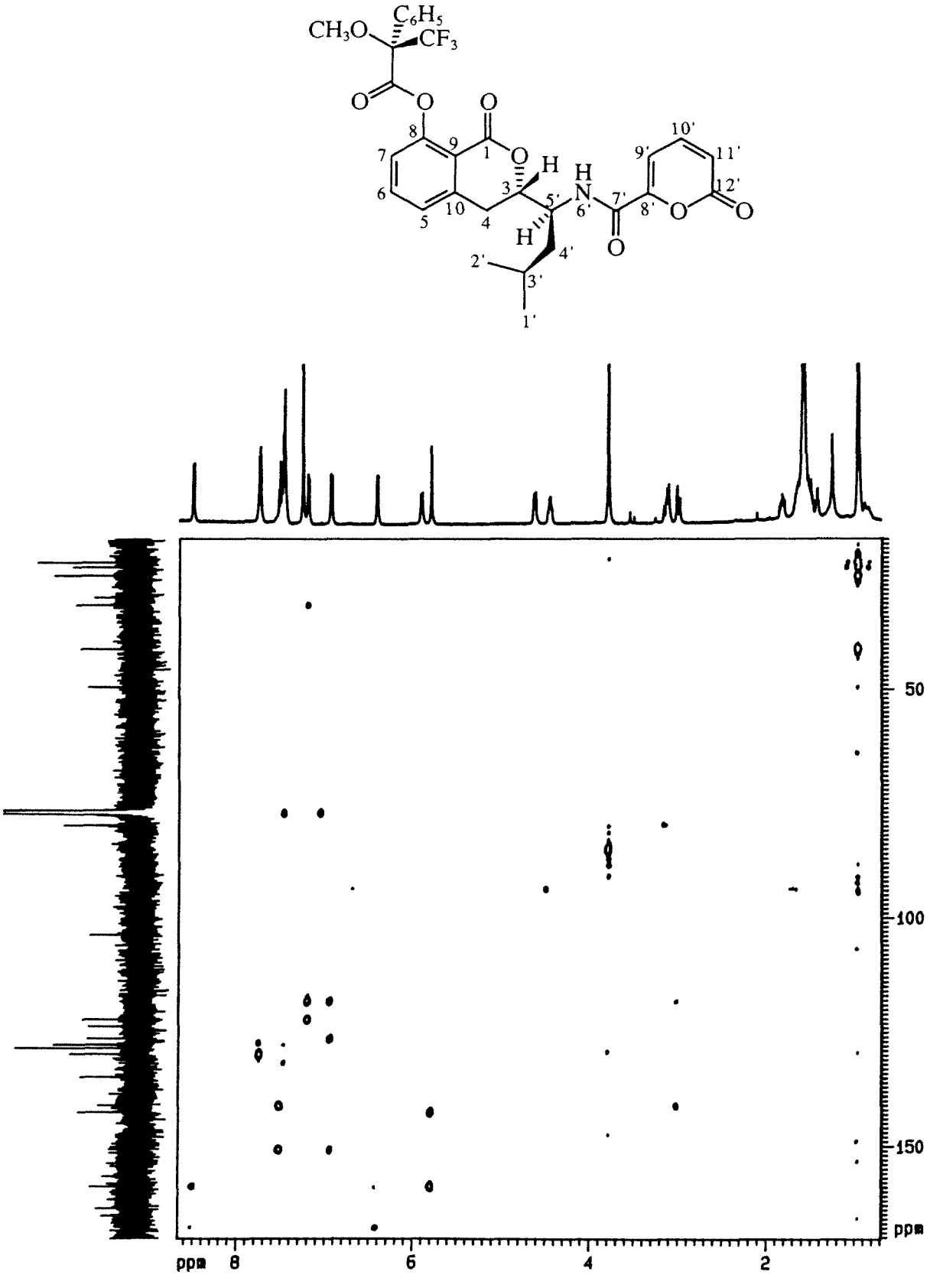

Figure 88. HMBC NMR spectrum of compound **58** (500 MHz ^{1}H NMR, $CDCl_3$).

8.3. Conclusion

A culture of the bacterium *Bacillus pumilus* (91Z50), isolated from a sediment sample collected in Georgia Strait, British Columbia, resulted in the isolation and structure elucidation of the new compound **57**, as well as the known compounds AI-77-B (**54**) and AI-77-F (**56**). Compound **57** was found to be a diastereomer of AI-77-F (**56**). The stereochemistry of the secondary alcohol in **57** could not be determined by the Moshers method since esterification of AI-77-F under basic conditions led to the opening of the butenolide ring and subsequent formation of a substituted pyran-2-one (**58**).

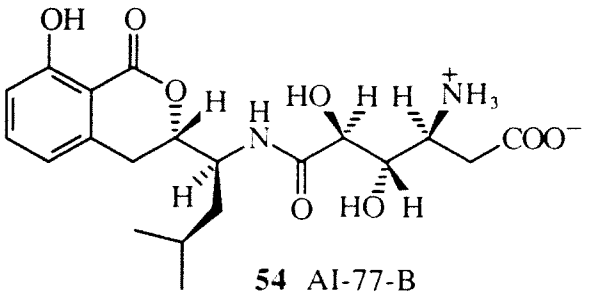

54 AI-77-B

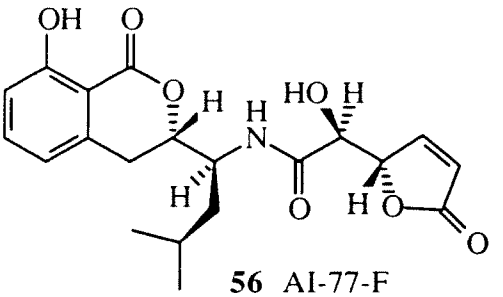

56 AI-77-F

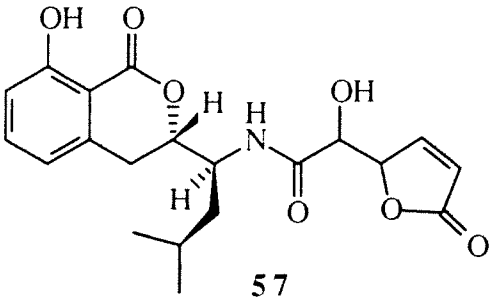

57

At a concentration of 100 µg/disc compound **54** showed antibacterial activity against methicillin-resistant *Staphylococcus aureus*, *S. aureus* and *S. saprophyticus*. Compounds **56** and **57** exhibited antibacterial activity only at concentrations greater than 100 µg/disc. Compound **54** also exhibited cytotoxic activity against P388 murine leukemia (ED_{50} = 2.6 µg/mL). In a structure-activity study on AI-77-B and related compounds, Shimojima and

Hayashi found that modifications of the amino acid moiety of AI-77-B significantly influenced the activity.[65c] The amino acid end group was required for activity. The isocoumarin skeleton was also required for activity.

The antimicrobial compound AI-77-B was originally isolated by Shimojima et al. from a terrestrial source of *Bacillus pumilus* obtained from a soil sample.[65] Aminocoumacin B, the same compound as AI-77-B, and other related compounds have been isolated by Itoh et al. from cultures of *B. pumilus* obtained from a soil sample collected in Nikko City, Tochigi Prefecture, Japan.[69] It is interesting that AI-77-B has also been isolated by the group of Elyakov in Vladivastok, USSR, from cultures of a marine isolate of *B. pumilus* obtained from the sponge *Dendrilla* sp..[70] These examples, together with the isolation of AI-77-B from the marine isolate 91Z50 presented in this thesis, show that isolates of *B. pumilus* obtained from soil samples and the marine environment in various parts of the world, produce AI-77-B and other related isocoumarin compounds. Since *B. pumilus* seems to be a common soil bacteria, and the fact that *B. pumilus* is capable of forming stable endospores that may be washed into the ocean, it seems likely that the marine isolates of *B. pumilus* may be of terrestrial origin.

Marine Bacteria: Unanswered Questions and Future Research

The results presented in this thesis have demonstrated that bacteria isolated from the marine environment are capable of producing structurally novel and biologically active secondary metabolites. However, several fundamental issues relating to research in the field of marine microorganisms need to be addressed. These include: i) What is a marine bacterium? ii) Do marine bacteria produce unique metabolites not observed from terrestrial microorganisms? iii) Are the bacteria isolated from the ocean indigenous to the marine environment? iv) When is a natural product considered marine or terrestrial?

It is difficult to answer these questions and the results presented in this thesis are not conclusive. In the current literature, the term marine bacteria is used freely and often refers to any bacterium isolated from the marine environment. Zobell and Upham[71] in 1944 suggested that bacteria found in the ocean at places remote from possible terrestrial contamination, and which require sea water for growth upon initial isolation, could be regarded as marine bacteria. A universal definition of a marine bacterium would be useful, but this may not be possible due to the diverse species of bacteria in the ocean, many of which belong to genera that up to now have been considered "terrestrial".

The compounds isolated from the four bacterial species presented in this thesis have demonstrated that marine bacteria are capable of producing novel compounds. This is illustrated by the isolation of oncorhyncolide (**34**), a metabolite of the bacterium *Serratia odorifera*. Oncorhyncolide has a unique structure that is apparently not seen in other microbial metabolites isolated from terrestrial sources. However, all four bacterial species produced metabolites that have identical or similar structures to metabolites isolated from terrestrial microorganisms. Cultures of *Serratia odorifera* produced the known antimicrobial compounds aminopyrrolonitrin (**32**)[33] and prodigiosin (**33**).[34] Both compounds have been isolated from terrestrial sources. A marine isolate of *Pseudomonas fluorescens* produced andrimid (**41**) and the new natural products moiramides A to C (**38** to **40**). Andrimid was originally isolated from a terrestrial source of the bacterium *Enterobacter* sp..[51] Cultures of *Pseudomonas* sp. 91V47 produced the

rhizoxin analogs **44** to **50**. Rhizoxin analogs have been previously isolated from the fungi *Rhizopus chinensis*[59a] and *Rhizopus* sp. No. F-1360,[59b] organisms that are very different from the bacterium *Pseudomonas* sp. 91V47. In addition, the known compound AI-77-B (**57**) has been isolated from cultures of a marine *B. pumilus*. Terrestrial sources of this bacterium also produce AI-77-B.[65,69]

The isolation of a bacterium, usually considered terrestrial, from a marine environment does not necessarily mean that this organism is a contaminant in the ocean or that it is a halotolerant terrestrial bacterium. *Bacillus pumilus* has been isolated from both the marine and terrestrial environments. It is possible that a number of bacteria are common in both the marine and terrestrial environments and that they produce similar or identical natural products.

Historically, the classification of natural products as marine or terrestrial has been based on the origin of the initial source organism. However, the isolation of a previously known "terrestrial" metabolite from cultures of a bacterium isolated from the marine environment does not exclude this metabolite from being considered a marine natural product. With the increasing number of metabolites being isolated from bacteria inhabiting the marine environment, many of which are similar in structure to previously known terrestrial microbial metabolites, the classification of natural products needs to be re-evaluated.

The standard techniques used today for culturing bacteria provide us with less than five percent of the bacteria in a marine sample that can be observed by microscopic methods. These standard methods usually result in the isolation of bacteria belonging to common genera found from terrestrial sources. Therefore, we need to target the large percent of bacteria that are not cultured under standard conditions for future developments. This will require a better understanding of the physiological requirements of marine bacteria and the development of alternative culturing techniques. In addition, the marine environment offers regions of extreme pressure and temperature and we will need to develop culturing techniques to target microorganisms surviving in these extreme environments. Bacteria found in these areas may have very different biosynthetic capabilities than those of terrestrial origin.

EXPERIMENTAL SECTION

General materials and methods

The ^{1}H NMR spectra were recorded on Bruker WH-400 and Bruker AMX-500 spectrometers. Chemical shifts were referenced to either tetramethylsilane (TMS, δ 0.00 ppm) or the residual solvent peaks as a secondary reference ($CDCl_3$ δ 7.26 ppm, C_6D_6 δ 7.15 ppm, CD_3OD δ 3.30 ppm, DMSO-d6 δ 2.49 ppm). The ^{13}C and APT spectra were recorded on Varian XL-300 (75 MHz) and Bruker AMX-500 (125 MHz) spectrometers. ^{13}C chemical shifts were referenced to the residual solvent peaks ($CDCl_3$ δ 77.0 ppm, C_6D_6 δ 128.0 ppm, CD_3OD δ 49.0 ppm, DMSO-d6 δ 39.5 ppm). COSY, NOE difference and double resonance experiments were performed on a Bruker WH-400 spectrometer. HMQC and HMBC experiments were conducted on a Bruker AMX-500 spectrometer.

Low and high resolution electron impact (EI) mass spectra were recorded on Kratos AEI MS-59 and AEI MS-50 mass spectrometers, respectively. Low resolution desorption chemical ionization (DCI) mass spectra were performed on a Delsi-Nermag R-10-10 C quadrupole mass spectrometer using ammonia as the reagent gas. Low and high resolution liquid secondary ion mass spectra (LSIMS) were recorded on a Kratos Concept II HQ mass spectrometer using 3-nitrobenzylalcohol as the sample matrix.

Infrared (IR) spectra of samples applied as films on sodium chloride plates were recorded on a Perkin-Elmer 1600 Fourier Transform (FT) spectrometer. Ultraviolet-visible spectra were recorded on a Bausch and Lomb Spectronic-2000 spectrophotometer. Optical rotations and circular dichroism (CD) spectra were measured using a Jasco J-710 spectropolarimeter.

Normal and reversed-phase thin layer chromatographies (TLC) were performed using Merck type 5554 aluminium backed Kieselgel 60 F254 silica and Whatman $MKC_{18}F$ plates respectively. TLC plates were visualized by UV (254 nm) or by the use of H_2SO_4, vanillin or ninhydrin spray reagents. Further information on the preparation of spray reagents is provided

by Stahl.[72] XAD-4 resin was used to adsorb the organic material from the supernatant of a bacterial culture. Sephadex LH-20 (bead size 25-100 μ) was used for size exclusion chromatography. Normal phase flash chromatography was accomplished using Merck silica gel G60 (230-400 mesh) or Sigma type H TLC grade silica gel (10-40 μ, no binder). Radial thin layer chromatography was performed on a Harrison Research Chromatotron model 7924 and a FMI model RPG-150 lab pump. Chromatotron plates were made from Merck silica gel 60 PF-254 with $CaSO_4.1/2H_2O$ as a binder. Reversed-phase open column chromatography was carried out using reversed-phase silica prepared according to the literature.[73]

Samples were prepared for HPLC purification by application to Waters Sep-Pak C18 and silica cartridges according to package instructions. High performance liquid chromatography (HPLC) separations used one of two systems. The first was comprised of a Waters 501 HPLC pump connected to a Waters model 440 absorbance detector and a Perkin-Elmer LC-25 RI detector. The other system consisted of a Waters 600E multisolvent delivery system equipped with a Waters 486 tunable absorbance detector. Reversed-phase HPLC separations were performed using Alltech C18 5 μ analytical and C18 10 μ semi-prep columns. Normal phase HPLC separations utilized an Alltech silica 5 μ analytical column.

Solvents for extractions and column chromatographies were Fisher or BDH reagent grade. All HPLC solvents were BDH Omnisolve or Fisher HPLC grade. All reagents were commercial grade and were used without further purification. Exceptions were pyridine and triethylamine which were distilled and stored over BaO and 4 Å Linde type molecular sieves, respectively.

Antimicrobial assays against the bacteria *Staphylococcus aureus*, methicillin-resistant *S. aureus*, *S. saprophyticus* and *Enterococcus faecalis*, the yeast *Candida albicans* and the fungus *Rhizoctonia solani* were carried out using the disc diffusion method. Antimicrobial assays for andrimid and moiramides A to C were conducted by Dr. Valerie Bernan, American Cyanamide, Pearl River, NY. Cytotoxicity bioassays against mouse P388 (in vitro) leukemia cell line were performed under the supervision of Dr. Theresa M. Allen of the Department of Pharmacology, University of Alberta.

Bacterial culture conditions

Cultures of *Serratia odorifera* 91-157, *Pseudomonas* 91V47 and *Bacillus pumilus* 91Z50 were grown at room temperature in liquid shake cultures in one liter Erlenmeyer flasks containing 500 mL of tryptic soy broth medium (Difco) supplemented with 1 % sodium chloride (except for 91-157 which was grown without a salt supplement). The cultures were harvested by centrifugation (8000 rpm, 10 minutes) or by filtration (Millipore Pellicon Cassette System, 45 μm filter) four or five days after inoculation. The marine isolate *Pseudomonas fluorescens* 91QQ48 was cultured as lawns on solid media containing tryptic soy broth medium (Difco), 1 % agar (Bacto agar, Difco) and 1 % sodium chloride at room temperature for three days.

Samples of these bacteria are preserved in 1 mL vials in liquid nitrogen.

Secondary metabolites from *Serratia odorifera* (91-157)

The Gram-negative *Serratia odorifera* 91-157 was isolated from a surface water sample taken near a Chinook salmon (*Oncorhyncus tshawytscha*) farm in Georgia Strait, British Columbia. *Serratia odorifera* was grown at room temperature in liquid shake culture in 1/2 strength tryptic soy broth medium. Thirty-six one liter Erlenmeyer flasks containing 500 mL of medium were each inoculated with 2 mL of an actively growing culture of *Serratia odorifera* and the cultures were harvested by centrifugation four days after inoculation. The supernatant was passed over a column of XAD-4 resin packed in water, the column was washed with water, and the adsorbed organic material was eluted with methanol. Evaporation of the methanol eluate in vacuo gave a crude residue which exhibited antimicrobial activity against *Staphylococcus aureus*, *Bacillus subtilus*, the yeast *Candida albicans* and the fungus *Rhizoctonia solani*. The crude residue was partitioned between water (200 mL) and ethyl acetate (5 x 250 mL). The combined ethyl acetate extracts were dried over Na_2SO_4, filtered and concentrated in vacuo to

yield a pungent dark red oil (1.3 g). The antimicrobial activity was found to reside in the organic extract.

Fractionation of the organic soluble materials by Sephadex LH-20 (3:1 methanol/dichloromethane) yielded eighty-eight fractions which were analyzed by TLC and pooled to give six major fractions. The second fraction exhibited weak antibacterial activity and the sixth fraction was active against the fungus *Rhizoctonia solani*. The sixth LH-20 fraction contained the antimicrobial compound aminopyrrolonitrin (**32**) (1 mg).[33] Aminopyrrolonitrin was purified by reversed-phase HPLC (4:6 water/methanol). The second fraction was applied to a reversed-phase Sep-Pak and eluted with a step gradient of solvents beginning with 7:3 water/methanol through methanol. A late eluting fraction resulted in the isolation of the antibiotic red pigment, prodigiosin (**33**).[34] Purification of the first fraction from the Sep-Pak by reversed-phase HPLC (7:3 water/methanol) gave pure oncorhyncolide (**34**) (16 mg). Oncorhyncolide was isolated as an unstable oil and was acetylated with acetic anhydride and pyridine (0.5 mL of each, room temperature, 20 hours) under an atmosphere of nitrogen to give the relatively stable diacetate (**35**).[35] The antibiotic pigment prodigiosin was also isolated from the cell pellet after centrifugation. The cells were freeze-dried and extracted with diethyl ether to yield 2.26 g of a crude red oil. Half of the crude extract was applied to a silica gel flash column and eluted with a step gradient from dichloromethane (100 %) to ethyl acetate (100 %). The fractions showing a pink TLC spot (R_f = 0.48, ethyl acetate) were pooled and concentrated in vacuo to yield 110 mg of a dark red oil containing the known compound prodigiosin.

Aminopyrrolonitrin (32)[33]

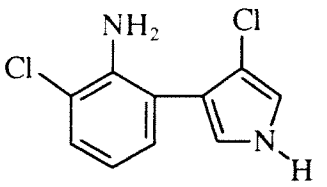

Aminopyrrolonitrin (**32**) was isolated as a yellow oil; IR (film), ν_{max}: 3426, 3384, 1610 1069 cm^{-1}; ^1H NMR ($CDCl_3$, 400 MHz), δ: 4.23 (bs, 2H); 6.71 (t, J = 7.8 Hz, 1H); 6.84 (t, J = 2.6 Hz, 1H); 6.88 (t, J = 2.6 Hz, 1H); 7.09 (dd, J = 7.6,1.5 Hz, 1H); 7.24 (dd, J = 8.0, 1.5 Hz, 1H); 8.33 (bs, 1H) ppm; ^{13}C NMR ($CDCl_3$, 75 MHz), δ: 112.2, 116.1, 117.1, 117.9, 119.2, 119.4, 120.0, 128.5, 130.0, 141.7 ppm; HREIMS $C_{10}H_8N_2Cl_2$ (M^+) m/z: 226.0067 (ΔM +0.3 mmu); LREIMS, m/z (formula, relative intensity): 226 ($C_{10}H_8N_2Cl_2$, 85.4), 191 ($C_{10}H_8N_2Cl$, 67.5), 190 ($C_{10}H_7N_2Cl$, 100), 156 ($C_{10}H_8N_2$, 95.2).

Prodigiosin (33)[34p]

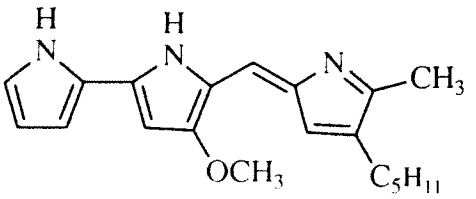

Prodigiosin (**33**) was isolated as a red oil; ^1H NMR ($CDCl_3$, 400 MHz), δ: 0.87 (t, J = 6.9 Hz, 3H), 1.25-1.32 (m, 6H), 2.38 (t, J = 7.5 Hz, 2H), 2.53 (s, 3H), 3.99 (s, 3H), 6.07 (d, J = 1.5 Hz, 1H), 6.33 (m, 1H), 6.67 (d, J = 2.0 Hz, 1H), 6.91 (m, 1H), 6.94 (s, 1H), 7.21 (bs, 1H), 12.54 (bs, 1H), 12.69 (bs, 1H) ppm; HREIMS $C_{20}H_{25}N_3O$ (M^+) m/z: 323.1995 (ΔM -0.2 mmu); LREIMS, m/z (formula, relative intensity): 323 ($C_{20}H_{25}N_3O$, 41.2), 266 ($C_{16}H_{16}N_3O$, 100.0).

Oncorhyncolide (34)

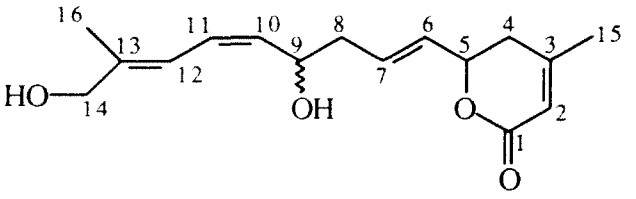

Oncorhyncolide (**34**) was isolated as an unstable colourless oil; $[\alpha]_D$ -36° (c = 3.1, methanol); IR (film), ν_{max}: 3400, 1690 cm^{-1}; ^1H NMR (benzene-d_6, 400 MHz), δ: 1.14 (bs, 3H), 1.36 (dd, J = 17.7, 4.4 Hz, 1H), 1.54 (ddm, J = 17.7, 10.3, ≈1 Hz, 1H), 1.58 (bs, 3H), 1.87 (t, J = 6 Hz, 1H), 2.17 (m, 1H), 2.29 (m, 1H), 3.90 (d, J = 5.9 Hz, 1H), 4.24 (m, 1H), 4.53 (m, 1H), 5.33 (dd, J = 15.5, 5.9 Hz, 1H), 5.37 (t, J = 8.8 Hz, 1H), 5.56 (bs, 1H), 5.67 (m, 1H), 6.23 (dt, J = 11.4, ≈1 Hz, 1H), 6.41 (dm, J = 11.6, ≈1 Hz, 1H) ppm; HREIMS $C_{16}H_{22}O_4$ (M^+) m/z: 278.1527, (ΔM +0.9 mmu); LREIMS, m/z (formula, relative intensity): 278 ($C_{16}H_{22}O_4$, 0.8), 260 ($C_{16}H_{20}O_3$, 13.4), 244 ($C_{16}H_{20}O_2$, 6.4), 126 ($C_7H_{10}O_2$, 100).

Oncorhyncolide diacetate (35)

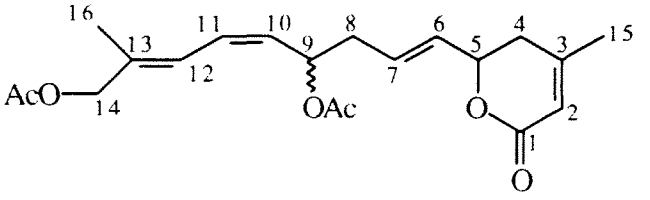

Oncorhyncolide diacetate (**35**) was isolated as a colourless oil; IR (film), ν_{max}: 1728 cm^{-1}; ^1H NMR (benzene-d_6, 400 MHz), δ: 1.19 (bs, 3H), 1.41 (dd, J = 17.6, 4.2 Hz, 1H), 1.46 (bs, 3H), 1.63 (m, 1H), 1.68 (s, 3H), 1.75 (s, 3H), 2.21 (m, 1H), 2.30 (m, 1H), 4.27 (m, 1H), 4.35 (d, J = 13.5 Hz, 1H), 4.44 (d, J = 13.5 Hz, 1H), 5.37 (t, J = 10.0 Hz, 1H), 5.39

(dd, J = 15.5, 6.0 Hz, 1H), 5.52 (m, 1H), 5.62 (bs, 1H), 5.93 (m, 1H), 6.21 (dt, J = 11.5, <1 Hz, 1H), 6.54 (dm, J = 11.5, ≈1 Hz, 1H) ppm; ^{13}C NMR (benzene-d_6, 125 MHz), δ: 14.0, 20.4, 20.7, 22.1, 34.4, 37.9, 68.8, 69.0, 76.3, 117.3, 121.7, 127.3, 128.3, 128.9, 131.5, 136.0, 154.9, 163.5, 169.5, 169.8 ppm; HREIMS $C_{18}H_{22}O_4$ (M^+ -AcOH) m/z: 302.1519 (ΔM +0.1 mmu); LRDCIMS (NH_3), $C_{20}H_{26}O_4$ (M + NH_4) m/z: 380 (relative intensity 47.7).

Biosynthesis of Oncorhyncolide

Liquid shake cultures of *Serratia odorifera* 91-157 (12 x 1 L flasks each containing 500 mL of 1/2 strength tryptic soy broth) were fed [1-^{13}C: 1 g], [2-^{13}C: 0.5 g], [1,2-$^{13}C_2$: 0.25 g] and [2-^{13}C,$^{2}H_3$: 0.5 g] labelled sodium acetate in separate experiments. The labelled precursors were added in two pulses 30 and 50 hours after inoculation and the cultures were harvested by centrifugation after four days. The supernatant was passed over a column of XAD-4 resin packed in water, the resin was washed with water and the adsorbed organic material was eluted with methanol. Evaporation of the methanol eluate in vacuo gave a crude residue which was dissolved in water (100 mL) and partitioned with ethyl acetate (3 x 100 mL). The ethyl acetate extract was fractionated by Sephadex LH-20 (3:1 methanol/dichloromethane). The fraction containing oncorhyncolide (**34**) was acetylated with acetic anhydride and pyridine (0.5 mL of each, room temperature, 20 hours) under an atmosphere of nitrogen. Removal of excess reagents under reduced pressure gave a crude oil which was purified by radial thin layer chromatography (silica gel: EtOAc/hexane 4:6) to yield the pure oncorhyncolide diacetate (**35**).[42]

[1-^{13}C]Sodium acetate

^{13}C NMR (benzene-d_6, 125 MHz), δ (% enrichment above natural abundance): 14.0 (0.4), 20.4 (0.4), 20.7 (0.3), 22.1 (0.3), 34.4 (0.0), 37.9 (0.0), 68.8 (0.6), 69.0 (11.4), 76.3 (7.9),

117.3 (0.6), 121.7 (0.0), 127.3 (10.0), 128.3 (9.6), 128.9 (0.4), 131.5 (0.4), 136.0 (10.3), 154.9 (9.9), 163.5 (7.8), 169.5 (-0.3), 169.8 (0.7) ppm.

[2-^{13}C]Sodium acetate

^{13}C NMR (benzene-d_6, 125 MHz), δ (% enrichment above natural abundance): 14.0 (4.1), 20.4 (0.2), 20.7 (0.0), 22.1 (2.6), 34.4 (3.5), 37.9 (4.6), 68.8 (4.5), 69.0 (0.3), 76.3 (0.0), 117.3 (2.9), 121.7 (3.6), 127.3 (0.3), 128.3 (0.4), 128.9 (4.5), 131.5 (4.0), 136.0 (0.3), 154.9 (0.1), 163.5 (0.2), 169.5 (0.1), 169.8 (0.0) ppm.

[1,2-$^{13}C_2$]Sodium acetate

^{13}C NMR (benzene-d_6, 125 MHz), δ: 14.0 (s), 20.4 (s), 20.7 (s), 22.1 (s), 34.4 ($^1J_{C3.C4}$ = 36.9 Hz), 37.9 ($^1J_{C7.C8}$ = 43.1 Hz, acetone-d_6), 68.8 ($^1J_{C13.C14}$ = 47.4 Hz), 69.0 ($^1J_{C9.C10}$ = 50.2 Hz), 76.3 ($^1J_{C5.C6}$ = 49.8 Hz), 117.3 ($^1J_{C1.C2}$ = 68.3 Hz), 121.7 ($^1J_{C11.C12}$ = 56.2 Hz), 127.3 ($^1J_{C11.C12}$ = 56.2 Hz), 128.3 ($^1J_{C7.C8}$ = 43.1 Hz, acetone-d_6), 128.9 ($^1J_{C9.C10}$ = 49.8 Hz), 131.5 ($^1J_{C5.C6}$ = 50.6 Hz), 136.0 ($^1J_{C13.C14}$ = 47.4 Hz), 154.9 ($^1J_{C3.C4}$ = 37.7 Hz), 163.5 ($^1J_{C1.C2}$ = 68.3 Hz), 169.5 (s), 169.8 (s) ppm.

Secondary metabolites from *Pseudomonas fluorescens* (91QQ48)

Moiramide A (38)

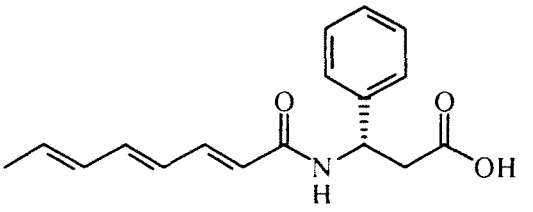

Moiramide A (**38**) was isolated as an amorphous white solid; CD (methanol): $[\Theta]_{212.4}$ 13080, $[\Theta]_{244.8}$ -11230, $[\Theta]_{292.6}$ -6003; UV (methanol), λ_{max} (ε): 293.8 (27421) nm; IR (film), ν_{max}: 3281, 1698, 1648 cm^{-1}; ^1H NMR (DMSO-d_6, 400 MHz), δ: 1.76 (d, J = 6.6 Hz, 3H), 2.68 (m, 2H), 5.25 (dd, J = 15.3 8.3 Hz, 1H), 5.89 (m, 1H), 6.00 (d, J = 15.0 Hz, 1H), 6.18 (ddd, J = 15.0, 10.7, 1.5 Hz, 1H), 6.25 (dd, J = 14.8, 11.3 Hz, 1H), 6.53 (dd, J = 14.8, 10.7, Hz, 1H), 7.00 (dd, J = 15.0, 11.3 Hz, 1H), 7.22 (m, 1H), 7.30 (d, J = 4.1 Hz, 4H), 8.48 (d, J = 8.3 Hz, 1H), 12.25 (bs, 1H) ppm; ^{13}C NMR (DMSO-d_6, 125 MHz), δ: 18.2, 40.9, 49.5, 124.1, 126.4 (2C), 126.9, 128.0, 128.2 (2C), 131.4, 133.3, 138.9, 139.4, 142.6, 164.2, 171.6 ppm; HREIMS $C_{17}H_{19}NO_3$ (M^+) m/z: 285.1366 (ΔM +0.1 mmu); LREIMS m/z (formula, relative intensity): 285 ($C_{17}H_{19}NO_3$, 36.1), 164 ($C_9H_{10}NO_2$, 100.0), 121 (C_8H_9O, 68.4).

Moiramide B (39)

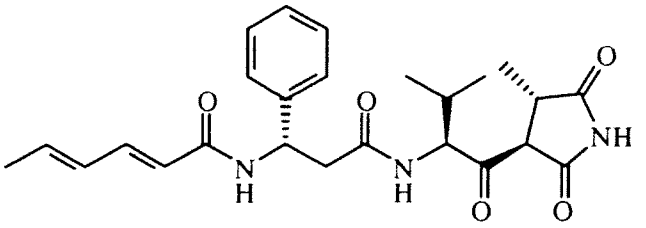

Moiramide B (**39**) was isolated as an amorphous white solid; CD (methanol): $[\Theta]_{214.0}$ 6302, $[\Theta]_{237.6}$ -24140, $[\Theta]_{289.0}$ 570, $[\Theta]_{311.4}$ -3187; UV (methanol), λ_{max} (ε): 255.9 (29040) nm; IR (film), ν_{max}: 3272, 1725 (sh), 1712, 1658, 1633, 1538 cm^{-1}; ^1H NMR (DMSO-d_6, 400 MHz), δ: 0.74 (d, J = 6.7 Hz, 3H), 0.79 (d, J = 6.7 Hz, 3H), 1.07 (d, J = 7.3 Hz, 3H), 1.78 (d, J = 6.5 Hz, 3H), 2.28 (m, 1H), 2.63 (dd, J = 14.3, 6.0 Hz, 1H), 2.76 (dd, J = 14.3, 8.6 Hz, 1H), 2.90 (dd, J = 7.3, 5.5 Hz, 1H), 3.91 (d, J = 5.5 Hz, 1H), 4.61 (dd, J = 8.4, 5.4 Hz, 1H), 5.27 (m, 1H), 5.92 (d, J = 15.1 Hz, 1H), 6.06 (m, 1H), 6.19 (dd, J = 15.0, 10.8 Hz, 1H), 6.95 (dd, J = 15.1, 10.8 Hz, 1H), 7.20 (m, 1H), 7.3 (m, 4H), 8.08 (d, J = 8.4 Hz, 1H), 8.37 (d, J = 8.4 Hz, 1H), 11.33 (bs, 1H) ppm; ^{13}C NMR (DMSO-d_6, 125 MHz), δ: 14.5, 17.2, 18.2, 19.4, 28.1, 38.9, 41.9, 49.8, 57.8, 63.0, 122.9, 126.4 (2C), 126.8, 128.2 (2C), 129.9, 136.6, 139.4, 142.8, 164.4, 169.8, 173.7, 180.0, 203.3 ppm; HREIMS $C_{25}H_{31}N_3O_5$ (M^+) m/z: 453.2262 (ΔM -0.1 mmu); LREIMS m/z (formula, relative intensity): 453 ($C_{25}H_{31}N_3O_5$, 5.0), 358 ($C_{19}H_{24}N_3O_4$, 14.0), 242 ($C_{15}H_{16}NO_2$, 69.4), 200 ($C_{13}H_{14}NO$, 39.0), 146 (C_9H_8NO, 63.0), 95 (C_6H_7O, 100).

Moiramide C (40)

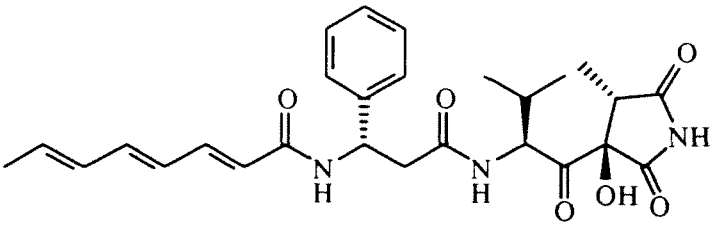

Moiramide C (**40**) was isolated as an amorphous white solid; CD (methanol): $[\Theta]_{218.0}$ -2075, $[\Theta]_{237.8}$ -12360, $[\Theta]_{303.2}$ 4971; UV (methanol), λ_{max} (ε): 289.2 (29771) nm; IR (film), ν_{max}: 3247, 1729 (sh), 1717, 1636, 1608, 1541 cm^{-1}; ^1H NMR (DMSO-d_6, 400 MHz), δ: 0.61 (d, J = 6.8 Hz, 3H), 0.71 (d, J = 7.1 Hz, 3H), 0.81 (d, J = 6.8 Hz, 3H), 1.76 (d, J = 6.4 Hz, 3H), 2.50 (m, 1H), 2.66 (d, J = 7.4 Hz, 2H), 2.89 (q, J = 7.1 Hz, 1H), 5.18 (dd, J = 9.4, 3.4 Hz, 1H), 5.25 (m, 1H), 5.90 (m, 1H), 5.99 (d, J = 15.1 Hz, 1H), 6.18 (ddd, J = 15.0, 10.9, 1.5 Hz, 1H), 6.24 (dd, J = 15.0, 11.4 Hz, 1H), 6.53 (dd, 15.0, 10.9, Hz, 1H), 6.98 (dd, J = 15.1, 11.4 Hz, 1H), 6.99 (s, 1H), 7.19 (m, 1H), 7.3 (m, 4H), 7.83 (d, J = 9.4 Hz, 1H), 8.33 (d, J = 8.5 Hz, 1H), 11.41 (bs, 1H) ppm; ^{13}C NMR (DMSO-d_6, 125 MHz), δ: 7.7, 15.9, 18.2, 19.7, 27.4, 41.8, 48.6, 49.9, 58.0, 86.8, 124.2, 126.3 (2C), 126.7, 128.0, 128.0 (2C), 131.4, 133.2, 138.8, 139.2, 142.7, 164.1, 169.5, 174.8, 176.6, 208.6 ppm; HREIMS $C_{27}H_{33}N_3O_6$ (M^+) m/z: 495.2378 (ΔM +0.9 mmu); LREIMS m/z (formula, relative intensity): 495 ($C_{27}H_{33}N_3O_6$, 0.6), 146 (C_9H_8NO, 91.8), 121 (C_8H_9O, 39.7).

Andrimid (41)[51]

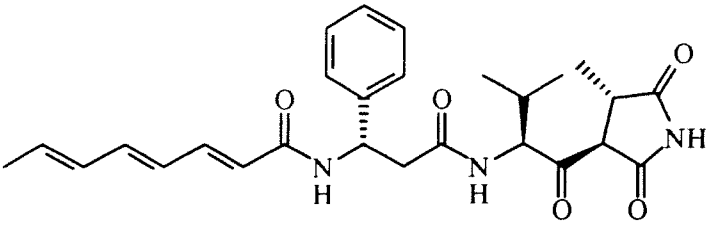

Andrimid (**41**) was isolated as an amorphous white solid; CD (methanol): $[\Theta]_{215.8}$ 4944, $[\Theta]_{240.2}$ -11480, $[\Theta]_{274.8}$ -567, $[\Theta]_{309.0}$ -6096; UV (methanol), λ_{max} (ε): 292.1 (35759) nm; IR (film), ν_{max}: 3282, 1712, 1650, 1644, 1538, 1531 cm^{-1}; ^1H NMR (DMSO-d_6, 400 MHz), δ: 0.74 (d, J = 6.7 Hz, 3H), 0.80 (d, J = 6.7 Hz, 3H), 1.07 (d, J = 7.3 Hz, 3H), 1.78 (d, J = 6.5 Hz, 3H), 2.29 (m, 1H), 2.65 (dd, J = 14.3, 6.1 Hz, 1H), 2.76 (dd, J = 14.3, 8.5 Hz, 1H), 2.91 (dd, J = 7.3, 5.5 Hz, 1H), 3.92 (d, J = 5.5 Hz, 1H), 4.63 (dd, J = 8.4, 5.4 Hz, 1H), 5.28 (m, 1H), 5.89 (m, 1H), 6.01 (d, J = 15.1 Hz, 1H), 6.17 (ddd, J = 15.2, 10.8, 1 Hz, 1H), 6.25 (dd, J = 14.8, 11.3 Hz, 1H), 6.53 (dd, 14.8, 10.8, Hz, 1H), 7.00 (dd, J = 15.1, 11.3 Hz, 1H), 7.2 (m, 1H), 7.3 (m, 4H), 8.09 (d, J = 8.4 Hz, 1H), 8.40 (d, J = 8.5 Hz, 1H), 11.35 (bs, 1H) ppm; ^{13}C NMR (DMSO-d_6, 125 MHz), δ: 14.5, 17.2, 18.2, 19.3, 28.1, 38.9, 41.9, 49.8, 57.8, 63.0, 124.2, 126.4 (2C), 126.8, 128.0, 128.2 (2C), 131.4, 133.3, 138.8, 139.4, 142.8, 164.2, 169.8, 173.6, 179.9, 203.3 ppm; HREIMS $C_{27}H_{33}N_3O_5$ (M^+) m/z: 479.2416 (ΔM -0.4 mmu); LREIMS m/z (formula, relative intensity): 479 ($C_{27}H_{33}N_3O_5$, 358 ($C_{19}H_{24}N_3O_4$,17.5), 268 ($C_7H_{18}NO_2$, 81.7),146 (C_9H_8NO, 74.5), 121 (C_8H_9O, 100.0).

Prodigiosin (33)[34p]

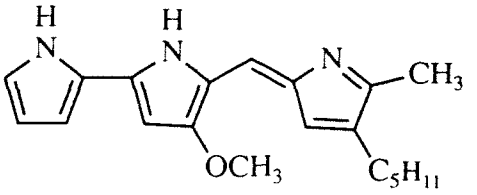

Prodigiosin (**33**) was isolated as a red powder; ^{1}H NMR ($CDCl_3$, 400 MHz), δ: 0.88 (t, J = 6.9 Hz, 3H), 1.25-1.35 (m, 6H), 2.32 (t, J = 7.9 Hz, 2H), 2.55 (s, 3H), 4.00 (s, 3H), 6.07 (bs, 1H), 6.35 (dd, J = 3.7, 2.5 Hz, 1H), 6.66 (bs, 1H), 6.91 (m, 1H), 6.94 (s, 1H), 7.25 (m, 1H), 12.57 (bs, 1H), 12.76 (bs, 1H); HREIMS $C_{20}H_{25}N_3O$ (M^+) m/z: 323.2006 (ΔM +0.8 mmu); LREIMS, m/z (formula, relative intensity): 323 ($C_{20}H_{25}N_3O$, 98.7), 266 ($C_{16}H_{16}N_3O$, 100.0).

Biosynthesis of Andrimid

Pseudomonas fluorescens 91QQ48 was grown as lawns on solid media. Four aluminium trays (23 x 33 x 5 cm) each containing 500 mL of tryptic soy broth medium, 1 % agar and 1 % sodium chloride were each inoculated with 2 mL of an actively growing liquid culture of *P. fluorescens*. The cultures were incubated for 3 days at room temperature. After this time the cells were gently scraped off the solid media. The agar medium was sectioned into 3 x 3 cm cubes and immersed in ethyl acetate. After 24 hours the solvent was decanted, dried over sodium sulfate and concentrated in vacuo to obtain a pungent dark red oil. The ethyl acetate extraction of the agar was repeated three times to yield 0.65 g of the crude oil.

The crude extract was chromatographed on a Sephadex LH-20 column eluted with ethyl acetate/methanol/water (8:2:1). TLC analysis indicated the presence of andrimid in fractions fourteen to twenty. These fractions were pooled and concentrated in vacuo to give a pink powder. Reversed-phase column chromatography (65:35 methanol/phosphate buffer, pH 6.87)

of the andrimid containing fraction allowed the separation of the pink pigment prodigiosin which remained on the top of the column. The andrimid containing fractions were pooled and concentrated in vacuo to remove the methanol. The aqueous residue was exhaustively extracted with ethyl acetate. Further purification by reversed-phase HPLC (65:35 methanol/phosphate buffer, pH 6.87) gave pure andrimid (50 mg).[51]

The labelled precursors [1-^{13}C: 0.5 g]valine, [1-^{13}C: 1 g]sodium acetate, [1,2-^{13}C: 0.5 g]sodium acetate), [1,2-$^{13}C_2$: 250 mg]glycine and [1,2-$^{13}C_2$,^{15}N: 100 mg]glycine were dissolved in water and filter sterilized before adding to the culture medium (4 x 500 mL tryptic soy broth, 1 % agar, 1 % sodium chloride) just before pouring the media into the aluminium trays in separate experiments. Andrimid was isolated by the procedure outlined above.

[1-^{13}C]Valine

^{13}C NMR (DMSO-d_6, 125 MHz), δ (% enrichment above natural abundance): 14.5 (0.0), 17.2 (0.0), 18.2 (0.1), 19.3 (0.1), 28.1 (0.0), 38.9 (0.0), 41.9 (0.1), 49.8 (0.0), 57.8 (-0.1), 63.0 (0.0), 124.2 (0.1), 126.4 (0.0), 126.8 (0.1), 128.0 (0.0), 128.2 (0.1)), 131.4 (0.1), 133.3 (0.1), 138.8 (0.0), 139.4 (0.1), 142.8 (0.1), 164.2 (0.1), 169.8 (0.0), 173.6 (0.0), 179.9 (0.0), 203.3 (22.4) ppm.

[1-^{13}C]Sodium acetate

^{13}C NMR (DMSO-d_6, 125 MHz), δ (% enrichment above natural abundance): 14.5 (0.0), 17.2 (0.0), 18.2 (-0.1), 19.3 (0.1), 28.1 (0.0), 38.9 (1.1), 41.9 (0.1), 49.8 (0.0), 57.8 (-0.2), 63.0 (0.1), 124.2 (-0.1), 126.4 (0.1), 126.8 (-0.1), 128.0 (-0.3), 128.2 (0.1)), 131.4 (-0.2), 133.3 (17.2), 138.8 (18.7), 139.4 (17.7), 142.8 (0.1), 164.2 (21.7), 169.8 (0.2), 173.6 (18.4), 179.9 (-0.1), 203.3 (0.1) ppm.

[1,2-$^{13}C_2$]Sodium acetate

^{13}C NMR (DMSO-d_6, 125 MHz), δ: 14.5, 17.2, 18.2 ($^1J_{C7'''.C8'''}$ = 43.0) , 19.3, 28.1, 38.9, 41.9, 49.8, 57.8 ($^1J_{C2.C3}$ = 42.8 Hz), 63.0, 124.2 ($^1J_{C1'''.C2'''}$ = 64.4 Hz), 126.4 (2C), 126.8, 128.0 ($^1J_{C3'''.C4'''}$ = 56.3 Hz), 128.2 (2C), 131.4 ($^1J_{C5'''.C6'''}$ = 55.7 Hz), 133.3 ($^1J_{C7'''.C8'''}$ = 43.0), 138.8 ($^1J_{C5'''.C6'''}$ = 55.7 Hz), 139.4 ($^1J_{C3'''.C4'''}$ = 56.3 Hz), 142.8, 164.2 ($^1J_{C1'''.C2'''}$ = 64.4 Hz), 169.8, 173.6 ($^1J_{C2.C3}$ = 42.8 Hz), 179.9, 203.3 ppm.

[1,2-$^{13}C_2$]Gycine

^{13}C NMR (DMSO-d_6, 125 MHz), δ: 14.5, 17.2, 18.2, 19.3, 28.1, 38.9 ($^1J_{C4.C5}$ = 45.8 Hz), 41.9, 49.8, 57.8, 63.0, 124.2, 126.4 (2C), 126.8, 128.0, 128.2 (2C), 131.4, 133.3, 138.8, 139.4, 142.8, 164.2, 169.8, 173.6, 179.9 ($^1J_{C4.C5}$ = 45.8 Hz), 203.3 ppm.

[1,2-$^{13}C_2$,^{15}N]Glycine

^{13}C NMR (DMSO-d_6, 125 MHz), δ: 14.5, 17.2, 18.2, 19.3, 28.1, 38.9 ($^1J_{C4.C5}$ = 45.8 Hz; $^2J_{C4.N1}$ = 5.7 Hz), 41.9, 49.8, 57.8, 63.0, 124.2, 126.4 (2C), 126.8, 128.0, 128.2 (2C), 131.4, 133.3, 138.8, 139.4, 142.8, 164.2, 169.8, 173.6, 179.9 ($^1J_{C4.C5}$ = 45.8 Hz; $^1J_{C5.N1}$ = 12.4 Hz), 203.3 ppm.

Secondary metabolites from *Pseudomonas* sp. 91V47

The bacterial isolate 91V47, obtained from an abalone collected off Cortez Island in Georgia Strait, British Columbia, was identified as a pseudomonad. *Pseudomonas* sp. 91V47 was grown at room temperature in liquid shake culture in tryptic soy broth. Thirty-six one liter Erlenmeyer flasks containing 500 mL of medium plus 1 % sodium chloride were each inoculated with 2 mL of an actively growing culture of *Pseudomonas* sp. 91V47 and the cultures were harvested by filtration five days after inoculation. The supernatant was passed over a column of XAD-4 resin packed in water, the column was washed with water, and the adsorbed organic material was eluted with methanol. Evaporation of the methanol eluate in vacuo gave a crude residue which was found to be cytotoxic. The crude residue was partitioned between water (200 mL) and ethyl acetate (5 x 250 mL). The combined ethyl acetate extracts were dried over sodium sulfate, filtered and concentrated in vacuo to yield a pungent brown oil. The cytotoxic activity was found to reside in the organic extract (in vitro P388 murine leukemia, ED_{50} = 0.0287 μg/mL). Three batches of bacteria were grown to yield 7.74 g of the crude extract.

Fractionation of the organic soluble materials by Sephadex LH-20 (eluent: 3:1 methanol/dichloromethane) yielded two hundred fractions which were analyzed by TLC and pooled to give thirteen major fractions. The third fraction was found to be cytotoxic. The polar constituents of the third LH-20 fraction were purified by reversed-phase HPLC (eluent: 4:6 methanol/0.025M phosphate, buffer pH 6.78) and yielded eleven fractions. Each fraction was concentrated in vacuo to remove the methanol and the aqueous residue was exhaustively extracted with ethyl acetate. Further purification by reversed-phase HPLC (eluent: methanol/ 0.025M phosphate buffer, pH 6.78) yielded three new natural products **44** (15 mg), **45** (12 mg) and **46** (8 mg). The third fraction contained a less polar, purple staining TLC spot (R_f = 0.32, silica, ethyl acetate) on spraying with vanillin. Purification of the less polar purple spot by normal phase silica HPLC (eluent: 2:3 and 1:1 hexane/ethyl acetate) yielded the new compounds **47** (8 mg), **48** (1 mg) and **49** (2 mg) as well as the known compound WF-1360C (**50**) (9 mg).[59]

WF-1360C (50)[59]

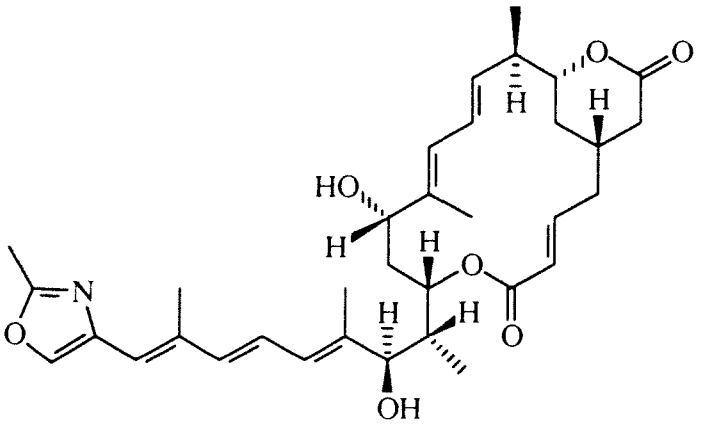

WF-1360C (**50**) was isolated as an amorphous white solid; IR (film), ν_{max}: 3418 (br), 1715 cm^{-1}; ^1H NMR ($CDCl_3$, 400 MHz), δ: 0.70 (m, 1H), 0.97 (d, J = 6.9 Hz, 3H), 1.22 (d, J = 6.6 Hz, 3H), 1.75 (m, 1H), 1.80 (m, 1H), 1.81 (s, 3H), 1.89 (s, 3H), 1.90 (m, 1H), 1.97 (m, 1H), 2.08 (m, 1H), 2.12 (m, 1H), 2.14 (s, 3H), 2.15 (m, 1H), 2.29 (m, 1H), 2.46 (s, 3H), 2.55 (m, 1H), 2.77 (dm, J = 14.9 Hz, 1H), 3.70 (m, 1H), 3.90 (d, J = 6.3 Hz, 1H), 4.00 (dd, J = 10.6, 2.6 Hz, 1H), 4.70 (dd, J = 10.6, 5.1 Hz, 1H), 5.19 (dd, J = 15.2, 9.6 Hz, 1H), 5.63 (d, 15.7 Hz, 1H), 5.85 (d, J = 10.9 Hz, 1H), 6.21 (dd, J = 10.9 Hz, 1H), 6.25 (s, 1H), 6.25 (dd, J = 15.2, 10.9 Hz, 1H), 6.40 (d, J = 15.2 Hz, 1H), 6.58 (dd, J = 15.2, 10.9 Hz, 1H), 6.80 (m, 1H), 7.53 (s, 1H) ppm; ^{13}C NMR ($CDCl_3$, 125 MHz), δ: 9.7, 11.0, 12.8, 13.8, 14.4, 16.5, 29.6, 33.5, 34.6, 36.8, 38.3, 40.0, 45.2, 74.8, 77.6, 78.3, 83.2, 120.4, 124.2, 124.4, 126.3, 126.7, 129.7, 134.7, 135.9, 137.0, 137.4, 138.3, 138.7, 139.2, 146.8, 160.9, 166.2, 170.3 ppm; HREIMS $C_{34}H_{45}NO_7$ (M^+) m/z: 579.3202 (ΔM +0.6 mmu); LREIMS m/z (formula, relative intensity): 579 ($C_{34}H_{45}NO_7$, 8.3), 561 ($C_{34}H_{43}NO_6$, 41.9).

Compound 44

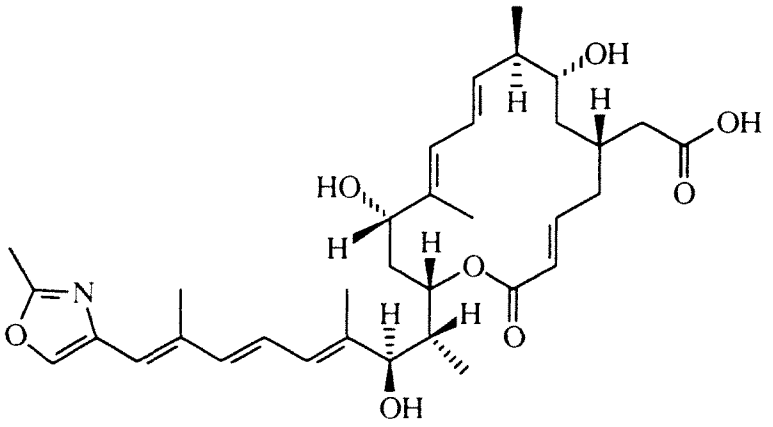

Compound **44** was isolated as an unstable white solid; IR (film), ν_{max}: 3400 (br), 1710 cm^{-1}; ^1H NMR (DMSO-d_6, 400 MHz), δ: 0.78 (m, 1H), 0.84 (d, J = 6.7 Hz, 3H), 0.90 (d, J = 7.3 Hz, 3H), 1.61 (s, 3H), 1.64 (m, 1H), 1.75 (m, 1H), 1.78 (s, 3H), 1.81 (m, 1H), 1.82 (m, 1H), 1.82 (m, 1H), 1.85 (m, 1H), 1.88 (m, 1H), 2.04 (dd, J = 16.2, 4.9 Hz, 1H), 2.15 (s, 3H), 2.25 (m, 1H), 2.39 (s, 3H), 2.83 (m, 1H), 2.90 (dd, J =16.2, 3.2 Hz, 1H), 3.68, (m, 1H), 3.70, (m, 1H), 4.51 (d, J = 6.1 Hz, 1H), 4.62 (dd, J = 9.7, 3.2 Hz, 1H), 4.67 (d, J = 3.0 Hz, 1H), 4.83 (d, J = 4.5 Hz, 1H), 5.10 (dd, J = 15.2, 9.6 Hz, 1H), 5.53 (d, J = 11.0 Hz, 1H), 5.58 (d, J = 15.6 Hz, 1H), 6.05 (dd, J = 15.2, 10.8 Hz, 1H), 6.08 (d, J = 10.0 Hz, 1H), 6.23 (s, 1H), 6.39 (d, J = 15.1 Hz, 1H), 6.55 (m, 1H), 6.60 (m, 1H), 8.01 (s, 1H), 11.98 (s, 1H) ppm; ^{13}C NMR (DMSO-d_6, 125 MHz), δ: 9.8, 10.6, 12.1, 13.3, 14.0, 17.0, 33.0, 34.2, 36.4, 37.6, 40.0, 40.1, 45.8, 73.1, 75.7, 77.0, 77.4, 119.6, 123.3, 124.2, 124.6, 125.5, 127.6, 136.2, 136.4, 136.9, 137.1, 138.2, 138.6, 140.6, 147.8, 160.4, 165.0, 174.0 ppm; HRLSIMS (positive ion, 3-nitrobenzylalcohol matrix), $C_{34}H_{48}NO_8$ $(M + H)^+$ m/z: 598.33982. (ΔM +1.83 mmu); LRLSIMS (positive ion, 3-nitrobenzylalcohol matrix), m/z (formula, relative intensity): 598 ($C_{34}H_{48}NO_8$, 2.0), 580 ($C_{34}H_{44}NO_7$, 2.6), 562 ($C_{34}H_{44}NO_6$,1.7).

Compound 45

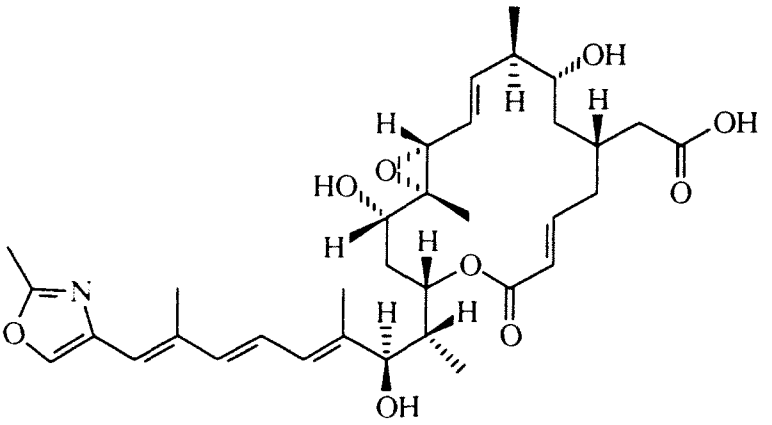

Compound **45** was isolated as an unstable white solid; IR (film), ν_{max}: 3420 (br), 1714 cm^{-1}; ^1H NMR (DMSO-d_6, 400 MHz), δ: 0.86 (d, J = 6.8 Hz, 3H), 0.94 (d, J = 6.6 Hz, 3H), 0.95 (m, 1H), 1.17 (s, 3H), 1.52 (m, 1H), 1.75 (m, 1H), 1.78 (s, 3H), 1.85 (m, 1H), 1.85 (m, 1H), 1.90 (m, 1H), 2.10 (m, 1H), 2.13 (s, 3H), 2.15 (m, 1H), 2.20 (m, 1H), 2.30 (m, 1H), 2.39 (s, 3H), 2.40 (m, 1H), 2.78 (dd, J = 10.5, 2.5 Hz, 1H), 2.84 (d, J = 8.1 Hz, 1H), 2.98 (m, 1H), 3.69, (d, J = 7.6 Hz, 1H), 4.46 (d, J = 6.6 Hz, 1H), 4.64 (dd, J = 9.7, 3.6 Hz, 1H), 4.87 (d, J = 4.5 Hz, 1H), 5.01 (d, J = 3.8 Hz, 1H), 5.08 (dd, J = 15.6, 8.1 Hz, 1H), 5.32 (dd, J = 15.6, 9.2 Hz, 1H), 5.74 (d, J = 15.6 Hz, 1H), 6.05 (d, J = 11.0 Hz, 1H), 6.22 (s, 1H), 6.35 (d, J = 15.2 Hz, 1H), 6.57 (dd, J = 15.2, 11.0 Hz, 1H), 6.67 (m, 1H), 8.00 (s, 1H), 12.06 (s, 1H) ppm: ^{13}C NMR (DMSO-d_6, 125 MHz), δ: 9.6, 10.8, 12.0, 13.4, 14.0, 17.4, 30.6, 33.4, 34.6, 37.8, 39.7, 40.0, 44.9, 60.7, 64.7, 70.7, 73.8, 76.9, 77.5, 119.7, 124.5, 124.9, 125.6, 125.8, 136.2, 136.6, 137.1, 138.2, 140.2, 140.5, 145.5, 160.5, 164.6, 173.7 ppm; HRLSIMS (positive ion, 3-nitrobenzylalcohol matrix), $C_{34}H_{48}NO_9$ $(M + H)^+$ m/z: 614.33214 (ΔM -0.77 mmu); LRLSIMS (positive ion, 3-nitrobenzylalcohol matrix), m/z (formula, relative intensity): 614 ($C_{34}H_{48}NO_9$, 5.2), 596 ($C_{34}H_{46}NO_8$, 3.8), 578 ($C_{34}H_{44}NO_7$, 1.5).

Compound 46

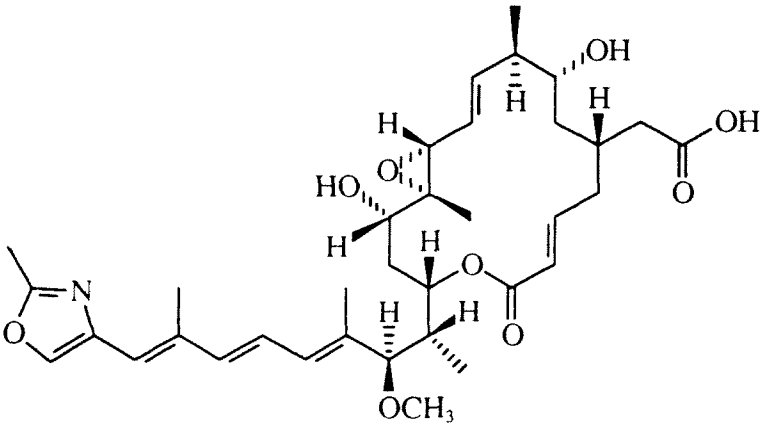

Compound **46** was isolated as an unstable white solid; IR (film), ν_{max}: 3428 (br), 1713 cm^{-1}; ^1H NMR (DMSO-d_6, 400 MHz), δ: 0.91 (d, J = 6.7 Hz, 3H), 0.94 (d, J = 6.6 Hz, 3H), 0.95 (m, 1H), 1.19 (s, 3H), 1.52 (m, 1H), 1.65 (m, 1H), 1.76 (s, 3H), 1.85 (m, 1H), 1.88 (m, 1H), 1.93 (m, 1H), 2.08 (m, 1H), 2.16 (s, 3H), 2.20 (m, 1H), 2.23 (m, 1H), 2.33 (m, 1H), 2.41 (s, 3H), 2.42 (m, 1H), 2.77 (dm, J = 10.1, Hz, 1H), 2.84 (d, J = 8.0 Hz, 1H), 3.00 (m, 1H), 3.08 (s, 3H), 3.28, (d, J = 8.8 Hz, 1H), 4.47 (d, J = 6.5 Hz, 1H), 4.63 (dd, J = 9.6, 3.2 Hz, 1H), 5.07 (d, J = 3.9 Hz, 1H), 5.07 (dd, J = 15.6, 8.0 Hz, 1H), 5.33 (dd, J = 15.6, 9.2 Hz, 1H), 5.76 (d, J = 15.5 Hz, 1H), 6.13 (d, J = 11.0 Hz, 1H), 6.27 (s, 1H), 6.42 (d, J = 15.1 Hz, 1H), 6.63 (dd, J = 15.1,11.0 Hz, 1H), 6.69 (m, 1H), 8.04 (s, 1H), 12.07 (s, 1H) ppm; ^{13}C NMR (DMSO-d_6, 125 MHz), δ: 10.1, 10.7, 11.3, 13.4, 14.0, 17.4, 30.6, 33.2, 34.6, 37.8, 38.9, 40.0, 44.9, 55.6, 60.6, 64.6, 70.7, 72.9, 76.9, 88.2, 120.3, 124.0, 124.7, 125.8, 128.8, 136.0, 136.1, 137.3, 137.5, 138.1, 140.2, 145.8, 160.5, 164.6, 173.7 ppm; HRLSIMS (positive ion, 3-nitrobenzylalcohol matrix), $C_{35}H_{50}NO_9$ $(M + H)^+$ m/z: 628.34436 (ΔM -4.20 mmu); LRLSIMS (positive ion, 3-nitrobenzylalcohol matrix), m/z (formula, relative intensity): 628 ($C_{35}H_{50}NO_9$, 12.8), 627 ($C_{34}H_{49}NO_9$, 7.2), 610 ($C_{34}H_{48}NO_8$, 2.4), 596 ($C_{33}H_{46}NO_8$, 7.8).

Compound 47

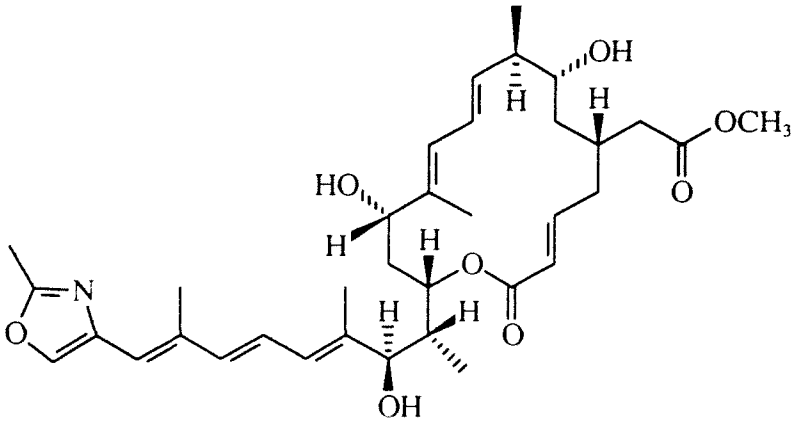

Compound **47** was isolated as an amorphous white solid; IR (film), ν_{max}: 3412 (br), 1731 (sh), 1715 cm^{-1}; ^1H NMR ($CDCl_3$, 400 MHz), δ: 0.92 (d, J = 6.9 Hz, 3H), 0.96 (m, 1H), 1.05 (d, J = 6.5 Hz, 3H), 1.76 (s, 3H), 1.81 (s, 3H), 1.90 (m, 1H), 1.90 (m, 1H), 1.95 (m, 1H), 1.97 (m, 1H), 2.02 (m, 1H), 2.04 (m, 1H), 2.10 (m, 1H), 2.13 (s, 3H), 2.35 (m, 1H), 2.40 (m, 1H), 2.46 (s, 3H), 2.81 (dd, J = 15.6, 4.4 Hz, 1H), 3.11 (m, 1H), 3.68 (s, 3H), 3.91 (bs, 1H), 4.06 (bd, J = 10.6 Hz, 1H), 4.90 (dd, J = 10.3, 6.8 Hz, 1H), 5.25 (dd, J = 15.1, 9.6 Hz, 1H), 5.61 (dd, 15.4, 1.6 Hz, 1H), 5.81 (d, J = 10.8 Hz, 1H), 6.13 (dd, J = 15.1, 10.8 Hz, 1H), 6.24 (s, 1H), 6.26 (d, J = 11.0 Hz, 1H), 6.39 (d, J = 15.1 Hz, 1H), 6.57 (dd, J = 15.1, 11.0 Hz, 1H), 6.80 (m, 1H), 7.52 (s, 1H) ppm; ^{13}C NMR ($CDCl_3$, 125 MHz), δ: 9.7, 10.5, 13.6, 13.8, 14.4, 16.6, 34.3, 34.5, 37.1, 39.2, 40.5, 40.6, 46.1, 51.6, 73.8, 75.7, 77.2, 78.7, 120.2, 123.0, 124.5, 126.0, 126.6, 128.1, 135.8, 137.1, 137.8, 137.9, 138.1, 138.3, 138.8, 149.3, 160.8, 166.7, 173.8 ppm; HREIMS $C_{35}H_{49}NO_8$ (M^+) m/z: 611.3449 (ΔM -0.9 mmu); LREIMS m/z (formula, relative intensity): 611 ($C_{35}H_{49}NO_8$, 0.4), 593 ($C_{35}H_{47}NO_7$, 4.0), 579 ($C_{34}H_{45}NO_7$, 5.5), 561 ($C_{34}H_{43}NO_6$, 27.8).

Compound 48

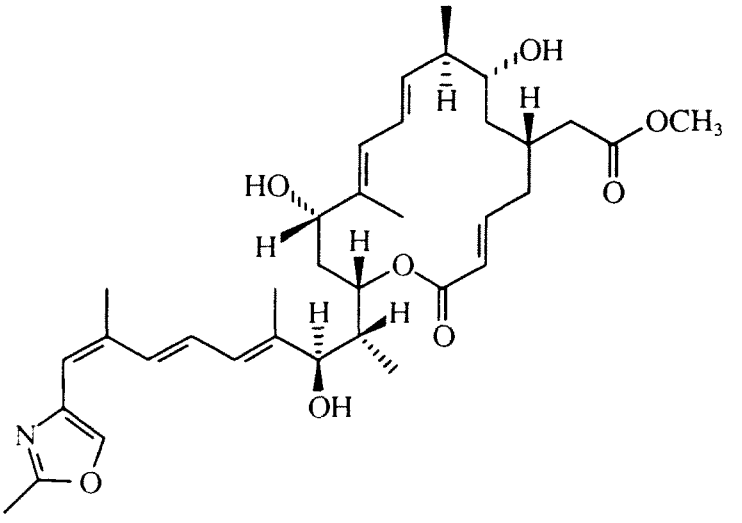

Compound **48** was isolated as a white solid: IR (film), ν_{max}: 3404 (br), 1715 cm^{-1}; ^1H NMR ($CDCl_3$, 500 MHz), δ: 0.92 (d, J = 6.9 Hz, 3H), 0.95 (m, 1H), 1.05 (d, J = 6.5 Hz, 3H), 1.77 (s, 3H), 1.81 (s, 3H), 1.90 (m, 1H), 1.90 (m, 1H), 1.95 (m, 1H), 1.95 (m, 1H), 2.00 (m, 1H), 2.03 (s, 3H), 2.05 (m, 1H), 2.10 (m, 1H), 2.35 (m, 1H), 2.40 (m, 1H), 2.45 (s, 3H), 2.81 (dd, J = 15.6, 4.0 Hz, 1H), 3.11 (m, 1H), 3.68 (s, 3H), 3.93 (bs, 1H), 4.06 (bd, J = 10.7 Hz, 1H), 4.89 (dd, J = 9.8, 7.2 Hz, 1H), 5.24 (dd, J = 15.1, 9.6 Hz, 1H), 5.61 (dd, 15.7, 1.0 Hz, 1H), 5.80 (d, J = 10.8 Hz, 1H), 6.06 (s, 1H), 6.13 (dd, J = 15.1, 10.8), 6.33 (d, J = 11.0 Hz, 1H), 6.62 (dd, J = 15.3, 11.0 Hz, 1H), 6.80 (m, 1H), 7.34 (d, J = 15.3 Hz, 1H), 7.47 (s, 1H) ppm; ^{13}C NMR ($CDCl_3$, 125 MHz), δ: 9.8, 10.6, 13.5, 13.9, 16.7, 20.9, 34.4, 34.5, 37.1, 39.2, 40.5, 40.6, 46.1, 51.6, 74.0, 75.9, 77.5, 78.6, 117.6, 123.1, 126.5, 126.5, 126.7, 128.1, 131.1, 135.8, 135.9, 137.7, 138.0, 138.3, 138.6, 149.3, 161.5, 166.8, 173.8 ppm; HREIMS $C_{35}H_{49}NO_8$ (M^+) m/z: 611.3463 (ΔM +0.5 mmu).

Compound 49

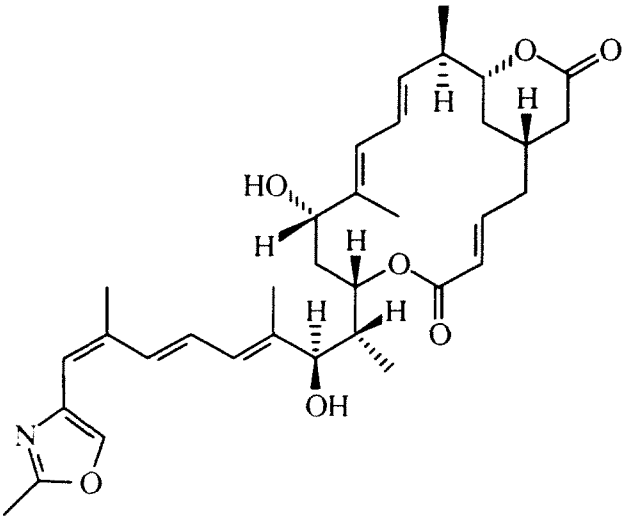

Compound 55 was isolated as a white solid; IR (film), ν_{max}: 3415 (broad), 1714 cm^{-1}; ^1H NMR ($CDCl_3$, 500 MHz), δ: 0.70 (m, 1H), 0.98 (d, J = 6.7 Hz, 3H), 1.20 (d, J = 6.4 Hz, 3H), 1.75 (m, 1H), 1.80 (m, 1H), 1.81 (s, 3H), 1.88 (m, 1H), 1.89 (s, 3H), 1.97 (m, 1H), 2.04 (s, 3H), 2.10 (m, 1H), 2.15 (m, 1H), 2.15 (m, 1H), 2.30 (m, 1H), 2.45 (s, 3H), 2.55 (m, 1H), 2.77 (dd, J = 18.1, 3.1 Hz, 1H), 3.69 (m, 1H), 3.92 (bs, 1H), 4.00 (d, J = 10.1 Hz, 1H), 4.68 (dd, J = 10.3, 5.3 Hz, 1H), 5.18 (dd, J = 15.2, 9.6 Hz, 1H), 5.64 (d, 15.8 Hz, 1H), 5.83 (d, J = 10.7 Hz, 1H), 6.07, (s, 1H), 6.25 (dd, J = 15.2, 10.7 Hz, 1H), 6.29 (d, J = 11.2 Hz, 1H), 6.62 (dd, J = 15.3, 11.2 Hz, 1H), 6.79 (m, 1H), 7.40, (d, J = 15.3 Hz, 1H), 7.47 (s, 1H) ppm; ^{13}C NMR ($CDCl_3$, 125 MHz), δ: 9.7, 11.0, 12.7, 13.9, 16.6, 20.9, 29.7, 33.9, 34.6, 36.8, 38.3, 40.1, 45.3, 75.1, 78.0, 78.2, 83.2, 117.6, 124.2, 126.0, 126.5, 127.3, 129.7, 131.8, 134.6, 135.6, 136.1, 138.3, 138.7, 139.4, 146.7, 161.3, 166.3, 170.3 ppm; HREIMS $C_{34}H_{45}NO_7$ (M^+) m/z: 579.3188 (ΔM +0.6 mmu); LREIMS m/z (formula, relative intensity): 579 ($C_{34}H_{45}NO_7$, 4.7).

Secondary metabolites from *Bacillus pumilus* (91Z50)

Bacterial isolate 91Z50, obtained from a sediment sample in Georgia Strait, British Columbia, was identified as the Gram-positive *Bacillus pumilus*. *B. pumilus* was grown at room temperature in liquid shake culture in tryptic soy broth. Thirty-six one liter Erlenmeyer flasks containing 500 mL of medium plus 1 % sodium chloride were each inoculated with 2 mL of an actively growing culture of *Bacillus pumilus* and the cultures were harvested by filtration five days after inoculation. The supernatant was passed over a column of XAD-4 resin packed in water, the column was washed with water, and the adsorbed organic material was eluted with methanol. Evaporation of the methanol eluate in vacuo gave a crude residue which exhibited antibacterial activity against *Staphylococcus aureus*, methicillin-resistant *S. aureus*, *S. saprophyticus* and *Enterococcus faecalis*. The crude residue was partitioned between water (200 mL) and ethyl acetate (5 x 250 mL). The combined ethyl acetate extracts were dried over Na_2SO_4, filtered and concentrated in vacuo to yield a pungent brown oil. The antibacterial activity was found to reside in the organic extract. Three batches of bacteria were cultured to yield 10.64 g of the oil.

Fractionation of the organic soluble materials by Sephadex LH-20 (3:1 methanol/dichloromethane) yielded one hundred and thirty fractions which were analyzed by TLC and pooled to give six major fractions. The first three fractions showed antibacterial activity against the four test organisms, *Staphylococcus aureus*, methicillin-resistant *S. aureus*, *S. saprophyticus* and *Enterococcus faecalis*. The second LH-20 fraction was applied to a reversed-phase column and eluted with water/methanol (1:4). TLC analysis yielded seven fractions. The second fraction contained an interesting purple TLC spot on reversed-phase silica (R_f = 0.39, 1:4 water/methanol) after spraying with ninhydrin. Further purification of the fraction containing the purple spot by reversed-phase preparative TLC (1:4 water/methanol) and reversed-phase HPLC (6:4 water/methanol) yielded the known antimicrobial compound AI-77-B (**54**) (22 mg).[65d] Acetylation of AI-77-B with acetic anhydride and pyridine (0.5 mL of each, room temperature, 20 hours) under an atmosphere of nitrogen gave the triacetate **55**.[65d]

The third antimicrobial fraction was applied to a Sephadex LH-20 column and eluted with ethyl acetate/methanol/water (8:2:1). One hundred and forty fractions were collected, analyzed by TLC and pooled to yield six fractions. The second fraction showed antimicrobial activity. Recycling of this active fraction on Sephadex LH-20 (ethyl acetate/methanol/water, 8:2:1) gave an interesting fraction containing two green TLC spots (R_f = 0.39, 0.52) on spraying with ninhydrin. Application of this fraction to a TLC silica flash column (3:6 hexane/ethyl acetate) yielded the known compound AI-77-F (**56**) (6 mg)[65d] and the new compound **57** (5 mg).

AI-77-B (54)[65d]

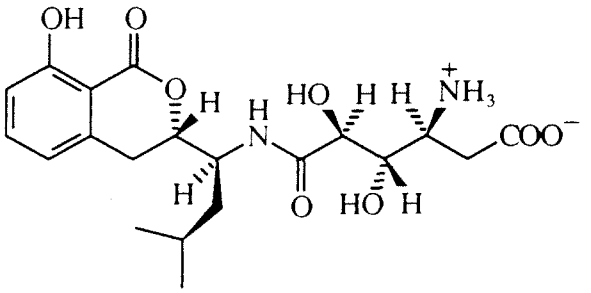

AI-77-B (**54**) was isolated as an amorphous white solid; UV (methanol), λ_{max}; 244 nm (ε = 7540), 312 nm (ε = 5161); CD (methanol), Θ_{198} -47770, Θ_{219} 8726, Θ_{229} 3601, Θ_{241} 7306, Θ_{260} -7312, Θ_{284} -137, Θ_{317} -2065; IR (film), ν_{max}: 3238 (broad), 1671, 1665, 1654 cm^{-1}; ^1H NMR (CD_3OD, 400 MHz), δ: 0.94 (d, J = 6.5 Hz, 3H), 0.97 (d, J = 6.5 Hz, 3H), 1.44 (m, 1H), 1.72 (m, 1H), 1.82 (m, 1H), 2.52 (m, 1H), 2.59 (m, 1H), 2.92 (dd, J = 16.5, 3.0 Hz, 1H), 3.09 (dd, J = 16.5, 12.2 Hz, 1H), 3.59 (bs, 1H), 3.92 (m, 1H), 4.14 (d, J = 5.3 Hz, 1H), 4.35 (dt, 10.6, 3.4 Hz, 1H), 4.66 (dt, 12.2, 3.0 Hz, 1H), 6.78 (d, J = 7.4 Hz, 1H), 6.83 (d, J = 8.4 Hz, 1H), 7.44 (dd, J = 8.4, 7.4 Hz, 1H) ppm; ^1H NMR (DMSO-d_6, 400 MHz), δ: 0.85 (d, J = 6.3 Hz, 3H), 0.89 (d, J = 6.3 Hz, 3H), 1.33 (m, 1H), 1.66 (m, 2H), 2.13 (m, 1H), 2.27 (m, 1H), 2.85 (dd, J = 16.5, 2.3 Hz, 1H), 3.05 (dd, 16.5, 12.4 Hz, 1H), 3.24 (m, 1H), 3.64 (m, 1H), 3.93 (d, J = 5.5 Hz), 4.19 (m, 1H), 4.68 (dm, J = 12.4 Hz, 1H), 6.81 (d, J = 7.5 Hz, 1H), 6.84 (d, J = 8.4 Hz, 1H), 7.47 (dd, J = 8.4, 7.5 Hz, 1H), 7.84 (d, J = 9.3

Hz, 1H) ppm; ^{13}C NMR (CD_3OD, 125 MHz), δ:22.0, 23.8, 25.8, 30.9, 35.1, 40.7, 50.4, 52.6, 73.2 (2C), 82.7, 109.4, 116.7, 119.5, 137.5, 141.6, 163.2, 171.0, 175.2, 178.2 ppm; HREIMS, $C_{20}H_{26}N_2O_7$ (M - H_2O) m/z: 406.1740 (ΔM +0.0 mmu); LREIMS, m/z (formula, relative intensity): 389 ($C_{20}H_{23}NO_7$, 4.3), 371 ($C_{20}H_{21}NO_6$, 2.8), 307 ($C_{16}H_{21}NO_5$, 4.4), 244 ($C_{11}H_{20}N_2O_4$, 46.6), 227 ($C_{11}H_{17}NO_4$, 31.3), 201 ($C_{13}H_{13}O_2$, 33.6); LRDCIMS (NH_3), m/z (formula, relative intensity): 425 ($C_{20}H_{29}N_2O_8$, 2), 424 ($C_{20}H_{28}N_2O_8$, 1), 407 ($C_{20}H_{27}N_2O_7$, 82).

AI-77-B Acetate 55[65d]

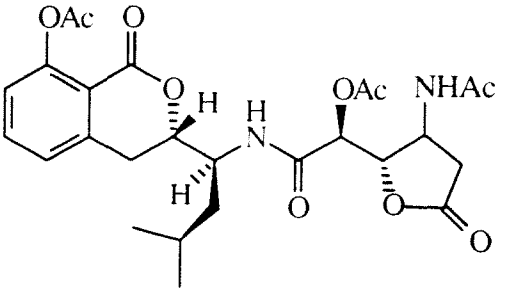

Compound **55** was isolated as a pale yellow oil; IR (film), ν_{max}: 3310, 1771, 1757, 1729, 1670 cm^{-1}; ^1H NMR ($CDCl_3$, 400 MHz), δ: 0.88 (d, J = 6.4 Hz, 3H), 0.93 (d, J = 6.4 Hz, 3H), 1.38 (m, 1H), 1.69 (m, 2H), 1.88 (s, 3H), 2.15 (s, 3H), 2.34 (s, 3H), 2.55 (dd, J = 18.4, 3.7 Hz, 1H), 2.89 (dd, J = 16.5, 3.0 Hz, 1H), 3.01 (m, 2H), 4.31 (m, 1H), 4.48 (dt, J = 11.7, 3.0 Hz, 1H), 4.72 (bs, 2H), 5.40 (m, 1H), 6.67 (d, J = 5.0 Hz, 1H), 6.81 (d, J = 9.4 Hz, 1H), 7.04 (d, J = 8.0 Hz, 1H), 7.16 (d, J = 7.6 Hz, 1H), 7.54 (dd, J = 8.0, 7.6 Hz, 1H) ppm; ^{13}C NMR ($CDCl_3$, 125 MHz), δ: 20.8, 21.2, 21.7, 22.9, 23.2, 24.6, 31.1, 35.3, 40.2, 47.6, 49.5, 73.4, 79.9, 83.4, 117.4, 123.0, 125.7, 134.9, 141.2, 151.8, 162.0, 166.2, 169.6, 169.9, 170.8, 174.7 ppm; HREIMS, $C_{26}H_{32}N_2O_{10}$ (M^+) m/z: 532.2060 (ΔM +0.3 mmu); LREIMS, m/z (formula, relative intensity): 532 ($C_{26}H_{32}N_2O_{10}$, 0.2), 490 ($C_{24}H_{30}N_2O_9$, 5.4), 268 ($C_{13}H_{20}N_2O_4$, 91.6).

AI-77-F (56)[65d]

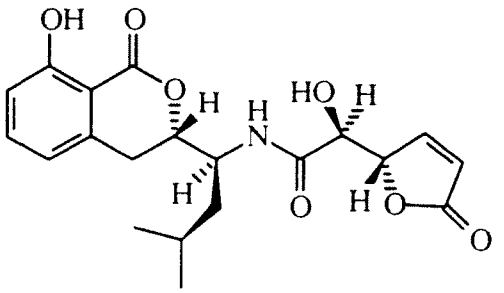

AI-77-F (**56**) was isolated as an amorphous white solid; UV (methanol), λ_{max}; 243 nm (ε = 8072), 312 nm (ε = 5099); CD (methanol), Θ_{201} -87030, Θ_{223} -7875, Θ_{226} -8151, Θ_{242} 5646, Θ_{260} -1027, Θ_{284} 1, Θ_{313} -1839; IR (film), ν_{max}: 3323 (broad), 1758, 1672, cm^{-1}; ^1H NMR ($CDCl_3$, 400 MHz), δ: 0.96 (d, J = 6.5 Hz, 3H), 0.98 (d, J = 6.5 Hz, 3H), 1.48 (m, 1H), 1.61 (m, 1H), 1.85 (m, 1H), 2.88 (dd, J = 16.5, 3.0 Hz, 1H), 3.06 (dd, J = 16.5, 12.3 Hz, 1H), 4.38 (m, 1H), 4.58 (d, J = 4.4 Hz, 1H), 4.63 (dt, J = 12.3, 2.5 Hz, 1H), 5.46 (m, 1H), 6.23 (dd, J = 5.7, 1.8 Hz, 1H), 6.71 (d, J = 7.4 Hz, 1H), 6.88 (d, J = 8.5 Hz, 1H), 7.37 (dd, J = 5.7, 1.2 Hz, 1H), 7.42 (dd, J = 8.5, 7.4 Hz, 1H), 10.73 (s, 1H) ppm; ^1H NMR (DMSO-d_6, 400 MHz), δ: 0.83 (d, J = 6.5 Hz, 3H), 0.90 (d, J = 6.5 Hz, 3H), 1.31 (m, 1H), 1.68 (m, 2H), 2.96 (d, J = 6.2 Hz, 2H), 4.16 (m, 1H), 4.40 (bs, 1H), 4.68 (m, 1H), 5.35 (m, 1H), 6.19 (d, J = 5.1 Hz, 1H), 6.26 (dd, J = 5.7, 1.9 Hz, 1H), 6.83 (d, J = 6.3 Hz, 1H), 6.85 (d, J = 7.7 Hz, 1H), 7.49 (m, 2H), 7.81 (d, J = 9.5 Hz, 1H), 10.80 (s, 1H) ppm; ^{13}C NMR ($CDCl_3$, 125 MHz), δ: 21.6, 23.1, 24.9, 30.3, 40.3, 49.3, 70.7, 80.9, 83.6, 108.1, 116.3, 118.2, 123.4, 136.5, 139.1, 152.4, 162.2, 169.3, 169.4, 172.7 ppm; HREIMS, $C_{20}H_{23}NO_7$ (M^+) m/z: 389.1478 (ΔM +0.3 mmu); LREIMS, m/z (formula, relative intensity): 389 ($C_{20}H_{23}NO_7$, 0.4), 371 ($C_{20}H_{21}NO_6$, 0.5), 227 ($C_{11}H_{17}NO_4$, 6.8), 209 ($C_{11}H_{15}NO_3$, 10.4), 163 ($C_9H_7O_3$, 16.9), 135 ($C_8H_7O_2$, 20.0), 86 ($C_8H_{12}N$, 100.0).

Compound 57

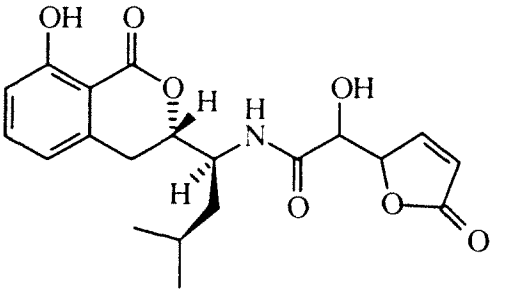

Compound **57** was isolated as a white solid; UV (methanol), λ_{max}; 244 nm (ε = 7261), 312 nm (ε = 4743); CD (methanol), Θ_{194} -64450, Θ_{214} 49050, Θ_{239} 9403, Θ_{261} -5896, Θ_{286} 553, Θ_{314} -752; IR (film), ν_{max}: 3327 (broad), 1760, 1673 cm^{-1}; ^1H NMR ($CDCl_3$, 400 MHz), δ: 0.95 (d, J = 6.5 Hz, 3H), 0.97 (d, J = 6.5 Hz, 3H), 1.47 (m, 1H), 1.67 (m, 1H), 1.83 (m, 1H), 2.84 (dd, J = 16.5, 3.0 Hz, 1H), 3.02 (dd, J = 16.5, 12.5 Hz, 1H), 4.33 (d, J = 5.3 Hz, 1H), 4.37 (m, 1H), 4.59 (dt, J = 12.4, 2.5 Hz, 1H), 5.31 (ddd, J = 5.3, 2.0, 1.5 Hz, 1H), 6.19 (dd, J = 5.8, 2.0 Hz, 1H), 6.69 (d, J = 7.4 Hz, 1H), 6.86 (d, J = 8.4 Hz, 1H), 6.91 (d, J = 9.7 Hz, 1H), 7.40 (dd, J = 8.4, 7.4 Hz, 1H), 7.66 (dd, J = 5.8, 1.5 Hz, 1H), 10.73 (s, 1H) ppm; ^1H NMR (DMSO-d_6, 400 MHz), δ: 0.86 (d, J = 6.4 Hz, 3H), 0.91 (d, J = 6.4 Hz, 3H), 1.32 (m, 1H), 1.67 (m, 2H), 2.96 (d, J = 7.5 Hz, 2H), 4.21 (m, 1H), 4.32 (dd, J = 6.4, 2.7 Hz, 1H), 4.68 (m, 1H), 5.42 (m, 1H), 5.99 (d, J = 6.5 Hz, 1H), 6.24 (dd, J = 5.7, 2.0 Hz, 1H), 6.84 (d, J = 7.4 Hz, 1H), 6.85 (d, J = 8.4 Hz, 1H), 7.48 (dd, J = 8.4, 7.4 1H), 7.62 (d, J = 9.6 Hz, 1H), 7.71 (dd, J = 5.7, 1.5 Hz, 1H), 10.80 (s, 1H) ppm; ^{13}C NMR ($CDCl_3$, 125 MHz), δ: 21.8, 23.1, 24.7, 30.3, 40.5, 49.4, 72.0, 81.0, 83.5, 108.0, 116.3, 118.2, 122.9, 136.5, 139.1, 153.6, 162.2, 169.3, 169.4, 172.3 ppm; HREIMS, $C_{20}H_{23}NO_7$ (M^+) m/z: 389.1481 (ΔM +0.7 mmu); LREIMS, m/z (formula, relative intensity): 389 ($C_{20}H_{23}NO_7$, 0.2), 371 ($C_{20}H_{21}NO_6$, 0.9), 227 ($C_{11}H_{17}NO_4$, 6.8), 209 ($C_{11}H_{15}NO_3$, 8.5), 163 ($C_9H_7O_3$, 18.2), 135 ($C_8H_7O_2$, 22.5), 86 ($C_8H_{12}N$, 100.0).

Moshers esterification

(S)-(+)-2-methoxy-2-phenyl-2-(trifluoromethyl) acetic acid chloride (MPTA-Cl), (5 μL), prepared according to the literature,[66] was added to a solution of AI-77-F (**72**) (1 mg), triethylamine (5 μL), dimethylaminopyridine (1 crystal) in $CDCl_3$ (100 μL).[67] After one hour the chloroform was evaporated. The residue was applied to a normal phase silica Sep-Pak and eluted with 1:1 ethyl acetate/hexane. Purification by normal phase HPLC (1:1 ethyl acetate/hexane) yielded the pure R-MPTA ester **58**.

Compound 58

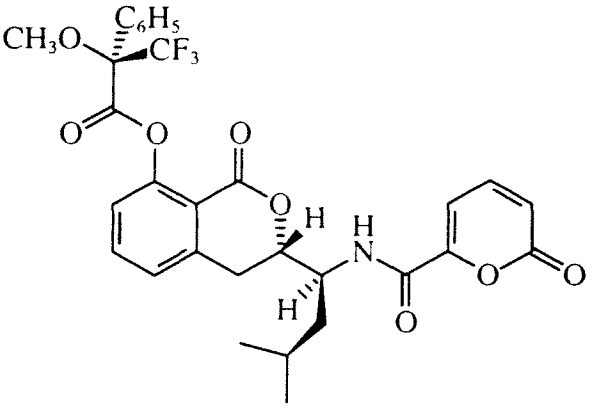

Compound **58** was isolated as a pale yellow film; IR (film), ν_{max}: 3320, 1790, 1766, 1732, 1673; ^1H NMR ($CDCl_3$, 400 MHz), δ: 0.95, (d, J = 2.8 Hz, 3H), 0.97 (d, J = 2.8 Hz, 3H), 1.50 (m, 1H), 1.65 (m, 1H), 1.82 (m, 1H), 2.99 (dd, J = 16.4, 3.3 Hz, 1H), 3.13 (dd, J = 16.4, 11.3 Hz, 1H), 3.79 (s, 3H), 4.45 (m, 1H), 4.62 (m, 1H), 5.79 (s, 1H), 5.88 (d, J = 10.0 Hz, 1H), 6.41 (dd, 5.6, 1.7 Hz, 1H), 6.94 (d, J = 8.0 Hz, 1H), 7.19 (d, J = 8.0 Hz, 1H), 7.46-7.48 (m, 3H), 7.51 (t, J = 8.0 Hz, 1H), 7.74 (m, 1H), 7.75 (m, 1H), 8.50 (d, J = 5.6 Hz, 1H); ^{13}C NMR ($CDCl_3$, 125 MHz), δ:21.9, 23.0, 24.8, 31.3, 41.0, 49.5, 79.8, 103.8, 122.1, 123.7, 126.3, 127.7 (2C), 128.5 (2C), 129.8, 134.8, 138.5, 141.1, 142.6, 156.7, 158.9, 163.6, 165.3 ppm; HREIMS, $C_{30}H_{28}NO_8F_3$ (M^+) m/z: 3587.1171 (ΔM +0.4 mmu); LREIMS, m/z (formula, relative intensity): 587 ($C_{30}H_{28}NO_8F_3$, 3.5), 464 ($C_{24}H_{25}NO_5F_3$, 1.6), 379 ($C_{19}H_{14}O_5F_3$, 6.7), 208 ($C_{11}H_{14}NO_3$, 65.2), 189 ($C_9H_8OF_3$, 100.0).

Appendix 1.

Nuclear Magnetic Resonance Techniques

Nuclear magnetic resonance (NMR) techniques have been employed in this thesis to aid in the structural elucidation of the new natural products. A simple, non-quantum mechanical description of the NOE difference, COSY, HMQC and HMBC experiments, along with an example of each will be presented in this appendix. A number of books and reviews provide a more detailed explanation of the theory of one-dimensional and two-dimensional NMR.[74] Tables of chemical shifts and coupling constants are also readily available.[75]

One-dimensional NMR experiments

The time sequence for a one-dimensional experiment is shown in Figure A1. The preparation time allows the sample to reach thermal equilibrium. A radiofrequency pulse is applied and data collection starts at the end of the evolution period with the detection time. During the evolution time (t_1, a constant), additional pulses may be applied, scalar spin-spin interactions can be applied by gating the decoupler channel, or dipolar couplings (through-space) may take place.

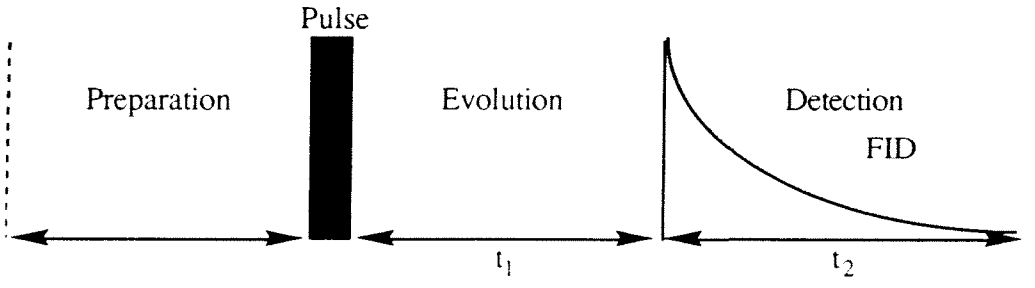

Figure A1. Time sequence for a one-dimensional NMR experiment.[76]

The nuclear Overhauser effect difference experiment

In this thesis the nuclear Overhauser effect difference spectrum (NOEDS) was used to determine stereochemical features of the new metabolites. When two protons (H_A and H_X) are close to each other in space, saturation of H_A by the application of a selective radiofrequency pulse alters the intensity of the signal H_X. This change in intensity is known as the nuclear Overhauser effect (NOE) and it is a consequence of the through space dipolar coupling between H_A and H_X. Subtraction of the unperturbed FID as a result of off-resonance irradiation from the perturbed FID (with NOE) and subsequent Fourier transform generates a spectrum containing only the NOE enhanced signals, the NOEDS. The NOE difference spectrum contains a signal at δ_X, the chemical shift of the NOE, and a large negative signal at δ_A, the chemical shift of the irradiated proton. NOEs are usually positive for small molecules in a non-viscous solvent, however, larger molecules may give rise to negative NOEs.[74c] The intensity of the signal is inversely proportional to the sixth power of the distance between the two protons, H_A and H_X.

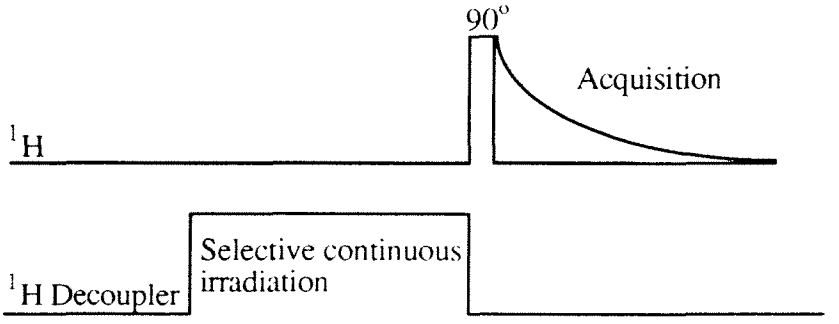

Figure A2. The pulse sequence for an NOE difference experiment.[77]

The pulse sequence for a NOEDS experiment is given in Figure A2. This experiment consists of the sequential acquisition of ^1H spectra with gated decoupling.

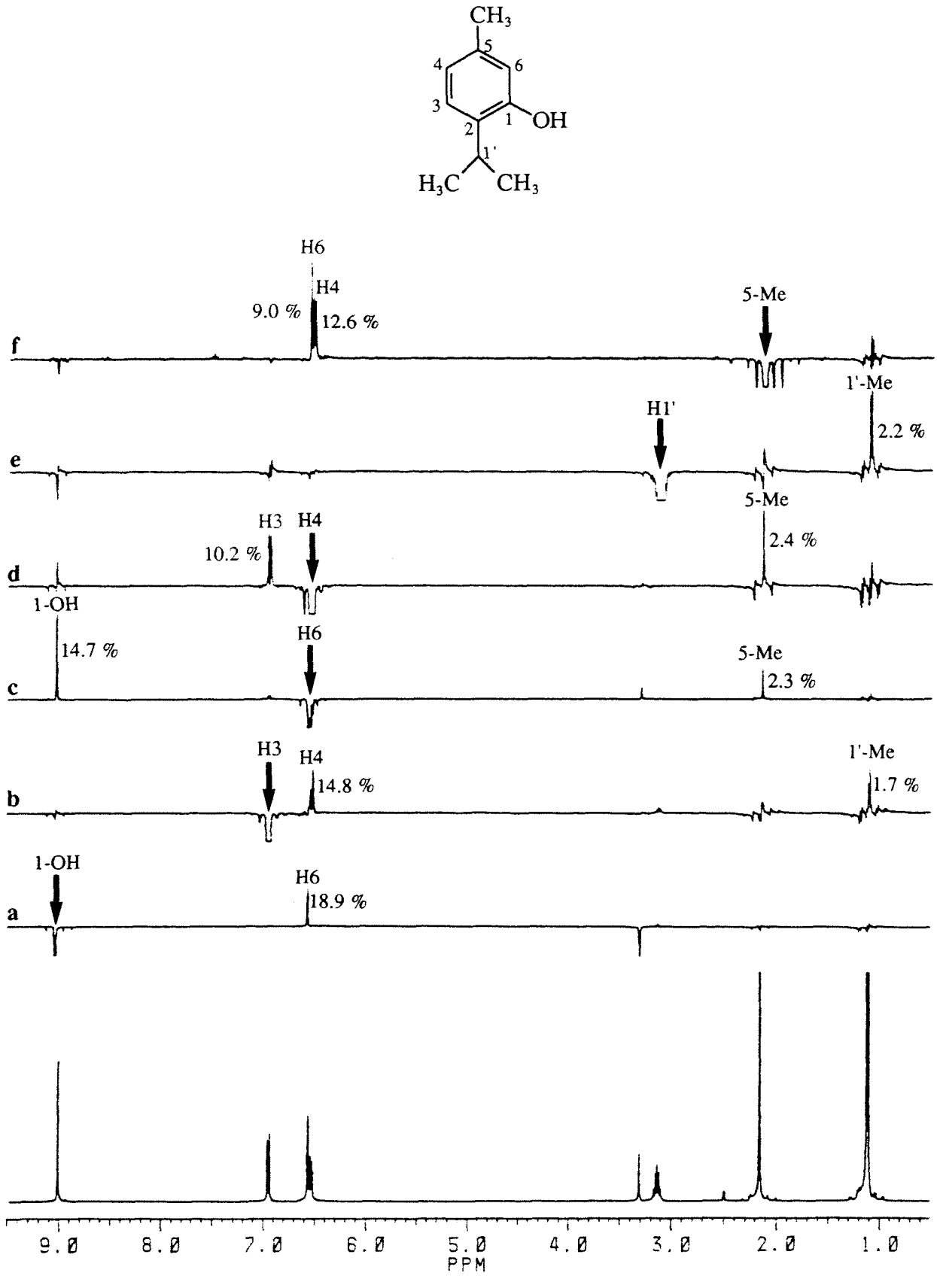

Figure A3. NOE difference spectra of thymol (400 MHz, DMSO-d_6).

In gated decoupling the decoupler is turned on and a specific resonant frequency is irradiated allowing the build up of NOE. The decoupler is then turned off and a 90° pulse is applied followed by the acquisition of FID. All the NOEDS experiments in this thesis were recorded on a Bruker WH-400 spectrometer with a decoupler power of 47-51 dB and a preparation delay of 6 seconds. The preparation delay allowed the system to come to thermal equilibrium between irradiations. The NOE enhancements in this thesis were calculated as a percent of the irradiated peak (large negative peak). A one-proton irradiated peak was assigned to -100 %. The percent NOEs do not provide an accurate measurement of the distance between protons but they do provide some indication of the strength of the NOE.

The NOE difference spectra of thymol, a simple organic molecule, are shown in Figure A3. The off-resonance spectrum of thymol is shown at the bottom of the figure. In spectrum **b** the aromatic proton at δ 6.95 (H3) was irradiated inducing NOEs at δ 6.53 (H4) and δ 1.11 (1'-Me). Irradiation of the methyl singlet at δ 2.15 (5-Me) resulted in the enhancement of the H4 and H6 resonances at δ 6.53 and δ 6.56 respectively (spectrum **f**). The results from selected NOEDS are summarized in Figure A4.

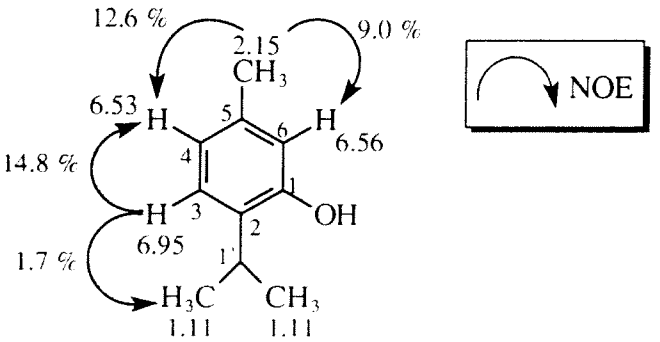

Figure A4. Results from selected NOE difference experiments on thymol.

Two-dimensional NMR experiments

The time sequence for a two-dimensional (2D) NMR experiment is shown in Figure A5. It has the time sequence "preparation - evolution - detection" as in the 1D experiment illustrated in Figure A1. In a 1D NMR experiment the receiver signal $S(t_2)$ is solely a function of the detection time t_2 but in a 2D NMR experiment the evolution time t_1 is variable. The mixing period consists of pulses and fixed delays. At the end of the mixing period the chemical shifts of the observed nuclei are recorded. During the course of n experiments the evolution time, t_1, is increased by a constant time increment Δt_1. A separate FID is detected in t_2 for each t_1 increment. Therefore, the receiver signal is dependent on two time variables, t_1 and t_2, i.e. $S(t_1,t_2)$ and the data is Fourier transformed twice. Fourier transformation of the data with respect to t_2 provides n conventional spectra that are phase or amplitude modulated. The phase or amplitude modulation contains information about homo or heteronuclear coupling or dipolar coupling and originates by varying the delays and pulses during the evolution period. Fourier transformation in the second dimension, with respect to t_1, leads to a second frequency domain that may contain information about coupling constants or chemical shifts.

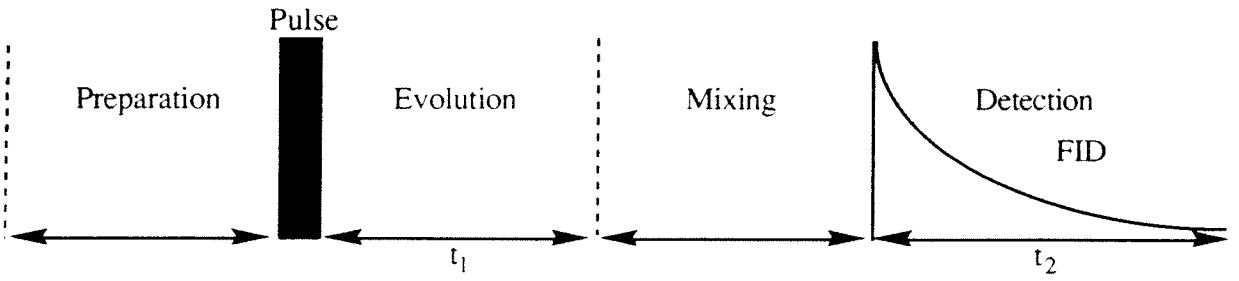

Figure A5. Time sequence for a two-dimensional NMR experiment.[74a]

The ^1H-^1H COSY experiment

The homonuclear correlated spectroscopy (COSY) experiment was used in this thesis to determine proton connectivities. A series of 1D homonuclear decoupling experiments can provide the same information as the COSY experiment. The advantage of a COSY experiment over its 1D analog is that information about all the scalar couplings of a molecule is provided in a short time even when the 1D ^1H NMR spectrum is congested.

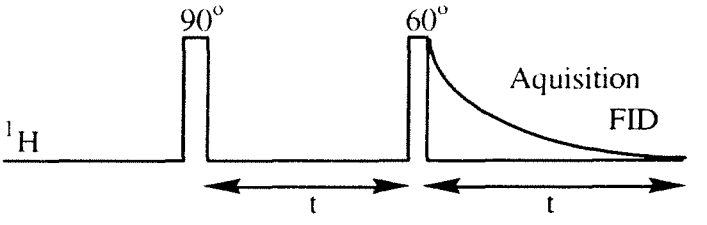

Figure A6. The pulse sequence for a COSY experiment.[78]

The pulse sequence for the acquisition of a COSY60 experiment is provided in Figure A6. Following the preparation time a 90° pulse is applied and produces transverse magnetization. The magnetization precesses at its Larmor frequency (ν_0) in the x,y plane during t_1. At the end of the evolution time t_1 a second pulse, 60°, is applied that transfers coherence from the protons that have evolved during t_1 to protons with which they are scalar coupled. Fourier transformation with respect to t_1 leads to a series of proton spectra that are modulated by scalar coupling. A second Fourier transformation gives a 2D NMR spectrum with the ^1H chemical shift on both axis. The COSY spectrum contains a signal on the diagonal at (δ_A,δ_A) when protons are correlated to themselves. Cross peaks or off-diagonal peaks arise from scalar coupling when $\nu_1 \neq \nu_2$ and have coordinates (δ_A,δ_B) and (δ_B,δ_A).

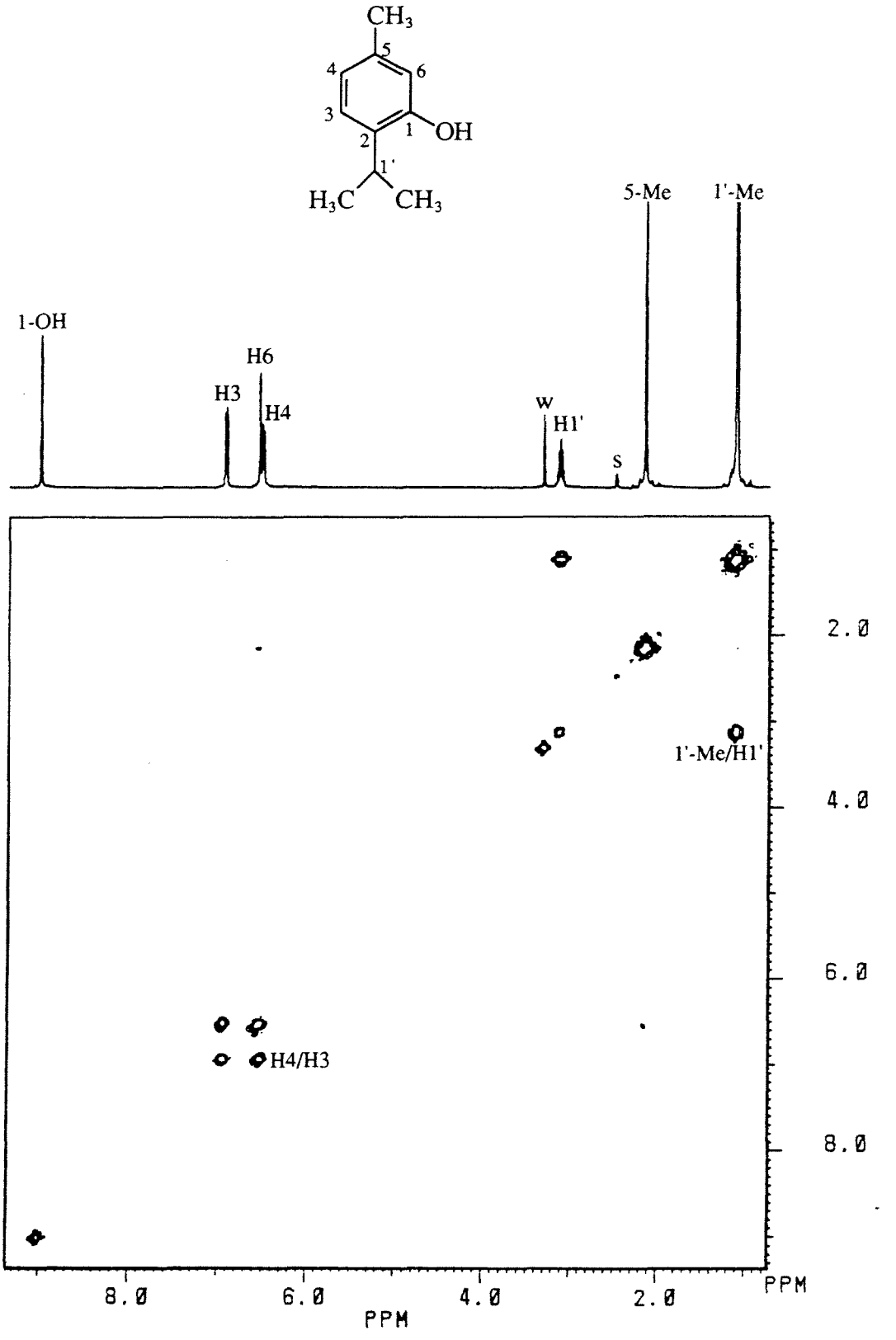

Figure A7. ^{1}H COSY NMR spectrum of thymol (400 MHz, DMSO-d_6).

The entire COSY spectrum of thymol is shown in Figure A7. Diagonal peaks appear on a line from the bottom left hand corner to the upper right hand corner of the spectrum, occurring at the intersection of the same signal on both axes. Peaks that appear elsewhere are cross peaks and indicate coupling. Two isolated spin systems are observed for thymol. The resonance at δ 1.11 (1'-Me), integrating for six protons, shows a correlation with the methine resonance at δ 3.13 (H1'). The doublet at δ 6.53 (H4) shows a COSY correlation (cross peak) to a doublet at δ 6.94 (H3). The COSY correlations for thymol are summarized in Figure A8.

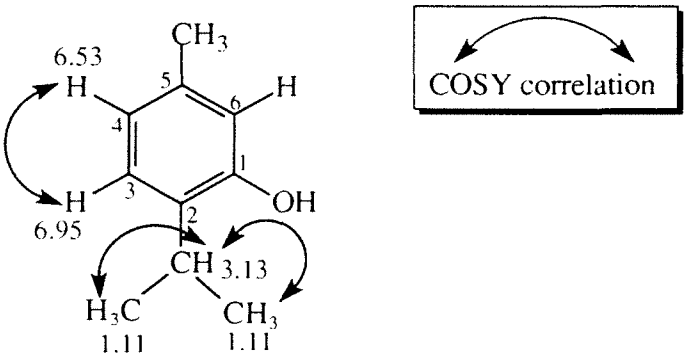

Figure A8. COSY correlations for thymol.

The HMQC experiment

The ^{1}H-detected heteronuclear multiple-quantum coherence (HMQC)[79] experiment was used in this thesis to determine one bond ^{1}H-^{13}C connectivities and it is often referred to as an inverse-detected experiment. An HMQC experiment provides the same information as the ^{13}C-detected heteronuclear correlation[80] (HETCOR) experiment. The advantage of the HMQC experiment is that the FID is acquired in the ^{1}H domain and the greater sensitivity of the ^{1}H nucleus in the NMR experiment means that the HMQC experiment requires less sample and/or less time to obtain the data than in the analogous HETCOR experiment.

The pulse sequence for the HMQC experiment is depicted in Figure A9. The Bird pulse is employed at the beginning of the pulse sequence to suppress signals from protons not coupled to ^{13}C nuclei. Typical values for the delays Δ ($1/2^{1}J_{CH}$) and τ (optimized to eliminate ^{1}H-^{12}C bonded signals) used in the HMQC experiments in this thesis were 3.5 ms and 0.7 s, respectively. Fourier transformation with respect to t_2 results in a series of ^{1}H spectra modulated by one bond ^{1}H-^{13}C scalar coupling. A second Fourier transformation with respect to t_1 results in a 2D spectrum with proton chemical shifts along the F_2 axis and carbon chemical shifts along the F_1 axis. Proton-carbon correlations are observed at (F_1,F_2).

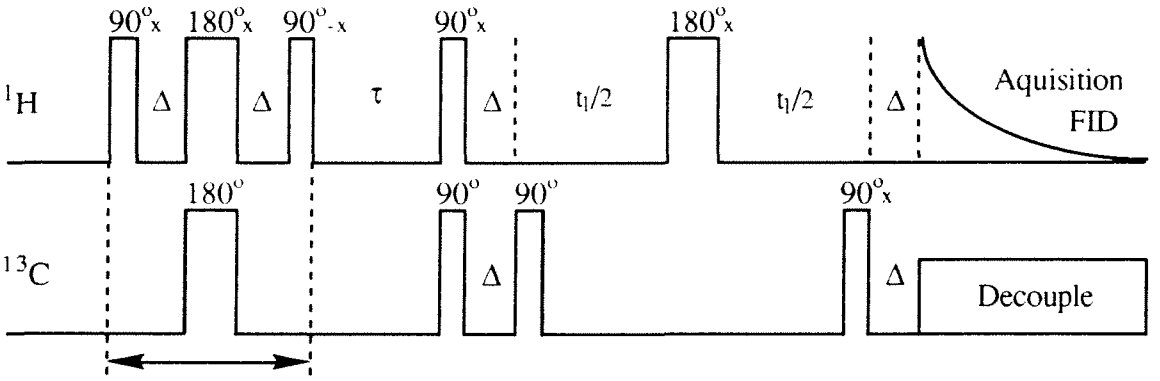

Figure A9. Pulse sequence for the HMQC experiment.[79]

The HMQC spectrum of thymol is provided in Figure A10. This spectrum shows correlations between carbons and their attached protons. The three aromatic protons at δ 6.53, δ 6.56 and δ 6.95 show correlations to the carbons at δ 119.7, δ 115.2 and δ 125.7 respectively. The methine carbon at δ 3.13 is correlated to the carbon at δ 26.2. Intense correlations are observed for the upfield methyl resonances. The methyl resonance at δ 2.15 is correlated to the carbon at δ 20.7 and the methyl doublet at δ 1.11, integrating for six protons, is correlated to the carbon resonance at δ 22.6.

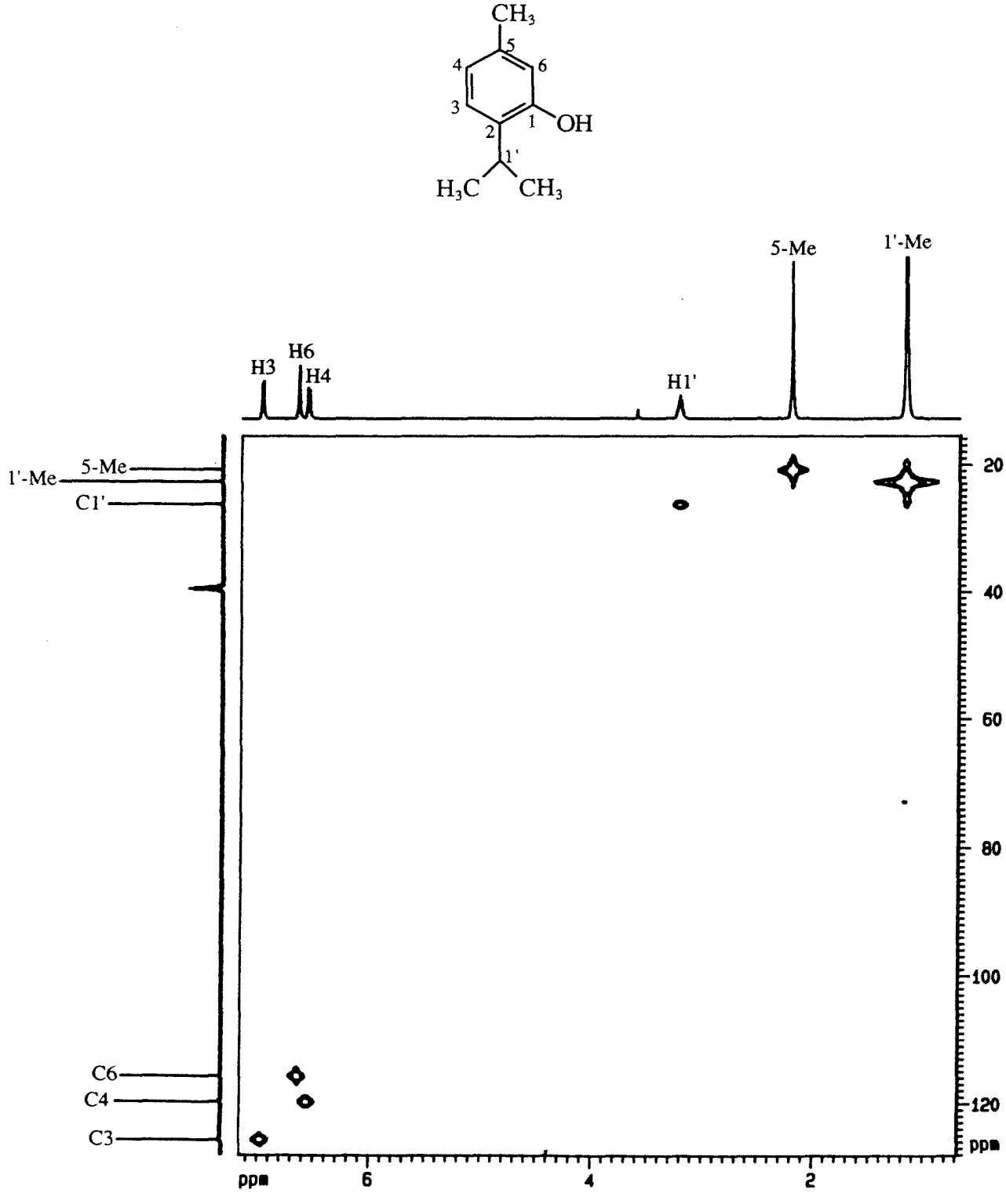

Figure A10. HMQC NMR spectrum of thymol (500 MHz ^{1}H NMR, DMSO-d_6).

The HMBC experiment

The ^{1}H-detected multiple-bond heteronuclear multiple-quantum coherence (HMBC)[81] experiment is similar to the HMQC experiment but it has been optimized for long range, two and three bond, ^{1}H-^{13}C connectivities. This experiment is analogous to the ^{13}C-detected correlation to long range coupling (COLOC)[82] experiment. The ^{1}H-detected HMBC experiment is more sensitive than the COLOC experiment and it can provide ^{1}H-^{13}C connectivities through heteroatoms and allows the unambiguous assignment of quaternary carbon atoms.

The pulse sequence for the HMBC experiment is provided in Figure A11. One-bond correlations are eliminated from this experiment by using a low-pass J-filter, consisting of a 90° proton pulse, a delay Δ_1, followed by a 90° carbon pulse, at the beginning of the pulse sequence. Typical values for the delays Δ_1 ($1/2^{1}J_{CH}$) and Δ_2 (optimized for long range J_{CH}) used for the HMBC experiments in this thesis were 3.5 ms and 60 ms, respectively. Fourier transformation results in a 2D spectrum with ^{1}H chemical shifts along the F_2 axis and ^{13}C chemical shifts along the F_1 axis. Two and three bond ^{1}H-^{13}C correlations are observed as cross peaks at (F_2,F_1). The HMBC spectrum of thymol is given in Figure A12.

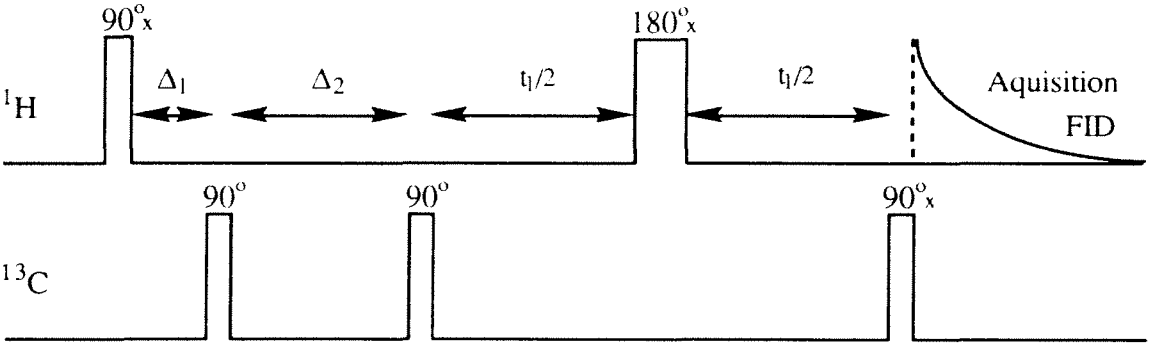

Figure A11. Pulse sequence for the HMBC experiment.[81]

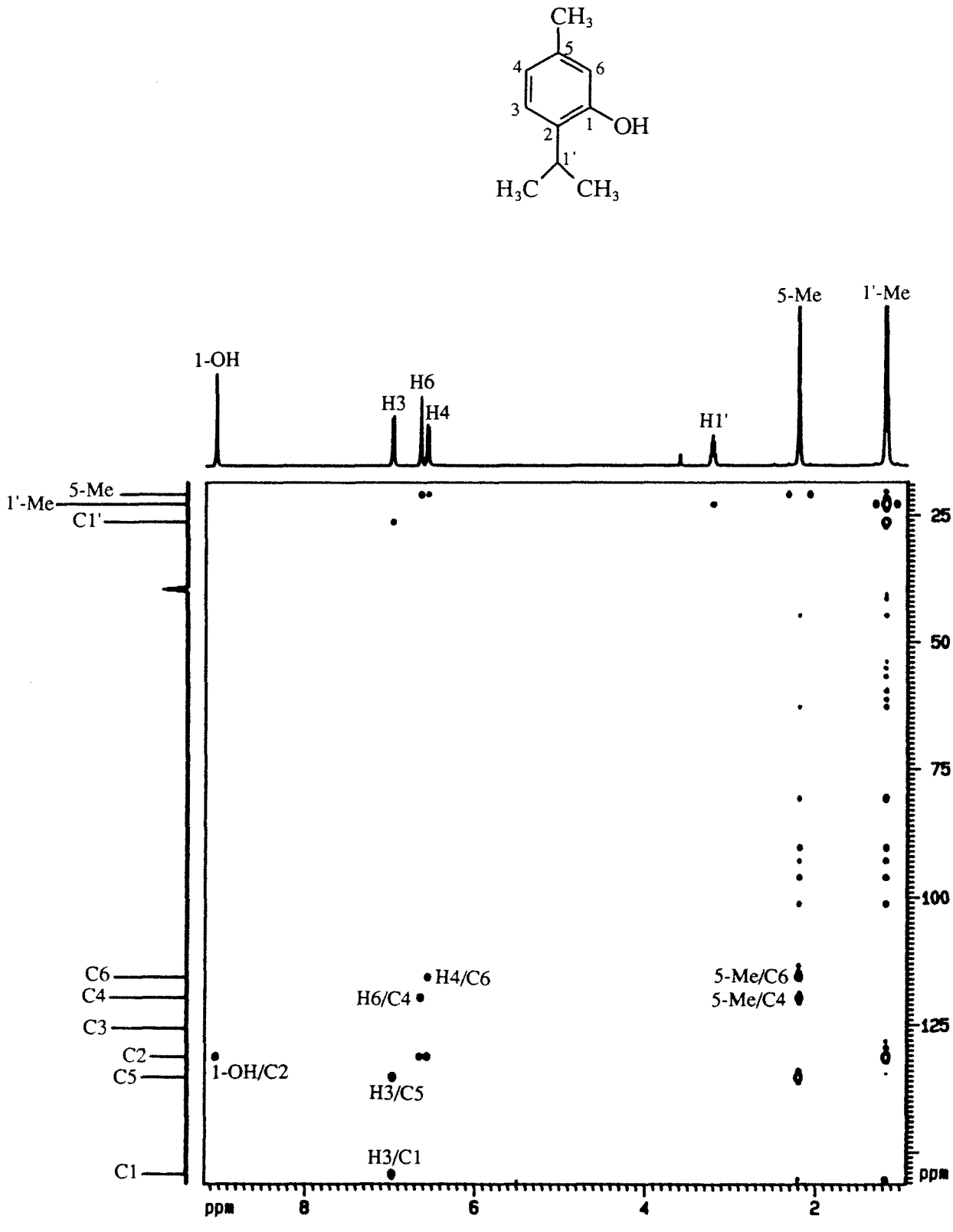

Figure A12. HMBC NMR spectrum of thymol (500 MHz ^{1}H NMR, DMSO-d_6).

Large noise peaks for the methyl signals running along the F_1 axis appear in the spectrum. Methyl peaks show cross peaks which are three times more intense than methine peaks. Plotting a higher contour level will decrease this noise but it will weaken cross peaks from the other groups. The intense methyl cross peaks are easily distinguished from the noise. The methyl resonance at δ 2.15 is correlated to the carbon resonances at δ 115.7, 119.7 and 135.3. The phenolic proton is correlated to the quaternary carbon at δ 131.3. The HMBC experiment shows correlations from protons to carbons two and three bonds distant. Selected HMBC correlations for thymol are summarized in Figure A13.

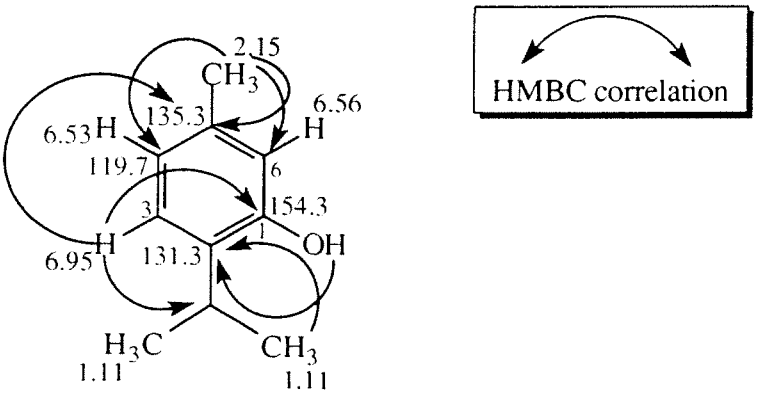

Figure A13. Selected HMBC correlations for thymol.

References

1. a) Cohen, M. L. *Science* **1992**, 257, 1050. b) Neu, H. S. *Science* **1992**, 257, 1064.

2. Fleming, A. *Brit. J. Exp. Pathol.* **1929**, 10, 226.

3. a) Chain, E.; Florey, H. W.; Gardner, A. D. *Lancet* **1940**, 2, 226. b) Abraham, E. P.; Chain, E.; Fletcher, C. M. *Lancet* **1941**, 3, 177.

4. Levy, S. B. *The Antibiotic Paradox*; Plenum Press: New York, 1992; pp 39-40.

5. Waksman, S. A. Ed., *Streptomycin*; Williams and Wilkins: Baltimore, 1949.

6. De Gaxia *Zentralblatt für Hygiene und Infektionkrankheiten* **1989**, 6, 162.

7. Rosenfeld, W. D.; Zobell, C. *J. Bacteriol.* **1947**, 54, 393.

8. Grein, A.; Meyers, S. P. *J. Bacteriol.* **1958**, 76, 457.

9. a) Austin, B. *Marine Microbiology*; Cambridge University Press: Cambridge, 1988. b) Fenical, W.; Jenson, P. R. In *Marine Biotechnology, Volume I;* Attaway, D. H.; Zaborsky, O. R., Eds.; Plenum Press: New York, 1993; pp 419-457.

10. a) Kuster, E. and Neumeirer, W. *Backeriol. Suppl.* **1981**, 11, 315. b) Okami, Y.; Okazaki, T. In *Norcardia and Streptomycetes*; Mordarski, M.; Kurylowicz, W.; Leljaszewicz, W., Eds.; Gustav Fisher Verlag: Stuggart, Germany, 1978; pp 145-151. c) Okami, Y.; Okazaki, T. *J. Ferment. Technol.* **1975**, 53, 833. d) Tresner, H. D., Hayes, J. A.; Backus, E. J. *Appl. Microbiol.* **1968**, 16, 1134.

11. Jensen, P. R.; Dwight, R.; Fenical, W. *Appl. Environ. Microbial.* **1991**, 57, 1102.

12. a) Austin, B. *J. Appl. Bacteriol.* **1989**, 67, 461. b) Fenical, W. *Chem. Rev.* **1993**, 93, 1673. c) Kobayashi, J.; Ishibashi, M. *Chem. Rev.* **1993**, 93, 1753.

13 a) Takahashi, A.; Kurasawa, S.; Ikeda, D.; Okami, Y.; Takeuchi, T. *J. Antibiotics* **1989**, 42, 1556. b) Takahashi, A.; Ikeda, D.; Nakamura, H.; Naganawa, H.; Kurasawa, S.; Okami, Y.; Takeuchi, T. *J. Antibiotics* **1989**, 42, 1562.

14. Pathirana, C.; Jensen, P. R.; Dwight, R.; Fenical, W. *J. Org. Chem.* **1992**, 57, 740.

15. Pathirana, C.; Tapiolas, D.; Jensen, P. R.; Dwight, R.; Fenical, W. *Tetrahedron Lett.* **1991**, 32, 2323.

16. Gustafson, K.; Roman, M.; Fenical, W. *J. Am. Chem. Soc.* **1989**, 111, 7519.

17. a) Kameyama, T.; Takahashi, A.; Kurasawa, S.; Ishizuka, M.; Okami, Y.; Takeuchi, T.; Umezawa, H. *J. Antibiotics* **1987**, 40, 1664. b) Takahashi, A.; Nakamura, H.; Kameyama, T.; Kurasawa, S.; Naganawa, H.; Okami, Y.; Takeuchi, T.; Umezawa, H. *J. Antibiotics* **1987**, 40, 1671.

18. a) Okami, Y.; Okazaki, T.; Kitahara, T.; Umezawa, H. *J. Antibiotics* **1976**, 39, 1019. b) Nakamura, H.; Iitaka, Y.; Kitahara, T.; Okazaki, T.; Okami, Y. *J. Antibiotics* **1977**, 30, 714. c) Sato, K.; Okazaki, T.; Maeda, K.; Okami, Y. *J. Antibiotics* **1978**, 31, 632.

19. a) Hütter, R.; Keller-Schierlein, W.; Knüsel, F.; Prelog, V.; Rodgers, G. C., Jr.; Suter, P.; Vogel, G.; Voser, W.; Zähner, H. *Helv. Chim. Acta* **1967**, 50, 1533. b) Dunitz, J. D.; Hawley, D. M.; Miklos, D.; White, D. N. J.; Berlin, Yu.; Marusic, R.; Prelog, V. *Helv. Chim. Acta* **1971**, 54, 1709.

20. Okami, Y.; Hotta, K.; Yoshida, M.; Ikeda, D.; Kondo, S.; Umezawa, H. *J. Antibiotics* **1979**, 32, 964.

21. a) Nara, T.; Yamamoto, M.; Kawamoto, I.; Takayama, K.; Okachi, R.; Takasawa, S.; Sato, T.; Sato, S. *J. Antibiotics* **1977**, 30, 533. b) Okachi, R.; Takasawa, S.; Sato, T.; Sato, S.; Yamamoto, M.; Kawamoto, I.; Nara, T. *J. Antibiotics* **1977**, 30, 541. c) Egan, R. S.; Stanaszek, R. S.; Cirovic, M.; Mueller, S. L.; Tadanier, J.; Martin, J. R.; Collum, P.; Goldstein, A. W.; De Vault, R. L.; Sinclair, A. C.; Fager, E. E.; Mitscher, L. A. *J. Antibiotics* **1977**, 30, 552.

22. a) Deushi, T,; Iwasaki, A.; Kamiya, K.; Kunieda, T.; Mizoguchi, T.; Nakayama, M.; Itoh, H.; Mori, T.; Oda, T. *J. Antibiotics* **1979**, 32, 173. b) Iwasaki, A.; Itoh, H.; Mori, T. *J. Antibiotics* **1979**, 32, 180. c) Deushi, T.; Nakayama, M.; Watanabe, I.; Moira, T. *J. Antibiotics* **1979**, 32, 187.

23. Pathirana, C.; Jensen, P. R.; Fenical, W. *Tetrahedron Lett.* **1992**, 33, 7663.

24. Shin-Ya, K.; Imai, S.; Furihata, K.; Hayakawa, Y.; Kato, Y.; Vanduyne, G. D.; Clardy, J.; Seto, H. *J. Antibiotics* **1990**, 43, 444.

25. Wessels, P.; Göhrt, A.; Zeeck, A.; Drautz, H.; Zähner, H. *J. Antibiotics* **1991**, 44, 1013.

26. Kosuge, T.; Tsuji, K.; Hirai, K.; Fukuyama, T. *Chem. Pharm. Bull.* **1985**, 33, 3059.

27. Yotsu, M.; Yamazaki, T.; Meguro, Y.; Endo, A.; Murata, M.; Naoki, H.; Yasumoto, T. *Toxicon* **1987**, 25, 225.

28. Gil-Turnes, M. S.; Hay, M. E.; Fenical, W. *Science* **1989**, 246, 116.

29. Stierle, A. C.; Cardellina, J. H.; Singleton, F. L. *Experientia* **1988**, 44, 1021.

30. a) Elyakov, G. B.; Kuznetsova, T.; Mikhailov, V. V.; Maltsev, I. I.; Voinov, V. G.; Fedoreyev, S. A. *Experentia* **1991**, 47, 632. b) Voinov, V. G.; El'kin, Yu. N.; Kuznetsova, T. A.; Mal'tsev, I. I.; Mikhailov, V. V.; Sasunkevich, V. A. *J. Chromat.* **1991**, 586, 360.

31. Shigemori, H.; Bae, M.-A.; Yazawa, K.; Sasaki, T.; Kobayashi, J. *J. Org Chem.* **1992**, 57, 4317.

32. Kelly, M. T. University of British Columbia in Vancouver, personal communication.

33. a) Hamill, R.; Elander, R.; Mabe, J.; Gorman, M. *Antimicrob. Agents Chemother.* **1967**, 388. b) Martin, L. L.; Chang, C.-J.; Floss, H. G.; Mabe, J. A.; Hagaman, E. W.;

Wenkert, E. *J. Am. Chem. Soc.* **1972**, 94, 8942. c) Roitman, J. N.; Mahoney, N. E.; Janisiewicz, W. J.; Benson, M. *J. Agric. Food Chem.* **1990**, 38, 538.

34. Isolation and Characterization: a) Wrede, F.; Rothhass, A. *Z. Physiol. Chem.* **1934**, 226, 95 and references cited therein. Biosynthesis: b) Wasserman, H. H.; McKeon, J. E.; Santer, U. V. *Biochem. Biophys. Res. Commun.* **1960**, 3, 146. c) Santer, U. V.; Vogel, H. J. *J. Fed. Proc.* **1956**, 15, 345. d) Santer, U. V.; Vogel, H.J. *Biochem. Biophys. Acta* **1956**, 19, 578. e) Cushley, R. J.; Anderson, D. R.; Lipsky, S. R.; Sykes, R. J.; Wasserman, H. H. *J. Am. Chem. Soc.* **1971**, 93, 6284. f) Cushley, R. J.; Sykes, R. J.; Shaw, C.-K.; Wasserman, H. H. *Can. J. Chem.* **1975**, 53, 148. g) Gerber, N. N.; McInnes, A. G.; Smith, D. G.; Walter, J. A.; Wright, J. L. C.; Vining, L. C. *Can J. Chem.* **1978**, 56, 1155. Structure determination (total synthesis, partial synthesis): h) Gerber, N. N. *Tetrahedron Lett.* **1983**, 24, 2797. i) Wasserman, H. H.; McKeon, J. E.; Smith, L.; Forgione, P. *J. Am. Chem. Soc.* **1960**, 82, 506. j) Wasserman, H. H.; McKeon, J. E.; Smith, L.; Forgione, P. *Tetrahedron Suppl.* **1966**, 8 (part II), 647. k) Rapport, H.; Holden, K. G. *J. Am. Chem. Soc.* **1960**, 82, 5510. l) Rapport, H.; Holden, K. G. *J. Am. Chem. Soc.* **1962**, 84, 635. m) Castro, A. J.; Deck, J. F.; Hugo, M. T.; Lowe, E. J.; Marsh, J. P., Jr.; Pfeiffer, B. J. *J. Org. Chem.* **1963**, 28, 857. n) Castro, A. J.; Corwin, A. H.; Waxham, F. J.; Beilby, A. L. *J. Org. Chem.* **1959**, 24, 455. o) Boger, D. L.; Patel, M. *Tetrahedron Lett.* **1987**, 28, 2499. p) Boger, D. L.; Patel, M. *J. Org. Chem.* **1988**, 53, 1405.

35. Needham, J.; Andersen, R. J.; Kelly, M. T. *Tetrahedron Lett.* **1991**, 32, 315.

36. a) Liverly, D. H.; Gorman, M.; Haney, M. E.; Mabe, J. A. *Antimicrob. Agents Chemother.* **1966**, 462. b) Floss, H. G.; Manni, P. E.; Hamill, R. L.; Mabe, J. A. *Biochem. Biophys. Res. Commun.* **1971**, 45, 781.

37. a) D'Aoust J. Y.; Kushner, D. J. *J. Bacteriol.* **1973**, 111, 340. b) Gauthier, M. J. *Int. J. Syst. Bacteriol.* **1976**, 26, 459.

38. DeFreitas, A. S. W.; Quilliam, M. A.; Walter, J. A.; Wright, J. L. C.; Pleasance, S. *J. Natl. Prod.* **1992**, 55, 1631.

39. a) Yue, S.; Duncan, J. S.; Yamamoto, Y. and Hutchinson, C. R. *J. Am. Chem. Soc.* **1987**, 109, 1253. b) Cane, D. E.; Yang, C. *J. Am. Chem. Soc.* **1987**, 109, 1255. c) Cane, D. E.; Yang, C.; Ott, W. R. *Proceedings of the Seventh International Symposium on Biology of Actinomycetes*; Japan Antibiotics Research Association: Tokyo, 1988; pp 395-400. d) Cane, D. E.; Ott, W. R. *J. Am. Chem. Soc.* **1988**, 110, 4840. e) Spavold, Z. M.; Robinson, J. A. *J. Chem. Soc., Chem. Commun.* **1988**, 4. f) Yoshizawa, Y.; Li, Z.; Resse, P. B.; Vederas, J. C. *J. Am. Chem. Soc.* **1990**, 112, 3212. g) Staunton, J.; Sutkowski, A. C. *J. Chem. Soc., Chem. Commun.* **1991**, 1108. h) Staunton, J.; Sutkowski, A. C. *J. Chem. Soc., Chem. Commun.* **1991**, 1110. i) Jacobs, A.; Staunton, J.; Sutkowski, A. C. *J. Chem. Soc., Chem. Commun.* **1991**, 1113. j) Cane, D. E.; Prabhakaran, P. C.; Tan, W.; Ott, W. R. *Tetrahedron Lett.* **1991**, 32, 5457. k) Li, Z.; Martin, F. M.; Vederas, J. C. *J. Am. Chem. Soc.* **1992**, 114, 1531. l) Cane, D. E.; Lambalot, R. H.; Prabhakaran, P. C.; Ott, W. *J. Am. Chem. Soc.* **1993**, 115, 522. m) Cane, D. E.; Tan, W.; Ott, W. R. *J. Am. Chem. Soc.* **1993**, 115, 527.

40. a) Kingston, D. G. I.; Kolpak, M. X.; LeFevre, J. W.; Borup-Grochtmann, I. *J. Am. Chem. Soc.* **1983**, 105, 5106. b) LeFevre, J. W.; Kingston, D. G. I. *J. Org. Chem.* **1984**, 49, 2588.

41. Grue-Sorensen, G; Spencer, I. D. *J. Am. Chem. Soc.* **1993**, 115, 2052.

42. Needham. J.; Andersen, R. J.; Kelly, M. T. *J. Chem. Soc., Chem. Commun.* **1992**, 1367.

43. Numa, S. Ed.: *Comprehensive Biochemistry*, Vol 7, Elsevier, Amsterdam 1984.

44. Staunton, J. *Angew. Chem. Int. Ed. Engl.* **1991**, 30, 1302.

45. Nakagawa, A.; Konda, Y.; Hatano, A.; Harigaya, Y.; Onda, M.; Omura, S. *J. Org. Chem.* **1988**, 53, 2660.

46. Kohl, W.; Irschik, H.; Reichenbach, H.; Höfle, G. *Liebigs Ann. Chem.* **1984**, 1088.

47. Trowitzsch, W.; Gerth, K.; Wray, V.; Höfle, G. *J. Chem. Soc. Chem. Commun.* **1983**, 1174.

48. Bobzin, S. C.; Moore, R. E. *Tetrahedron* **1993**, 49, 7615.

49. Wright, J. L. C., Institute for Marine Biosciences in Halifax, personal communication.

50 Ishiga, M., The University of British Columbia in Vancouver, personal communication

51. a) Fredenhagen, A.; Tamura, S. Y.; Kenny, P. T. M.; Komura, H.; Naya, Y.; Nakanishi, K.; Nishiyama, K.; Sugiura, M.; Kita, H. *J. Am. Chem. Soc.* **1987**, 109, 4409. b) McWhorter, W.; Fredenhagen, A.; Nakanishi, K.; Komura, H. *J. Chem. Soc., Chem, Commun.* **1989**, 299.

52. Needham, J.; Kelly, M. T.; Ishige, M.; Andersen, R. J. sumitted for publication in *J. Org. Chem.*

53. a) Buchanan, J. G; Hamblin, M. R.; Kumar, A.; Wightman, R. H. *J. Chem. Soc., Chem, Commun.* **1984**, 1515. b) Buchanan, J. G.; Kumar, A.; Wightman, R. H.; Field, S. J.; Young, D. W. *J. Chem. Soc., Chem. Commun.* **1984**, 1517.

54. a) Morishima, H.; Sawa, T.; Takita, T.; Aoyagi, T.; Takeuchi, T.; Umezawa, H. *J. Antibiotics* **1974**, 27, 267. b) Umezawa, H.; Aoyagi, T.; Morishima, H.; Matsuzaki, H.; Hamada, M.; Takeuchi, T. *J. Antibiotics* **1970**, 23, 259. c) Morishima, H.; Takita, T.; Aoyagi, T.; Takeuchi, T.; Umezawa, H. *J. Antibiotics* **1970**, 32, 263. c) Miyano, T.; Tomiyasu, M.; Iizuka, H.; Tomisaka, S.; Takita, T.; Aoyagi, T.; Umezawa, H. *J. Antibiotics* **1972**, 25, 491. d) Morishima, H.; Takita, T.; Umezawa, H. *J. Antibiotics* **1972**, 25, 551. e) Aoyagi, T.; Morishima, H.; Nishizawa, R.; Kunimoto, S.; Takeuchi, T.; Umezawa, H.; Ikezawa, H. *J. Antibiotics* **1972**, 25, 689. f) Morishima, H.; Takita, T.; Umezawa, H. *J. Antibiotics* **1973**, 26, 115. g) Kinoshita, M.; Aburaki, S.; Hagiwara, A.; Imai, J. *J. Antibiotics* **1973**, 26, 249. h) Aoyagi, T.; Yagisawa, Y.; Kumagai, M.; Hamada, M.; Morishima, H.; Takeuchi, T.; Umezawa, H. *J. Antibiotics* **1973**, 26, 539. i) Umezawa, H.; Miyano, T.; Murakami, T.; Takita, T.; Aoyagi, T.; Takeuchi, T.; Naganawa, H.; Morishima, H. *J. Antibiotics* **1973**, 26, 615.

55. Hasegawa, Y.; Nozu, Y.;Kuwana, N. *Agr. Biol. Chem.* **1976**, 40, 451.

56. Omura, S.; Imamura, N.; Kawakita, K.; Mori, Y.; Yamazaki, Y; Masuma, R.; Takahashi, Y.; Tanaka, H.; Huand, Lee-Yuan; Woodruff, H. B. *J. Antibiotics* **1986**, 39, 1079.

57. Klein, S. M.; Sagers, R. D. *J. Biol. Chem.* **1967**, 242, 298.

58. a) Sagers, R. D.; Gunsalus, I. C. *J. Bacteriol.* **1961**, 81, 541. b) Barker, H. A.; Volcan, B. E.; Cardon, B. P. *J. Biol. Chem.* **1948**, 173, 803.

59. a) Iwasaki, S.; Namikoshi, M.; Kobayashi, H.; Furukawa, J.; Okuda, S. *Chem. Pharm. Bull.* **1986**, 34, 1387. b) Kiyoto, S.; Kawai, Y.; Kawakita, T.; Kino, E.; Okuhara, M.; Uchida, I.; Tanaka, H.; Hashimoto, M.; Terano, H.; Kohsaka, M.; Aoki, H.; Imanaka, H. *J. Antibiotics* **1986**, 39, 762.

60. Iwasaki, S.; Kobayashi, H.; Furukawa, J.; Namikoshi, M.; Okuda, S.; Sato, Z.; Matsuda, I. and Noda, T. *J. Antibiotics* **1984**, 37, 354.

61 a) Tsuruo, T.; Oh-hara, T.; Iida, H.; Tsukagoshi, S.; Sato, Z.; Matsuda, I.; Iwasaki, S.; Okuda, S.; Shimizu, F.; Sasagawa, K.; Fukami, M.; Fukuda, K.; Arakawa, M. *Cancer Res.* **1986**, 46, 381. b) Takahashi, M.; Iwasaki, S.; Kobayashi, H.; Okuda, S.; Murai, T.; Sato, Y.; Haraguchi-Hiraoka, T.; Nagano, H. *J. Antibiotics* **1987**, 40, 66. c) Takahashi, M.; Iwasaki, S.; Kobayashi, H.; Okuda, S.; Murai, T.; Sato, Y. *Biochim. Biophys. Acta* **1987**, 926, 215. d) Takahashi, M.; Kobayashi, H.; Iwasaki, S. *Mol. Gen. Genet.* **1989**, 220, 53. e) Takahashi, M.; Matsumoto, S.; Iwasaki, S.; Yahara, I. *Mol. Gen. Genet.* **1990**, 222, 169. f) Bali, R.; Pettit, G.; Hamel, E. *Biochem. Pharmacol.* **1990**, 39, 1941. g) Kato, Y.; Ogawa, Y.; Imada, T.; Iwasaki, S.; Shimazaki, N.; Kobayashi, T.; Komai, T. *J. Antibiotics* **1991**, 44, 66. h) Sawada, T.; Hashimoto, Y.; Kobayashi, H.; Iwasaki, S. *Biochim. Biophys. Res. Commun.* **1991**, 178, 558. i) Waud, W. R.; Harrison, S. D. Jr.; Gilbert, K. S.; Laster, W. R. Jr.; Griswold, D. P. Jr. *Cancer Chemother. Pharmacol.* **1991**, 27, 456. j) Sullivan, A. S.; Prasad, V.; Roach, M. C.; Takahashi, M.; Iwasaki, S.; Ludueña, R. F. *Cancer Res.* **1990**, 50, 4277. k) McClean, S.; Whelan, R. D. H.; Hosking, L. K.; Hill, B. T. *Biochem. Soc. Trans.* **1991**, 19, 278S. l) Li, Y.; Kobayashi, H.; Tokiwa, Y.; Hashimoto, Y.; Iwasaki, S. *Biochem. Pharmacol.* **1992**, 43, 219. m) Li, Y.; Kobayashi, H.; Hashimoto, Y.; Iwasaki, S. *Biochem. Biophys. Res. Commun.* **1992**, 187, 722. n) Graham, M. A.; Bissett, D.; Setanoians, A.; Hamilton, T.; Kerr, D. J.; Henrar, R.; Kaye, S. B. *J. Natl. Cancer Inst.* **1992**, 84, 494.

62. a) Fujisawa Pharm. KK, JP Patent 61093186, 1986. b) Okuda, S.; Iwasaki, S.; Namikoshi, M.; Arakawa, Y.; Shimizu, N., JP Patent 62000087, 1987. c) Hirai, K.; Fujimoto, K.; Kobayashi, T., JP Patent 63246380, 1988. d) Kaneko, M.; Kamokari, M.; Kobayashi, T.; Sasagawa, K., EP Patent 350315, 1990. e) Iwasaki, S.; Kobayashi, T., JP Patent 02212490, 1990. f) Okuda, S.; Iwasaki, S.; Namikoshi, M.; Arakawa, M.; Shimizu, F., CA Patent 1271763, 1990. g) Komai, T.; Kawai, K.; Kinoshita, T.; Haruyama, H.; Kobayashi, T.; Sasagawa, K.; Iwasaki, S., JP Patent 03101680, 1991. h) Iwasaki, S.; Ogawa, J.; Kobayashi, T., JP Patent 03101679, 1991.

63. Iwasaki, S.; Namikoshi, M.; Kobayashi, H.; Furukawa, J.; Okuda, S.; Itai, A.; Kasuya, A.; Iitaka, Y.; Sato, Z. *J. Antibiotics* **1986**, 39, 424.

64. Kobayashi, H.; Iwasaki, S.; Yamada, E.; Okuda, S. *J. Chem. Soc., Chem. Commun.* **1986**, 1702.

65. a) Shimojima, Y.; Hayashi, H.; Ooka, T.; Shibukawa, M. *Agric. Biol. Chem.* **1966**, 46, 1823. b) Shimojima, Y.; Hayashi, H.; Ooka, T.; Shibukawa, M. *Tetrahedron Lett.* **1966**, 23, 5435. c) Shimojima, Y.; Hayashi, H. *J. Med. Chem.* **1967**, 26, 1370. d) Shimojima, Y.; Hayashi, H.; Ooka, T.; Shibukawa, M.; Iitaka, Y. *Tetrahedron* **1968**, 40, 2519. e) Kawai, A.; Hara, O.; Hamada, Y.; Shioiri, T. *Tetrahedron Lett.* **1988**, 29, 6331. f) Hamada, Y.; Kawai, A.; Kohno, Y.; Hara, O.; Shioiri, T. *J. Am. Chem. Soc.* **1989**, 111, 1524. g) Gesson, J. P.; Jacquesy, J. C.; Mondon, M. *Tetrahedron Lett.* **1989**, 30, 6503.

66. a) Dale, J. A.; Dull, D. L.; Mosher, H. S. *J. Org. Chem.* **1969**, 34, 2543. b) Dale, J. A.; Mosher, H. S. *J. Am. Chem. Soc.* **1957**, 95, 512. c) Sullivan, G. R.; Dale, J. A.; Mosher, H. S. *J. Org. Chem.* **1957**, 38, 2143. d) Ohtani, I.; Kusumi, T.; Kashman, Y.; Kakisawa, H. *J. Am. Chem. Soc.* **1991**, 113, 4092. e) Kusumi, T.; Fukushima, T.; Ohtani, I.; Kakisawa, H. *Tetrahedron Lett.* **1991**, 32, 2939.

67. Ward, D. E.; Rhee, C. K. *Tetrahedron Lett.* **1991**, 32, 7165.

68. Brogden, P. J.; Gabbutt, C. D.; Hepworth, J. D. In *Comprehensive Heterocyclic Chemistry, Volume 3*; Boulton, A. J. and McKillop, A. Eds.; Pergamon Press: 1984, pp 573-646.

69. a) Itoh, J.; Omoto, S.; Shomura, T; Nishizawa, N.; Miyado, S.; Yuda, Y.; Shibata, U.; Inouye, S. *J. Antibiotics* **1981**, 34, 611. b) Itoh, J.; Shomura, T.; Omoto, S.; Miyada, S.; Yuda, Y.; Shibata, U.;Inouye, S. *Agric. Biol. Chem.* **1982**, 46, 1255. c) Itoh, J.; Omoto, S.; Nishizawa, N.; Kodama, Y.; Inouye, S. *Agric. Biol. Chem.* **1982**, 46, 2659.

70. Elyakov, G. B. *Abstracts of Papers*, 7th International Symposium on Marine Natural Products, Capri, Italy; 1992, Abstract C15.

71. Zobell, C. E.; Upham, H. C. *Bull. Scripps Inst. Oceanogr.* **1944**, 5, 239.

72. Stahl, E.; Ed. Thin Layer Chromatography, 2nd Edition Springer-Verlag, Berlin, 1969.

73. Küsher, T. C.; Lindsten, G. R. *J. Org. Chem.* **1983**, 48, 3589.

74. a) Atta-ur-Rahman *One and Two Dimensional Spectroscopy*; Elsevier Science Publishers: New York, N.Y., 1989. b) Derome, A. E. *Modern NMR Techniques for Chemistry Research*; Pergamon Press: Oxford, 1987. c) Sanders, K. M.; Hunter, B. K. *Modern NMR Spectroscopy*, 2nd ed.; Oxford University Press: Oxford, 1992. d) Kessler, H.; Geheke, M.; Griesinger, C. *Angew. Chem. Int. Ed. Engl.* **1988**, 27, 490. e) Sadler, I. H. *Nat. Prod. Rep.* **1988**, 101.

75. Silverstein, R. M.; Bassler, G. C.; Morrill, T. C. *Spectrometric Identification of Organic Compounds*, Fourth Ed.; John Wiley and Sons: New York, 1981, pp. 181-304.

76. Benn, R.; Günther, H. *Angew. Chem. Int. Ed. Engl.* **1983**, 22, 350.

77. Sanders, J. K. M.; Mersh, J. D. *Prog. Nucl. Magn. Res.* **1982**, 15, 353.

78 Aue, W. P.; Bartholdi, E.; Ernst, R. R. *J. Chem. Phys.* **1976**, 64, 2229.

79. Bax, A. and Subramanian, S. *J. Magn. Reson.* **1986**, 67, 565.

80. a) Bax, A.; Morriss, G. A. *J. Magn. Reson.* **1981**, 42, 501. b) Bodenhausen, G.; Freeman, R. *J. Magn. Reson.* **1977**, 28, 471.

81. Bax, A.; Summers, M. F. *J. Am. Chem. Soc.* **1986**, 108, 2093.

82. Kessler, H.; Griesinger, C.; Zarbock, J.; Loosli, H. R. *J. Magn. Reson.* **1984**, 57, 331.